D 2015

U.PORTO
INSTITUTO DE CIÊNCIAS BIOMÉDICAS
UNIVERSIDADE DO PORTO

MECHANISMS OF ACTION AND ANTIMYCOBACTERIAL ACTIVITY OF ANTIMICROBIAL PEPTIDES

TÂNIA MARTINS DA SILVA
TESE DE DOUTORAMENTO APRESENTADA
AO INSTITUTO DE CIÊNCIAS BIOMÉDICAS ABEL SALAZAR
DA UNIVERSIDADE DO PORTO EM
CIÊNCIAS BIOMÉDICAS

Tânia Martins da Silva

Mechanisms of action and antimycobacterial activity of antimicrobial peptides

Tese de Candidatura ao grau de Doutor em Ciências Biomédicas submetida ao Instituto de Ciências Biomédicas Abel Salazar

Orientador – Prof. Doutora Maria Salomé Gomes
Categoria – Professora Associada
Afiliação – Instituto de Ciências Biomédicas Abel Salazar (ICBAS) e Instituto de Biologia Molecular e Celular (IBMC) da Universidade do Porto

Co-Orientador – Prof. Doutora Margarida Bastos
Categoria – Professora Associada com Agregação
Afiliação – Centro de Investigação em Química (CIQ-UP), Departamento Química e Bioquímica, Faculdade de Ciências da Universidade do Porto

The work described on this thesis was conducted at the Iron and Innate Immunity group at Instituto de Biologia Molecular e Celular (IBMC) da Universidade do Porto and at the Nanostructures and Self-Organization group at Centro de Investigação em Química da Universidade do Porto (CIQ-UP).

The work was funded in part by grants (NORTE-07-0124-FEDER-000002-Host-Pathogen Interactions and NORTE-07-0162-FEDER-000088) of the Programa Operacional Regional do Norte (ON.2 – O Novo Norte) under the framework of Quadro de Referência Estratégico Nacional 2007/2013 (QREN), funded by Fundo Europeu de Desenvolvimento Regional (Feder). It also received support from Fundação para a Ciência e Tecnologia (FCT) and European Social Funds through strategic projects, Pest-C/QUI/UI0081/2011 and Pest-C/QUI/UI0081/2013.

The author received a PhD fellowship (SFRH/BD/77564/2011) from FCT and financed by European Social Funds, Programa Operacional Potencial Humano (POPH) e Programa Operacional Capital Humano (POCH).

Agradecimentos

Gostava de agradecer a todas as pessoas que estiveram envolvidas neste trabalho, e que contribuíram para o seu desenvolvimento e realização.

Em primeiro lugar, agradecer às minhas orientadoras, Prof. Doutora Maria Salomé Gomes e Prof. Doutora Margarida Bastos, por toda a ajuda, sem elas este trabalho não seria possível.

Agradeço também à Fundação para a Ciência e Tecnologia (FCT) pelo financiamento da minha bolsa de doutoramento (SFRH/BD/77564/2011), ao programa doutoral em Ciências Biomédicas do Instituto de Ciências Biomédicas Abel Salazar (ICBAS) da Universidade do Porto, e à instituição de acolhimento, Instituto de Biologia Molecular e Celular (IBMC) da Universidade do Porto.

Ao Prof. Doutor Pedro Rodrigues, líder do grupo Iron and Innate Immunity do IBMC, e aos restantes membros, Ana Carolina Moreira, João Neves e Miguel Ramos. Aos ex-membros, Bárbara Magalhães, Carolina Caldas, Filipe Marques, Sandro Gomes, Sílvia Costa e Tânia Moniz.

A todas as pessoas do Centro de Investigação em Química da Universidade do Porto (CIQ-UP) e ao Departamento de Química e Bioquímica da Faculdade de Ciências da Universidade do Porto.

To Jan Bolscher (ACTA, Department of Oral Biochemistry, Amsterdam, The Netherlands), David Andreu (Departament de Ciències Experimentals i de la Salut, Universitat Pompeu Fabra, Barcelona, Spain) and Paula Gomes (Departamento de Química e Bioquímica, FCUP, Porto, Portugal) for providing the peptides, essentials for this work.

To Daniela Uhríková (Faculty of Pharmacy, J. A. Comenius University, Bratislava, Slovak Republic), Sergio Funari (DESY, Hamburg, Germany) and Bruno Silva (INL – International Iberian Nanotechnology Laboratory, Braga, Portugal), for all the help with the X-ray data and analysis.

Ao Rui Fernandes do Histology and Electron Microscopy Service e à Paula Sampaio da unidade de Advanced Light Microscopy do IBMC.

Às minhas amigas, Ana Carolina Moreira, Ana Santos, Célia Ramalho, Inês Vieira, Tânia Magalhães Silva e Tânia Moniz.

Finalmente, às pessoas mais importantes, aos meus pais e ao meu marido, obrigado.

Contents

Abbreviations List

AIDS	Acquired Immune Deficiency Syndrome
AMP	Antimicrobial Peptides
BMM	Bone marrow-derived macrophages
CA(1-7)M(2-9)	hybrid peptide containing amino acids 1-7 from cecropin A and 2-9 from melittin
CAM	CA(1-7)M(2-9)
CCL2	Chemokine (C-C motif) ligand 2
CD	Circular Dichroism
CFU	Colony forming unit
CL-DNA	Cationic liposomes-DNA system
D-LFcin17-30	D enantiomer of LFcin17-30
DMEM	Dulbecco's Modified Eagle's Medium
DSC	Differential Scanning Calorimetry
FBS	Fetal Bovine Serum
FWHM	Full width at half maximum
HBD	Human β-defensin
HDP	Host Defence Peptides
HEPES	4-(2-hydroxyethyl)-1-piperazineethanesulfonic acid
HIV	Human Immunodeficiency Virus
HNP	Human neutrophil peptide
HPLC	High performance liquid chromatography
IFN	Interferon
IL	Interleukin
ITC	Isothermal Titration Calorimetry
K	Lysine
LCCM	L929 cell conditioned medium
LF	Lactoferrin
LFampin265-284	lactoferrampin peptide containing amino acids 265-284 from bovine lactoferrin

LFchimera	Hybrid of LFcin17-30 and LFampin265-284 coupled by a special lysine linkage
LFcin	Lactoferricin
LFcin17-30	Lactoferricin peptide containing amino acids 17-30 from bovine lactoferrin
LFcin17-30 all K	LFcin17-30 with all arginines substituted by lysines
LFcin17-30 all R	LFcin17-30 with all lysines substituted by arginines
LPS	Lipopolysaccharide
LUVs	Large unilamellar vesicles
MAC	*Mycobacterium avium* Complex
M-CSF	Macrophage colony stimulating factor
MDR-TB	Multidrug-resistant tuberculosis
MRSA	Methicillin-resistant *Staphylococcus aureus*
NTM	Nontuberculous Mycobacteria
OLVs	Oligolamellar vesicles
P:L	Peptide-to-Lipid molar ratio
PBS	Phosphate buffered saline
PC	Phosphatidylcholine
PE	Phosphatidylethanolamine
PG	Phosphatidylglycerol
POPE	1-palmitoyl-2-oleoyl-*sn*-glycero-3-phosphoethanolamine
POPG	1-palmitoyl-2-oleoyl-*sn*-glycero-3-phospho-(1'-*rac*-glycerol)
R	Arginine
SAXD	Small Angle X-ray Diffraction
TAMRA	5(6)-carboxytetramethylrhodamine
TB	Tuberculosis
TNF	Tumour Necrosis Factor
WHO	World Health Organization
XDR-TB	Extensively-resistant tuberculosis

Abstract

The revolutionary discovery of penicillin in 1928 by Alexander Fleming held the promise of treatment and cure of all infectious diseases. Indeed, in the following decades the levels of bacterial infections largely declined with consequent large improvements for public health. However, nowadays we live in an era where bacterial resistance to antimicrobial agents is rapidly spreading throughout the world, putting at risk the success of treatments for infectious diseases, and thus placing them again as one of the world's major threats to global public health. To fight this tendency, new antimicrobial drugs must be introduced into the clinic, especially drugs with different paradigms from those of conventional antibiotics, and keeping resistance avoidance as one of the main goals. Antimicrobial peptides (AMP) are being extensively studied as a new potential alternative to fight infectious diseases. These peptides are widespread in nature and are characterized by a wide range of activity against several pathogens. Their mode of action is thought to rely on membrane destabilization through a variety of mechanisms that lead to cell death, possibly acting also on internal targets and/or through immunomodulation. Due to the nature of the main AMP target, the cytoplasmic membrane, and to the possibility of acting on different targets and by different mechanisms, it is believed that induction of resistance is less likely to occur for AMP than for conventional antibiotics.

The main goals of this thesis were to study the mechanisms of action of two families of AMP, cecropin A-melittin hybrids and lactoferrin peptides, and to assess the potential of lactoferricin peptides against *Mycobacterium avium*, an opportunistic intracellular pathogen.

The interaction of a cecropin A-melittin hybrid, CA(1-7)M(2-9), with bacterial model membranes composed of phosphatidylethanolamine (PE) and phosphatidylglycerol (PG) was evaluated through a number of biophysical techniques, such as Small Angle X-ray Diffraction, Differential Scanning Calorimetry, Isothermal Titration Calorimetry, Circular Dichroism and microscopy techniques. Our findings showed that the peptide's interaction takes place mainly at the surface (lipid heads level), without pore formation. Thus overall the results obtained indicate that CA(1-7)M(2-9) induces membrane condensation by disrupting the lipid vesicles and forming multilamellar structures in onion-like structures, with the peptide intercalated between the bilayers. We thus propose the "carpet model" as the best description of CA(1-7)M(2-9) mechanism of action with this bacterial model membranes, having membrane disruption as the final stage of its action.

In the case of lactoferrin peptides, LFcin17-30, LFampin265-284 and LFchimera, their mechanism of action was studied by X-ray diffraction with fungal model membranes

composed of phosphatidylcholine (PC) and phosphatidylglycerol (PG). The obtained results showed that although the three peptides belong to the same family, they interact differently with membranes. LFcin17-30 has a small effect on membrane structure, inducing mainly lipid segregation; LFampin265-284 induces the formation of a micellar cubic phase (Pm3n) that would thus completely disrupt the membrane; and LFchimera leads to membrane destruction through the formation of bicontinuous cubic phases (Im3m and Pn3m). Remarkably, these results are in very good agreement with the ones previously obtained for the action of these peptides against *Candida albicans*.

Lactoferricin, LFcin17-30, and variants obtained by specific amino acid substitutions were tested *in vitro* against *Mycobacterium avium*. Our results showed that all peptides were highly active against *M. avium* in broth culture, the most active peptides being the D enantiomer of LFcin17-30 (D-LFcin17-30) and the variant with all lysines substituted by arginines (LFcin17-30 all R). They all induced surface and ultra-structural changes upon contact with the mycobacteria, but no evident signs of membrane disruption were seen, leading us to propose that these lactoferricin peptides probably have an intracellular target within *M. avium*. Interestingly, when treating *M. avium*-infected macrophages, only D-LFcin17-30 had a significant activity against this pathogen. The combined administration of lactoferricin peptides and the conventional antibiotic ethambutol significantly increased the activity of all peptides and that of the antibiotic alone. Nevertheless, it did not surpassed the effect of D-LFcin17-30 alone. Further investigations on the mechanism of action of this particular peptide revealed that it does not co-localize with *M. avium* when inside macrophages, probably exerting its activity through modulation of the macrophage antimicrobial defence mechanisms.

With this work, we contributed to the elucidation of the mechanisms by which antimicrobial peptides interact with target membranes, showing a high heterogeneity of the mechanisms involved. We also highlighted the contribution of non-membrane disrupting mechanisms for the inhibitory effects of lactoferricin peptides. These lactoferricin peptides revealed potential as anti-mycobacterial agents in combination with the conventional antibiotic ethambutol and the D-enantiomer of LFcin17-30 as a highly active molecule against *M. avium*.

The work described in this thesis may contribute to the future development of effective antimicrobial peptides for the treatment of mycobacterial as well as other infectious diseases.

Resumo

A descoberta revolucionária da penicilina por Alexander Fleming em 1928 continha a promessa de tratar e curar todas as doenças infeciosas. Efetivamente, nas décadas que se seguiram, os níveis de infeções bacterianas diminuíram, levando a importantes melhorias na qualidade da saúde pública. No entanto, nos dias de hoje, a resistência das bactérias aos antibióticos está a espalhar-se rapidamente, sendo considerada uma das maiores ameaças mundiais para a saúde pública, colocando em risco o tratamento de infeções. Para combater este fenómeno, novos fármacos têm de ser introduzidos na clínica, de preferência com paradigmas diferentes dos antibióticos convencionais, em que a evasão à resistência bacteriana seja o principal objetivo. Neste âmbito, péptidos antimicrobianos (PAM) têm sido extensivamente estudados como uma nova alternativa para o combate de doenças infeciosas. Estes péptidos estão presentes na natureza e em quase todos os seres vivos, caraterizando-se por serem ativos contra uma vasta gama de agentes patogénicos. O mecanismo de ação dos PAM consiste na destabilização da membrana, por diferentes processos que conduzem à morte celular, podendo também atuar em alvos intracelulares e por imunomodulação. Devido à natureza do principal alvo destes péptidos, a membrana citoplasmática, e à possibilidade de atuarem em alvos diferentes por diferentes mecanismos, em princípio a indução de resistência é menos provável para os PAM do que para os antibióticos convencionais.

O objetivo desta tese foi determinar o mecanismo de ação de duas famílias de PAM, nomeadamente híbridos da cecropina A-melitina e péptidos derivados da lactoferrina, e ainda avaliar o potencial de péptidos derivados da lactoferricina contra um patogénio intracelular e oportunista, o *Mycobacterium avium*.

A interação de CA(1-7)M(2-9), um híbrido da cecropina A-melitina, com membranas modelo de bactérias, compostas por fosfatidiletanolamina (PE) e fosfatidilglicerol (PG), foi analisada através de várias técnicas biofísicas, como difração de raios-X, calorimetria diferencial de varrimento, calorimetria isotérmica de titulação, dicroísmo circular e técnicas de microscopia. Os resultados mostram que o péptido interage fortemente com a superfície da membrana, ao nível das cabeças lipídicas, sem mostrar evidência de formação de poros com estas membranas. Os resultados obtidos indicam que o CA(1-7)M(2-9) induz extensa condensação da membrana por disrupção das vesículas, formando uma estrutura multilamelar (tipo “cebola”) em que os péptidos se encontram intercalados entre as bicamadas. Propomos assim, que o modelo da carpete é o que melhor descreve o mecanismo de ação do CA(1-7)M(2-9) com este modelo de membranas bacterianas, com rutura vesicular como estado final.

O mecanismo de ação de péptidos derivados da lactoferrina, LFcin17-30, LFampin265-284 e LFchimera foi estudado por difração de raios-X com membranas modelo de membranas de fungos, compostas por fosfatidilcolina (PC) e PG. Os resultados mostram que apesar dos três péptidos pertencerem à mesma família, atuam por mecanismos diferentes. LFcin17-30 tem um efeito moderado nas membranas, induzindo apenas segregação lipídica; LFampin265-284 induz a formação de uma fase cúbica micelar (Pm3n) que irá levar à disrupção da membrana; LFchimera leva à destruição da membrana através da formação de fases cúbicas bicontínuas (Im3m e Pn3m). É de realçar o excelente acordo destes resultados com os obtidos anteriormente para o efeito destes péptidos contra *Candida albicans*.

Lactoferricina, LFcin17-30, e suas variantes obtidas por substituições de aminoácidos específicos, foram testadas *in vitro* contra *Mycobacterium avium*. Os nossos resultados mostram que todos os péptidos são ativos contra *M. avium* a crescer em culturas líquidas, sendo que o enantiómero D da LFcin17-30 (D-LFcin17-30) e a variante com todas as lisinas substituídas por argininas (LFcin17-30 all R) foram os péptidos mais ativos. Todas as lactoferricinas estudadas induziram alterações na superfície e na ultra-estrutura das micobactérias, mas sem sinais evidentes de disrupção membranar, e por isso propomos que estes péptidos têm provavelmente um alvo intracelular. Curiosamente, quando usados contra *M. avium* a crescer dentro de macrófagos, apenas o D-LFcin17-30 teve uma atividade significativa contra este agente patogénico. A administração combinada das lactoferricinas com o antibiótico etambutol aumentou significativamente a atividade de todos os péptidos e do antibiótico sozinho, sem no entanto ultrapassar o efeito do D-LFcin17-30 sozinho. Outras experiências com vista à clarificação do mecanismo de ação deste péptido revelaram que este não co-localiza com a micobactéria dentro dos macrófagos, estando provavelmente a exercer a sua atividade através da modulação dos mecanismos de defesa antimicrobianos dos macrófagos.

Com os resultados obtidos neste trabalho, conseguimos contribuir para a elucidação dos mecanismos de ação pelos quais os PAM interagem com as membranas alvo, mostrando uma grande heterogeneidade nos mecanismos envolvidos. Destaca-se também a contribuição de mecanismos que não envolvem disrupção membranar para a atividade das lactoferricinas. Estes péptidos em particular revelaram ser potenciais agentes antimicobacterianos, em particular em combinação com o antibiótico etambutol. Entre os péptidos estudados é de realçar o enantiómero D da LFcin17-30, que se revelou altamente eficaz contra *M. avium*.

O trabalho descrito nesta tese pode contribuir para o futuro desenvolvimento de péptidos antimicrobianos adequados ao tratamento de infeções por micobactérias, bem como por outros agentes.

Thesis Organization

This thesis is organized into three parts, Introduction, Results and Final Remarks.

- **Part I** comprises the introduction to the theme of the thesis, developing the more relevant topics, including also the objectives of the work.

- **Part II** encompasses four chapters of results, presented in the form of original scientific articles. In all four chapters the author of this thesis made substantial contributions for the design, conception, analysis and data interpretation, particularly:

    - **Chapters 5, 7 and 8 –** All the presented data was obtained and analysed by the author of this thesis with the collaboration of the remaining authors;
    - **Chapter 6 –** Only the DSC and CD data were not obtained by the author. However their analysis and interpretation, as well as their integration into the discussion and overall conclusions were made by the author of this thesis with the collaboration of the remaining authors.

- **Part III** contains the final remarks and future perspectives of the work.

PART I. INTRODUCTION

CHAPTER 1. Antimicrobial Peptides

We face at present an alarming situation regarding antibiotic resistance and the emergence of multidrug-resistant “super bugs”. The treatment of these infections is increasingly prone to failure and costly, strongly contributing to the terrible economic burden of global public health worldwide. Aggravating the problem, antimicrobial drug development is not keeping pace with the appearance of resistant pathogens. In the last 40 years, only three new classes of antibiotics for human use where discovered, and one of them is limited to topical application (Fischbach and Walsh 2009, Bassetti *et al.* 2013). World Health Organization (WHO) reported in 2014 that antibiotic resistance is spreading rapidly throughout the world and putting at risk the treatment of common infections. For instance, the failure of the treatment for gonorrhoea using last resort drugs (third-generation cephalosporins) has been reported in several countries and extensively drug-resistant tuberculosis has been identified in 100 countries (WHO 2015a). Also, methicillin-resistant *Staphylococcus aureus* (MRSA) are responsible for a high percentage of hospital-acquired infections that are spreading outside the hospital zones (Spellberg and Shlaes 2014, WHO 2015a). Within Europe, Portugal has one of the highest incidences of MRSA, as well as vancomycin-resistant *Enterococcus faecium* and multi-drug resistant *Acinetobacter* (DGS 2014).

Considering all this, we must acknowledge that we are moving towards a post-antibiotic era, where new antimicrobial strategies must emerge. In this context, antimicrobial peptides (AMP) are a new potential alternative for fighting infectious diseases.

Antimicrobial peptides are a large group of compounds that exhibit antimicrobial activity towards several pathogens. They are produced by almost all living organisms, as a primitive and conserved part of their immune defence system (Ganz and Lehrer 1999). These peptides are multifunctional and act in concert with other immune mechanisms providing a first line of defence against invading organisms, having evolved in nature to protect their hosts against diverse pathogens, such as bacteria, fungi, protozoa, and virus, as well as cancer cells (Zasloff 2002, Wiesner and Vilcinskas 2010). AMP production can be constitutive or induced as a response to inflammation, infection or injury, depending on the organism, cell type and peptide. They can also be expressed systemically, or they can be localized in specific sites more frequently exposed to pathogens, such as the skin or mucosa, or in some blood cell types, such as neutrophils, eosinophils and platelets (Yeung *et al.* 2011, Mansour *et al.* 2014). Although their mechanism of action is a matter of debate, AMP can exhibit a wide range of activities that include disrupting the pathogens membrane, acting on internal targets, immunomodulation, among others (see chapter 1.3), increasing their efficacy and capacity to evade potential resistance mechanisms (Nguyen

et al. 2011). Due to their multifunctional roles in both innate and adaptive immunity (see chapter 1.4), antimicrobial peptides can also be called host defence peptides (for an extensive review see (Mansour *et al.* 2014)).

Since the discovery of AMP and their potential as antimicrobial drugs, intensive research has been made not only to discover new peptides and characterize them, but also to drive their clinical use. So far more than 2600 antimicrobial peptides have been described in The Antimicrobial Peptide Database – APD (http://aps.unmc.edu/AP/main.php). Their described activities are equally vast, including antibacterial, antiviral, antifungal, antiparasitic, anticancer, antiprotist, insecticidal, spermicidal, chemotactic, wound healing, antioxidant and protease inhibitors (Wang *et al.* 2009).

1.1. Structural characteristics

Antimicrobial peptides vary widely in many aspects, such as length, sequence, structure, activity and source. As a result of such diversity, there is no universal target or mechanism of action for this class of compounds. Even so, membranes are believed to be the main target for most peptides. AMP are classified as small peptides (<50 amino acids), the majority of which have a positive charge at neutral pH due to the presence of arginine and lysine residues, and about 50% of hydrophobic residues. Their cationic character allows them to interact more easily with negatively charged membranes, such as prokaryotic membranes, than with zwitterionic membranes, as is the case of animal cells (membrane selectivity will be discussed later in more detail, see chapter 1.2) (Teixeira *et al.* 2012). When in solution, AMP usually have a random structure; however, when in contact with membranes they adopt an amphipathic structure where hydrophobic and cationic residues will segregate into different faces. This separation is essential for their mechanism of action as the positively charged face will establish the first contact with the membrane through electrostatic interactions whereas the non-polar face will interact with the lipid acyl chains, allowing the peptide to insert into the membrane through hydrophobic and van der Walls interactions (Hancock and Chapple 1999, Teixeira *et al.* 2012). Although the structural characteristics just mentioned are known to be important, their correlation with antimicrobial activity is not simple. Usually the increase in the number of positive residues correlates with an increase in the antibacterial activity, but above a certain threshold, the higher cationicity will result in a higher haemolytic activity and consequent toxicity for the host, with no improvement in the antibacterial activity (Bessalle *et al.* 1992, Giangaspero *et al.* 2001, Jiang *et al.* 2008). The same occurs with the hydrophobicity. The increased number of hydrophobic residues, which leads to large hydrophobic surfaces, usually

contributes to higher toxicity towards host cells, with no improvement in the antimicrobial activity (Shin *et al.* 2001, Kondejewski *et al.* 2002, Jiang *et al.* 2008). The same could be described for the length, amino acid composition, and secondary structure. Therefore, in a diverse and wide group of compounds such as antimicrobial peptides, there are no universal characteristics that guarantee a good antimicrobial peptide with high and selective activity.

Due to their diversity, classification of AMP is not trivial. Most authors classify them based on their secondary structure, but it could also be based on their origin.

The most common classification based on the secondary structure divides AMP into three groups – alpha-helical peptides, beta-sheet peptides and extended peptides. **Alpha-helical peptides** are the largest group, the most studied peptides being the cecropins from the cecropia moth, melittin from the bee venom toxin, magainins expressed in the skin and intestine of frogs and cathelicidins present in mammals (Teixeira *et al.* 2012). **Beta-sheet peptides** contain a defined number of beta-strands with few or no helical domains. This structure is usually stabilized by the presence of disulphide bonds, as in the case of lactoferricin obtained from lactoferrin and present in mammals, protegrin from pigs, and defensins, present in several vertebrates (Nguyen *et al.* 2011, Teixeira *et al.* 2012). The last group of AMP is the **extended peptides**. These peptides do not fold into regular secondary structures and are composed of a high number of certain amino acids, like histidine (histatins), tryptophan (indolicidins) and arginine and proline (PR-39) (Nguyen *et al.* 2011).

1.2. Selective toxicity

Independently of how AMP exert their activity, they will interact with the pathogen cellular membrane but also with the host membranes. This interaction must be as selective as possible to prevent toxic effects to the host cells. Melittin, from the bee venom, was one of the first described membrane-active peptides (Habermann 1972), but it is well known for its haemolytic properties, which prevented its clinical use. However, it remains until today one of the well described and characterized antimicrobial peptides. In the evaluation of the activity of AMP, the cytotoxicity of these peptides towards mammalian cells should always be addressed. There are many different cytotoxicity assays that can be performed, but their outcome strongly depends on many factors such as the origin and life storage of the mammalian cells, the peptide-to-cell ratio, the medium used, and therefore the results must be carefully analysed (van 't Hof *et al.* 2001). Based on the results of cytotoxicity assays together with the antimicrobial activity of AMP, the selectivity index, defined as the

ratio between cytotoxic activity and antimicrobial activity, can be determined, being a useful tool to predict the potential of a given AMP as a therapeutic agent.

One of the major factors underlying AMP selectivity is the membrane lipid composition, which varies considerably between eukaryotic and prokaryotic cells (Teixeira *et al.* 2012). Cytoplasmic membranes of mammalian cells are mostly constituted by phospholipids and cholesterol. Phospholipids are asymmetrically distributed between the inner and the outer leaflet of the bilayer exposing predominately zwitterionic phosphatidylcholine (PC) and sphingomyelin to the extracellular side. On the other hand, bacterial cytoplasmic membranes do not have cholesterol and are mainly composed of zwitterionic phosphatidylethanolamine (PE) and negatively charged phosphatidylglycerol (PG) and cardiolipin, conferring an overall negative charge to the outer side of the cytoplasmic membrane (Lohner and Blondelle 2005, Lohner 2009, Teixeira *et al.* 2012). There are also differences in the membrane potential, which is less negative in eukaryotes (-15 mV) than in prokaryotes (-140 mV) (van 't Hof *et al.* 2001, Steinstraesser *et al.* 2011). Since one of the main principles of peptide activity is thought to be electrostatic interaction with membranes, the higher amount of negatively charged lipids (Teixeira *et al.* 2012), a higher negative electrical potential (van 't Hof *et al.* 2001, Steinstraesser *et al.* 2011) and the lack of sterols like cholesterol (Benachir *et al.* 1997, Raghuraman and Chattopadhyay 2004, Sood and Kinnunen 2008) turns bacterial membranes into a preferred target for AMP. Nonetheless, it should be noted that in the case of bacteria, before reaching the cytoplasmic membrane, the peptides have to overcome other barriers. In the case of Gram-positive bacteria, a thick peptidoglycan layer embedded with teichoic and lipoteichoic acids (which are negatively charged) is present around the cell. For Gram-negative bacteria the cell wall consists of an outer lipid membrane layer, with a unique and highly asymmetrical composition (negatively charged lipopolysaccharides are located in the outer leaflet and phospholipids are confined to the inner leaflet) and a layer of peptidoglycan (much thinner than that of Gram-positive bacteria) between the inner and the outer membranes (Cabeen and Jacobs-Wagner 2005, Lohner and Blondelle 2005, Lohner 2009). Therefore in normal conditions the overall charge of a bacterial cell wall is negative, increasing the chances of interaction with AMP over mammalian cells.

Antimicrobial peptides can also kill eukaryotic pathogens, such as fungi and protozoa. The specificity here also relies on charge, since these pathogens have a higher percentage of anionic phospholipids in the outer leaflet than mammalian cells (Wassef *et al.* 1985, Cintra *et al.* 1986, Seabra *et al.* 2004, Wanderley *et al.* 2006). The same happens for cancer cells. Although they are mammalian cells, their neoplastic transformation introduces significant changes in the cytoplasmic membrane, such as the exposure of

phosphatidylserine (negatively charged) that is usually confined to the inner leaflet, the higher expression of O-glycosylated mucins, sialic acids linked to glycoproteins and glycolipids, and heparin sulphates, all these leading to an overall negative charge, rendering them more susceptibility to AMP activity. Also, these cells have increased number of microvilli, which leads to increase in cell surface area exposed to AMP. In some cases, cancer cells also have lower levels of cholesterol increasing their fluidity and therefore their susceptibility to AMP's action (Riedl *et al.* 2011, Teixeira *et al.* 2012, Gaspar *et al.* 2013).

1.3. Mechanisms of action

The mechanism of action of antimicrobial peptides is not fully understood but properties such as the secondary structure, overall charge and hydrophobicity, play important roles in their interaction with pathogen membranes. Other parameters also have to be considered, for instance, the membrane lipid composition, the peptide-to-lipid molar ratio, and environmental conditions like ionic strength and pH (Lohner and Blondelle 2005). Due to the high diversity of AMP and their properties there is no universal mechanism for their action. However, there are some proposed mechanisms providing possible ways to understand how the peptides exert their antimicrobial activity. Overall these mechanisms rely on the same steps: **adsorption** of AMP onto the membrane due to electrostatic interactions between the cationic peptides and the head groups of anionic phospholipids; **conformational change** upon membrane contact; **attachment** and **insertion** into the membrane as the concentration of peptide increases; **membrane permeability** that could lead to cell death or not; and finally, translocation to the cytoplasm and possible **intracellular killing** (Brogden 2005).

According to the **barrel-stave model** (figure 1), peptides large enough (~ 22 amino acids) form transmembrane aqueous channels/pores by inserting into the hydrophobic core perpendicularly to the membrane plane where the hydrophobic region of the peptide is aligned with the acyl chains of the phospholipids while the hydrophilic peptide regions form the inner surface of the pore channel (figure 1). The continuous recruitment of peptides to the membrane increases the pore size leading to leakage of the cells contents, membrane depolarization and thereby cell death (Nguyen *et al.* 2011). The peptides arrangement in the membrane causes high repulsion due to their charges, and this can culminate in the disintegration of the pore. This model is only possible for peptides with not too high charge and high hydrophobic, and it is believed that the number of peptides acting by this mechanism is low. An example is alamethicin from the fungus *Trichoderma*

viridis, perforin, produced by cytotoxic T lymphocytes and NK cells, and complement component C9 (Wiesner and Vilcinskas 2010).

The **carpet model** (figure 1) proposes that the membrane surface is covered by the peptides, parallel aligned to the bilayer surface, in a “carpet-like” manner, diminishing the fluidity of the membrane. When the concentration of the peptide reaches a threshold value, the integrity of the membrane is lost due to the disruption of the bilayer curvature, that can happen through transient toroidal pores or other peptide/lipid structures, leading eventually to membrane micellization and cell death (figure 1) (Teixeira *et al.* 2012).

The formation of **toroidal or wormhole pores** (figure 1) can be seen as representing one of the possible final stages of the previous carpet model, where the formation of pores leads to disruption of the membranes. In fact, these two models have been unified in the so-called **“Shai-Matzusaki-Huang” model** that proposes that peptides bind parallel to the membrane with the apolar amino acids penetrating partly into the hydrophobic core, while the cationic residues interact with the head groups of anionic phospholipids, inducing membrane thinning and a high curvature strain. To release this strain the orientation of the peptides changes from parallel to perpendicular, causing bending of the membrane interface towards the hydrophobic interior, maintaining the contact between the peptides and the charged head groups from the phospholipids. These events lead to the formation of water-filled toroidal pores composed of the peptides and the lipid head groups (figure 1). Upon disintegration of the pores, some peptides can be translocated to the inner leaflet of the membranes reaching the cytoplasm or the membrane can be disrupted due to depolarization or micellization, resulting in cell death (Nicolas 2009, Rivas *et al.* 2009).

Other mechanisms of action have recently been suggested that do not imply a membranolytic activity. These do not necessarily exclude each other, or even the models explained above. In the **aggregate channel model**, the peptides insert into the membrane and cluster into short-lived transmembrane aggregates which allows not only the peptides to cross the membrane, but also the leakage of ions and other molecules (Teixeira *et al.* 2012). **Lipid segregation** is the formation of lipid-peptide domains as a result of lateral segregation of anionic and zwitterionic lipids induced by the presence of the positively charged peptide (figure 1). This can cause small leakage of intracellular contents, depolarization due to a dissipation of the membrane potential, and also membrane destabilization due to changes in the curvature strain. These will affect the function of membrane proteins and biological processes, with harmful consequences for the cell (Nguyen *et al.* 2011, Teixeira *et al.* 2012). In the **sinking raft model**, the peptides induce a mass imbalance between the two leaflets due to preferential binding to some

lipid domains. As the curvature of the membrane increases, the peptides sink into the bilayer forming transient pores that allow not only the peptide translocation to the cytosol but also the leakage of intracellular metabolites (Teixeira *et al.* 2012). In the **electroporation model**, the interaction between peptide and membrane creates an electric potential difference in the membrane. When this difference reaches a certain threshold, pores can be formed by molecular electroporation, allowing the peptides to translocate (figure 1) (Nguyen *et al.* 2011, Teixeira *et al.* 2012). Another model predicts the **formation of non-lamellar phase structures**, such as hexagonal and cubic phases formed by membrane lipids (figures 1 and 6 – see chapter 2), which could induce membrane disruption or could affect the establishment of lipid domains in the cellular membrane. These domains are important for many biological processes such endocytosis (induced by lipid rafts) and for the activity of membrane proteins, thus disturbing them could culminate in the impairment of membrane function and eventually cell death (Luzzati 1997, Lohner 2009, Haney *et al.* 2010, Teixeira *et al.* 2012).

Whatever the mechanism is, peptide interaction with membranes can induce cell death by the dissipation of transmembrane electrochemical ion gradients, loss of metabolites, lipid asymmetry and eventually lysis of the cell (Wiesner and Vilcinskas 2010). However, an increasing amount of research has shown that membrane permeabilization alone may not be sufficient to cause cell death. Some AMP can be translocated to the cytoplasm, with or without permeabilizing the cytoplasmic membrane, and bind to DNA, RNA and proteins. This interaction can culminate in inhibition of several cellular processes such as cell wall synthesis, protein synthesis, enzymatic activity and even membrane septum formation, which would lead to cell death (Brogden 2005, Li *et al.* 2012). Buforin is an example of a non-lytic peptide that although having high antimicrobial activity this does not correlate with lysis of the bacterial membrane. Instead the peptide translocates efficiently to the cytoplasm, probably through the formation of short-lived toroidal pores, enabling this peptide to enter the cell and act on intracellular targets (Kobayashi *et al.* 2000, Kobayashi *et al.* 2004, Henriques *et al.* 2006).

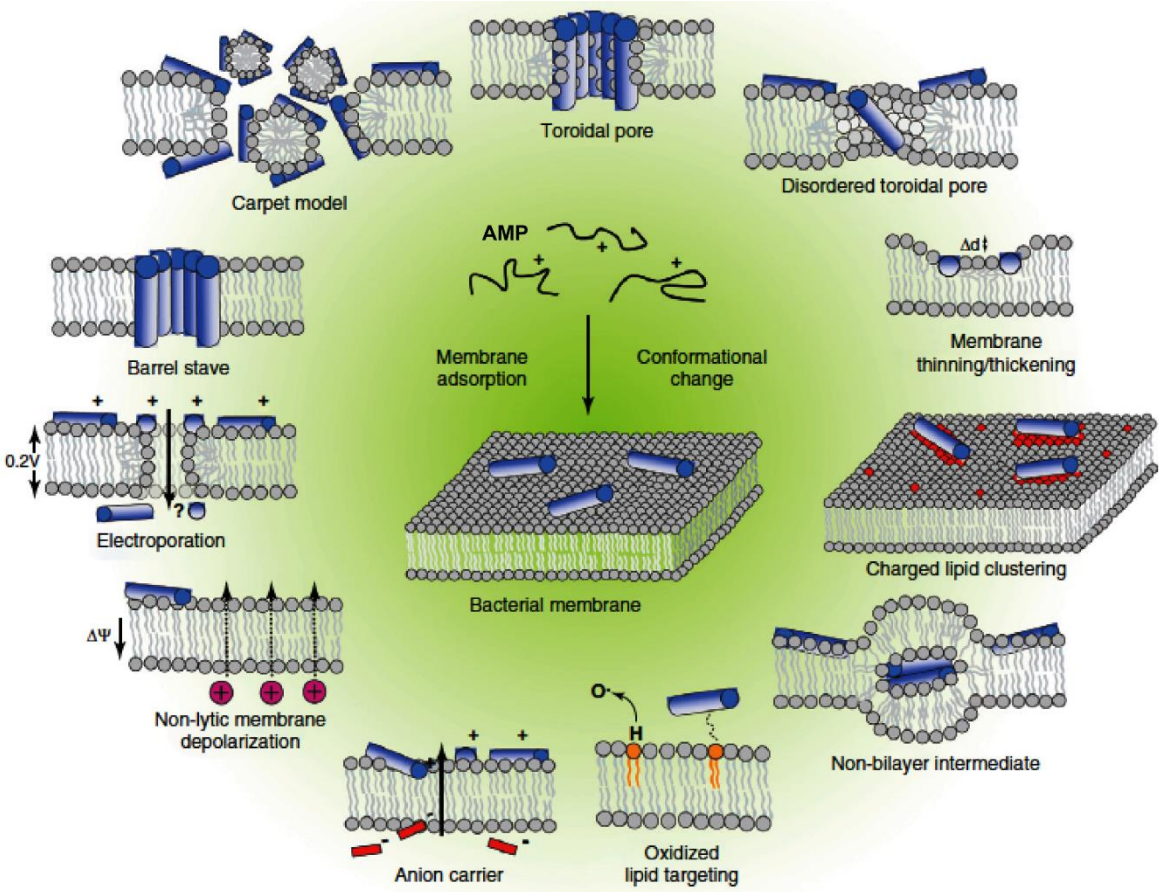

Figure 1– Proposed mechanisms of action for AMP. Illustration of some of the proposed events/mechanisms occurring at the cytoplasmic membrane after an initial interaction of antimicrobial peptides with the membranes (adapted from: (Nguyen *et al.* 2011)).

1.4. Host Defence Peptides

More recently, antimicrobial peptides have been increasingly recognized for their multifunctional roles in innate and adaptive immunity, being this effect in some cases more significant than their direct antimicrobial activity. The combination of these different but complementary functions is essential for the efficient control of infections in the host organism. Thus, in response to an infection, antimicrobial peptides can promote bacterial clearance through direct killing but also through the establishment of immune cell circuits, leading some authors to re-name them “host defence peptides” (HDP) (Auvynet and Rosenstein 2009, Guaní-Guerra *et al.* 2010, Yeung *et al.* 2011).

In humans, the two major classes of HDP are the defensins and the cathelicidins. These peptides can be found in neutrophils, monocytes, mast cells, epithelial cells, among others. They can be expressed constitutively, as beta-defensin 1 (HBD1) in keratinocytes, or

induced by an inflammatory stimulus like beta-defensin 2 (HBD2) that is present in epithelial cells, and is induced by lipopolysaccharide (LPS) and tumour necrosis factor alpha (TNF-alpha) (Arnett and Seveau 2011, Mansour *et al.* 2014). Their immunomodulatory activities are vast, including, recruitment of immune cells; inhibition of the production of pro-inflammatory cytokines such as TNF-alpha, IL-6 and IL-8, and at the same time enhancing anti-inflammatory cytokines (IL-10 and chemokines); induction of cellular differentiation and activation; modulation of adaptive immunity by recruiting T cells; regulation of several cellular processes such as autophagy, apoptosis and pyroptosis, and also the promotion of wound healing (Mansour *et al.* 2014).

The importance of HDP for the health of the host was demonstrated by studies where their enhanced expression increased resistance to bacterial infections in mice (Bals *et al.* 1999, Salzman *et al.* 2003). On the other hand, mice lacking endogenous cathelicidin (CRAMP) or beta-defensin were more susceptible to streptococcal infections being this effect reversed by administration of exogenous cathelicidin (Nizet *et al.* 2001, Fukumoto *et al.* 2005). Moreover, and as a consequence of the immunomodulatory activities, HDP are also involved in autoimmunity. Increased expression of these peptides is associated with different inflammatory conditions such as cystic fibrosis, psoriasis, and others (Guaní-Guerra *et al.* 2010). On the other hand, lack or decreased amounts of HDP is related to increased susceptibility to infections in diseases such as morbus Kostmann (Putsep *et al.* 2002).

1.5. Resistance to AMP

Induction of resistance is thought to be less likely for AMP when compared to conventional antibiotics. This is mostly due to the fast kinetics of the antimicrobial process, to the possibility of acting on multiple targets and to the fact that their main molecular target – the membrane- is highly conserved and essential for pathogen survival. Although in principle acquiring resistance to AMP is more difficult, it has been pointed that it might have more severe consequences if it led to cross-resistance to innate human antimicrobial peptides (host defence peptides) (Samuelsen *et al.* 2005, Hancock and Sahl 2006, Habets and Brockhurst 2012). Some studies have already pointed out the existence of resistance to AMP, while others suggest some possible mechanisms, based on the documented mechanisms of resistance to peptide antibiotics such as polymyxin B and daptomycin, which have a similar mechanism of action as AMP, acting on the cell membrane (Maria-Neto *et al.* 2015).

Since the basis of antimicrobial activity is an initial electrostatic interaction between the cationic peptides and the pathogen, the first resistance mechanisms which could be predicted would be a reduction of the negative charge at the pathogen surface. In fact, electrostatic repulsion of AMP can arise from several modifications of the bacterial surface, some of which were already documented, such as: the addition of the positively charged lysine to phosphatidylglycerol (lysyl-PG) by staphylococci and clostridia, the incorporation of aminoarabinose and ethanolamine on the lipid A of LPS in some Gram-negative bacteria, or L-rhamnosylation and esterification of teichoic acids by D-alanine in Gram positives (Bauer and Shafer 2015, Carvalho *et al.* 2015, Joo and Otto 2015, LaRock and Nizet 2015, Maria-Neto *et al.* 2015, Nuri *et al.* 2015).

It has also been described that bacteria can induce the production of secreted or cell-surface proteins that irreversibly bind or cleave AMP and glycopolymeric matrices that trap the peptides preventing their access to the bacterial cytoplasmic membrane. Additionally, some of the efflux pumps involved in antibiotic expulsion have been shown to be able to export AMP (Bauer and Shafer 2015, Joo and Otto 2015, LaRock and Nizet 2015, Matamouros and Miller 2015). Increased resistance can also be achieved by changing membrane fluidity by modification of fatty acid acylation pattern of lipid A of LPS (Koprivnjak and Peschel 2011, Bauer and Shafer 2015, LaRock and Nizet 2015, Nuri *et al.* 2015). Another form of bacterial resistance is the formation of biofilms, since, usually, the susceptibility to AMP of bacterial biofilm is lower than that of bacteria in the planktonic state (Nuri *et al.* 2015).

It has been recently described that bacteria can sense the presence of AMP and activate resistance mechanisms, through either two-components or three-components sensor-transducer response systems (Joo and Otto 2015, Matamouros and Miller 2015). The activation of these sensor systems will result in the changes on the above mentioned surface charge and rigidity, cell wall and membrane thickness or membrane fluidity (Nuri *et al.* 2015). It is thought that these systems evolved to guarantee that such alterations, which often come with a high energy burden or loss of fitness to the bacteria are activated only when needed.

1.6. AMP in the clinic: Will it be possible?

Since the discovery of the potential of antimicrobial peptides as new therapies to fight infectious diseases, there has been a tremendous effort to try to get these peptides into the clinic. Cationic peptides such as polymyxin B and gramicidin S have been used for a long time in the clinic as topical agents, and the lantibiotic nisin, produced by fermentation

using *Lactococcus lactis* is used as an antimicrobial food additive (Hancock and Sahl 2006).

Several AMP are in different stages of clinical trials for a variety of applications such as diabetic foot ulcers, prevention of catheter-related infections, acne therapy, among others. However, their success has been limited. There are some AMP that have reached the last stages of clinical trials but, so far, none has been approved (Steinstraesser *et al.* 2011, Seo *et al.* 2012). As drug candidates, AMP present some disadvantages due to their peptidic nature, including reduced activity in the presence of salts and divalent cations, susceptibility to pH changes, proteases and other plasma components' activity, resulting in low metabolic stability and bioavailability, and reduced *in vivo* half-lives (Rotem and Mor 2009). The route of administration is also a problem. If administered orally, they most probably would be degraded upon encounter with the enzymes from the digestive tract, and if injected, besides the susceptibility to the proteases in the blood, they could trigger immune responses that neutralize the active component or induce allergic reactions. Other safety considerations raise many concerns. They can cross-react with receptors for neuropeptides and peptide hormones, and the rapid degradation of AMP could lead to unwanted levels of amino acids for which some patients are sensitive, such as glutamate (Chinese restaurant syndrome) and phenylalanine (phenylketonuria) (van 't Hof *et al.* 2001). The high cost of production associated with peptide synthesis is another major drawback in the clinical application of these peptides.

All the above factors contribute to the current limitations of the use of AMP as topical drugs for the treatment of skin and wound infections (Wiesner and Vilcinskas 2010).

Different approaches have been adopted to try to overcome these problems. Several classes of modified antimicrobial peptides have appeared, including AMP mimetics, hybrid AMP, AMP congeners, stabilized AMP, AMP conjugates and immobilized AMP (Brogden and Brogden 2011). All these compounds derive from natural AMP as the result of modifications to the peptide composition, or are molecules that imitate their structure and function. Some of the strategies employed consist of i) the use of D-amino acids (rather than L-amino acids) which are resistant to proteases but have higher costs when compared with L-amino acids; ii) the use of nonpeptidic backbones (peptidomimetics); iii) conjugation with a specific antibody or receptor, and micelles or liposomes, for improved stability and "targeted" delivery; iv) pro-drug molecules, among others (Hancock and Sahl 2006, Brogden and Brogden 2011).

In the work described in this thesis, two classes of AMP – cecropin A-melittin hybrids and lactoferrin peptides – were studied for their mechanisms of action and the potential of

modifications that can result in improved clinical potential. These two classes of peptides will thus be described here in more detail.

1.7. Cecropin A-melittin peptides

Cecropin A, with 37 amino acids, was the first antimicrobial peptide from an insect to be reported (Steiner *et al.* 1981). It is active against Gram-negative and Gram-positive bacteria (Steiner *et al.* 1981, Andreu *et al.* 1983, Boman and Hultmark 1987, Andreu *et al.* 1992), forms an amphipathic α-helix when in contact with lipid membranes (Steiner 1982, Silvestro and Axelsen 2000) and acts by forming voltage-dependent channels that collapse the ionic gradients (Diaz-Achirica *et al.* 1994).

Melittin, from the bee venom toxin, has a variety of toxic properties namely a high haemolytic activity (Mackler and Kreil 1977). This peptide adopts a α-helical conformation aggregating into tetramers (Vogel 1981, Lafleur *et al.* 1991), and is used as a model of a cytolytic peptide to monitor lipid–protein interactions using a variety of biophysical techniques (Raghuraman and Chattopadhyay 2007).

These two peptides, cecropin A and melittin, are composed of hydrophilic and hydrophobic domains separated by a flexible hinge region, adopting α-helix – hinge – α-helix conformation. The hydrophobic region of cecropin A is localized on its C-terminal whereas in melittin it is localized on the N-terminal (Merrifield *et al.* 1982, Holak *et al.* 1988, Fink *et al.* 1989, Raghuraman and Chattopadhyay 2007). In an attempt to obtain antimicrobial peptides with strong bactericidal activity and low haemolytic properties, Boman, *et al.* in 1989 synthesized for the first time **cecropin A-melittin hybrids**, and they found that these hybrids had better antimicrobial properties than the parental compounds (Boman *et al.* 1989). In particular, a hybrid formed by the first 8 amino acids of the cationic region of cecropin A and the first 18 amino acids of the hydrophobic and non-haemolytic region of melittin (CA(1-8)M(1-18)) exhibited a wider spectrum of antimicrobial activity and improved potency in comparison to cecropin A, without the cytotoxic effects of melittin (Wade *et al.* 1990). In the continuation of this work, Andreu *et al.* in 1992 synthesized shorter hybrids that retained significant activity when compared to the larger versions of the hybrid, especially **CA(1-7)M(2-9)** (Andreu *et al.* 1992).

The mechanism of action of these hybrids is thought to be membrane disruption due to the formation of toroidal pores and/or disintegration of the membrane due to a detergent-like action (Andreu *et al.* 1992, Diaz-Achirica *et al.* 1994, Juvvadi *et al.* 1996, Diaz-Achirica *et al.* 1998, Abrunhosa *et al.* 2005, Sato and Feix 2006, Pistolesi *et al.* 2007, Bastos *et al.* 2008, Ferre *et al.* 2009, Milani *et al.* 2009, Teixeira *et al.* 2010). Supporting

this is the fact that the antimicrobial activity of the hybrid peptides composed of all D-amino acids was equivalent to that of the hybrids with L-amino acids. This strongly indicates that the peptides do not act by interacting with chiral receptors in the lysis and killing of the pathogens, but instead follow a non-specific membranolytic way of action (Wade *et al.* 1990, Merrifield *et al.* 1995, Diaz-Achirica *et al.* 1998, Arias *et al.* 2006). Cecropin A-melittin hybrids are active against several different Gram-positive and Gram-negative bacteria, and protozoan *in vitro* (Andreu *et al.* 1992, Piers *et al.* 1994, Chicharro *et al.* 2001, Rodriguez-Hernandez *et al.* 2006, Fernandez-Reyes *et al.* 2010), can synergize with antibiotics for the control of MRSA infections (Giacometti *et al.* 2004, Mataraci and Dosler 2012), and have proven efficacy on *in vivo* model of dog leishmaniasis (Alberola *et al.* 2004) and in an experimental pseudomonas keratitis model in rabbits (Nos-Barbera *et al.* 1997). Interestingly, they strongly interact with LPS protecting from induced lethal endotoxic shock *in vivo* (Gough *et al.* 1996). These hybrids can also be involved in the regulation of the host defence. Arias *et al.* (Arias *et al.* 2006) showed that CA(1-8)M(1-18) was capable of activating murine macrophages by inducing the expression of NOS2 due to unspecific but limited membrane permeation. More recently, Salomone *et al*., constructed a chimeric peptide between a cecropin A-melittin derivative and an arginine-rich Tat peptide, from the HIV-1 Tat protein, successfully obtaining a cell-penetrating peptide that can be used as a tool for gene-delivery applications (Salomone *et al.* 2012, Salomone *et al.* 2013).

1.8. Lactoferrin peptides

Lactoferrin (LF) is a mammalian iron-binding glycoprotein of 80 kDa that belongs to the transferrin family (Brock 2002). Contrary to transferrin, that appears primarily in the bloodstream delivering iron to the cells, lactoferrin is mostly found in exocrine secretions, like milk, tear fluid and seminal plasma, and in neutrophil granules playing an important role in maternal and innate immunity (Wiesner and Vilcinskas 2010). This is a multifunctional protein that has antibacterial, antiviral, antifungal and antiparasitic activities and can protect against cancer development and metastasis owing to its immunomodulatory potential (Brock 2002, Wiesner and Vilcinskas 2010). The antibacterial activity of lactoferrin was first thought to be due only to the sequestration of iron, an essential nutrient, from bacteria (Jenssen and Hancock 2009). Now, it is known that allied to that, the existence of particular domains, such as the highly cationic N1 terminal domain, where lactoferricin and lactoferrampin can be found, are crucial for the antimicrobial activities of lactoferrin (Tomita *et al.* 1991).

Lactoferricin is obtained by pepsin digestion of lactoferrin (Tomita *et al.* 1991, Bellamy *et al.* 1992b, Kuwata *et al.* 1998) and has been extensively studied (Wakabayashi *et al.* 2003, Gifford *et al.* 2005). The bovine peptide is constituted by 25 amino acids, corresponding to the amino acids 17-41 in the native protein (bovine lactoferrin), forming a looped structure with a disulphide bond between two cysteine residues (Bellamy *et al.* 1992a). The antimicrobial spectrum of activity of lactoferricin ranges from several Gram-negative to Gram-positive bacteria (Bellamy *et al.* 1992a, Bellamy *et al.* 1992b), fungi (Bellamy *et al.* 1994), protozoan and viruses (Gifford *et al.* 2005). Lactoferricin has been shown to have antitumor effects, like inhibition of tumour metastasis, suppression of tumour-induced angiogenesis and significant reduction of solid tumour (fibrosarcomas, melanomas, colon carcinomas) size in mice, without affecting erythrocytes or fibroblasts (Yoo *et al.* 1997b, Eliassen *et al.* 2002). This peptide can also have immunomodulatory properties, playing a role in the innate and adaptive immune system, including the induction of apoptosis in several cancer cell lines without harming normal mammalian cells (Yoo *et al.* 1997a, Mader *et al.* 2005, Furlong *et al.* 2006, Mader *et al.* 2007, Furlong *et al.* 2010, Pan *et al.* 2013), and the inhibition of septic shock by binding to endotoxins (Yamauchi *et al.* 1993).

Groenink, *et al.* in 1999 synthesized shorter peptides with sequences homologous to the N-terminal domain of bovine and human lactoferricin, and found that among the peptides tested, bovine lactoferricin containing amino acids 17-30 (**LFcin17-30**) had the highest number of positively charged residues and the highest antimicrobial activity against both Gram-positive and Gram-negative bacteria (Groenink *et al.* 1999). Recent studies showed that this peptide is active against different pathogens such as *Escherichia coli*, *Staphylococcus aureus*, *Candida albicans*, *Leishmania*, among others (van der Kraan *et al.* 2005b, Flores-Villasenor *et al.* 2010, Lopez-Soto *et al.* 2010, Silva *et al.* 2012), and can potentiate the effect of classical antimicrobial drugs aiming the use of low doses and therefore low toxicity (Leon-Sicairos *et al.* 2006, Sanchez-Gomez *et al.* 2011).

Another peptide in the N1 domain of bovine lactoferrin was identified by the group of Jan G. Bolscher, namely **lactoferrampin** containing the amino acids 268-284 (LFampin268-284). This peptide exhibited antimicrobial activity against a broad range of pathogens, especially against *Candida albicans* and several bacteria (van der Kraan *et al.* 2004). Systematic studies, using the initial sequence of lactoferrampin to obtain other peptides by truncation and or extension, have shown that lactoferrampin 265-284 (**LFampin265-284**) was the shortest and most active peptide, in particular against *Candida albicans* (van der Kraan *et al.* 2005a, van der Kraan *et al.* 2005b). The three extra amino acids (Aspartic acid-Leucine-Isoleucine) did not confer any additional positive charge (one of the most important characteristics of AMP) since the first is negatively

charged and the other two are uncharged. Instead, this N-terminal sequence endowed lactoferrampin with a high tendency to adopt a more stable amphipathic α-helix, enhancing in this way its microbicidal activity (van der Kraan *et al.* 2005a, van der Kraan *et al.* 2006, Haney *et al.* 2007, Adao *et al.* 2011, Haney *et al.* 2012a).

Lactoferricin and lactoferrampin are spatially close in lactoferrin (figure 2), making it plausible that they cooperate in many of the beneficial properties of this protein. To test if these peptides would form a functional unit, a chimeric peptide (**LFchimera**) containing **LFcin17-30** and **LFampin265-284** was synthesized by Jan G. Bolscher (Bolscher *et al.* 2009b). To try to mimic the spatial topology of these two peptides in lactoferrin, LFcin17-30 and LFampin265-284 are coupled by their C-terminals to the α- and ε-amino groups, respectively, of an additional lysine, leaving the two N-terminals as free ends (figure 2) (Haney *et al.* 2012b). **LFchimera** displays a strong activity against a wide variety of pathogens such as *Escherichia coli*, *Pseudomonas aeruginosa, Vibrio parahaemolyticus, Staphylococcus aureus, Entamoeba histolytica, Candida albicans, Leishmania pifanoi*, *Burkholderia* and *Streptococcus pneumonia*, which is maintained under different physiological conditions (including high ionic strength and rich growth medium) (Bolscher *et al.* 2009b, Leon-Sicairos *et al.* 2009, Flores-Villasenor *et al.* 2010, Lopez-Soto *et al.* 2010, Bolscher *et al.* 2012, Flores-Villasenor *et al.* 2012a, Silva *et al.* 2012, Kanthawong *et al.* 2014, Leon-Sicairos *et al.* 2014). Additionally, it was recently found that LFchimera can protect mice against a lethal infection with enterohemorrhagic *E. coli* (Flores-Villasenor *et al.* 2012b).

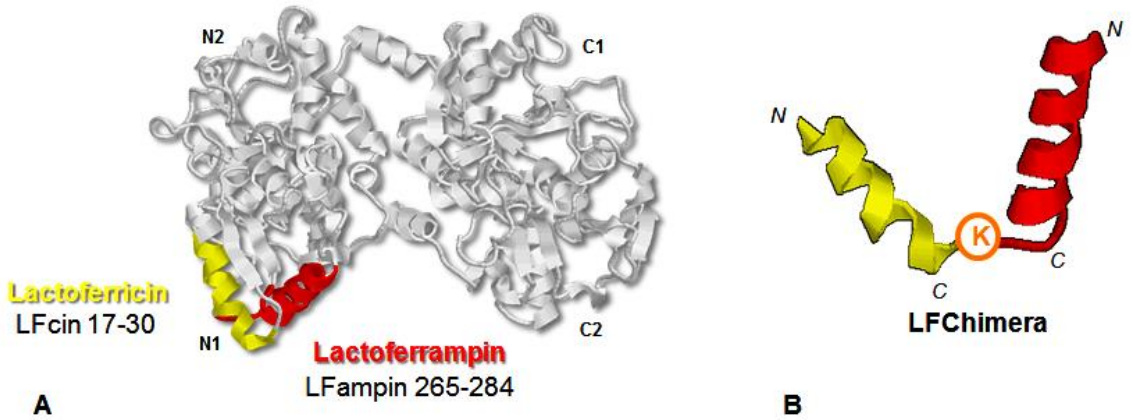

Figure 2 – Lactoferrin peptides. A) Ribbon diagram of bovine lactoferrin with LFcin17-30 (yellow) and LFampin265-284 (red). **B)** Designed of LFchimera composed by LFcin17-30 and LFampin265-284 coupled by an additional lysine (K) (adapted from: (Bolscher *et al.* 2009b)).

CHAPTER 2. Antimicrobial peptides and model membranes

The mechanism of action of AMP is complex and not entirely understood. Due to the high diversity of AMP it is now recognized that there is no universal mechanism for their action. Further, they can act in multiple ways, making it challenging to unravel all the molecular events resulting from their action. However, experimental data obtained so far clearly indicates that biological membranes are the main target of AMP. The use of liposomes, aimed at mimicking the biological membrane, allows the study of the activity of AMP in a highly controlled way, allowing easy modulation of lipid composition, and the informative use of numerous biophysical techniques. Studies on liposomes have been crucial to understand AMP modes of action and help a more rational design of AMP. In the work described in this thesis, lipid model membranes were used to study their interaction with AMP using several biophysical techniques, which are briefly presented below.

2.1. Lipid model membranes as a tool to study AMP activity

Biological membranes are mainly composed of a lipid matrix that anchors all other components, like proteins, glycoproteins and glycolipids that perform crucial functions in the life of the cell. Phospholipids, the building blocks of the cellular membranes, are amphiphilic molecules composed of a hydrophilic head group and a hydrophobic tail that consist of hydrocarbon chains. The lipid composition varies among different organisms and even among cell types of the same organism. The phospholipid distribution between the inner and outer leaflets of the lipid bilayer is asymmetrical, and some lipids are more common in one leaflet (Pozo Navas *et al.* 2005). The view of lipid molecules as only a scaffold for proteins is rapidly changing towards dynamic and active molecules, involved in various biological processes that are crucial to the life of the cell. In this context, the physical properties of membranes (such as fluidity and shape) are also increasingly recognized as fundamental for the proper functioning of the cell (Luzzati 1997, Haney *et al.* 2010).

Lipid organization upon contact with water is highly variable, depending on their intrinsic properties, on the composition of the medium (pH, ionic strength, additives, etc.), as well as on temperature and water content. The use of X-ray diffraction and other biophysical techniques reveals that lipids can assume different conformations or phases when in contact with water. For several lipids, systematic studies of phase transitions in relation to temperature and water content were performed, generating complex phase diagrams (figure 3).

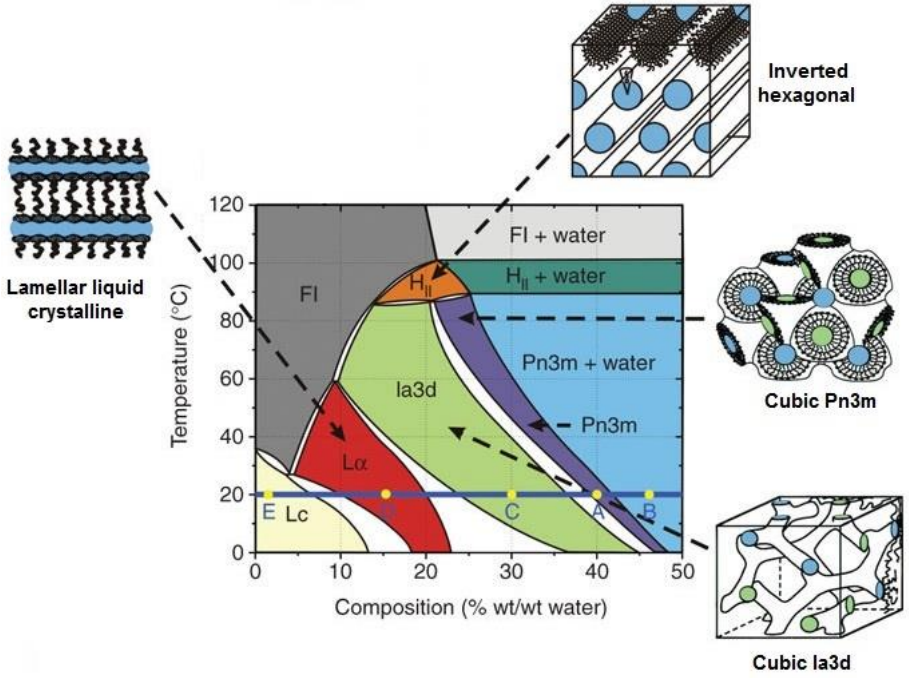

Figure 3 – Temperature-composition phase diagram of monoolein. The phases formed by the lipid monoolein depend on temperature and hydration as illustrated in this phase diagram (adapted from: (Qiu and Caffrey 2000)).

The tendency to form a certain phase, *e.g.* lamellar, hexagonal, cubic, depends among other factors on the geometric shape of the phospholipid molecule (Haney *et al.* 2010). Lipids where the hydrocarbon chain and the head group have similar cross-sectional areas will have a cylindrical shape (*e.g.* phosphatidylcholine and phosphatidylserine), and will tend to assume a planar bilayer structure, *i.e.* lamellar structure (figure 4A). When the head group area is smaller than the hydrocarbon chain, the structure is well represented by an inverted truncated cone (*e.g.* phosphatidylethanolamine) (figure 4B). When part of a membrane, these will favour a negative curvature and inverted hexagonal (H_{II}) phases. Finally, lipids with the head group area larger than the hydrocarbon chain will appear as a cone (*e.g.* lysophosphatidylcholine), forming preferentially structures like normal hexagonal (H_I) phase or micelles with a positive curvature (figure 4C) (Haney *et al.* 2010).

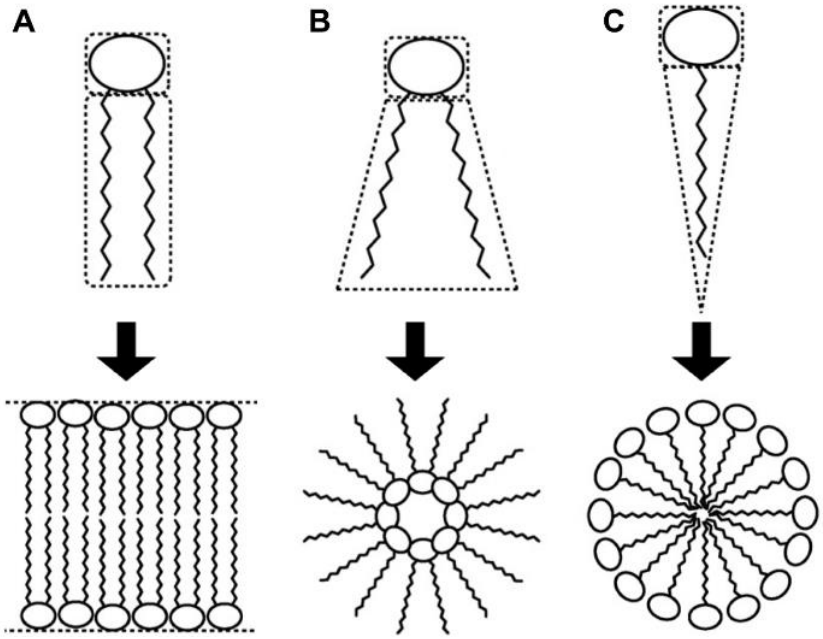

Figure 4 – Relation between the geometric shape of the phospholipid molecule and the structure favoured. A) Cylindrical shape phospholipids tend to assume lamellar structure. **B)** Inverted truncated cone shaped phospholipids favour a negative curvature of the membrane and can form inverted micelles or inverted hexagonal phases (H_{II}). **C)** Cone shaped phospholipids favour a positive curvature of the membrane forming normal hexagonal phases (H_I) or micelles (adapted from (Haney *et al.* 2010)).

The functional structure of a biological membrane is a planar lipid bilayer in a lamellar phase (figure 5 and 6). Lamellar phases still include significant variations in their properties, depending on the lipids present and on the environment. The most common phases are

- the **liquid crystalline** or **fluid lamellar phase** ($\mathbf{L_\alpha}$) where the hydrocarbon chains are in a "melted", fluid state (figure 5) allowing easy lateral lipid movement and even flip-flop, fundamental conditions for membrane reorganization upon external stimulus;
- the **gel lamellar phase** ($\mathbf{L_\beta}$) in which the hydrocarbon chains are extended and much more rigid (figure 5) (Haney *et al.* 2010), occurs at lower temperatures that the ones where the liquid crystalline phase is stable.
- Other gel lamellar phases such as **tilted** ($\mathbf{L_{\beta'}}$), **interdigitated** ($\mathbf{L_{\beta I}}$) and **rippled** ($\mathbf{P_{\beta'}}$) phase have been described for some lipids (Seddon and Templer 1995).

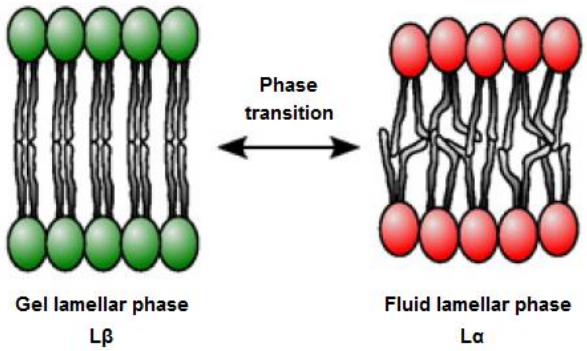

Figure 5 – Lamellar phases. Schematic representation of the structure and orientation of the phospholipids' hydrocarbon chains in two lamellar phases, gel (L_β) and fluid (L_α) (adapted from: (Tresset 2009)).

The typical lipid state in biological membranes is the liquid crystalline or fluid lamellar phase. Although usually the maintenance of a stable bilayer is essential for normal membrane function, it is well known that in some cases membranes containing high amounts of non-lamellar phase-forming lipids (*e.g.* phosphatidylethanolamine) have the ability to form more complex 3D morphologies, adopting non-lamellar structures such as hexagonal and cubic phases (figure 6), that are believed to play important roles in some biological processes (Luzzati 1997, Lohner 2009). **Hexagonal phases** (figure 4 and 6) are formed by phospholipids cylinders oriented in a hexagonal lattice. In the case of the normal hexagonal phase (H_I), the hydrocarbon chains represent the centre of the cylinder (figures 4C and 6B), whereas in the inverted hexagonal phase (H_{II}) the head groups are oriented towards the core of the cylinder that is filled with water (figures 4B and 6C). The H_{II} is implied for instance, in membrane fusion processes, whereas few lipids adopt H_I (Tresset 2009, Haney *et al.* 2010). **Cubic phases** are part of a large family of phases that are complex and diverse, and can be divided essentially into two classes, bicontinuous and micellar phases (Luzzati *et al.* 1997). The bicontinuous phases consist of a single bilayer folded into a three-dimensional cubic network separating two disjointed water compartments with continuous regions of both polar (hydrophilic head groups) and non-polar (hydrocarbon chains) structures (Ia3d, Pn3m, Im3m) (figure 6 D, E and F). The micellar phases are impervious to water-soluble components, and their structure is made of disjointed micelles with different sizes for a more efficient packing on a cubic lattice (*e.g.* Fd3m, Pm3n) (figure 6G) (Luzzati *et al.* 1997, Tresset 2009). Cubic phases are abundant in the biological world being present in the plasma membrane of archaebacteria, in the endoplasmic reticulum and in the mitochondria of mammalian cells. These phases are

also involved in biological processes such as membrane fusion and fat digestion (Luzzati 1997, Tresset 2009).

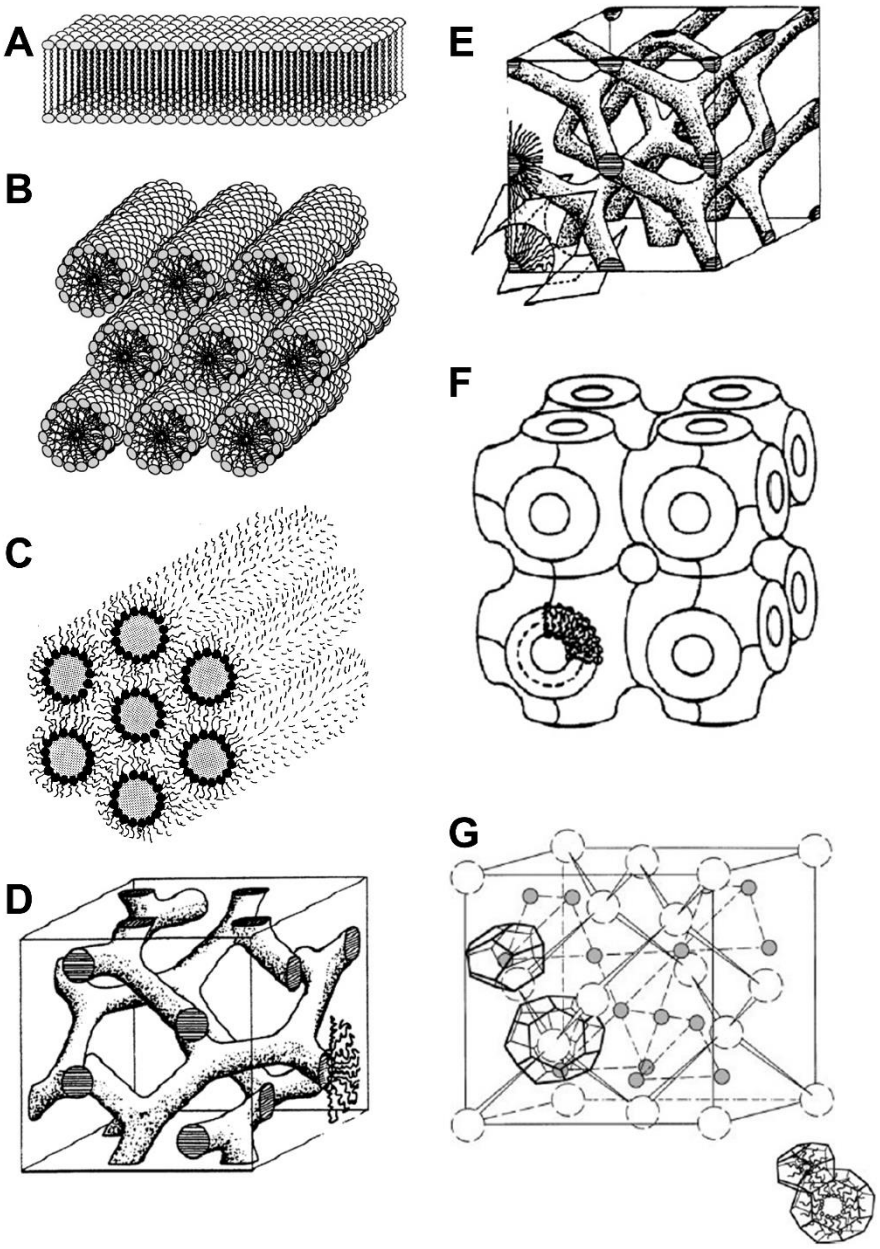

Figure 6 – Lamellar and non-lamellar phases. Schematic representation of lamellar phase (A), normal hexagonal phase (H_I) (B), inverted hexagonal phase (H_{II}) (C), bicontinuous cubic phases, Ia3d (D), Pn3m (E) and Im3m (F), and a micellar cubic phase, Fd3m (G) (adapted from (Seddon and Templer 1995, Tresset 2009, Haney *et al.* 2010)).

When studying the interaction of antimicrobial peptides with membranes, it is crucial to understand if AMP are capable of altering the phospholipid phase behaviour and, if so, to correlate these changes in lipid polymorphism with models for the biological effects of AMP. Model membranes are particularly useful for that aim, as their properties can be

easily modulated, by varying phospholipid compositions, and easily analysed by using different techniques (*e.g.* calorimetry, X-ray diffraction, neutron scattering, fluorescence spectroscopy). They are very simplified models of complex structures enabling the discrimination of the different effects in the global mechanism of action. They can provide information that enables the understanding of the changes in polymorphism induced by AMP (*e.g.* the induction or disappearance of a certain phase), and how AMP affect the overall structure and stability of the membrane. In this way the mechanism of action of AMP can be clarified, and the conclusions may lead to a fine-tuning of new peptides to obtain better therapeutic agents.

The phospholipid compositions most widely used to mimic the erythrocytes membranes for the study of AMP are zwitterionic membranes of phosphatidylcholine (PC), with or without cholesterol. The combination of PC and phosphatidylglycerol (PG) or phosphatidylethanolamine (PE) and PG are used to mimic the cytoplasmic membrane of pathogens, which usually have a global negative charge. For bacterial membranes, it is more common to use model membranes of PE and PE/PG mixtures, as these are the more common phospholipids in bacteria, whereas for mimicking fungus, membranes mainly composed of PC and PG are used (Teixeira *et al.* 2012). Few studies have addressed the importance of the hydrocarbon chain in the AMP/membrane interaction. In some cases, there has been some evidence that AMP may not only be sensitive to the head group type but also to the overall lipid composition of the membrane (Sevcsik *et al.* 2007, Sevcsik *et al.* 2008). Therefore, efforts are now being made to include variations in this parameter in model membrane studies. More elaborate models could also be used by the introduction of sphingomyelin and sterols when mimicking eukaryotic membranes and cardiolipin for prokaryotic ones, or even by using membrane extracts obtained from bacteria. However, data analysis from these systems is much more complex. It should be stressed that the main paradigm of model studies is to “keep it simple”, to enable significant discriminative analysis of interaction effects. For that reason, most of the studies use model membranes composed of only one lipid or binary lipid mixtures.

2.2. Biophysical techniques to study AMP activity

2.2.1. Circular Dichroism

Circular Dichroism (CD) is a spectroscopic technique used to study the orientation and secondary structure of a peptide when in contact with membranes. Structures such as α-helix, β-sheet, β-turn, random and others, have positive and/ or negative peaks giving rise to unique profiles enabling their identification and discrimination (Brahms and Brahms

1980). As mentioned before (chapter 1.1), AMP in solution are usually characterized by a random coil structure, but upon contact with lipid membranes they tend to adopt a defined secondary structure. These conformational changes depend not only on the nature of the peptide, but also on the membranous environment, affecting parameters such as attachment and insertion in the membrane and, therefore, AMP activity (Abrunhosa *et al.* 2005, Adao *et al.* 2011).

2.2.2. Differential Scanning Calorimetry

As mentioned before, lipids adopt different phases according to their characteristics and the environment where they are inserted. Changes in temperature (among other factors) can lead to a temperature-induced transition between these phases, referred as thermotropic mesomorphism (Seddon and Templer 1995). Differential Scanning Calorimetry (DSC) is a non-destroying technique that allows the determination of the heat involved in a thermotropic transition in solids, liquids and suspensions as well as the temperature at which transitions occur (Cooper *et al.* 2001). In a DSC experiment, the sample is heated at a constant rate, and as the sample undergoes temperature-induced phase transitions, it will release or absorb heat, which is measured throughout the experiment and recorded as a function of temperature. DSC studies allow the determination of the transition temperature (T_m), the transition enthalpy (ΔH) and cooperativity of a certain thermotropic phase transition (Cooper *et al.* 2001). DSC allows the study of the effects of peptides on liposomes by comparing the calorimetric profiles obtained for the pure lipid system with those of the peptide/lipid mixtures at various peptide-to-lipid molar ratios (P:L), and thus the evaluation of the influence of the peptide on the thermotropic transitions (*e.g.* the gel to liquid-crystalline transition) of different membranes (Lohner and Prenner 1999, Haney *et al.* 2010). This technique is a good screening tool to obtain information about the peptide's activity and specificity (Lohner and Prenner 1999, Abrunhosa *et al.* 2005, Bolscher *et al.* 2009a, Teixeira *et al.* 2010, Adao *et al.* 2011) before going into experiments with cells.

2.2.3. Isothermal Titration Calorimetry

Isothermal Titration Calorimetry (ITC) measures the heat resulting from the interaction of two biomolecules (titrant and titrated) at a given temperature, allowing the determination of the thermodynamic parameters that characterize the interaction (O'Brien *et al.* 2001). The titration of a ligand (*e.g.* antimicrobial peptide) to a macromolecular assembly (*e.g.* lipid membrane) results in a heat change (heat will either be absorbed or released) that

will be monitored throughout the experiment, enabling the quantitative characterization of the energetics of the interaction. Depending on the type and the conditions of the experiment, thermodynamic parameters such as equilibrium constant (*K*), interaction stoichiometry (N) and enthalpy (Δ*H*) can be retrieved. From those, the remaining thermodynamic parameters, Gibbs energy (Δ*G*) and entropy (Δ*S*) can be easily calculated, providing a complete thermodynamic characterization of the interaction at one temperature (O'Brien *et al.* 2001). When experiments are performed at different temperatures, the change in heat capacity (ΔC_p) can be calculated and is a fundamental parameter when the hydrophobic effect is involved (O'Brien *et al.* 2001). The overall analysis of the ITC profile, the thermodynamic parameters and the physical-chemical properties of the compounds allow the understanding of the characteristics of the interaction process. Since all chemical reactions involve changes in enthalpy, this information is very important in many applications, such as pharmaceutical development of new drugs, vehicles for drug delivery, food industry, surfactant/polymers applications, among others.

To analyse ITC data, a model for the interaction is always needed. In the case of macromolecule/ligand interaction (*e.g.* protein-protein interaction), a **ligand-binding model** is appropriate, with a defined stoichiometry. The analysis will then provide the association constant (K_a) the enthalpy change (Δ*H*) and the stoichiometry (N) (O'Brien *et al.* 2001). When membranes are involved, the most appropriate model is the **partition model**, as long as the membrane is not destroyed upon partition. In the case of partition, the ligand is distributed between the aqueous and the membrane phase, in a concentration ratio that depends on its affinity for the two phases. We can thus obtain the partition constant (K_p) and the enthalpy (Δ*H*) of the process (Wieprecht *et al.* 1999, Seelig 2004). If the ligand and/or the membrane are charged, the obtained partition constant is an **apparent** one, and the electrostatic effect have to be dealt with to obtain the **intrinsic** partition constant (Heiko 2004).

Although other methods (*e.g*. fluorescence spectroscopy, zeta potential, Electron paramagnetic resonance – EPR) can provide the partition constant, the advantage of ITC is that it can measure directly the interaction enthalpy, and provide complete thermodynamic information from one ITC run (Seelig 1997).

In the case of AMP and membrane interaction, the information provided by ITC characterizes the AMP affinity for different membranes (K_p value) (Abraham *et al.* 2005) as well as its energetics – association, helix formation, the importance of charge effects, among others (Seelig 2004). In many cases, information on the mechanism of action can

also be derived from proper interpretation of ITC results (Wieprecht *et al.* 2000, Abraham *et al.* 2005, Bastos *et al.* 2008).

2.2.4. X-ray Diffraction

X-ray diffraction is a powerful tool to characterize the structure of lipid mesophases and polymorphic changes in the lipid bilayer. Lipid dispersions in water form structures with long-range periodic order that can be analysed by X-ray techniques, in particular by diffraction methods, as these periodic structures will diffract the X-rays in a particular pattern depending on the existent phase and the respective space group. If an ordered mesophase is present (*e.g.* lamellar, hexagonal and cubic phases), sharp Bragg peaks will appear in the low-angle region of the diffraction pattern. These Bragg reflections have reciprocal spacing in characteristic ratios for each phase allowing their identification (Seddon and Templer 1995). Typically, depending on the lipid and temperature, liposomes form lamellar or hexagonal phases. However, the presence of an antimicrobial peptide can induce structural changes, by altering the lattice parameter, changing the transition temperature and or leading to the disappearance or appearance of phases. Understanding the type of polymorphic structure that is present in a peptide-lipid mixture can lead to a deeper knowledge of the mechanism of action of the peptide (Hickel *et al.* 2008, Haney *et al.* 2010, Bastos *et al.* 2011, Pabst *et al.* 2012).

CHAPTER 3. *Mycobacterium*

Tuberculosis (TB) remains one of the leading causes of human death worldwide (Nathan 2014, WHO 2015b). Although the mortality associated with TB has decreased, in 2014 WHO reported that 1.5 million people died from this infection (WHO 2015b). The incidence of multidrug and extensively drug-resistant TB (MDR-TB and XDR-TB) has been increasing worldwide, with more than 100 countries reporting cases of XDR-TB (Falzon *et al.* 2015, WHO 2015b).

The genus *Mycobacterium* includes not only *Mycobacterium tuberculosis* but other pathogenic species such as *M. leprae* and *M. ulcerans*, as well as a multitude of non-pathogenic species usually referred to as nontuberculous mycobacteria (NTM). More than 150 species of NTM are known, being ubiquitous in the environment, present in water, soil, dust and plants (Tortoli 2006, Falkinham 2015). The consequences of mycobacterial infection depend on the virulence of the infecting *Mycobacterium* and the resistance of the host. In humans, the outcome can range from relatively mild and transient symptoms to a widely disseminated disease (Pieters 2001, Tortoli 2009). NTM can be the cause of several types of infections, such as pulmonary (one of the most common), cutis and soft tissue, bone and joint, and lymphonodal infections (Tortoli 2009). Disseminated disease occurs in immunocompromised patients, especially in HIV-infected patients, but also in patients with cancer, organ or stem cell transplant, with genetic immunodeficiencies, and patients undertaking therapies for immune-mediated inflammatory diseases (Tortoli 2009, Henkle and Winthrop 2015). The prevalence of NTM infections has been increasing worldwide, followed by a decrease in TB (Cassidy *et al.* 2009, Brode *et al.* 2014), and thus stressing the importance of these NTM and the infections caused by them.

3.1. Mycobacterial cell wall

Mycobacteria are irregular rods, aerobic, and unable to form spores (Prescott *et al.* 2002). *Mycobacterium* species are characterized by an extremely complex and highly impermeable cell wall, composed of three main components, the mycolic acids, a highly branched arabinogalactan (AG) polysaccharide and a cross-linked network of peptidoglycan, being called the mAGP complex (figure 7) (Jankute *et al.* 2015). The covalent linkage between these three layers results in a hydrophobic envelope of extremely low fluidity and high impermeability. Also intercalated between the mycolic acids, there is an outer layer containing various free lipids such as phenolic glycolipids and sulpholipids, among others. The outmost layer of the cell wall that some authors refer to as capsule, is mainly composed of polysaccharides and proteins (Abdallah *et al.* 2007,

Guenin-Mace *et al.* 2009, Jankute *et al.* 2015). This unique cell wall is critical for the capacity of mycobacterial pathogens to survive inside the host and to resist chemotherapy (Guenin-Mace *et al.* 2009). The presence of mycolic acids and other lipids outside the peptidoglycan layer also makes mycobacteria acid-fast. This means these bacteria are not stained by the Gram method but retain the primary stain fuchsin, when subject to the Ziehl-Neelsen method (Prescott *et al.* 2002).

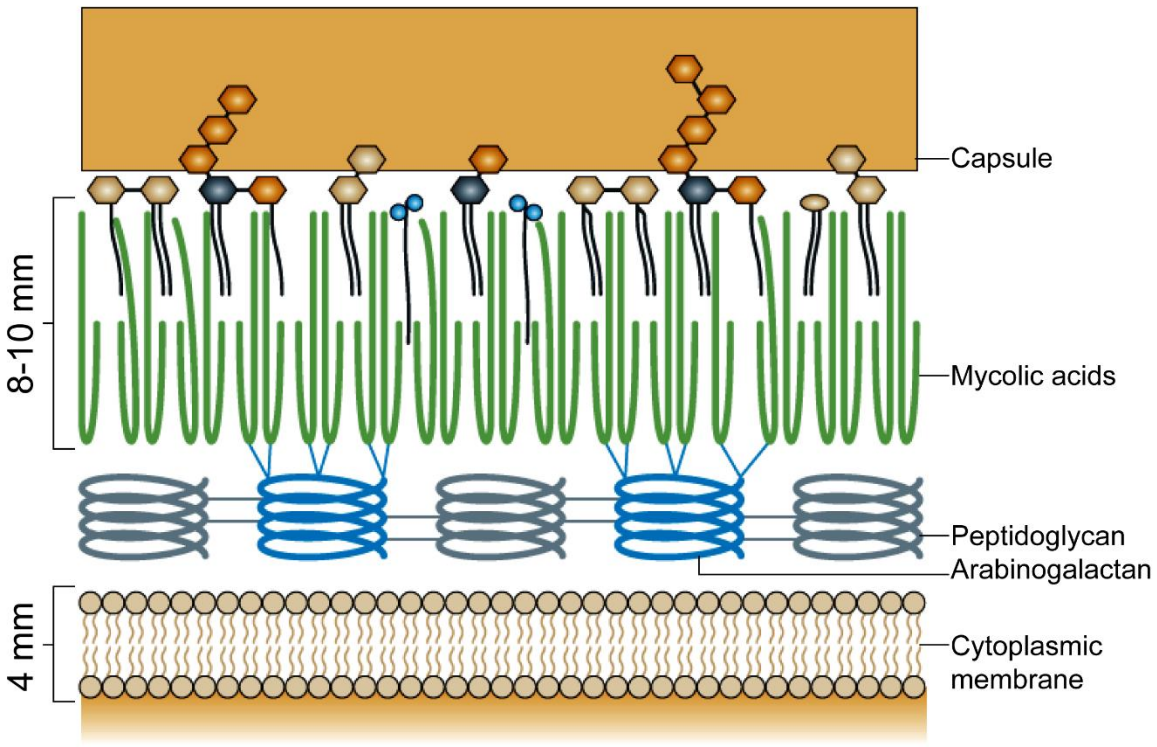

Figure 7 – Mycobacterial cell wall. Schematic representation of one of the current views of the mycobacterial cell wall (adapted from: (Abdallah *et al.* 2007)).

Mycobacterium plasma membrane, which is protected by the cell wall, is an asymmetric bilayer essentially composed of lipids and proteins, as any biological membrane. The phospholipid composition is very similar to all the other bacterial membranes containing essentially phosphatidylethanolamine, phosphatidylglycerol, diphosphatidylglycerol, and phosphatidylinositol mannosides, these last three conferring the membranes an overall negative charge (Guenin-Mace *et al.* 2009).

3.2. *Mycobacterium avium*

Mycobacterium avium complex (MAC), compromising *M. avium* and *M. intracellulare*, is the most common cause of NTM infections in immunocompromised hosts. Disseminated MAC was one of the first opportunistic infections detected in AIDS patients remaining until today a substantial cause of morbidity and mortality among these patients (Tortoli 2009). Infection of AIDS patients by *M. avium* occurs in advanced stages of the disease when the levels of CD4+ T cells are very low. *M. avium* can also infect patients with other debilitating diseases, especially restrictive and obstructive pulmonary diseases, that compromise the immune system, such as chronic obstructive pulmonary disease, emphysema, chronic bronchitis and children with lymphadenitis (Appelberg 2006b).

M. avium, similar to other mycobacteria, is a facultative intracellular pathogen residing mainly inside macrophages. The outcome of *M. avium* infections, along with other mycobacteria, directly depends on the virulence of the infecting mycobacteria and the resistance of the host. After being phagocytized by macrophages, the mycobacteria reside inside the phagosomes of the host cells inhibiting the phagosome-lysosome fusion, and, therefore, the formation of the phagolysosome (Appelberg 2006b, de Chastellier 2009). The phagolysosome, designed to protect the host against invading pathogens, is characterized by an acidic environment containing proteolytic enzymes that degrade the content of the vacuole (Pieters 2001). By inhibiting the phagosome-lysosome fusion, mycobacteria escape from harmful environments (*e.g.* acidic pH), but at the same time maintain the interaction with endosomes, allowing the access to nutrients, and ensuring their survival and proliferation inside the host (Appelberg 2006b, Appelberg 2006a).

The mechanism by which macrophages can inhibit the mycobacterial growth and the mechanisms used by mycobacteria to resist and live inside macrophages are only partially understood. *M. avium* can grow exponentially inside non-activated macrophages, this growth being more restrictive if the macrophages are activated with cytokines such as IFN-γ and TNF-alpha (Appelberg and Orme 1993, Appelberg *et al.* 1994, Appelberg 2006c). This activation can unblock the maturation of the phagosome which can culminate in the inhibition of the mycobacterial growth (Schaible *et al.* 1998, Via *et al.* 1998). Nutriprive mechanisms, restricting the access to nutrients, such as iron, may contribute to the elimination of the pathogen (Gomes *et al.* 1999b, Gomes and Appelberg 2002, Pais and Appelberg 2004, Appelberg 2006a, Appelberg 2006c, Silva-Gomes *et al.* 2013). This restriction of nutrients can come in many ways, including alterations in vesicular trafficking and phagosome-lysosome fusion (Pais and Appelberg 2004, Appelberg 2006a, Appelberg 2006c). The impact of phagosome maturation on *M. avium* viability is, however, not clear. For instance, co-infection of macrophages with *M. avium* and *Coxiella burnetii* resulted in

phagosome-lysosome fusion and, therefore, a decrease in the pH of the bacteria-containing organelle, which did not decrease the viability of *M. avium*, contrary to what occurred with *M. tuberculosis* (Gomes *et al.* 1999c). In other report, the induction of phagosome maturation by fatty acids inhibited the growth of both *M. tuberculosis* and *M. avium* (Anes *et al.* 2003).

Killing of *M. avium* by macrophages is independent of the respiratory burst or the production of nitric oxide (NO) (Gomes *et al.* 1999b, Gomes and Appelberg 2002, Appelberg 2006c), as opposed to *M. tuberculosis* and other pathogenic mycobacteria (Chan *et al.* 1995, MacMicking *et al.* 1997, Cooper *et al.* 2000).

Apoptosis has been described as a way to eliminate the pathogen by sacrificing the host cell (Gao and Kwaik 2000). Macrophages may undergo apoptosis after infection with *M. avium* (Gan *et al.* 1995, Fratazzi *et al.* 1997) which does not impact the viability of the mycobacteria, instead they use it as a way to spread the infection (Early *et al.* 2011). Autophagy is another catabolic process used by the cell as a mechanism of internal quality control, removing proteins, cytosolic components or damaged organelles, and it has emerged as a host antimicrobial defence mechanism capable of degrading intracellular pathogens (Deretic and Levine 2009). Autophagy induction via vitamin D3 inhibits *M. tuberculosis* growth (Gutierrez *et al.* 2004, Yuk *et al.* 2009, Selvaraj *et al.* 2015). In the case of *M. avium*, there are a few evidences of diminished ability to survive in autophagic vacuoles (de Chastellier and Thilo 2006, Early *et al.* 2011).

Understanding the mechanism by which the mycobacteria circumvent the host immune response, and the antimicrobial mechanisms of the macrophage responsible for controlling the microbial growth can open the way for the identification of novel targets and the development of new antimycobacterial drugs.

3.3. Treatment

Infections by mycobacteria are difficult to treat. Currently, the available treatments are poorly active, costly, toxic and require long periods of time that most often are not correctly followed by the patients, ultimately leading to increased levels of resistance. The primary treatment of all pathogenic mycobacteria consists of a combination of different antibiotics taken for several months. In the case of tuberculosis, the treatment varies according to the susceptibility of the isolated strain to the available drugs. The standard recommendations consist on a four antibiotic regime with isoniazid, rifampicin, pyrazinamide and ethambutol taken for 6 months. In the case of more resistant strains, fluoroquinolone or second-line injectable drugs, such as amikacin, kanamycin and

capreomycin are administrated (Koul *et al.* 2011). All these drugs are ineffective against extensively-drug resistant TB (XDR-TB), which has been increasing worldwide with reports in more than 100 countries (WHO 2015b).

In the case of NTM, the treatments were not designed for these infections but instead have been extrapolated from the TB experience. Macrolides, such as clarithromycin and azithromycin, are central for the treatment of NTM infections, together with other antimycobacterial drugs such as ethambutol, rifampin or rifabutin, taken for months to several years (Egelund *et al.* 2015, Philley and Griffith 2015). In the case of disseminated MAC, the administration of effective antiretroviral therapy in immunocompromised patients reduces the number of people at risk of developing the disease by elevating the number of CD4+ T cells (Horsburgh *et al.* 2001, Henkle and Winthrop 2015).

To achieve a better global control of mycobacterial infections, new antimycobacterial drugs should be developed to achieve shorten treatment duration, reduced daily pill burden and dose frequency, treatment of multidrug-resistant strains, and also the possibility of co-administration with anti-HIV drugs (Koul *et al.* 2011).

Intensive efforts have been made towards the discovery and application of alternative therapies, using for instance adjunctive immunomodulators such as picolinic acid (Pais and Appelberg 2000, Pais and Appelberg 2004, Cai *et al.* 2006), or iron chelators (Fernandes *et al.* 2010, Moniz *et al.* 2013, Moniz *et al.* 2015). These last compounds are of great interest as *M. avium* growth inside macrophages is directly proportional to the amount of iron available. Furthermore, AIDS patients have increased iron deposition in different tissues, favouring the growth of *M. avium*. The use of iron chelators, depriving the mycobacteria of an essential nutrient for their survival, is thus a promising road for the treatment of this disease (Gomes *et al.* 1999a, Gomes *et al.* 2001, Fernandes *et al.* 2010, Moniz *et al.* 2013, Moniz *et al.* 2015).

3.4. Mycobacteria as a target of AMP

Antimicrobial peptides have been described as displaying antimycobacterial activity, both through direct killing or immunomodulation (Shin and Jo 2011, Teng *et al.* 2015).

Cathelicidin peptide, LL-37, can kill *M. tuberculosis* both *in vitro* and *in vivo*, and its expression is increased in macrophages during mycobacterial infection (Rivas-Santiago *et al.* 2008, Sonawane *et al.* 2011, Rivas-Santiago *et al.* 2013, Santos *et al.* 2014). Also, it has been described that LL-37 can play a role in the induction and maturation of autophagy, activated by vitamin D3 in human monocytes, inhibiting the intracellular

mycobacterial growth (Liu *et al.* 2007, Yuk *et al.* 2009). Other effects of LL-37 have been pointed out, such as chemoattraction, regulation of apoptosis, induction of cytokines, among others, that altogether contribute to a better mycobacterial clearance (Shin and Jo 2011, Santos *et al.* 2014).

Defensins, such as human neutrophil peptide (HNP) and human β-defensin 2 (HBD-2), have also shown activity against *M. tuberculosis* and *M. avium*, *in vitro* and *in vivo* (Ogata *et al.* 1992, Sharma *et al.* 2000, Kisich *et al.* 2001, Sharma *et al.* 2001, Mendez-Samperio 2008, Rivas-Santiago *et al.* 2011). The combination of defensins with anti-tuberculosis drugs, like isoniazid and rifampicin, resulted in a significant reduction of intracellular mycobacteria, allowing the reduction of the drugs dosage and the duration of treatment (Kalita *et al.* 2004). Similar to cathelicidins, defensins are also involved in the innate immune defence against mycobacteria, including the regulation of inflammation, activation of NFκB and chemotactic effects (Shin and Jo 2011).

Hepcidin, besides playing an important role in iron metabolism (Ganz 2006), has been shown to have its expression increased in macrophages infected with mycobacteria, and to have a direct antimycobacterial activity against *M. tuberculosis* (Sow *et al.* 2007).

Several synthetic peptides have displayed antimycobacterial activity *in vitro* and also synergism with conventional drugs (Jena *et al.* 2011, Jiang *et al.* 2011, Ramon-Garcia *et al.* 2013, Khara *et al.* 2014).

The increasing number of reports describing the antimycobacterial activity of different AMP highlights the potential of these peptides to be used as new drugs for fighting mycobacterial infections.

CHAPTER 4. Objectives of this thesis

Antimicrobial peptides comprise a vast array of compounds, which are promising potential alternatives to treat infectious diseases. With increasing levels of resistance and therefore, failure of the existing drugs, there is a demand for new and more effective antimicrobial compounds. Antimicrobial peptides are part of the innate immune defence mechanisms of almost all living organisms and they can act in multiple ways against pathogens avoiding resistance more easily than conventional drugs. The general goals of this work were to assess the activity of several peptides against *Mycobacterium avium* and to investigate the mechanisms of action of different peptides using lipid model membranes.

In order to achieve these general goals, several tasks were performed, with more focused objectives, which are detailed below:

- To characterize the interaction of a cecropin A-melittin hybrid peptide (CA(1-7)M(2-9)) with lipid model membranes using Circular Dichroism, Differential Scanning Calorimetry, Isothermal Titration Calorimetry, X-ray diffraction and microscopy techniques (chapter 5).
- To characterize the interaction of three peptides derived from lactoferrin (lactoferricin (LFcin17-30), lactoferrampin (LFampin265-284) and LFchimera) with model membranes by Circular Dichroism, Differential Scanning Calorimetry and X-ray diffraction. To correlate the observed effects with the previously reported structural changes of *Candida albicans* upon treatment with these peptides (chapter 6).
- To evaluate the activity of lactoferricin (LFcin17-30), against *Mycobacterium avium* growing in broth culture. To identify the most relevant structural characteristics of the peptide for antimicrobial activity, using variants obtained by specific amino acid substitutions. To investigate the mechanism of action of these peptides, using scanning and transmission electron microscopy (chapter 7).
- To evaluate the effect of lactoferricin (LFcin17-30) peptide and its variants against *Mycobacterium avium* growing inside macrophages, its natural host cells. To elucidate the mechanisms by which the peptides impact on the intramacrophagic growth of *M. avium*. To investigate the possibility of a synergistic effect of the peptides with conventional antibiotics (chapter 8).

References

Abdallah A. M., Gey van Pittius N. C., Champion P. A., Cox J., Luirink J., Vandenbroucke-Grauls C. M., Appelmelk B. J. and Bitter W. (2007). Type VII secretion - mycobacteria show the way. *Nat Rev Microbiol*. 5(11):883-891.

Abraham T., Lewis R. N., Hodges R. S. and McElhaney R. N. (2005). Isothermal titration calorimetry studies of the binding of the antimicrobial peptide gramicidin S to phospholipid bilayer membranes. *Biochemistry*. 44(33):11279-11285.

Abrunhosa F., Faria S., Gomes P., Tomaz I., Pessoa J. C., Andreu D. and Bastos M. (2005). Interaction and Lipid-Induced Conformation of Two Cecropin−Melittin Hybrid Peptides Depend on Peptide and Membrane Composition. *J Phys Chem B*. 109(36):17311-17319.

Adao R., Nazmi K., Bolscher J. G. and Bastos M. (2011). C- and N-truncated antimicrobial peptides from LFampin 265 - 284: Biophysical versus microbiology results. *J Pharm Bioallied Sci*. 3(1):60-69.

Alberola J., Rodriguez A., Francino O., Roura X., Rivas L. and Andreu D. (2004). Safety and efficacy of antimicrobial peptides against naturally acquired leishmaniasis. *Antimicrob Agents Chemother*. 48(2):641-643.

Andreu D., Merrifield R. B., Steiner H. and Boman H. G. (1983). Solid-phase synthesis of cecropin A and related peptides. *Proc Natl Acad Sci U S A*. 80(21):6475-6479.

Andreu D., Ubach J., Boman A., Wahlin B., Wade D., Merrifield R. B. and Boman H. G. (1992). Shortened cecropin A-melittin hybrids. Significant size reduction retains potent antibiotic activity. *FEBS Lett*. 296(2):190-194.

Anes E., Kuhnel M. P., Bos E., Moniz-Pereira J., Habermann A. and Griffiths G. (2003). Selected lipids activate phagosome actin assembly and maturation resulting in killing of pathogenic mycobacteria. *Nat Cell Biol*. 5(9):793-802.

Appelberg R. (2006a). Macrophage nutriprive antimicrobial mechanisms. *J Leukoc Biol*. 79(6):1117-1128.

Appelberg R. (2006b). Pathogenesis of Mycobacterium avium infection. *Immunol Res*. 35(3):179-190.

Appelberg R. (2006c). Pathogenesis of Mycobacterium avium infection: typical responses to an atypical mycobacterium? *Immunol Res*. 35(3):179-190.

Appelberg R., Castro A. G., Pedrosa J., Silva R. A., Orme I. M. and Minoprio P. (1994). Role of gamma interferon and tumor necrosis factor alpha during T-cell-independent and -dependent phases of Mycobacterium avium infection. *Infect Immun*. 62(9):3962-3971.

Appelberg R. and Orme I. M. (1993). Effector mechanisms involved in cytokine-mediated bacteriostasis of Mycobacterium avium infections in murine macrophages. *Immunology*. 80(3):352-359.

Arias C., Guizy M., Luque-Ortega J. R., Guerrero E., de la Torre B. G., Andreu D., Rivas L. and Valenzuela C. (2006). The induction of NOS2 expression by the hybrid cecropin A-melittin antibiotic peptide CA(1-8)M(1-18) in the monocytic line RAW 264.7 is triggered by a temporary and reversible plasma membrane permeation. *Biochim Biophys Acta*. 1763(1):110-119.

Arnett E. and Seveau S. (2011). The multifaceted activities of mammalian defensins. *Curr Pharm Des*. 17(38):4254-4269.

Auvynet C. and Rosenstein Y. (2009). Multifunctional host defense peptides: Antimicrobial peptides, the small yet big players in innate and adaptive immunity. *FEBS J*. 276(22):6497-6508.

Bals R., Weiner D. J., Moscioni A. D., Meegalla R. L. and Wilson J. M. (1999). Augmentation of innate host defense by expression of a cathelicidin antimicrobial peptide. *Infect Immun*. 67(11):6084-6089.

Bassetti M., Merelli M., Temperoni C. and Astilean A. (2013). New antibiotics for bad bugs: where are we? *Ann Clin Microbiol Antimicrob*. 12:22.

Bastos M., Bai G., Gomes P., Andreu D., Goormaghtigh E. and Prieto M. (2008). Energetics and partition of two cecropin-melittin hybrid peptides to model membranes of different composition. *Biophys J*. 94(6):2128-2141.

Bastos M., Silva T., Teixeira V., Nazmi K., Bolscher J. G. M., Funari S. S. and Uhríková D. (2011). Lactoferrin-Derived Antimicrobial Peptide Induces a Micellar Cubic Phase in a Model Membrane System. *Biophys J*. 101(3):L20-L22.

Bauer M. E. and Shafer W. M. (2015). On the in vivo significance of bacterial resistance to antimicrobial peptides. *Biochim Biophys Acta*. 1848(11 Pt B):3101-3111.

Bellamy W., Takase M., Wakabayashi H., Kawase K. and Tomita M. (1992a). Antibacterial spectrum of lactoferricin B, a potent bactericidal peptide derived from the N-terminal region of bovine lactoferrin. *J Appl Bacteriol*. 73(6):472-479.

Bellamy W., Takase M., Yamauchi K., Wakabayashi H., Kawase K. and Tomita M. (1992b). Identification of the bactericidal domain of lactoferrin. *Biochim Biophys Acta*. 1121(1-2):130-136.

Bellamy W., Yamauchi K., Wakabayashi H., Takase M., Takakura N., Shimamura S. and Tomita M. (1994). Antifungal properties of lactoferricin B, a peptide derived from the N-terminal region of bovine lactoferrin. *Lett Appl Microbiol*. 18(4):230-233.

Benachir T., Monette M., Grenier J. and Lafleur M. (1997). Melittin-induced leakage from phosphatidylcholine vesicles is modulated by cholesterol: a property used for membrane targeting. *Eur Biophys J*. 25(3):201-210.

Bessalle R., Haas H., Goria A., Shalit I. and Fridkin M. (1992). Augmentation of the antibacterial activity of magainin by positive-charge chain extension. *Antimicrob Agents Chemother*. 36(2):313-317.

Bolscher J., Nazmi K., van Marle J., van 't Hof W. and Veerman E. (2012). Chimerization of lactoferricin and lactoferrampin peptides strongly potentiates the killing activity against Candida albicans. *Biochem Cell Biol*. 90(3):378-388.

Bolscher J. G., Adao R., Nazmi K., van den Keybus P. A., van 't Hof W., Nieuw Amerongen A. V., Bastos M. and Veerman E. C. (2009a). Bactericidal activity of LFchimera is stronger and less sensitive to ionic strength than its constituent lactoferricin and lactoferrampin peptides. *Biochimie*. 91(1):123-132.

Bolscher J. G. M., Adão R., Nazmi K., van den Keybus P. A. M., van 't Hof W., Nieuw Amerongen A. V., Bastos M. and Veerman E. C. I. (2009b). Bactericidal activity of LFchimera is stronger and less sensitive to ionic strength than its constituent lactoferricin and lactoferrampin peptides. *Biochimie*. 91(1):123-132.

Boman H. G. and Hultmark D. (1987). Cell-free immunity in insects. *Annu Rev Microbiol*. 41:103-126.

Boman H. G., Wade D., Boman I. A., Wahlin B. and Merrifield R. B. (1989). Antibacterial and antimalarial properties of peptides that are cecropin-melittin hybrids. *FEBS Lett*. 259(1):103-106.

Brahms S. and Brahms J. (1980). Determination of protein secondary structure in solution by vacuum ultraviolet circular dichroism. *J Mol Biol*. 138(2):149-178.

Brock J. H. (2002). The physiology of lactoferrin. *Biochem Cell Biol*. 80(1):1-6.

Brode S. K., Daley C. L. and Marras T. K. (2014). The epidemiologic relationship between tuberculosis and non-tuberculous mycobacterial disease: a systematic review. *Int J Tuberc Lung Dis*. 18(11):1370-1377.

Brogden K. A. (2005). Antimicrobial peptides: pore formers or metabolic inhibitors in bacteria? *Nat Rev Microbiol*. 3(3):238-250.

Brogden N. K. and Brogden K. A. (2011). Will new generations of modified antimicrobial peptides improve their potential as pharmaceuticals? *Int J Antimicrob Agents*. 38(3):217-225.

Cabeen M. T. and Jacobs-Wagner C. (2005). Bacterial cell shape. *Nat Rev Microbiol*. 3(8):601-610.

Cai S., Sato K., Shimizu T., Yamabe S., Hiraki M., Sano C. and Tomioka H. (2006). Antimicrobial activity of picolinic acid against extracellular and intracellular Mycobacterium avium complex and its combined activity with clarithromycin, rifampicin and fluoroquinolones. *J Antimicrob Chemother*. 57(1):85-93.

Carvalho F., Atilano M. L., Pombinho R., Covas G., Gallo R. L., Filipe S. R., Sousa S. and Cabanes D. (2015). L-Rhamnosylation of Listeria monocytogenes Wall Teichoic Acids Promotes Resistance to Antimicrobial Peptides by Delaying Interaction with the Membrane. *PLoS Pathog*. 11(5):e1004919.

Cassidy P. M., Hedberg K., Saulson A., McNelly E. and Winthrop K. L. (2009). Nontuberculous mycobacterial disease prevalence and risk factors: a changing epidemiology. *Clin Infect Dis*. 49(12):e124-129.

Chan J., Tanaka K., Carroll D., Flynn J. and Bloom B. R. (1995). Effects of nitric oxide synthase inhibitors on murine infection with Mycobacterium tuberculosis. *Infect Immun*. 63(2):736-740.

Chicharro C., Granata C., Lozano R., Andreu D. and Rivas L. (2001). N-terminal fatty acid substitution increases the leishmanicidal activity of CA(1-7)M(2-9), a cecropin-melittin hybrid peptide. *Antimicrob Agents Chemother*. 45(9):2441-2449.

Cintra W. M., Silva-Filho F. C. and De Souza W. (1986). The surface charge of Toxoplasma gondii: a cytochemical and electrophoretic study. *J Submicrosc Cytol*. 18(4):773-781.

Cooper A., Nutley M. A. and Wadood A. (2001). Differential scanning microcalorimetry. Chapter 11, In **Protein-Ligand Interactions: hydrodynamics and calorimetry**. Edited by S. E. Harding and B. Z. Chowdhry. United Sates, Oxford University Press.

Cooper A. M., Segal B. H., Frank A. A., Holland S. M. and Orme I. M. (2000). Transient loss of resistance to pulmonary tuberculosis in p47(phox-/-) mice. *Infect Immun*. 68(3):1231-1234.

de Chastellier C. (2009). The many niches and strategies used by pathogenic mycobacteria for survival within host macrophages. *Immunobiology*. 214(7):526-542.

de Chastellier C. and Thilo L. (2006). Cholesterol depletion in Mycobacterium avium-infected macrophages overcomes the block in phagosome maturation and leads to the reversible sequestration of viable mycobacteria in phagolysosome-derived autophagic vacuoles. *Cell Microbiol*. 8(2):242-256.

Deretic V. and Levine B. (2009). Autophagy, immunity, and microbial adaptations. *Cell Host Microbe*. 5(6):527-549.

DGS (2014) Portugal - Prevenção e Controlo de Infeções e de Resistência aos Antimicrobianos em números - 2014. Direção-Geral da Saúde. from http://www.dgs.pt/estatisticas-de-saude/estatisticas-de-saude/publicacoes/portugal-controlo-da-infecao-e-resistencia-aos-antimicrobianos-em-numeros-2014.aspx

Diaz-Achirica P., Prieto S., Ubach J., Andreu D., Rial E. and Rivas L. (1994). Permeabilization of the mitochondrial inner membrane by short cecropin-A-melittin hybrid peptides. *Eur J Biochem*. 224(1):257-263.

Diaz-Achirica P., Ubach J., Guinea A., Andreu D. and Rivas L. (1998). The plasma membrane of Leishmania donovani promastigotes is the main target for CA(1-8)M(1-18), a synthetic cecropin A-melittin hybrid peptide. *Biochem J*. 330 (Pt 1):453-460.

Early J., Fischer K. and Bermudez L. E. (2011). Mycobacterium avium uses apoptotic macrophages as tools for spreading. *Microb Pathog*. 50(2):132-139.

Egelund E. F., Fennelly K. P. and Peloquin C. A. (2015). Medications and monitoring in nontuberculous mycobacteria infections. *Clin Chest Med*. 36(1):55-66.

Eliassen L. T., Berge G., Sveinbjornsson B., Svendsen J. S., Vorland L. H. and Rekdal O. (2002). Evidence for a direct antitumor mechanism of action of bovine lactoferricin. *Anticancer Res*. 22(5):2703-2710.

Falkinham J. O., 3rd (2015). Environmental sources of nontuberculous mycobacteria. *Clin Chest Med*. 36(1):35-41.

Falzon D., Mirzayev F., Wares F., Baena I. G., Zignol M., Linh N., Weyer K., Jaramillo E., Floyd K. and Raviglione M. (2015). Multidrug-resistant tuberculosis around the world: what progress has been made? *Eur Respir J*. 45(1):150-160.

Fernandes S. S., Nunes A., Gomes A. R., de Castro B., Hider R. C., Rangel M., Appelberg R. and Gomes M. S. (2010). Identification of a new hexadentate iron chelator capable of restricting the intramacrophagic growth of Mycobacterium avium. *Microbes Infect*. 12(4):287-294.

Fernandez-Reyes M., Diaz D., de la Torre B. G., Cabrales-Rico A., Valles-Miret M., Jimenez-Barbero J., Andreu D. and Rivas L. (2010). Lysine N(epsilon)-trimethylation, a tool for improving the selectivity of antimicrobial peptides. *J Med Chem*. 53(15):5587-5596.

Ferre R., Melo M. N., Correia A. D., Feliu L., Bardaji E., Planas M. and Castanho M. (2009). Synergistic effects of the membrane actions of cecropin-melittin antimicrobial hybrid peptide BP100. *Biophys J*. 96(5):1815-1827.

Fink J., Boman A., Boman H. G. and Merrifield R. B. (1989). Design, synthesis and antibacterial activity of cecropin-like model peptides. *Int J Pept Protein Res*. 33(6):412-421.

Fischbach M. A. and Walsh C. T. (2009). Antibiotics for emerging pathogens. *Science*. 325(5944):1089-1093.

Flores-Villasenor H., Canizalez-Roman A., de la Garza M., Nazmi K., Bolscher J. G. and Leon-Sicairos N. (2012a). Lactoferrin and lactoferrin chimera inhibit damage caused by enteropathogenic Escherichia coli in HEp-2 cells. *Biochimie*. 94(9):1935-1942.

Flores-Villasenor H., Canizalez-Roman A., Reyes-Lopez M., Nazmi K., de la Garza M., Zazueta-Beltran J., Leon-Sicairos N. and Bolscher J. G. (2010). Bactericidal effect of bovine lactoferrin, LFcin, LFampin and LFchimera on antibiotic-resistant Staphylococcus aureus and Escherichia coli. *Biometals*. 23(3):569-578.

Flores-Villasenor H., Canizalez-Roman A., Velazquez-Roman J., Nazmi K., Bolscher J. G. and Leon-Sicairos N. (2012b). Protective effects of lactoferrin chimera and bovine lactoferrin in a mouse model of enterohaemorrhagic Escherichia coli O157:H7 infection. *Biochem Cell Biol*. 90(3):405-411.

Fratazzi C., Arbeit R. D., Carini C. and Remold H. G. (1997). Programmed cell death of Mycobacterium avium serovar 4-infected human macrophages prevents the mycobacteria from spreading and induces mycobacterial growth inhibition by freshly added, uninfected macrophages. *J Immunol*. 158(9):4320-4327.

Fukumoto K., Nagaoka I., Yamataka A., Kobayashi H., Yanai T., Kato Y. and Miyano T. (2005). Effect of antibacterial cathelicidin peptide CAP18/LL-37 on sepsis in neonatal rats. *Pediatr Surg Int*. 21(1):20-24.

Furlong S. J., Mader J. S. and Hoskin D. W. (2006). Lactoferricin-induced apoptosis in estrogen-nonresponsive MDA-MB-435 breast cancer cells is enhanced by C6 ceramide or tamoxifen. *Oncol Rep*. 15(5):1385-1390.

Furlong S. J., Mader J. S. and Hoskin D. W. (2010). Bovine lactoferricin induces caspase-independent apoptosis in human B-lymphoma cells and extends the survival of immune-deficient mice bearing B-lymphoma xenografts. *Exp Mol Pathol*. 88(3):371-375.

Gan H., Newman G. W. and Remold H. G. (1995). Plasminogen activator inhibitor type 2 prevents programmed cell death of human macrophages infected with Mycobacterium avium, serovar 4. *J Immunol*. 155(3):1304-1315.

Ganz T. (2006). Hepcidin--a peptide hormone at the interface of innate immunity and iron metabolism. *Curr Top Microbiol Immunol*. 306:183-198.

Ganz T. and Lehrer R. I. (1999). Antibiotic peptides from higher eukaryotes: biology and applications. *Mol Med Today*. 5(7):292-297.

Gao L. Y. and Kwaik Y. A. (2000). The modulation of host cell apoptosis by intracellular bacterial pathogens. *Trends Microbiol*. 8(7):306-313.

Gaspar D., Veiga A. S. and Castanho M. A. (2013). From antimicrobial to anticancer peptides. A review. *Front Microbiol*. 4:294.

Giacometti A., Cirioni O., Kamysz W., D'Amato G., Silvestri C., Simona Del Prete M., Lukasiak J. and Scalise G. (2004). In vitro activity and killing effect of the synthetic hybrid cecropin A-melittin peptide CA(1-7)M(2-9)NH(2) on methicillin-resistant nosocomial isolates of Staphylococcus aureus and interactions with clinically used antibiotics. *Diagn Microbiol Infect Dis*. 49(3):197-200.

Giangaspero A., Sandri L. and Tossi A. (2001). Amphipathic alpha helical antimicrobial peptides. *Eur J Biochem*. 268(21):5589-5600.

Gifford J. L., Hunter H. N. and Vogel H. J. (2005). Lactoferricin: a lactoferrin-derived peptide with antimicrobial, antiviral, antitumor and immunological properties. *Cell Mol Life Sci*. 62(22):2588-2598.

Gomes M. S. and Appelberg R. (2002). NRAMP1- or cytokine-induced bacteriostasis of Mycobacterium avium by mouse macrophages is independent of the respiratory burst. *Microbiology*. 148(10):3155-3160.

Gomes M. S., Boelaert J. R. and Appelberg R. (2001). Role of iron in experimental Mycobacterium avium infection. *J Clin Virol*. 20(3):117-122.

Gomes M. S., Dom G., Pedrosa J., Boelaert J. R. and Appelberg R. (1999a). Effects of iron deprivation on Mycobacterium avium growth. *Tuber Lung Dis*. 79(5):321-328.

Gomes M. S., Flórido M., Pais T. F. and Appelberg R. (1999b). Improved Clearance of Mycobacterium avium Upon Disruption of the Inducible Nitric Oxide Synthase Gene. *J Immunol*. 162(11):6734-6739.

Gomes M. S., Paul S., Moreira A. L., Appelberg R., Rabinovitch M. and Kaplan G. (1999c). Survival of Mycobacterium avium and Mycobacterium tuberculosis in Acidified Vacuoles of Murine Macrophages. *Infect Immun*. 67(7):3199-3206.

Gough M., Hancock R. E. and Kelly N. M. (1996). Antiendotoxin activity of cationic peptide antimicrobial agents. *Infect Immun*. 64(12):4922-4927.

Groenink J., Walgreen-Weterings E., van 't Hof W., Veerman E. C. I. and Nieuw Amerongen A. V. (1999). Cationic amphipathic peptides, derived from bovine and human

lactoferrins, with antimicrobial activity against oral pathogens. *FEMS Microbiol Lett*. 179(2):217-222.

Guaní-Guerra E., Santos-Mendoza T., Lugo-Reyes S. O. and Terán L. M. (2010). Antimicrobial peptides: General overview and clinical implications in human health and disease. *Clin Immunol*. 135(1):1-11.

Guenin-Mace L., Simeone R. and Demangel C. (2009). Lipids of pathogenic Mycobacteria: contributions to virulence and host immune suppression. *Transbound Emerg Dis*. 56(6-7):255-268.

Gutierrez M. G., Master S. S., Singh S. B., Taylor G. A., Colombo M. I. and Deretic V. (2004). Autophagy is a defense mechanism inhibiting BCG and Mycobacterium tuberculosis survival in infected macrophages. *Cell*. 119(6):753-766.

Habermann E. (1972). Bee and wasp venoms. *Science*. 177(4046):314-322.

Habets M. G. and Brockhurst M. A. (2012). Therapeutic antimicrobial peptides may compromise natural immunity. *Biol Lett*. 8(3):416-418.

Hancock R. E. and Chapple D. S. (1999). Peptide antibiotics. *Antimicrob Agents Chemother*. 43(6):1317-1323.

Hancock R. E. and Sahl H. G. (2006). Antimicrobial and host-defense peptides as new anti-infective therapeutic strategies. *Nat Biotechnol*. 24(12):1551-1557.

Haney E. F., Lau F. and Vogel H. J. (2007). Solution structures and model membrane interactions of lactoferrampin, an antimicrobial peptide derived from bovine lactoferrin. *Biochim Biophys Acta*. 1768(10):2355-2364.

Haney E. F., Nathoo S., Vogel H. J. and Prenner E. J. (2010). Induction of non-lamellar lipid phases by antimicrobial peptides: a potential link to mode of action. *Chem Phys Lipids*. 163(1):82-93.

Haney E. F., Nazmi K., Bolscher J. G. and Vogel H. J. (2012a). Influence of specific amino acid side-chains on the antimicrobial activity and structure of bovine lactoferrampin. *Biochem Cell Biol*. 90(3):362-377.

Haney E. F., Nazmi K., Bolscher J. G. and Vogel H. J. (2012b). Structural and biophysical characterization of an antimicrobial peptide chimera comprised of lactoferricin and lactoferrampin. *Biochim Biophys Acta*. 1818(3):762-775.

Heiko H. (2004). The microcalorimetry of lipid membranes. *J Phys Condens Matter*. 16(15):R441.

Henkle E. and Winthrop K. L. (2015). Nontuberculous mycobacteria infections in immunosuppressed hosts. *Clin Chest Med*. 36(1):91-99.

Henriques S. T., Melo M. N. and Castanho M. A. (2006). Cell-penetrating peptides and antimicrobial peptides: how different are they? *Biochem J*. 399(1):1-7.

Hickel A., Danner-Pongratz S., Amenitsch H., Degovics G., Rappolt M., Lohner K. and Pabst G. (2008). Influence of antimicrobial peptides on the formation of nonlamellar lipid mesophases. *Biochim Biophys Acta*. 1778(10):2325-2333.

Holak T. A., Engstrom A., Kraulis P. J., Lindeberg G., Bennich H., Jones T. A., Gronenborn A. M. and Clore G. M. (1988). The solution conformation of the antibacterial peptide cecropin A: a nuclear magnetic resonance and dynamical simulated annealing study. *Biochemistry*. 27(20):7620-7629.

Horsburgh C. R., Gettings J., Alexander L. N. and Lennox J. L. (2001). Disseminated Mycobacterium avium Complex Disease among Patients Infected with Human Immunodeficiency Virus, 1985–2000. *Clin Infect Dis*. 33(11):1938-1943.

Jankute M., Cox J. A., Harrison J. and Besra G. S. (2015). Assembly of the Mycobacterial Cell Wall. *Annu Rev Microbiol*. 69(1):405-423.

Jena P., Mishra B., Leippe M., Hasilik A., Griffiths G. and Sonawane A. (2011). Membrane-active antimicrobial peptides and human placental lysosomal extracts are highly active against mycobacteria. *Peptides*. 32(5):881-887.

Jenssen H. and Hancock R. E. (2009). Antimicrobial properties of lactoferrin. *Biochimie*. 91(1):19-29.

Jiang Z., Higgins M. P., Whitehurst J., Kisich K. O., Voskuil M. I. and Hodges R. S. (2011). Anti-tuberculosis activity of alpha-helical antimicrobial peptides: de novo designed L- and D-enantiomers versus L- and D-LL-37. *Protein Pept Lett*. 18(3):241-252.

Jiang Z., Vasil A. I., Hale J. D., Hancock R. E., Vasil M. L. and Hodges R. S. (2008). Effects of net charge and the number of positively charged residues on the biological activity of amphipathic alpha-helical cationic antimicrobial peptides. *Biopolymers*. 90(3):369-383.

Joo H. S. and Otto M. (2015). Mechanisms of resistance to antimicrobial peptides in staphylococci. *Biochim Biophys Acta*. 1848(11 Pt B):3055-3061.

Juvvadi P., Vunnam S., Merrifield E. L., Boman H. G. and Merrifield R. B. (1996). Hydrophobic effects on antibacterial and channel-forming properties of cecropin A-melittin hybrids. *J Pept Sci*. 2(4):223-232.

Kalita A., Verma I. and Khuller G. K. (2004). Role of Human Neutrophil Peptide-1 as a Possible Adjunct to Antituberculosis Chemotherapy. *J Infect Dis*. 190(8):1476-1480.

Kanthawong S., Puknun A., Bolscher J. G., Nazmi K., van Marle J., de Soet J. J., Veerman E. C., Wongratanacheewin S. and Taweechaisupapong S. (2014). Membrane-active mechanism of LFchimera against Burkholderia pseudomallei and Burkholderia thailandensis. *Biometals*. 27(5):949-956.

Khara J. S., Wang Y., Ke X. Y., Liu S., Newton S. M., Langford P. R., Yang Y. Y. and Ee P. L. (2014). Anti-mycobacterial activities of synthetic cationic alpha-helical peptides and their synergism with rifampicin. *Biomaterials*. 35(6):2032-2038.

Kisich K. O., Heifets L., Higgins M. and Diamond G. (2001). Antimycobacterial agent based on mRNA encoding human beta-defensin 2 enables primary macrophages to restrict growth of Mycobacterium tuberculosis. *Infect Immun*. 69(4):2692-2699.

Kobayashi S., Chikushi A., Tougu S., Imura Y., Nishida M., Yano Y. and Matsuzaki K. (2004). Membrane Translocation Mechanism of the Antimicrobial Peptide Buforin 2. *Biochemistry*. 43(49):15610-15616.

Kobayashi S., Takeshima K., Park C. B., Kim S. C. and Matsuzaki K. (2000). Interactions of the novel antimicrobial peptide buforin 2 with lipid bilayers: proline as a translocation promoting factor. *Biochemistry*. 39(29):8648-8654.

Kondejewski L. H., Lee D. L., Jelokhani-Niaraki M., Farmer S. W., Hancock R. E. and Hodges R. S. (2002). Optimization of microbial specificity in cyclic peptides by modulation of hydrophobicity within a defined structural framework. *J Biol Chem*. 277(1):67-74.

Koprivnjak T. and Peschel A. (2011). Bacterial resistance mechanisms against host defense peptides. *Cell Mol Life Sci*. 68(13):2243-2254.

Koul A., Arnoult E., Lounis N., Guillemont J. and Andries K. (2011). The challenge of new drug discovery for tuberculosis. *Nature*. 469(7331):483-490.

Kuwata H., Yip T. T., Tomita M. and Hutchens T. W. (1998). Direct evidence of the generation in human stomach of an antimicrobial peptide domain (lactoferricin) from ingested lactoferrin. *Biochim Biophys Acta*. 1429(1):129-141.

Lafleur M., Samson I. and Pezolet M. (1991). Investigation of the interaction between melittin and dipalmitoylphosphatidylglycerol bilayers by vibrational spectroscopy. *Chem Phys Lipids*. 59(3):233-244.

LaRock C. N. and Nizet V. (2015). Cationic antimicrobial peptide resistance mechanisms of streptococcal pathogens. *Biochim Biophys Acta*. 1848(11 Pt B):3047-3054.

Leon-Sicairos N., Angulo-Zamudio U. A., Vidal J. E., Lopez-Torres C. A., Bolscher J. G., Nazmi K., Reyes-Cortes R., Reyes-Lopez M., de la Garza M. and Canizalez-Roman A. (2014). Bactericidal effect of bovine lactoferrin and synthetic peptide lactoferrin chimera in Streptococcus pneumoniae and the decrease in luxS gene expression by lactoferrin. *Biometals*. 27(5):969-980.

Leon-Sicairos N., Canizalez-Roman A., de la Garza M., Reyes-Lopez M., Zazueta-Beltran J., Nazmi K., Gomez-Gil B. and Bolscher J. G. (2009). Bactericidal effect of lactoferrin and lactoferrin chimera against halophilic Vibrio parahaemolyticus. *Biochimie*. 91(1):133-140.

Leon-Sicairos N., Reyes-Lopez M., Ordaz-Pichardo C. and de la Garza M. (2006). Microbicidal action of lactoferrin and lactoferricin and their synergistic effect with metronidazole in Entamoeba histolytica. *Biochem Cell Biol*. 84(3):327-336.

Li Y., Xiang Q., Zhang Q., Huang Y. and Su Z. (2012). Overview on the recent study of antimicrobial peptides: origins, functions, relative mechanisms and application. *Peptides*. 37(2):207-215.

Liu P. T., Stenger S., Tang D. H. and Modlin R. L. (2007). Cutting edge: vitamin D-mediated human antimicrobial activity against Mycobacterium tuberculosis is dependent on the induction of cathelicidin. *J Immunol*. 179(4):2060-2063.

Lohner K. (2009). New strategies for novel antibiotics: peptides targeting bacterial cell membranes. *Gen Physiol Biophys*. 28(2):105-116.

Lohner K. and Blondelle S. E. (2005). Molecular mechanisms of membrane perturbation by antimicrobial peptides and the use of biophysical studies in the design of novel peptide antibiotics. *Comb Chem High Throughput Screen*. 8(3):241-256.

Lohner K. and Prenner E. J. (1999). Differential scanning calorimetry and X-ray diffraction studies of the specificity of the interaction of antimicrobial peptides with membrane-mimetic systems. *Biochim Biophys Acta*. 1462(1-2):141-156.

Lopez-Soto F., Leon-Sicairos N., Nazmi K., Bolscher J. G. and de la Garza M. (2010). Microbicidal effect of the lactoferrin peptides lactoferricin17-30, lactoferrampin265-284, and lactoferrin chimera on the parasite Entamoeba histolytica. *Biometals*. 23(3):563-568.

Luzzati V. (1997). Biological significance of lipid polymorphism: the cubic phases. *Curr Opin Struct Biol*. 7(5):661-668.

Luzzati V., Delacroix H., Gulik A., Gulik-Krzywicki T., Mariani P. and Vargas R. (1997). Chapter 1 The Cubic Phases of Lipids. In **Current Topics in Membranes**. Edited by M. E. Richard, Academic Press. Volume 44: 3-24.

Mackler B. F. and Kreil G. (1977). Honey bee venom melittin: correlation of nonspecific inflammatory activities with amino acid sequences. *Inflammation*. 2(1):55-65.

MacMicking J. D., North R. J., LaCourse R., Mudgett J. S., Shah S. K. and Nathan C. F. (1997). Identification of nitric oxide synthase as a protective locus against tuberculosis. *Proc Natl Acad Sci U S A*. 94(10):5243-5248.

Mader J. S., Richardson A., Salsman J., Top D., de Antueno R., Duncan R. and Hoskin D. W. (2007). Bovine lactoferricin causes apoptosis in Jurkat T-leukemia cells by sequential permeabilization of the cell membrane and targeting of mitochondria. *Exp Cell Res*. 313(12):2634-2650.

Mader J. S., Salsman J., Conrad D. M. and Hoskin D. W. (2005). Bovine lactoferricin selectively induces apoptosis in human leukemia and carcinoma cell lines. *Mol Cancer Ther*. 4(4):612-624.

Mansour S. C., Pena O. M. and Hancock R. E. (2014). Host defense peptides: front-line immunomodulators. *Trends Immunol*. 35(9):443-450.

Maria-Neto S., de Almeida K. C., Macedo M. L. and Franco O. L. (2015). Understanding bacterial resistance to antimicrobial peptides: From the surface to deep inside. *Biochim Biophys Acta*.

Matamouros S. and Miller S. I. (2015). S. Typhimurium strategies to resist killing by cationic antimicrobial peptides. *Biochim Biophys Acta*. 1848(11 Pt B):3021-3025.

Mataraci E. and Dosler S. (2012). In vitro activities of antibiotics and antimicrobial cationic peptides alone and in combination against methicillin-resistant Staphylococcus aureus biofilms. *Antimicrob Agents Chemother*. 56(12):6366-6371.

Mendez-Samperio P. (2008). Role of antimicrobial peptides in host defense against mycobacterial infections. *Peptides*. 29(10):1836-1841.

Merrifield E. L., Mitchell S. A., Ubach J., Boman H. G., Andreu D. and Merrifield R. B. (1995). D-enantiomers of 15-residue cecropin A-melittin hybrids. *Int J Pept Protein Res*. 46(3-4):214-220.

Merrifield R. B., Vizioli L. D. and Boman H. G. (1982). Synthesis of the antibacterial peptide cecropin A (1-33). *Biochemistry*. 21(20):5020-5031.

Milani A., Benedusi M., Aquila M. and Rispoli G. (2009). Pore forming properties of cecropin-melittin hybrid peptide in a natural membrane. *Molecules*. 14(12):5179-5188.

Moniz T., Nunes A., Silva A. M., Queiros C., Ivanova G., Gomes M. S. and Rangel M. (2013). Rhodamine labeling of 3-hydroxy-4-pyridinone iron chelators is an important contribution to target Mycobacterium avium infection. *J Inorg Biochem*. 121:156-166.

Moniz T., Silva D., Silva T., Gomes M. S. and Rangel M. (2015). Antimycobacterial activity of rhodamine 3,4-HPO iron chelators against Mycobacterium avium: analysis of the contribution of functional groups and of chelator's combination with ethambutol. *Med Chem Commun*. 6(12):2194-2203.

Nathan C. (2014). Drug-resistant tuberculosis: a new shot on goal. *Nat Med*. 20(2):121-123.

Nguyen L. T., Haney E. F. and Vogel H. J. (2011). The expanding scope of antimicrobial peptide structures and their modes of action. *Trends Biotechnol*. 29(9):464-472.

Nicolas P. (2009). Multifunctional host defense peptides: intracellular-targeting antimicrobial peptides. *FEBS J*. 276(22):6483-6496.

Nizet V., Ohtake T., Lauth X., Trowbridge J., Rudisill J., Dorschner R. A., Pestonjamasp V., Piraino J., Huttner K. and Gallo R. L. (2001). Innate antimicrobial peptide protects the skin from invasive bacterial infection. *Nature*. 414(6862):454-457.

Nos-Barbera S., Portoles M., Morilla A., Ubach J., Andreu D. and Paterson C. A. (1997). Effect of hybrid peptides of cecropin A and melittin in an experimental model of bacterial keratitis. *Cornea*. 16(1):101-106.

Nuri R., Shprung T. and Shai Y. (2015). Defensive remodeling: How bacterial surface properties and biofilm formation promote resistance to antimicrobial peptides. *Biochim Biophys Acta*. 1848(11 Pt B):3089-3100.

O'Brien R., Chowdhry B. Z. and Ladbury J. E. (2001). Isothermal titration calorimetry of biomecules. Chapter 10, In **Protein-Ligand Interactions: hydrodynamics and calorimetry**. Edited by S. E. Harding and B. Z. Chowdhry. United Sates, Oxford University Press.

Ogata K., Linzer B. A., Zuberi R. I., Ganz T., Lehrer R. I. and Catanzaro A. (1992). Activity of defensins from human neutrophilic granulocytes against Mycobacterium avium-Mycobacterium intracellulare. *Infect Immun*. 60(11):4720-4725.

Pabst G., Zweytick D., Prassl R. and Lohner K. (2012). Use of X-ray scattering to aid the design and delivery of membrane-active drugs. *Eur Biophys J*. 41(10):915-929.

Pais T. F. and Appelberg R. (2000). Macrophage control of mycobacterial growth induced by picolinic acid is dependent on host cell apoptosis. *J Immunol*. 164(1):389-397.

Pais T. F. and Appelberg R. (2004). Induction of Mycobacterium avium growth restriction and inhibition of phagosome-endosome interactions during macrophage activation and apoptosis induction by picolinic acid plus IFNgamma. *Microbiology*. 150(Pt 5):1507-1518.

Pan W. R., Chen P. W., Chen Y. L., Hsu H. C., Lin C. C. and Chen W. J. (2013). Bovine lactoferricin B induces apoptosis of human gastric cancer cell line AGS by inhibition of autophagy at a late stage. *J Dairy Sci*. 96(12):7511-7520.

Philley J. V. and Griffith D. E. (2015). Treatment of slowly growing mycobacteria. *Clin Chest Med*. 36(1):79-90.

Piers K. L., Brown M. H. and Hancock R. E. (1994). Improvement of outer membrane-permeabilizing and lipopolysaccharide-binding activities of an antimicrobial cationic peptide by C-terminal modification. *Antimicrob Agents Chemother*. 38(10):2311-2316.

Pieters J. (2001). Entry and survival of pathogenic mycobacteria in macrophages. *Microbes Infect*. 3(3):249-255.

Pistolesi S., Pogni R. and Feix J. B. (2007). Membrane insertion and bilayer perturbation by antimicrobial peptide CM15. *Biophys J*. 93(5):1651-1660.

Pozo Navas B., Lohner K., Deutsch G., Sevcsik E., Riske K. A., Dimova R., Garidel P. and Pabst G. (2005). Composition dependence of vesicle morphology and mixing properties in a bacterial model membrane system. *Biochim Biophys Acta*. 1716(1):40-48.

Prescott L. M., Harley J. P. and Klein D. A. (2002). Microbiology. Boston, McGraw Hill.

Putsep K., Carlsson G., Boman H. G. and Andersson M. (2002). Deficiency of antibacterial peptides in patients with morbus Kostmann: an observation study. *Lancet*. 360(9340):1144-1149.

Qiu H. and Caffrey M. (2000). The phase diagram of the monoolein/water system: metastability and equilibrium aspects. *Biomaterials*. 21(3):223-234.

Raghuraman H. and Chattopadhyay A. (2004). Interaction of melittin with membrane cholesterol: a fluorescence approach. *Biophys J*. 87(4):2419-2432.

Raghuraman H. and Chattopadhyay A. (2007). Melittin: a membrane-active peptide with diverse functions. *Biosci Rep*. 27(4-5):189-223.

Ramon-Garcia S., Mikut R., Ng C., Ruden S., Volkmer R., Reischl M., Hilpert K. and Thompson C. J. (2013). Targeting Mycobacterium tuberculosis and Other Microbial Pathogens Using Improved Synthetic Antibacterial Peptides. *Antimicrob Agents Chemother*. 57(5):2295-2303.

Riedl S., Zweytick D. and Lohner K. (2011). Membrane-active host defense peptides--challenges and perspectives for the development of novel anticancer drugs. *Chem Phys Lipids*. 164(8):766-781.

Rivas-Santiago B., Hernandez-Pando R., Carranza C., Juarez E., Contreras J. L., Aguilar-Leon D., Torres M. and Sada E. (2008). Expression of cathelicidin LL-37 during Mycobacterium tuberculosis infection in human alveolar macrophages, monocytes, neutrophils, and epithelial cells. *Infect Immun*. 76(3):935-941.

Rivas-Santiago B., Rivas Santiago C. E., Castaneda-Delgado J. E., Leon-Contreras J. C., Hancock R. E. and Hernandez-Pando R. (2013). Activity of LL-37, CRAMP and antimicrobial peptide-derived compounds E2, E6 and CP26 against Mycobacterium tuberculosis. *Int J Antimicrob Agents*. 41(2):143-148.

Rivas-Santiago C. E., Rivas-Santiago B., Leon D. A., Castaneda-Delgado J. and Hernandez Pando R. (2011). Induction of beta-defensins by l-isoleucine as novel immunotherapy in experimental murine tuberculosis. *Clin Exp Immunol*. 164(1):80-89.

Rivas L., Luque-Ortega J. R. and Andreu D. (2009). Amphibian antimicrobial peptides and Protozoa: Lessons from parasites. *Biochim Biophys Acta*. 1788(8):1570-1581.

Rodriguez-Hernandez M. J., Saugar J., Docobo-Perez F., de la Torre B. G., Pachon-Ibanez M. E., Garcia-Curiel A., Fernandez-Cuenca F., Andreu D., Rivas L. and Pachon J. (2006). Studies on the antimicrobial activity of cecropin A-melittin hybrid peptides in colistin-resistant clinical isolates of Acinetobacter baumannii. *J Antimicrob Chemother*. 58(1):95-100.

Rotem S. and Mor A. (2009). Antimicrobial peptide mimics for improved therapeutic properties. *Biochim Biophys Acta*. 1788(8):1582-1592.

Salomone F., Cardarelli F., Di Luca M., Boccardi C., Nifosi R., Bardi G., Di Bari L., Serresi M. and Beltram F. (2012). A novel chimeric cell-penetrating peptide with membrane-disruptive properties for efficient endosomal escape. *J Control Release*. 163(3):293-303.

Salomone F., Cardarelli F., Signore G., Boccardi C. and Beltram F. (2013). In vitro efficient transfection by CM(1)(8)-Tat(1)(1) hybrid peptide: a new tool for gene-delivery applications. *PLoS One*. 8(7):e70108.

Salzman N. H., Ghosh D., Huttner K. M., Paterson Y. and Bevins C. L. (2003). Protection against enteric salmonellosis in transgenic mice expressing a human intestinal defensin. *Nature*. 422(6931):522-526.

Samuelsen O., Haukland H. H., Jenssen H., Kramer M., Sandvik K., Ulvatne H. and Vorland L. H. (2005). Induced resistance to the antimicrobial peptide lactoferricin B in Staphylococcus aureus. *FEBS Lett*. 579(16):3421-3426.

Sanchez-Gomez S., Japelj B., Jerala R., Moriyon I., Fernandez Alonso M., Leiva J., Blondelle S. E., Andra J., Brandenburg K., Lohner K. and Martinez de Tejada G. (2011). Structural features governing the activity of lactoferricin-derived peptides that act in synergy with antibiotics against Pseudomonas aeruginosa in vitro and in vivo. *Antimicrob Agents Chemother*. 55(1):218-228.

Santos J. C., Silva-Gomes S., Silva J. P., Gama M., Rosa G., Gallo R. L. and Appelberg R. (2014). Endogenous cathelicidin production limits inflammation and protective immunity to Mycobacterium avium in mice. *Immun Inflamm Dis*. 2(1):1-12.

Sato H. and Feix J. B. (2006). Osmoprotection of bacterial cells from toxicity caused by antimicrobial hybrid peptide CM15. *Biochemistry*. 45(33):9997-10007.

Schaible U. E., Sturgill-Koszycki S., Schlesinger P. H. and Russell D. G. (1998). Cytokine activation leads to acidification and increases maturation of Mycobacterium avium-containing phagosomes in murine macrophages. *J Immunol*. 160(3):1290-1296.

Seabra S. H., de Souza W. and Damatta R. A. (2004). Toxoplasma gondii exposes phosphatidylserine inducing a TGF-beta1 autocrine effect orchestrating macrophage evasion. *Biochem Biophys Res Commun*. 324(2):744-752.

Seddon J. M. and Templer R. H. (1995). Chapter 3 - Polymorphism of Lipid-Water Systems. In **Handbook of Biological Physics**. Edited by R. Lipowsky and E. Sackmann, North-Holland. Volume 1: 97-160.

Seelig J. (1997). Titration calorimetry of lipid-peptide interactions. *Biochim Biophys Acta*. 1331(1):103-116.

Seelig J. (2004). Thermodynamics of lipid-peptide interactions. *Biochim Biophys Acta*. 1666(1-2):40-50.

Selvaraj P., Harishankar M. and Afsal K. (2015). Vitamin D: Immuno-modulation and tuberculosis treatment. *Can J Physiol Pharmacol*. 93(5):377-384.

Seo M. D., Won H. S., Kim J. H., Mishig-Ochir T. and Lee B. J. (2012). Antimicrobial peptides for therapeutic applications: a review. *Molecules*. 17(10):12276-12286.

Sevcsik E., Pabst G., Jilek A. and Lohner K. (2007). How lipids influence the mode of action of membrane-active peptides. *Biochim Biophys Acta*. 1768(10):2586-2595.

Sevcsik E., Pabst G., Richter W., Danner S., Amenitsch H. and Lohner K. (2008). Interaction of LL-37 with model membrane systems of different complexity: influence of the lipid matrix. *Biophys J*. 94(12):4688-4699.

Sharma S., Verma I. and Khuller G. K. (2000). Antibacterial activity of human neutrophil peptide-1 against Mycobacterium tuberculosis H37Rv: in vitro and ex vivo study. *Eur Respir J*. 16(1):112-117.

Sharma S., Verma I. and Khuller G. K. (2001). Therapeutic potential of human neutrophil peptide 1 against experimental tuberculosis. *Antimicrob Agents Chemother*. 45(2):639-640.

Shin D. M. and Jo E. K. (2011). Antimicrobial Peptides in Innate Immunity against Mycobacteria. *Immune Netw*. 11(5):245-252.

Shin S. Y., Lee S. H., Yang S. T., Park E. J., Lee D. G., Lee M. K., Eom S. H., Song W. K., Kim Y., Hahm K. S. and Kim J. I. (2001). Antibacterial, antitumor and hemolytic activities of alpha-helical antibiotic peptide, P18 and its analogs. *J Pept Res*. 58(6):504-514.

Silva-Gomes S., Bouton C., Silva T., Santambrogio P., Rodrigues P., Appelberg R. and Gomes M. S. (2013). Mycobacterium avium infection induces H-ferritin expression in mouse primary macrophages by activating Toll-like receptor 2. *PLoS One*. 8(12):e82874.

Silva T., Abengozar M. A., Fernandez-Reyes M., Andreu D., Nazmi K., Bolscher J. G., Bastos M. and Rivas L. (2012). Enhanced leishmanicidal activity of cryptopeptide chimeras from the active N1 domain of bovine lactoferrin. *Amino Acids*. 43(6):2265-2277.

Silvestro L. and Axelsen P. H. (2000). Membrane-induced folding of cecropin A. *Biophys J*. 79(3):1465-1477.

Sonawane A., Santos J. C., Mishra B. B., Jena P., Progida C., Sorensen O. E., Gallo R., Appelberg R. and Griffiths G. (2011). Cathelicidin is involved in the intracellular killing of mycobacteria in macrophages. *Cell Microbiol*. 13(10):1601-1617.

Sood R. and Kinnunen P. K. (2008). Cholesterol, lanosterol, and ergosterol attenuate the membrane association of LL-37(W27F) and temporin L. *Biochim Biophys Acta*. 1778(6):1460-1466.

Sow F. B., Florence W. C., Satoskar A. R., Schlesinger L. S., Zwilling B. S. and Lafuse W. P. (2007). Expression and localization of hepcidin in macrophages: a role in host defense against tuberculosis. *J Leukoc Biol*. 82(4):934-945.

Spellberg B. and Shlaes D. (2014). Prioritized current unmet needs for antibacterial therapies. *Clin Pharmacol Ther*. 96(2):151-153.

Steiner H. (1982). Secondary structure of the cecropins: antibacterial peptides from the moth Hyalophora cecropia. *FEBS Lett*. 137(2):283-287.

Steiner H., Hultmark D., Engstrom A., Bennich H. and Boman H. G. (1981). Sequence and specificity of two antibacterial proteins involved in insect immunity. *Nature*. 292(5820):246-248.

Steinstraesser L., Kraneburg U., Jacobsen F. and Al-Benna S. (2011). Host defense peptides and their antimicrobial-immunomodulatory duality. *Immunobiology*. 216(3):322-333.

Teixeira V., Feio M. J. and Bastos M. (2012). Role of lipids in the interaction of antimicrobial peptides with membranes. *Prog Lipid Res*. 51(2):149-177.

Teixeira V., Feio M. J., Rivas L., De la Torre B. G., Andreu D., Coutinho A. and Bastos M. (2010). Influence of Lysine Nε-Trimethylation and Lipid Composition on the Membrane Activity of the Cecropin A-Melittin Hybrid Peptide CA(1−7)M(2−9). *J Phys Chem B*. 114(49):16198-16208.

Teng T., Liu J. and Wei H. (2015). Anti-mycobacterial peptides: from human to phage. *Cell Physiol Biochem*. 35(2):452-466.

Tomita M., Bellamy W., Takase M., Yamauchi K., Wakabayashi H. and Kawase K. (1991). Potent antibacterial peptides generated by pepsin digestion of bovine lactoferrin. *J Dairy Sci*. 74(12):4137-4142.

Tortoli E. (2006). The new mycobacteria: an update. *FEMS Immunol Med Microbiol*. 48(2):159-178.

Tortoli E. (2009). Clinical manifestations of nontuberculous mycobacteria infections. *Clin Microbiol Infect*. 15(10):906-910.

Tresset G. (2009). The multiple faces of self-assembled lipidic systems. *PMC Biophys*. 2(1):3.

van 't Hof W., Veerman E. C., Helmerhorst E. J. and Amerongen A. V. (2001). Antimicrobial peptides: properties and applicability. *Biol Chem*. 382(4):597-619.

van der Kraan M. I., Groenink J., Nazmi K., Veerman E. C., Bolscher J. G. and Nieuw Amerongen A. V. (2004). Lactoferrampin: a novel antimicrobial peptide in the N1-domain of bovine lactoferrin. *Peptides*. 25(2):177-183.

van der Kraan M. I., Nazmi K., Teeken A., Groenink J., van 't Hof W., Veerman E. C., Bolscher J. G. and Nieuw Amerongen A. V. (2005a). Lactoferrampin, an antimicrobial

peptide of bovine lactoferrin, exerts its candidacidal activity by a cluster of positively charged residues at the C-terminus in combination with a helix-facilitating N-terminal part. *Biol Chem*. 386(2):137-142.

van der Kraan M. I., Nazmi K., van 't Hof W., Amerongen A. V., Veerman E. C. and Bolscher J. G. (2006). Distinct bactericidal activities of bovine lactoferrin peptides LFampin 268-284 and LFampin 265-284: Asp-Leu-Ile makes a difference. *Biochem Cell Biol*. 84(3):358-362.

van der Kraan M. I., van Marle J., Nazmi K., Groenink J., van 't Hof W., Veerman E. C., Bolscher J. G. and Nieuw Amerongen A. V. (2005b). Ultrastructural effects of antimicrobial peptides from bovine lactoferrin on the membranes of Candida albicans and Escherichia coli. *Peptides*. 26(9):1537-1542.

Via L. E., Fratti R. A., McFalone M., Pagan-Ramos E., Deretic D. and Deretic V. (1998). Effects of cytokines on mycobacterial phagosome maturation. *J Cell Sci*. 111 (Pt 7):897-905.

Vogel H. (1981). Incorporation of melittin into phosphatidylcholine bilayers. Study of binding and conformational changes. *FEBS Lett*. 134(1):37-42.

Wade D., Boman A., Wahlin B., Drain C. M., Andreu D., Boman H. G. and Merrifield R. B. (1990). All-D amino acid-containing channel-forming antibiotic peptides. *Proc Natl Acad Sci U S A*. 87(12):4761-4765.

Wakabayashi H., Takase M. and Tomita M. (2003). Lactoferricin derived from milk protein lactoferrin. *Curr Pharm Des*. 9(16):1277-1287.

Wanderley J. L., Moreira M. E., Benjamin A., Bonomo A. C. and Barcinski M. A. (2006). Mimicry of apoptotic cells by exposing phosphatidylserine participates in the establishment of amastigotes of Leishmania (L) amazonensis in mammalian hosts. *J Immunol*. 176(3):1834-1839.

Wang G., Li X. and Wang Z. (2009). APD2: the updated antimicrobial peptide database and its application in peptide design. *Nucleic Acids Res*. 37(Database issue):D933-937.

Wassef M. K., Fioretti T. B. and Dwyer D. M. (1985). Lipid analyses of isolated surface membranes of Leishmania donovani promastigotes. *Lipids*. 20(2):108-115.

WHO (2015a) Antimicrobial Resistance. Fact Sheet Nº 194. World Health Organization Media Center. Accessed on September 2015, from http://www.who.int/mediacentre/factsheets/fs194/en/

WHO (2015b) Global tuberculosis report 2015. World Health Organization. from http://www.who.int/tb/publications/global_report/en/

Wieprecht T., Apostolov O., Beyermann M. and Seelig J. (2000). Membrane binding and pore formation of the antibacterial peptide PGLa: thermodynamic and mechanistic aspects. *Biochemistry*. 39(2):442-452.

Wieprecht T., Beyermann M. and Seelig J. (1999). Binding of antibacterial magainin peptides to electrically neutral membranes: thermodynamics and structure. *Biochemistry*. 38(32):10377-10387.

Wiesner J. and Vilcinskas A. (2010). Antimicrobial peptides: The ancient arm of the human immune system. *Virulence*. 1(5):440-464.

Yamauchi K., Tomita M., Giehl T. J. and Ellison Iii R. T. (1993). Antibacterial activity of lactoferrin and a pepsin-derived lactoferrin peptide fragment. *Infect Immun*. 61(2):719-728.

Yeung A. T., Gellatly S. L. and Hancock R. E. (2011). Multifunctional cationic host defence peptides and their clinical applications. *Cell Mol Life Sci*. 68(13):2161-2176.

Yoo Y. C., Watanabe R., Koike Y., Mitobe M., Shimazaki K., Watanabe S. and Azuma I. (1997a). Apoptosis in human leukemic cells induced by lactoferricin, a bovine milk protein-derived peptide: involvement of reactive oxygen species. *Biochem Biophys Res Commun*. 237(3):624-628.

Yoo Y. C., Watanabe S., Watanabe R., Hata K., Shimazaki K. and Azuma I. (1997b). Bovine lactoferrin and lactoferricin, a peptide derived from bovine lactoferrin, inhibit tumor metastasis in mice. *Jpn J Cancer Res*. 88(2):184-190.

Yuk J. M., Shin D. M., Lee H. M., Yang C. S., Jin H. S., Kim K. K., Lee Z. W., Lee S. H., Kim J. M. and Jo E. K. (2009). Vitamin D3 induces autophagy in human monocytes/macrophages via cathelicidin. *Cell Host Microbe*. 6(3):231-243.

Zasloff M. (2002). Antimicrobial peptides of multicellular organisms. *Nature*. 415(6870):389-395.

PART II. RESULTS

CHAPTER 5. Understanding the mechanism of action of a cecropin A-melittin hybrid antimicrobial peptide – a manifold biophysical approach

Understanding the mechanism of action of a cecropin A-melittin hybrid antimicrobial peptide - a manifold biophysical approach

Tânia Silva [a,b,c,d], Bruno Silva [e], Nuno Vale [f], Paula Gomes [f], Salomé Gomes [b,c,d], Sérgio S. Funari [g], Daniela Uhríková [h], Margarida Bastos [a,#]

[a] CIQ-UP – Centro de Investigação em Química, Departamento de Química e Bioquímica, Faculdade de Ciências, Universidade do Porto, 4169-007 Porto, Portugal;

[b] Instituto de Investigação e Inovação em Saúde, Universidade do Porto, Porto, Portugal;

[c] IBMC – Instituto de Biologia Molecular e Celular, Universidade do Porto, Porto, Portugal;

[d] ICBAS – Instituto de Ciências Biomédicas Abel Salazar, Universidade do Porto, Porto, Portugal;

[e] INL – International Iberian Nanotechnology Laboratory, Braga, Portugal;

[f] UCIBIO/REQUIMTE, Departamento de Química e Bioquímica, Faculdade de Ciências, Universidade do Porto, 4169-007 Porto, Portugal;

[g] HASYLAB, DESY, Hamburg, Germany;

[h] Faculty of Pharmacy, Comenius University, Bratislava, Slovak Republic.

Corresponding author: Margarida Bastos
Centro de Investigação em Química (CIQ-UP)
Department of Chemistry & Biochemistry
Faculty of Sciences, University of Porto,
R. Campo Alegre 697
4169-007 Porto, Portugal
Tel: +351 22 0402511
e-mail: mbastos@fc.up.pt

Abstract

The interaction of a cecropin A-melittin hybrid antimicrobial peptide, CA(1-7)M(2-9), with known antimicrobial action, was studied with bacterial model membranes of POPE/POPG 3:1 to contribute to an understanding of its mechanism of action. Several biophysical techniques were used to assess the structural and thermodynamics of the interaction. CA(1-7)M(2-9) disrupts the vesicles inducing membrane condensation, forming an onion-like structure of multilamellar held together by the intercalated peptides. DSC also indicated that the peptide induces extensive aggregation and stabilizes the gel lamellar phase suggesting a strong interaction with the membrane at the lipid heads level. Finally, ITC has shown that the energetics of the peptide/lipid interaction depend strongly on temperature, being endothermic in the gel lamellar phase and exothermic in the liquid crystalline phase. Further, the association ratio indicates that CA(1-7)M(2-9) only interacts with the outer leaflet, supporting the idea of a surface interaction with the membrane that leads to membrane condensation and not pore formation. Our results also indicate the existence of threshold value after which the behaviour changes. We thus propose that this peptide exerts its antimicrobial action through a carpet model where after a threshold concentration (related to membrane neutralization) there is membrane disruption and disintegration.

Introduction

Antimicrobial resistance is increasing rapidly, being one of the world's major health problem. Unfortunately, this is not being accompanied by the discovery of truly new drugs, but only 2nd and 3rd generation antibiotics (Fischbach and Walsh 2009, Bassetti *et al.* 2013). Nevertheless, intensive research exists aiming at the development of alternatives to the existing drugs. Among others, antimicrobial peptides (AMP) have being extensively studied, as a new antibiotic paradigm. These diverse group of compounds are widespread in nature being part of the innate immune system of almost all living organisms (Yeung *et al.* 2011). They are active against several pathogens, such as virus, protozoa, bacteria and fungi, acting primarily on the pathogen's membrane, but possibly having also intracellular targets (*e.g.* proteins, nucleic acids) and/or through immunomodulation (Nguyen *et al.* 2011, Mansour *et al.* 2014). This capacity of attacking in different fronts enables them to evade resistance more easily than conventional drugs (Nguyen *et al.* 2011). Several strategies have been employed to optimize the antimicrobial properties of these compounds with the main goal of decreasing their cytotoxicity towards host cells while maintaining or increasing their activity against pathogens. Further, attain a high selectivity index with AMP with the smallest possible number of amino acids (Haney and Hancock 2013).

One strategy that has been successfully used is hybridization, where parts of different peptides are combined into one molecule in order to optimize their individual characteristics (Brogden and Brogden 2011). Cecropin A-melittin hybrid peptides are one of the best examples of successful hybridization in the AMP field, and were first synthesized by Boman, *et al.* in 1989 (Boman *et al.* 1989). They are composed of the cationic region of cecropin A and the hydrophobic and non-haemolytic region of melittin. These hybrids have better antimicrobial properties than the parental compounds, with an improvement in the activity of cecropin A towards pathogens, together with a significant decrease in the haemolytic properties of melittin (Boman *et al.* 1989, Wade *et al.* 1990, Andreu *et al.* 1992). Their activity has been extensively studied, both on model membranes and pathogens, and their mechanism of action is thought to rely on membrane disruption due to the formation of toroidal pores and/or detergent-like action (Andreu *et al.* 1992, Diaz-Achirica *et al.* 1994, Juvvadi *et al.* 1996, Diaz-Achirica *et al.* 1998, Abrunhosa *et al.* 2005, Sato and Feix 2006, Pistolesi *et al.* 2007, Bastos *et al.* 2008, Ferre *et al.* 2009, Milani *et al.* 2009, Teixeira *et al.* 2010).

We have previously studied the interaction of CA(1-7)M(2-9) (or CAM), with model membranes of different compositions (Abrunhosa *et al.* 2005, Bastos *et al.* 2008, Teixeira *et al.* 2010). Following these works, we have now characterized the interaction of CAM

with model membranes of 1-palmitoyl-2-oleoyl-*sn*-glycero-3-phosphoethanolamine and 1-palmitoyl-2-oleoyl-*sn*-glycero-3-phospho-(1'-*rac*-glycerol) (POPE/POPG 3:1) using a variety of biophysical methods, in an attempt to ascertain its mechanism of action. The effect of the peptide was assessed by Small Angle X-ray Diffraction (SAXD), Differential Scanning Calorimetry (DSC), Isothermal Titration Calorimetry (ITC), Circular Dichroism (CD) and microscopy techniques.

Our results show that CAM interacts strongly with this negatively charged model membrane system, mainly through electrostatic interactions. We suggest that the peptide binds to the membrane until a threshold peptide/lipid ratio, after which it disrupts the vesicles inducing membrane condensation into a multilamellar system with the peptide intercalated within the lamellae, in an onion-like structure.

Material and Methods

Peptides

CA(1–7)M(2–9) or CAM (KWKLFKKIGAVLKVL-NH_2) was synthesized, purified, and characterized as described recently (Fernandez-Reyes *et al.* 2010). Peptide stock solutions were prepared in Phosphate Buffered Saline (PBS, 9.3 mM, 150 mM NaCl, pH 7.4) or HEPES buffer (HEPES 10 mM, 150 mM NaCl, pH=7.0) and stored at -20ºC until use.

Preparation of Liposomes

1-palmitoyl-2-oleoyl-*sn*-glycero-3-phosphoethanolamine (POPE) and 1-palmitoyl-2-oleoyl-*sn*-glycero-3-phospho-(1'-*rac*-glycerol) (POPG) (Avanti Polar Lipids, Alabama, USA) in a proportion 3:1, were dissolved in chloroform/methanol (3:1) and transferred to a round bottom flask, where a film was obtained by drying the solvent under a slow nitrogen stream. The film was thereafter kept under vacuum overnight to remove all traces of organic solvents. After drying, the lipid film was first warmed for 30 minutes at *ca.* 10 °C above the temperature of the gel-to-liquid crystalline phase transition (T_m) in a thermostated water bath, and afterwards hydrated with buffer, either HEPES (10 mM HEPES, 150 mM NaCl, pH 7.4) or PBS (9.3 mM, 150 mM NaCl, pH 7.4), kept at the same temperature. The oligolamellar vesicles (OLVs) were obtained by alternating gentle vortex with short periods in the thermostated water bath at ~35 °C. After this the OLVs were frozen in liquid nitrogen and thawed in the water bath at 35 °C, process being repeated 5 times.

Large unilamellar vesicles (LUVs) were obtained from the OLVs by extrusion in a 10 mL stainless steel extruder (Lipex Biomembranes, Vancouver, BC, Canada), inserted in a thermostated cell with a re-circulating water bath, at 35 °C. The samples were passed several times through polycarbonate filters (Nucleopore, Pleasanton, CA, USA) of decreasing pore size (600, 200 and 100 nm; 5, 10 and 10 times, respectively), under inert (N_2) atmosphere. The diameter of the vesicles were determined by Dynamic Light Scattering and found to be 101 $\pm$ 8 nm.

After preparation the lipid samples were kept overnight in the refrigerator at 4 °C before being used. The phospholipid concentration was determined by the phosphomolibdate method (McClare 1971).

Small Angle X-ray Diffraction

Peptide solution in the same buffer used for preparing the liposomes was added to POPE/POPG 3:1 OLVs at different peptide-to-lipid (P:L) molar ratios, and the mixtures were incubated for 30 min at 35 °C. The samples were then centrifuged at 13 000 rpm in a microcentrifuge at least for 15 min, and transferred into glass capillaries (Spezialglas Markröhrchen 1.5 mm capillaries, Glass Technik & Konstruktion – Müller & Müller OHG, Germany). In the transfer, care was taken to always have a significant amount of supernatant in the capillaries, to guarantee that all samples were studied at high water contents. The capillaries were sealed by flame, and stored at 4 °C, at least 3 days before use.

Small Angle X-ray diffraction (SAXD) experiments were performed at the synchrotron soft condensed matter beamline A2 in HASYLAB at Deutsches Elektronen Synchrotron (DESY), Hamburg, Germany, using a monochromatic radiation of λ=0.15 nm wavelength. Diffractograms were taken at selected temperatures, where the sample was equilibrated for 5 min before exposure to radiation, or by performing up and down temperature scans at a scan rate 1 °C/min, where diffractograms were recorded for 10 s every minute. The heating and cooling of the sample was regulated by a thermocouple connected to the temperature controller JUMO IMAGO 500 (JUMO GmbH & Co. KG, Fulda, Germany). The evacuated double-focusing camera was equipped with a linear position sensitive detector for WAXD and a 2D MarCCD detector or a linear position sensitive detector for SAXD. The raw data were normalized against the incident beam intensity. The SAXD patterns were calibrated using Ag behenate (Huang *et al.* 1993) or rat tail collagen (Roveri *et al.* 1980). Each Bragg diffraction peak was fitted by Lorentzians above a linear background by use of the Origin software program, to determine the position of maxima. The lamellar repeat distance (*d*) was determined as the inverse of the slope obtained from plotting s_n ($Å^{-1}$) *vs. n* (*n* = 1, 2 …, order of the diffraction peak), with the straight line passing through the origin (0,0). The uncertainty assigned to the parameter is the standard error of the slope, as obtained from the regression.

The domain size (*L*) can be estimated by fitting the shape of the lamellar Bragg peaks with the Caillé structure factor for stacks of membranes including finite size effects (Safinya *et al.* 1986, Silva *et al.* 2014). We find that a suitable approximation for *L* can also be obtained by fitting the Bragg peaks with a Lorentzian function, where $L \approx 1/\mathrm{FWHM}$ (note that the lamellar peak's full width at half maximum (FWHM) is defined in terms of momentum transfer $s=2\sin(\theta)/\lambda$, where $s=q/2\pi$). This method provides a good estimation of the domain size for broad peaks, but when the peaks become very narrow, the resolution of the instrument (which is not accounted here) will originate a systematic error,

with the calculated *L* being shifted to lower values. This systematic error does not affect our analysis, since we are interested in looking at the observed trends as a function of peptide content in the sample, not in obtaining accurate values. Once *L* is determined, the number of layers (n_L) per complexed particle can be easily obtained through the expression $n_L = L/d$ where *d* is the lamellar repeat distance.

Differential Scanning Calorimetry

Differential scanning calorimetry (DSC) was performed in a MicroCal VP-DSC microcalorimeter from Malvern (Worcestershire, UK). Blank experiments with HEPES buffer in both cells were performed overnight prior to sample loading, for subsequent blank correction. Samples were run against HEPES buffer in the reference cell, performing several successive heating and cooling scans for each sample, at a scanning rate of 60 °C/hour, over the temperature range 10 – 35 °C (OLVs) and 4– 35 °C (LUVs). The results provided here refer to the third heating scan, as we have observed that small differences always exit between the first and following scans, but in present case not after the third scan. The sample mixtures were prepared immediately before the DSC run, by adding the desired amount of peptide stock solution (in HEPES buffer) to the LUVs suspension. Samples with peptide-to-lipid molar ratios (P:L) from 1:50 to 1:10 were used. The solutions were previously degassed for 15 min. All procedures regarding sample preparation and handling (lag time at low temperature, time between mixtures, and start of the experiment) were kept constant in all experiments, to ensure that all samples had the same thermal history. In all cases, the reported DSC curves are only corrected for the respective blank experiment. In the case of pure liposome suspensions, T_m and the $\Delta_{trans}H$ were calculated by integration of the heat capacity versus temperature curve (C_p *versus* T), using a linear baseline to calculate the integral areas under the curves. In the case of peptide/lipid mixtures we only provide values for T_m (temperature of maximum C_p in C_p *vs.* T curves), as the shape of the curve shows that no correct $\Delta_{trans}H$ assignment can be made (see results).

Isothermal Titration Calorimetry

Isothermal Titration Calorimetry (ITC) measurements were performed in a MicroCal VP-ITC microcalorimeter from Malvern (Worcestershire, UK). Lipid-into-peptide titrations were performed by injecting 3-4 µL aliquots of POPE/POPG 3:1 LUVs (15 or 30 mM) into the calorimeter cell (*V* cell = 1.4323 mL) containing the peptide at concentrations between 10 and 25 µM. Titrations were performed at 5, 17 and 30 °C, injection speed 0.5 μLs^{-1},

stirring speed 459 rpm, and reference power 15 µcals^{-1}. For the experiments at 5 °C the room temperature was thermostated at ~15 °C, to guarantee that the lipid was in the gel phase throughout. The time between injections varied according to the used temperature. At 5 °C, very long times were needed to allow proper return to the baseline. A first injection of 1 µL was always performed to account for diffusion from/into the syringe tip during the equilibration period. Samples were run against HEPES buffer in the reference cell. All solutions were previously degassed for 15 min prior to calorimeter loading.

Titration experiments where aliquots of peptide solution of concentration 250 µM were titrated into liposome suspension contained in the cell (concentration 30 mM) were also performed, in an attempt to see whether a constant enthalpy was obtained for the peptide/liposome interaction, at extremely low P:L ratios.

Dilution experiments of LUVs suspensions into buffer, under the same experimental conditions were performed, to assess dilution effects, and compared with the values observed for the final peaks of each lipid into peptide titration run. Similar values were found, and thus the data treatment software used dealt with the dilution effects during data treatment.

ITC data analysis for the experiments in the fluid phase (30 °C) was made by use of two approaches. First, the raw data was imported to the NITPIC software (Keller *et al.* 2012) where the curves were treated and the peak areas calculated. Thereafter the obtained datasets were analyzed in terms of a surface partition model taking into account Coulombic interactions between free peptide molecules in the aqueous phase and the membrane, according to Gouy-Chapman theory (Vargas *et al.* 2013). For this, nonlinear least-squares fitting was performed in a Microsoft EXCEL spreadsheet (Microsoft, Redmond,WA) kindly provided by Sandro Keller (Vargas *et al.* 2013) using the PREMIUM SOLVER PLATFORM add-in (Frontline Systems, Incline Village, NV). Alternatively, the raw data was imported to the AFFINImeter software and analysed there using an *independent sites* model (https://www.affinimeter.com/).

Circular Dichroism

Circular Dichroism (CD) experiments were carried out in a Jasco J-815 spectropolarimeter (JASCO Corporation, Tokyo) equipped with a rectangular cell, path length of 1 mm. Scans were performed between 190 – 250 nm, with a scan speed of 100 nm/min, DIT 1 second, data pitch 0.1 nm and bandwidth 1.0 nm. The measurements were performed in PBS (9.3 mM, 150 mM NaF, pH 7.4). Spectra of pure liposome preparations (LUVs) were performed at the concentrations used in liposome/peptide mixtures, as blank experiments

to be subtracted from the liposome/peptide spectra. The peptide solution and liposome suspension (LUVs) were mixed just prior to each measurement, incubated at 35 °C for 30 min and measurements were performed thereafter at the same temperature. Each spectrum was the average of twelve accumulations. After blank correction, the observed ellipticity was converted to a mean residue molar ellipticity (θ) ($deg cm^2 dmol^{-1}$), based on the total amount of peptide in the mixture, considering all amino acids.

Confocal Microscopy

OLVs of POPE/POPG 3:1 were prepared as stated above with the addition of 0.3% Texas Red®-1,2-dihexadecanoyl-*sn*-glycero-3-phosphoethanolamine (Texas Red®-DHPE) (Molecular Probes). Mixtures of peptide solution and liposome suspension (OLVs) were prepared at different peptide-to-lipid (P:L) molar ratios, and were incubated for 30 min at 35 °C. A 15 µL drop of each sample, including the liposomes suspension without peptide, were placed in microscope slides and observed and photographed in a Laser Scanning Confocal Microscope Leica SP2 AOBS SE (Leica Microsystems, Germany).

Electron Microscopy

Negative staining electron microscopy was performed in samples of LUVs of POPE/POPG 3:1 and in mixtures of CAM with POPE/POPG 3:1 at different peptide-to-lipid (P:L) ratios and temperatures. Briefly, a 5 µL drop of each sample was placed on copper grids and allowed to stand for some minutes and thereafter the excess liquid was dried off with filter paper. Then a 5 µL drop of uranil acetate was added and incubated for few seconds, after which the excess was again removed with filter paper. For images of the gel phase, all these procedures were made at 4 °C to insure that the samples were in the gel phase before fixation. The samples were after observed and photographed in a Jeol JEM-1400 transmission electron microscope (TEM).

Results and Discussion

Small Angle X-ray Diffraction

Small Angle X-ray Diffraction (SAXD) experiments were performed to characterize the structure(s) present in liposome/peptide mixtures, and compare them with the ones shown by POPE/POPG 3:1 liposomes, to ascertain the changes in lipid structure induced by CAM.

In figure 1, representative X-ray diffraction patterns of the OLVs and OLV-peptide systems are shown for two temperatures, 10 (figure 1A) and 30 °C (figure 1B), corresponding to the gel (L_β) and liquid crystalline (L_α) phases. The pure POPE/POPG 3:1 OLVs below the gel-to-liquid crystalline phase transition (T_m) shows a lamellar pattern with an average spacing of 118 Å (figure 1A). The shape of the peaks is broad, as expected for OLVs, and the first lamellar peak is less intense than the second due to the proximity of a minimum in the membrane form factor to the first peak (Pozo Navas *et al.* 2005). The correlations between the layers in the OLVs are lost above the T_m, in L_α phase, as the membranes become unbound, and the lamellar peaks are replaced by diffuse scattering from the membrane form factor and perhaps by very weak correlations between the membranes. This observation agrees with the findings previously reported by Pozo Navas *et al.* for this system at different POPE/POPG ratios (Pozo Navas *et al.* 2005).

When the OLV dispersions are mixed with the CAM peptide, a fine white precipitate spontaneously forms, suggesting massive aggregation and condensation of the lipid bilayers induced by the peptide. The occurrence of this precipitate suggests the formation of large aggregates, as opposed to a scenario where the membranes would be dissolved to small structures like bicelles or micellar aggregates. The formation of such large membrane aggregates mediated by oppositely charged multivalent species (here, the peptide) is commonly observed for instance in the condensation of cationic liposomes by oppositely charged polyelectrolytes like DNA (Rädler *et al.* 1997, Koltover *et al.* 1998, Bouxsein *et al.* 2011) or even short-interference RNA (Bouxsein *et al.* 2007, Leal *et al.* 2010).

At 30 °C, above T_m, the mixed OLV-CAM systems in the L_α phase show a typical lamellar pattern (figure 1B) with a lamellar spacing *ca*. 50.6-53.8 Å that decreases with increase in peptide content. This spacing is much smaller than the average lamellar spacing observed for POPE/POPG 3:1 OLVs in the L_β phase, below T_m (118 Å), and also significantly smaller than the pure POPE lamellar spacing of *ca.* 62 Å for the same temperature range. This suggests that the CAM peptides are being intercalated within the interlamellar spacing, condensing the lamellar bilayers in a mechanism much similar to that one found

for condensation of cationic liposome-DNA (CL-DNA) systems (Rädler *et al.* 1997, Koltover *et al.* 1998, Bouxsein *et al.* 2011) in which a lamellar phase with DNA chains sandwiched between lipid bilayers is observed. However, in contrast to the CL-DNAs, a peak resulting from in-plane correlations between the peptides is not observed here above the transition temperature. This might be due to the small size of the peptides and correlates well with the difficulty in observing correlations between short non-sticky DNA pieces of 10 base pairs sandwiched between cationic membranes (Bouxsein *et al.* 2011). The width of the lamellar peaks in the mixed systems is much narrower than in the pure OLVs (figure 1), indicating that the presence of the peptides in the membranes makes them more tightly bound. Further, it decreases continuously as the peptide content in the system increases (*i.e.* as P:L increases) (figure 1), indicating an increase in the number of lamellar layers, condensed by the action of the positively charged peptides. This ordering effect can be clearly seen in values obtained for the number of layers (n_L) present (figure 2 and table S1). For the pure lipid system n_L is very small (~5 in L_β and~1 in L_α, figure 2 and table S1), in agreement with the literature (Pozo Navas *et al.* 2005). In the presence of the peptide, the n_L values increase as the peptide content increases, up to ~100 in both L_β and L_α for P:L=1:7 (figure 2 and table S1).

On cooling and reaching the T_m, new Bragg peaks appear for OLV-CAM system, still with an apparent lamellar pattern, but now the lowest Bragg peak (figure 1A, asterisk) indicates a spacing of ~110 Å, as if the structure suddenly doubled the lamellar spacing in the gel phase as compared to the liquid crystalline spacing ($d_{L\alpha}$ ~52Å). Curiously, the diffraction patterns of the mixed OLV-CAM systems and the pure POPE/POPG OLVs in the L_β phase are similar. The first Bragg peak (figure 1A, asterisk) is less intense than the second, and also the spacing from the first peak is similar in both systems (*ca.* 110 and 118 Å, respectively). It could be tempting to relate both behaviors, and claim that the lamellar phase found expands from ~52 to ~110 Å at temperatures below T_m. However, a deeper consideration of the physics at stake makes such a lamellar system with a spacing of ~110 Å unlikely. Both systems (with and without the peptide) should have extremely different bilayer-bilayer interactions, especially as regarding electrostatic interactions, since the peptide should neutralize most of the anionic charge from POPG. It is unlikely for the peptide-neutralized bilayers to keep such a large interlamellar spacing, especially with a large domain size that extends to dozens of bilayers. Indeed one possibility would be that the peptides would be expelled from the bilayers below T_m, so that the big lamellar aggregates expand to the size found for the pure OLVs, but that scenario also seems unrealistic, especially because the behavior is fully reversible in up-down-up-down temperature cycles. This makes it difficult to conceive a picture where the peptides would

leave and return systematically to the bilayers, inducing a bilayer expansion-condensation cycle induced by the temperature. Hence, the similarities between the scattering patterns in the systems with and without peptide are probably just a coincidence.

The hypothesis/model we find more realistic to justify the emergence of the new Bragg peaks below T_m (figure 1A, asterisk), is that of a scenario where on cooling, and by influence of the peptide, adjacent lipid membranes become distinct from each other (perhaps due to subtle changes in the lateral organization induced by the peptides). Therefore, the simple lamellar lattice (*d*) is replaced by a centered rectangular lattice, with the lattice parameter b_r (perpendicular to the lamellae) being now twice the lamellar repeat distance *d*, owing to the fact that adjacent bilayers are not completely similar (see model in figure 3). Therefore the values for the lamellar repeat distance are similar, being somewhat larger in the L_β phase (*d* ~65 Å) than in the L_α phase (~52 Å), as expected due to the more rigid hydrocarbon chains in the L_β phase. Despite adjacent bilayers not being completely similar, they still resemble each other to some extent, which would justify that the reflections with odd *n* value partially cancel by symmetry, leading to the observed smaller intensities of these peaks as compared to those with even *n* value. This is clearly seen in the first and second peaks in the L_β phase. Another interesting fact, is the appearance of a small extra peak at ~0.1 $Å^{-1}$ (sometimes a shoulder) close to the second Bragg peak, for the highest P:L ratios (1:10 and 1:7), and temperatures below T_m (figure 1A, arrows). Temperature cycles up and down between 10 and 80 °C and in independent samples with new peptide-lipid batches show that this behavior is completely reproducible, with this peak always appearing below T_m, in the L_β phase. Within the model described above, this peak could be related with the lattice parameter a_r (in the plane of the lamellae, figure 3).

This model seems physically more sound than implying the condensation-expansion of lamellae as the temperature is cycled below and above T_m, since it relies only on subtle changes in the bilayers, which change the lamellar 1D lattice into a 2D centered rectangular lattice. The subtle changes in the bilayers should be promoted by action of the peptide and stiffening of the alkyl chains below T_m. Such stiffening modulated by the peptides would be in perfect agreement with the reproducibility in the behavior as the temperature is cycled, since it only requires minor rearrangements in the lattice, without peptides having to be expelled from the lamellae. The ordering of the lamellae into a centered rectangular lattice could occur by a number of mechanisms, such as, for instance, induction of periodic grooves in the lamellae to better accommodate the peptide, as sketched in figure 3.

Differential Scanning Calorimetry

The effect of CAM on the thermotropic lipid transition was evaluated on both POPE/POPG 3:1 OLVs and LUVs, for varying P:L ratios. The peptide has a very strong effect on the lipid system, whether we use OLVs or LUVs (Figure 4 A and B, respectively). The lipid transition for the pure POPE/POPG 3:1 presents in both cases a profile that indicates non-ideal mixing between the two lipids (non-symmetric transition with low cooperativity), which have widely different transition temperatures, 24.7 °C for POPE and -5.3 °C for POPG (Pozo Navas *et al.* 2005). Indeed the transition is more cooperative in the case of OLVs when comparing to LUVs, due to higher number of layers. We obtained a T_m of 21.2 °C in the case of POPE/POPG 3:1 OLVs and 20.5 °C for LUVs (table 1). The OLVs value is in agreement with the values reported by Pozo Navas *et al.* (22.7 ºC for x_{POPG}=0.18 and 20.6 ºC for x_{POPG}=0.30) (Pozo Navas *et al.* 2005), and the LUVs value is in very good agreement with the one reported by Teixeira *et al*., 20.4 °C (Teixeira *et al.* 2010). As regarding the transition enthalpy, we obtained $\Delta_{trans}H$ of 21 kJmol^{-1} for OLVs and 24 kJmol^{-1} for LUVs, in fair agreement with Pozo Navas *et al.* value for OLVs (24.2 kJmol^{-1} for x_{POPG}=0.18 and 25.5 kJmol^{-1} for x_{POPG}=0.30) (Pozo Navas *et al.* 2005) and in good agreement with Teixeira *et al*. value for LUVs, 22 kJmol^{-1} (Teixeira *et al.* 2010).

When peptide is added to both OLVs and LUVs the T_m increases (table 1), indicating that the peptide stabilizes the gel phase, moving the transition to higher temperatures. Previously we have studied this system at lower P:L ratios (1:80), where the increase in T_m was already apparent (Teixeira *et al.* 2010), together with an increase in enthalpy (33.5 kJmol^{-1}), consistent with a stabilization of the L_β phase. This type of stabilizing effect has been reported by Schwieger *et al.* for the binding of poly(L-lysine) to DPPG membranes (Schwieger and Blume 2007). The initial stabilizing effect at low peptide concentrations must be the result of a more structured and compact lipid chain packing due to the electrostatic interaction of the peptide with polar lipid head groups, before significant segregation takes place.

Analysing now the curve's profile, in the case of OLVs, for the lowest P:L ratio (1:25), we can see in figure 4A that the peak height decreases and there is a significant drop in the baseline after the transition. These facts suggest that precipitation is taking place at this P:L ratio. The shoulder on the right is maintained, although shifted to higher temperatures, as occurs also with the main transition peak. As more peptide is present (P:L of 1:15 and 1:10) the transition shape changes significantly, becoming much less sharp. Further, very broad peaks appear on the low temperature side (~12 °C) (figure 4A) suggesting a progressive destabilization of the membrane organization.

In the case of LUVs (figure 4B) a drop in baseline after the transition is also observed for P:L ratios of 1:50 and 1:25, being even more significant than for OLVs. For the lowest P:L (1:50), the shape of the curve is significantly changed, showing higher cooperativity in the main peak and a higher temperature, together with a new peak appearing at 15.5 °C and a shoulder at 25.1 °C. We did observe a similar effect in the previous study, where at P:L of 1:40 two peaks still appeared (Teixeira *et al.* 2010). This indicates that at the lowest P:L ratios we have a peptide-mediated domain segregation. The first peak at low temperature can be assigned to a peptide-rich, POPG-enriched domain, and the second one, at a higher temperature, to a peptide-poor, POPE-enriched domain, consistent with the main transition temperatures of the pure lipids. As we increase the peptide content (P:L=1:25) the lower temperature peak becomes broader and moves to even lower temperatures (~12 °C), whereas the shoulder on the right of the main peak is maintained. At 1:15, the highest peptide-to-lipid ratio tested with LUVs, a dramatic effect similar to the one described above for the highest P:L ratios with OLVs was observed, in terms of curve shape and peaks position, and also found in the results previously reported (Teixeira *et al.* 2010). Therefore, in both cases (OLVs and LUVs) there appears to be a threshold concentration, after which the system behaviour changes. The existence of a threshold concentration has been reported for this peptide with different lipid systems. Bastos *et al.* suggest the value of 1:25 for the interaction with DMPC/DMPG 3:1 membranes, based on ITC results (Bastos *et al.* 2008), the same value being suggested by Pistolesi *et al.* for POPE/POPG/CL (70:25:5) (Pistolesi *et al.* 2007).

Circular Dichroism

The secondary structure of CAM was examined by Circular Dichroism (CD) in PBS buffer (9.3 mM PBS + 150 mM NaF) and in the presence of POPE/POPG 3:1 (figure 5). Measurements at different peptide concentrations in buffer showed that the peptide structure is not affected by concentration (results not shown). For the peptide in the presence of the membrane, the results at different P:L ratios were similar. In buffer the peptide is predominantly random (minimum at 198 nm), whereas in the presence of POPE/POPG 3:1 a α-helix structure is adopted, with well-defined minima around 208 and 222 nm (figure 5). The fraction of α-helix was calculated (Ladokhin and White 1999) to be 0.33, *i.e*., only ~5 amino acids are involved in the helix.

Isothermal Titration Calorimetry

The experiments at 30 °C (lipid in L_α phase) show a simple profile with an endothermic effect that drops to zero after a relatively small number of injections (Figures 6A and 7A). Even at the low peptide concentration used (10 or 15 µM) the steep binding isotherms reflect the large membrane affinity of the peptide, as found in similar systems (Scheidt *et al.* 2015). Attempts to use lower peptide concentration did not produce isotherms that could be analysed, due to the very small number of observed peaks.

The results were fitted first to a partition model with correction for electrostatic effects according to Gouy-Chapman theory (Seelig 2004, Vargas *et al.* 2013, Scheidt *et al.* 2015). In this model, the non-Coulombic interactions of a charged peptide with a lipid membrane are described as a partition equilibrium of the peptide between the interfacial aqueous phase (*i.e*., the aqueous phase adjacent to the membrane surface), and the lipid bilayer phase. This analysis provides values of the intrinsic partition constant, K_p, the molar transfer enthalpy from the aqueous phase to the bilayer phase, ΔH, and the effective charge of the peptide, z_{eff}, which determines the strength of Coulombic interactions between the peptide and the membrane.

The results obtained from the fitting of independent experiments at 30 °C when the peptide concentration in the cell was 15 µM and the lipid concentration in the syringe 30 mM (figure 8) lead to the values $K_p = (3.2 \times 10^5 \pm 2 \times 10^5)\ M^{-1}$, $\Delta H = (27 \pm 5)\ kJmol^{-1}$ and $z_{eff} = 4.7 \pm 0.4$. The overall quality of the fitting was acceptable (figure 8). The partition constant thus obtained agrees with the one previously determined by Time Resolved Fluorescence Spectroscopy (Teixeira *et al.* 2010), 5.1×10^5 (when transformed to M^{-1} by use of the lipid molar volume). The z_{eff} value found for the effective charge is somewhat smaller than the nominal charge (+6).

As the curves at 30 °C show a steep binding isotherm (figure 7A) we also did the fitting to a binding model, “independent binding sites model” (figure 9). As the positively charged peptide has a very strong interaction to the negatively charged bilayer, it is reasonable to also try this approach, and it has been used in recent publications (Arouri *et al.* 2013). In fact, the two constants (K_p and K_{app}) can be related, as has been previously shown (Bastos *et al.* 2004, Melo *et al.* 2011), and in limiting cases they are similar. The model used provides the microscopy binding constants K_{app} (*i.e*., per site), the enthalpy change ΔH, and the number of sites N. Thus, the total enthalpy observed can be calculated by multiplying the obtained ΔH by the number of “sites”. In this treatment we analysed two sets of data where the peptide concentration in the cell was 15 µM and the titrating lipid suspension was either 15 or 30 mM (see figure 9 for an example). The values retrieved

agree between the two sets of data, leading to average values K_{app} = (1.8x10^5± 0.7x10^5) M^{-1}, Δ*H* = (1.11 ± 0.02) kJmol^{-1} (per site) and number of sites N = 35 ± 4 (thus the total enthalpy observed is 39 ± 5 kJmol^{-1}). The N values can provide us information on the extent of interaction between the lipids and the peptide (Arouri *et al.* 2013). This last number indicates that we have ~35 lipids per peptide. Since the interaction of the peptide with the membranes is mostly electrostatically driven, and assuming that the peptide can escape the vesicle aggregates and redistribute upon new lipid addition, if we base our reasoning on the peptide effective charge referred above (4.7) a stoichiometry of 9 could be expected if the peptide would only bind to the outer leaflet, or ~5 if it could interact with both leaflets (based on POPG content), or 36 and 20, if based only total lipid content. The value retrieved for N (35±4) would thus indicate that the peptide interacts only with the outer layer. This is in line with the assumption taken in the partition model calculations where it was assumed that the peptide would only interact with the outer leaflet (γ=0.5). Therefore, within the confines of the difference between the models, we find the agreement satisfactory.

It is interesting to point that whereas similar results were obtained when the lipid concentration was varied between 15 and 30 mM as above in the case of the independent binding sites model, in the case of the partition treatment more significant variations were found. For this model, when the lipid concentration was kept at 15 mM but the peptide concentration was lower (10 µM) a good fit was obtained but leading to a K_p value that was higher (2.0x10^6 M^{-1}) and Δ*H* (16 kJmol^{-1}) and z_{eff} (3.5) smaller than the values obtained for the higher peptide concentration. At odds, when keeping the peptide concentration at 15 µM but decreasing the lipid concentration to 15 mM the K_p value decreased to 4.5 x10^4 M^{-1} but the values for the enthalpy and z_{eff} did not change significantly (28 kJmol^{-1} and 4.9, respectively). Further, when performing the reverse titration – peptide of concentration 250 µM titrated into 30 mM liposome suspension, the first injections had a slow increase in value up to the 5th one, with an average Δ*H* value of 5.6 ± 0.4 kJmol^{-1}, and were constant thereafter at an average value of 12.4±0.9 kJmol^{-1}. Thus not only were the values varying up to the 5th injection but also the constant enthalpy value retrieved is close to the one obtained for the lower peptide concentration (10 µM, not included in the calculation of the values presented here) but less than half the value retrieved for the other peptide concentrations used in the value reported above. These changes in thermodynamic parameters for different experimental conditions indicate that a simple partition model might not be the best choice for the present peptide/lipid system. In fact, in view of the results obtained in the SAXD experiments, and the interpretation we provided above of a condensation of the lamella by the peptide, the association model

tested might better describe the present system. Further, the indication extracted from the N value, suggesting interaction only with the outer layer, taken together with the SAXD results leads to the suggestion that the peptide associates with the lipids inducing vesicles destruction, forming lamellar structures with the peptide “sandwiched” between bilayers.

As regarding the experiments at 5 °C, where the lipid is in the gel phase, a very different behavior was obtained (figures 6C and 7C). The interaction was exothermic throughout. In the first part of the curve we can see a steep increase in Δ*H* values (in absolute value) up to a P:L ratio of 1:46, followed by a plateau region between 1:46 and 1:87, and thereafter the enthalpy values decrease at a slower pace towards zero. The initial increase in negative values shows that the peptide/lipid interaction is exothermic in the gel phase, reflecting probably the extensive aggregation of the liposomes (or lipid bilayers) by the peptide. The fact that the interaction was endothermic at higher and exothermic at lower temperatures indicates that this is not a simple process and that delicate balances among the various interactions (electrostatic, hydrophobic, partial dehydration of the lipid heads upon peptide binding, among others) exist that are moderated by temperature. It is interesting to observe that at all studied temperatures a similar P:L ratio of ~1:44 is found where a change in behavior occurs (figure 7). At 30 °C (figure 7A), it is the locus where the enthalpy becomes ~zero (only lipid dilution), *i.e.,* the end of the complexation process. At 17 °C (figure 7B), after this point the enthalpy becomes increasingly less negative, approaching the lipid dilution, indication also the end of the interaction process. Finally at 5 °C (figure 7C), it is the onset of a plateau region, observed between P:L ratios of 1:46 and 1:87. This P:L value must thus be a threshold that we propose reflects lipid saturation by the peptide. In terms of observed enthalpy, the existence of the plateau must reflect a range where phenomena of opposite enthalpy signs occur. Considering the interpretation of the interaction given above (see SAXD results) that the peptide disrupts the membrane forming bilayers stacks intercalated by the peptide, we propose that at this ratio (P:L=1:44) no more free peptide is available to interact with the lipids. Therefore, upon further injection of liposome suspension, the peptide can only redistribute among previous and new lipid layers. This implies disruption of the peptide lipid interaction (endothermic effect at this temperature), followed by association to new lipid layers (exothermic). Finally after P:L=1:87 the observed enthalpies only slowly tend to zero.

Finally at the intermediate temperatures, 17 °C (figure 7B) the ITC curve start at endothermic values, cross zero at P:L=1:35 and became increasingly negative up to P:L ratio of 1:44 after which it decreases (in absolute value) towards zero (figure 7B). At this temperature we have a mixture of gel and liquid crystalline phases, as shown by the DSC results (figure 4B). In the initial region of excess peptide, we interpret the positive values

as reflecting both the interaction with the L_α phase (endothermic) and the peptide-induced gel-to-liquid crystalline phase transition (endothermic) due to excess peptide, as for the same P:L ratios the observed enthalpy values are more positive than those encountered at 30 °C. After P:L=1:35 the negative values reflect the interaction with the L_β phase up to saturation at P:L=1:44. After the critical P:L ratio of 1:44, there is large excess lipid and the values decrease towards zero.

Finally we would like to point that the critical P:L ratio where a minimum in the enthalpy profiles occurs for all studied temperatures (around 1:44) is similar to the one found by Bhargava and Feix in a EPR study of the interaction of this peptide with POPE/POPG 80:20 (Bhargava and Feix 2004).

Fluorescence microscopy

In order to further investigate the mechanism of action of CAM on POPE/POPG 3:1 membranes, and to shed some light onto the structures formed, we have performed fluorescence microscopy using OLVs of POPE/POPG 3:1 labelled with Texas Red®-DHPE. Three different samples were visualized, the pure lipid mixture and two peptide/lipid mixtures at P:L of 1:25 and 1:10 (figure 10). The pure lipid mixture shows, as expected, oligolamellar vesicles of different sizes, well dispersed in the support (figure 10A). The mixtures present a completely different structure, with very large aggregates for both P:L ratios (figure 10 B, C, D and E). This is in line with the hypothesis of the peptide inducing extensive aggregation of the lipid system. Although in both cases an extensive aggregation is apparent, at the higher P:L ratio significantly larger aggregates are observed (figure 10 C and E), whereas a bridged network between smaller structures appears at P:L=1:25 (figure 10 B and D).

Electron Microscopy

The use of negative staining electron microscopy can provide some further insight on the structural characteristics of mixtures of CAM and LUVs of POPE/POPG 3:1. The system was studied at a temperature below T_m and for different P:L ratios (1:25 and 1:10). Some tests were also performed above T_m with poor results (data not shown). In the case of pure lipid mixture individual round vesicles are observed, revealing the presence of liposomes (figure 11A). When peptide is added, condensation occurs, with large aggregates being formed by multilamellar or disrupted vesicles (figure 11 B, C and D), in agreement with the observations by fluorescence microscopy (figure 10). The aggregates

are larger in the sample with higher peptide content at 1:10 as compared to 1:25 (figure 11 C and B, respectively), also in line with the observations by fluorescence microscopy (figure 10). In the enlargement presented in figure 11D we can easily see the different layers, in an “onion like” structure.

Conclusions

The system CAM/POPE/POPG (3:1) was studied using a number of different techniques, to unravel the mode of interaction of this peptide with the model membrane system, in an attempt to understand its antimicrobial mechanism of action.

The results obtained are consistent, and lead us to propose that CAM interacts strongly with the negatively charged membrane system, destroying the liposomes and leading to a lamellar stack of multilayers with peptide intercalated between them, in an onion-like structure. This is clearly shown by the SAXD results, where the increase in the number of layers upon peptide addition supports this suggestion. Further, the model we proposed to interpret the SAXD patterns reconciles the observed reversibility upon up and down temperature scans and the distances retrieved for the L_β and L_α phases. This behavior is similar to the condensation observed in CL-DNA systems, widely described in the literature (Rädler *et al.* 1997, Koltover *et al.* 1998, Bouxsein *et al.* 2011). Further, the fluorescence and electron microscopy results show the large difference between the pure lipid and the combined peptide/lipid system, in structures compatible to the proposed aggregation/condensation. We should add that preliminary NMR results showed that POPE/POPG 3:1 presents a vesicle structure, but in the presence of the peptide the peak symmetry is lost, with a shoulder appearing on the left indicating the presence of a lamellar structure (unpublished results).

Pistolesi *et al.* (Pistolesi *et al.* 2007) suggest that an initial interaction at low concentrations of membrane-bound peptide, occurs primarily near the membrane surface, with the peptide aligned parallel to the plane of the bilayer. With peptide insertion near the hydrophobic-hydrophilic interface, an expansion of the outer leaflet of the bilayer occurs, with continued accumulation of bound peptide, leading to membrane thinning as a prelude to pore formation or detergent-like disintegration of the bilayer. This would agree with our findings, suggesting that the end result is bilayer disintegration. It should also be pointed that a study by Ladokhin and White (Ladokhin and White 2001) showed that whereas melittin (a related peptide, as CAM is a cecropin A-melittin hybrid) induces release through pores of about 25 Å diameter in zwitterionic membranes (Ladokhin *et al.* 1997), release from POPG vesicles was found to be non-selective, *i.e.*, ‘detergent-like' (Ladokhin and White 2001).

The DSC experiments also showed that extensive aggregation takes place, in agreement with SAXD and microscopy findings. This precluded a quantitative analysis of the results obtained for peptide/lipid mixtures. Nevertheless, they indicate that at low P:L ratios the peptide stabilizes the L_β phase, a result that can arise from a strong, surface interaction.

When the peptide content is increased, extensive aggregation occurs, particularly after P:L=1:25.

Finally the ITC results showed that the enthalpy of interaction is endothermic in the L_α phase and exothermic in the L_β phase. Further, at temperatures of coexistence of both phases, at high P:L ratios the peptide interacts initially with the L_α phase and induces gel-to-liquid crystalline phase transition. In all cases a threshold P:L ratio of 1:44 was found, that we interpret as a saturation concentration. Moreover, the N value found from the treatment of the results in the L_α phase (~35 lipids per peptide) can provide information on the extent of interaction between the lipids and the peptide (Arouri *et al.* 2013). This value agrees with the one expected, considering the calculated effective charge (4.8), if we consider that the peptide only interacts with the outer lipid leaflet. This result is again in line with the peptide interaction at the level of the heads, inducing membrane condensation after a threshold value (related to charge neutralization) and not to pore formation. It should be noted that pore formation induced by CAM has been reported in other systems (Juvvadi *et al.* 1996, Sato and Feix 2006, Milani *et al.* 2009), however, our results are not compatible with such mechanism.

Thus, the overall results presented here strongly suggest that the mechanism of action of CAM can be described by the “carpet model” where the cationic peptide adsorbs to the partially negatively charged membrane, folding into α-helix and covering the membrane until a threshold concentration, inducing thereafter bilayer disruption with significant condensation into a multilamellar system. Since the system studied in this work is a good model of the bacterial membrane, where PE and PG are the most abundant phospholipids (Teixeira *et al.* 2012), the mechanism proposed here would lead to bacterial membrane destruction, loss of membrane potential and inner contents, ultimately leading to cell death.

Acknowledgements

The research received support from grants: NORTE-07-0162-FEDER-000088) of the Programa Operacional Regional do Norte (ON.2 – O Novo Norte) under the framework of Quadro de Referência Estratégico Nacional 2007/2013 (QREN), funded by Fundo Europeu de Desenvolvimento Regional (Feder) awarded to CIQ-UP; strategic projects, Pest-C/QUI/UI0081/2011 and Pest-C/QUI/UI0081/2013 from Fundação para a Ciência e Tecnologia (FCT) and European Social Funds, to CIQ-UP; PhD grant SFRH/BD/77564/2011 from FCT to TS; EC's 7th Framework Program (FP7/2007-2013) under grant agreement no. 226716 (HASYLAB project II-20090024 EC); SK-PT-0015-10 to DU, MB and TS.

Tables

Table 1 – Values of T_m for the gel-to-liquid crystalline phase transition of pure POPE/POPG 3:1 and mixtures with CAM at different P:L ratios as obtained from DSC.

P:L	T_m[a] / °C	
	OLVs	LUVs
0	21.2	20.5
1:50	-	21.1
1:25	22.0	20.6
1:15	23.2	22.1
1:10	23.0	-

[a] The estimated uncertainty in T_m is ± 0.1 °C (same liposomes preparation, used for the full P:L series) and ± 0.3 °C (within samples).

Figures

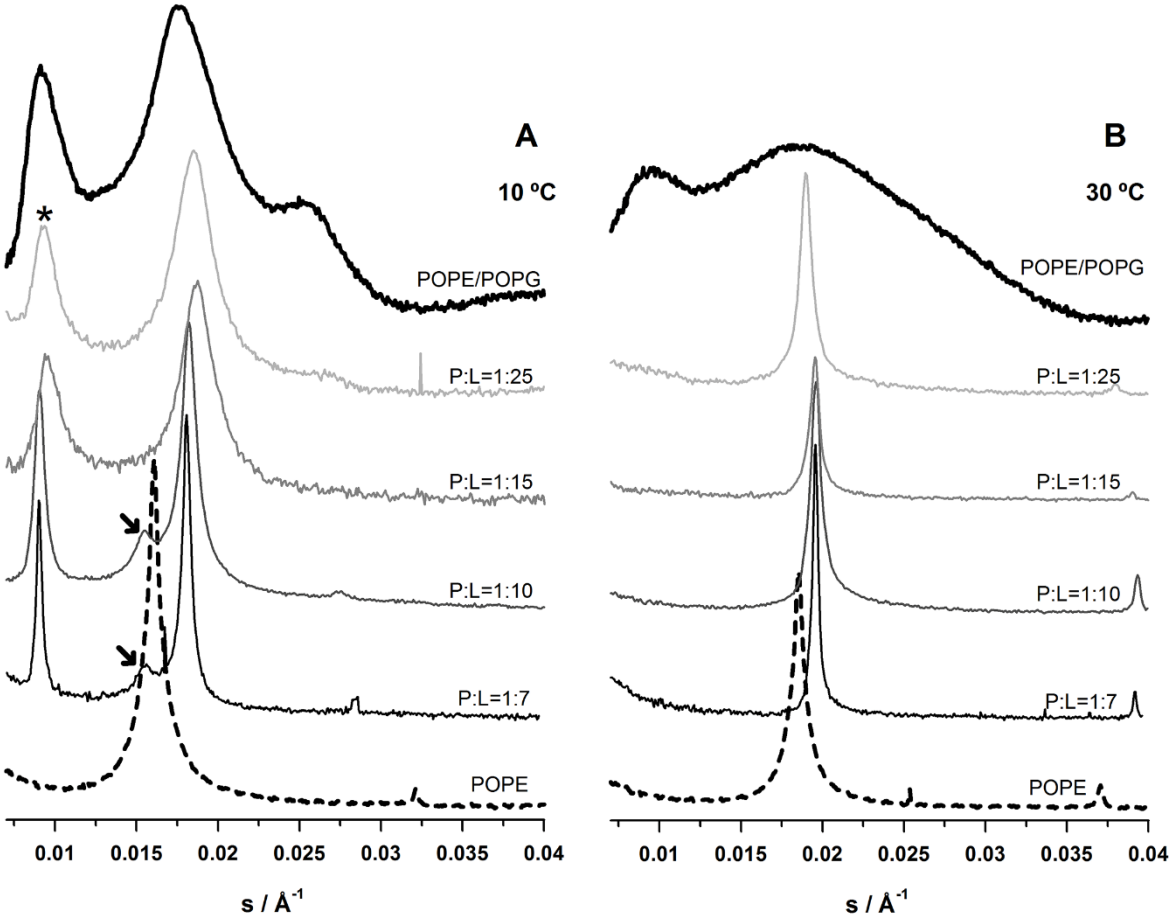

Figure 1 – SAX diffractograms of gel (L_β) (A) and liquid crystalline (Lα) (B) phases, for POPE, POPE/POPG 3:1 and CAM/POPE/POPG mixtures at different P:L ratios: 1:25, 1:15, 1:10 and 1:7, as marked in the figure. **A)** 10 °C; **B)** 30 °C.

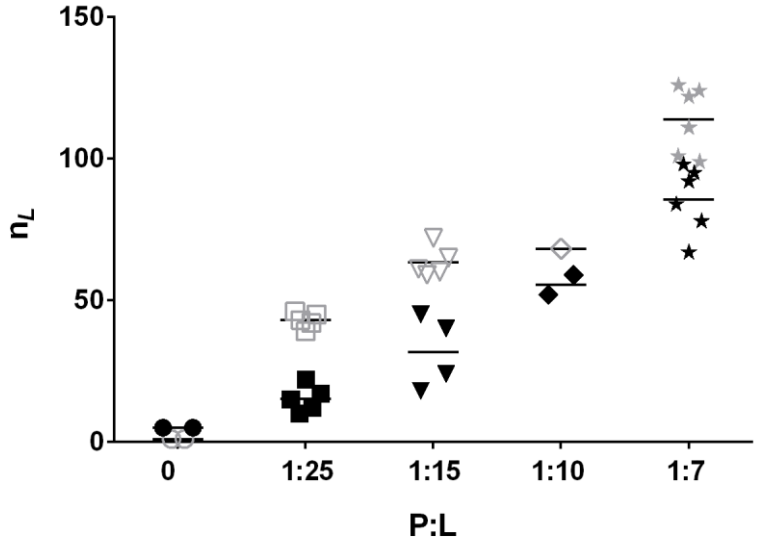

Figure 2 – Evolution of the number of domains (n_L) with increase in peptide content for mixtures of CAM and POPE/POPG 3:1 at different P:L molar ratios. Black symbols: 10 °C; grey symbols: 30 °C. Each symbol corresponds to a SAXD diffractogram, and the horizontal bar the average value for each group.

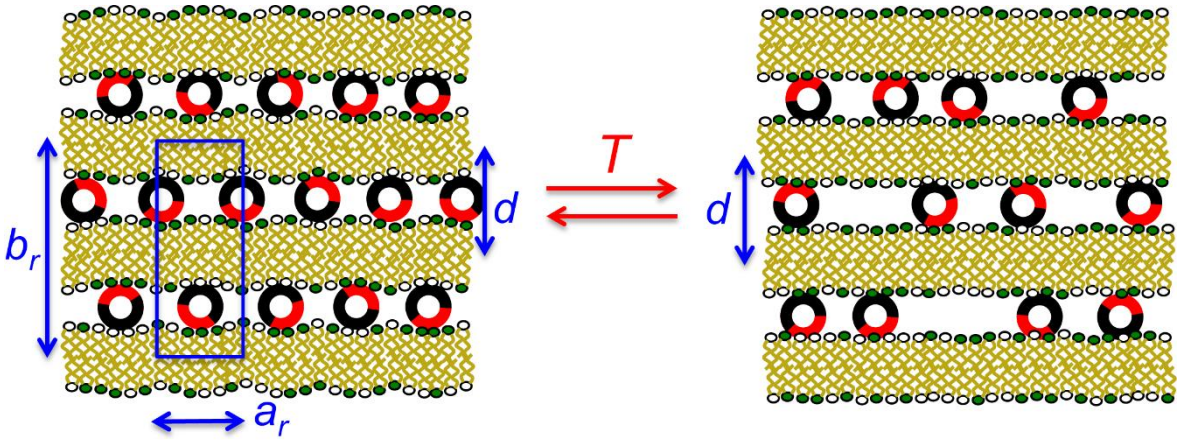

Figure 3 – Schematic representation of the proposed structural model, highlighting the condensed/complexed lamellar structure above T_m in the L_α phase (right) and its more ordered counterpart below T_m the L_β phase (left). The peptide cross-section is depicted with the hydrophobic domains in black and cationic domains in red. The figure suggests that the hydrophobic domains can interact more favorably with the PE head groups (small and zwitterionic, here colored in white) while the cationic domains interact favorably with the PG anionic head groups (colored green) of the next membrane, with both effects leading to the condensation of the membranes. Below T_m the stiffening of the alkyl chains, the small structural changes induced by the peptide and the possible more regular arrangement of the peptides, make neighboring bilayers distinct within a unit cell (note that the grooves in the neighboring lamellae are out-of-phase). Thus the unit cell can no longer be ascribed to a simple 1D lamellar lattice, requiring a 2D centered rectangular cell with the lattice parameter perpendicular to the planes (b_r) that becomes twice the lamellar repeat distance (d), and with the lattice parameter a_r in the plane of the lamellae. Because despite the slight differences between neighboring membranes, a large part of the structure is still similar, the odd-reflections are partially cancelled by symmetry and the therefore, the corresponding Bragg peaks have a smaller intensity than the even reflections.

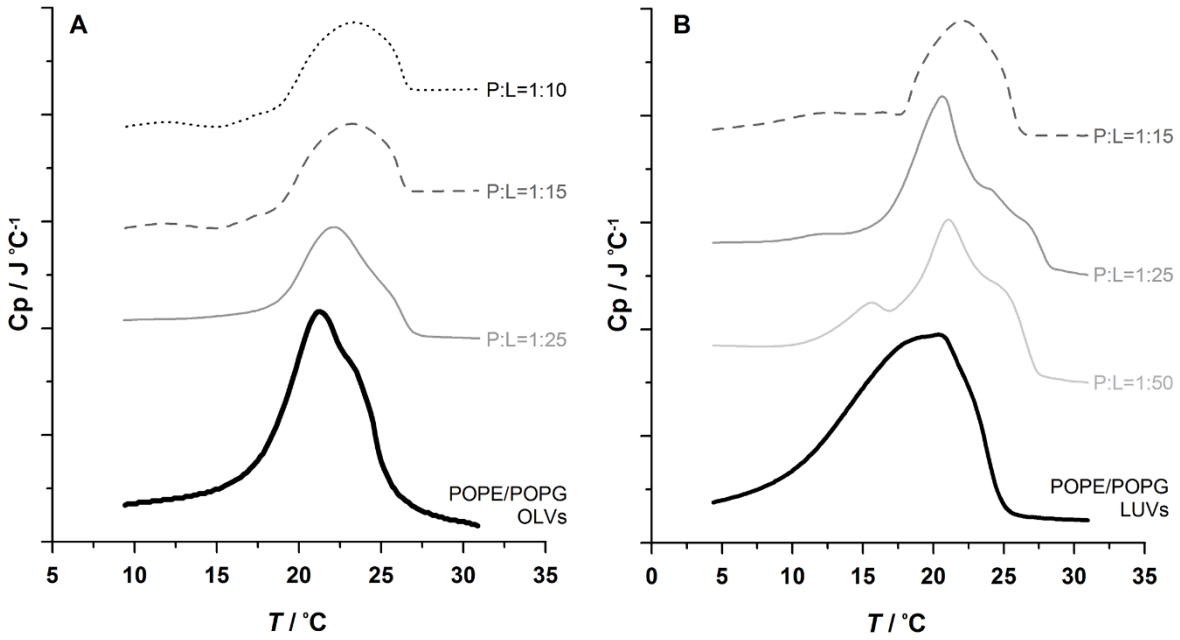

Figure 4 – DSC curves for POPE/POPG 3:1 and its mixture with CAM at different P:L molar ratios. **A)** OLVs of POPE/POPG 3:1 (solid black); P:L=1:25 (grey); P:L=1:15 (dashed grey); P:L=1:10 (dotted grey). **B)** LUVs of POPE/POPG 3:1 (solid black); P:L=1:50 (light grey); P:L=1:25 (grey); P:L=1:15 (dashed grey). The lipid concentration was 3 mM in all experiments.

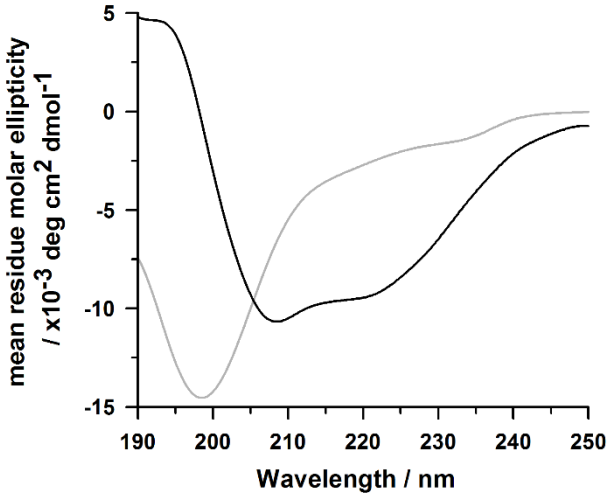

Figure 5 – CD spectra of CAM in buffer (25 µM) (grey) and in a mixture with POPE/POPG 3:1 (3 mM), at P:L=1:50 (black).

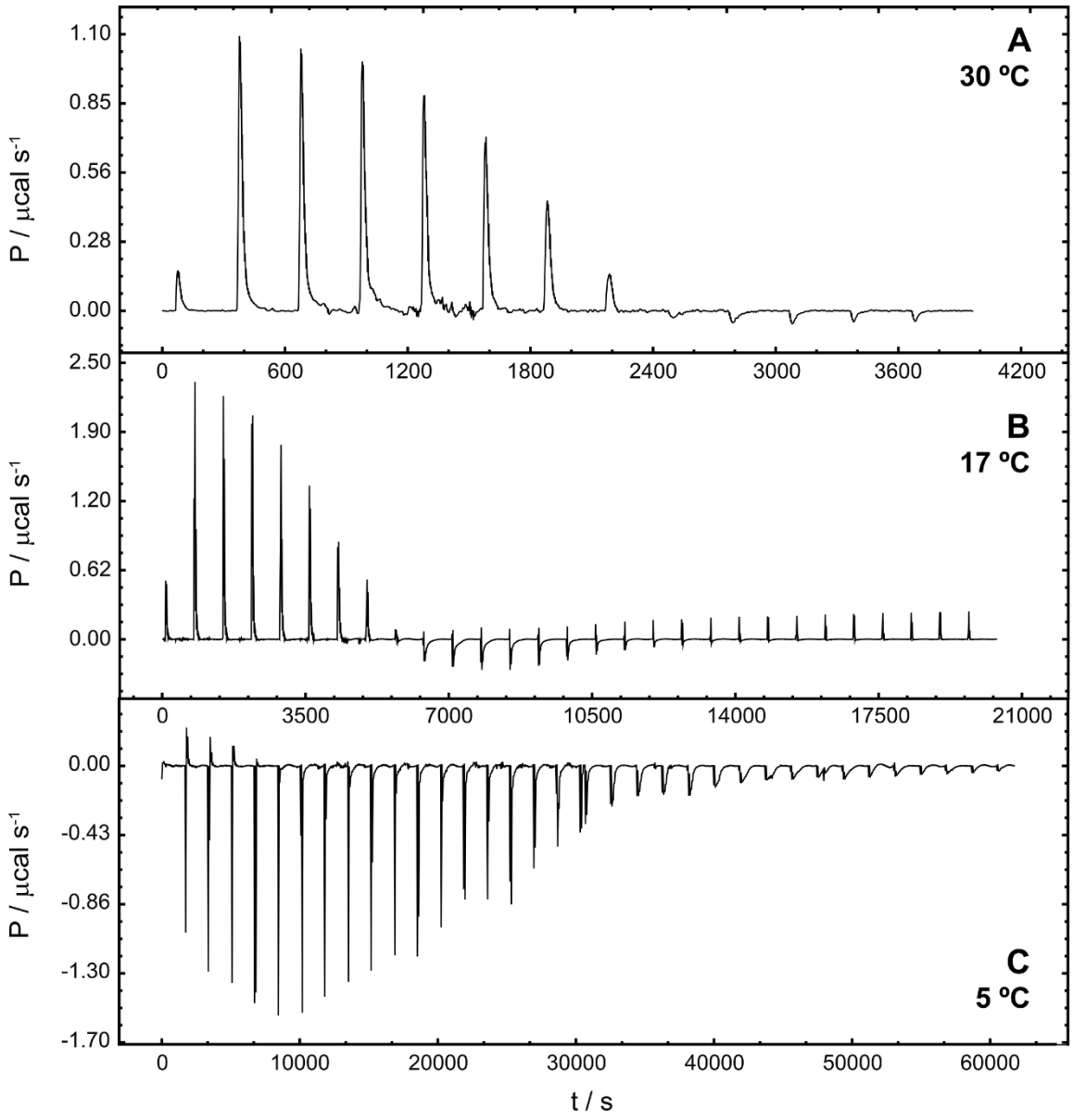

Figure 6 – ITC raw data for titration of CAM in buffer (15 µM) with POPE/POPG 3:1 (30 mM) at **A)** 30, **B)** 17 and **C)** 5 °C. The raw data was imported to the AFFINImeter software (www.affinimeter.com) and processed therein.

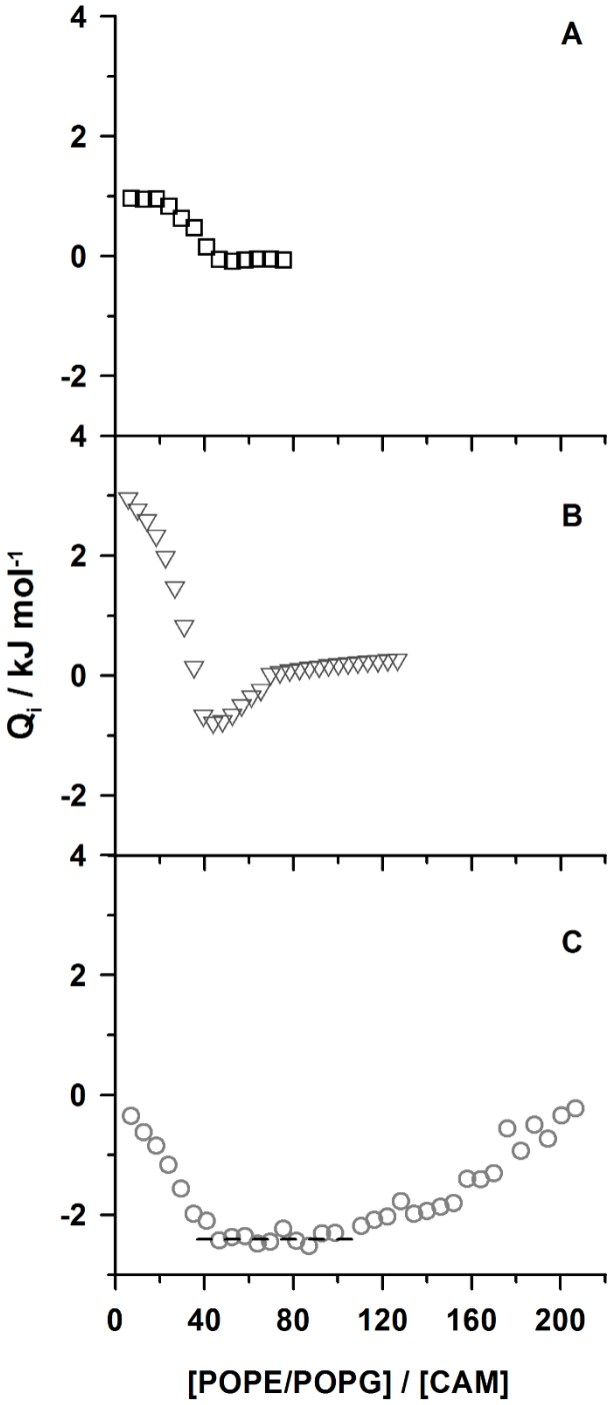

Figure 7 – Integrated peaks as a function of lipid-to-peptide ratio for titration of CAM in buffer (15 µM) with POPE/POPG 3:1 (30 mM) at **A)** 30, **B)** 17 and **C)** 5 °C. The baseline correction and integration were performed using the AFFINImeter software (www.affinimeter.com).

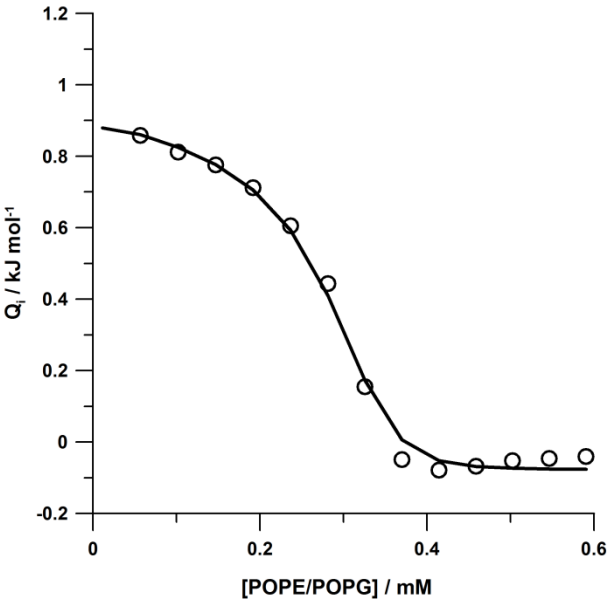

Figure 8 – Titration of CAM (15 µM) with POPE/POPG 3:1 (30 mM) at 30 °C. The integrated reactions heats normalized to the molar amount of injected lipid, Q_i, were obtained with the NITPIC software and are plotted as a function of lipid concentration in the cell. The data was analysed by use of a partition model taking into account Coulombic effects according to the Gouy-Chapman theory (Vargas *et al.* 2013). Experimental points are represented by circles and fitted values by the line.

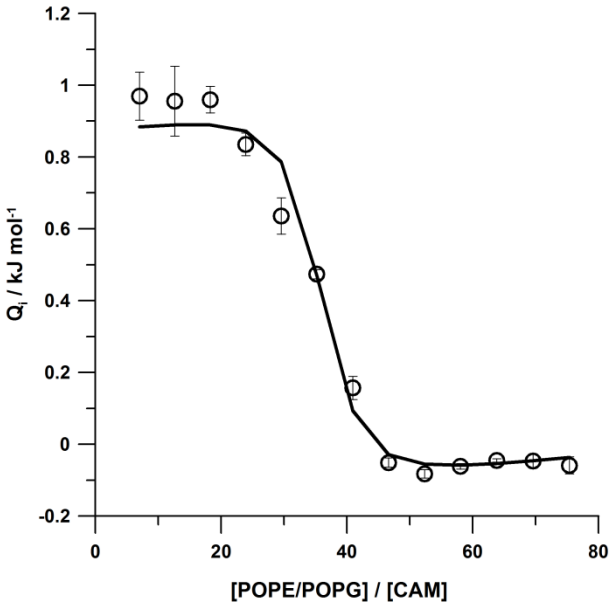

Figure 9 – Titration of CAM (15 µM) with POPE/POPG 3:1 (30 mM) at 30 °C. The integrated reactions heats normalized to the molar amount of injected lipid, Q_i, were obtained with the AFFINImeter software, and are plotted as a function of lipid-to-peptide ratio in the cell. The data was analysed using an "independent sites model" (AFFINImeter, www.affinimeter.com). Experimental points are represented by circles and fitted values by the line.

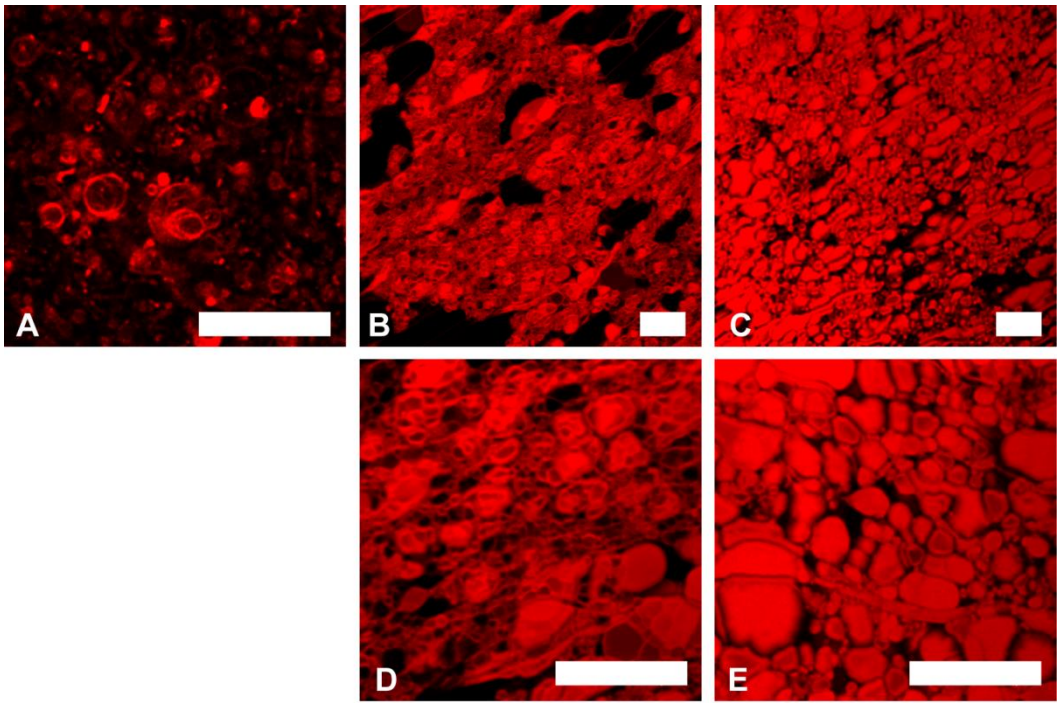

Figure 10 – Fluorescence confocal microscopy of POPE/POPG 3:1 (OLVs) containing 0.3% of Texas Red®-DHPE and its mixture with CAM at different P:L ratios. Upper panel: **A)** POPE/POPG 3:1; **B)** P:L=1:25; **C)** P:L=1:10. Lower panel: same mixtures as in the upper panel but at higher magnification: **D)** P:L=1:25; **E)** P:L=1:10. Scale bar: 15 µm.

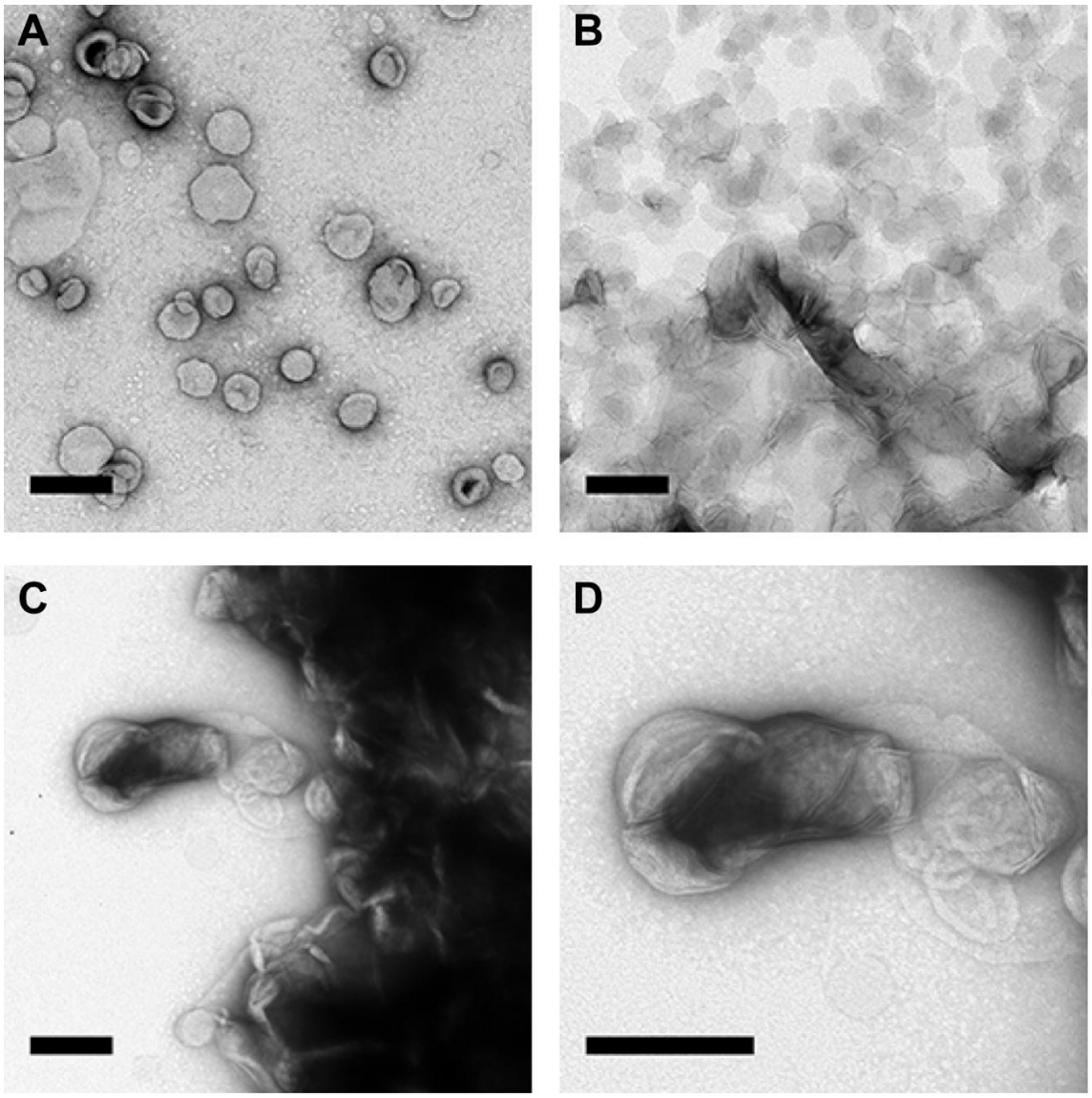

Figure 11 – Negative staining electron microscopy of POPE/POPG 3:1 (LUVs) and its mixture with CAM at different P:L ratios. Samples were incubated below T_m, in the gel state. **A)** POPE/POPG 3:1; **B)** P:L=1:25; **C)** P:L=1:10; **D)** higher magnification of **C**. Scale bar: 250 nm.

Supplementary Information

Table 1 – Number of layers calculated for CAM + POPE/POPG 3:1 mixtures at different peptide-to-lipid (P:L) molar ratio at 10 and 30 °C.

T / °C	P:L [a]	FWHM [b]	*d* / Å	Domain size *L*	Number of layers n_L
10	0	1.96E-03	111.4	510	5
		1.83E-03	117.2	546	5
	1:25	1.85E-03	55.5	541	10
		1.23E-03	54	813	15
		1.18E-03	50.35	847	17
		8.16E-04	55.5	1225	22
		1.51E-03	55.5	662	12
	1:15	7.66E-04	54.45	1305	24
		4.50E-04	55.25	2222	40
		1.06E-03	53.15	943	18
		4.05E-04	55.45	2469	45
	1:10	3.56E-04	54.45	2809	52
		3.10E-04	54.9	3226	59
	1:7	2.76E-04	54	3623	67
		2.20E-04	54	4545	84
		2.35E-04	54.45	4255	78
		1.96E-04	55.25	5102	92
		1.85E-04	55.25	5405	98
		1.91E-04	55.3	5236	95
30	0	7.84E-03	102	128	1
		1.26E-02	106.3	79	1
	1:25	4.15E-04	53	2410	45
		4.54E-04	52.6	2203	42
		4.04E-04	54	2475	46
		4.33E-04	53.9	2309	43
		4.69E-04	54.1	2132	39
	1:15	3.35E-04	51	2985	59
		3.20E-04	51.5	3125	61
		3.23E-04	51.4	3096	60
		2.99E-04	51.2	3344	65
		2.72E-04	51.4	3676	72
	1:10	2.89E-04	50.7	3460	68
	1:7	1.96E-04	50.3	5102	101
		2.00E-04	50.3	5000	99
		1.78E-04	50.7	5618	111
		1.59E-04	50.7	6289	124
		1.62E-04	50.8	6173	122
		1.56E-04	50.8	6410	126

[a] P:L – Peptide-to-lipid molar ratio

[b] FWHM – full width of the peak at half maximum

References

Abrunhosa F., Faria S., Gomes P., Tomaz I., Pessoa J. C., Andreu D. and Bastos M. (2005). Interaction and Lipid-Induced Conformation of Two Cecropin−Melittin Hybrid Peptides Depend on Peptide and Membrane Composition. *J Phys Chem B*. 109(36):17311-17319.

Andreu D., Ubach J., Boman A., Wahlin B., Wade D., Merrifield R. B. and Boman H. G. (1992). Shortened cecropin A-melittin hybrids. Significant size reduction retains potent antibiotic activity. *FEBS Lett*. 296(2):190-194.

Arouri A., Dathe M. and Blume A. (2013). The helical propensity of KLA amphipathic peptides enhances their binding to gel-state lipid membranes. *Biophys Chem*. 180-181:10-21.

Bassetti M., Merelli M., Temperoni C. and Astilean A. (2013). New antibiotics for bad bugs: where are we? *Ann Clin Microbiol Antimicrob*. 12:22.

Bastos M., Bai G., Gomes P., Andreu D., Goormaghtigh E. and Prieto M. (2008). Energetics and partition of two cecropin-melittin hybrid peptides to model membranes of different composition. *Biophys J*. 94(6):2128-2141.

Bastos M., Castro V., Mrevlishvili G. and Teixeira J. (2004). Hydration of ds-DNA and ss-DNA by neutron quasielastic scattering. *Biophys J*. 86(6):3822-3827.

Bhargava K. and Feix J. B. (2004). Membrane binding, structure, and localization of cecropin-mellitin hybrid peptides: a site-directed spin-labeling study. *Biophys J*. 86(1 Pt 1):329-336.

Boman H. G., Wade D., Boman I. A., Wahlin B. and Merrifield R. B. (1989). Antibacterial and antimalarial properties of peptides that are cecropin-melittin hybrids. *FEBS Lett*. 259(1):103-106.

Bouxsein N. F., Leal C., McAllister C. S., Ewert K. K., Li Y., Samuel C. E. and Safinya C. R. (2011). Two-dimensional packing of short DNA with nonpairing overhangs in cationic liposome-DNA complexes: from Onsager nematics to columnar nematics with finite-length columns. *J Am Chem Soc*. 133(19):7585-7595.

Bouxsein N. F., McAllister C. S., Ewert K. K., Samuel C. E. and Safinya C. R. (2007). Structure and gene silencing activities of monovalent and pentavalent cationic lipid vectors complexed with siRNA. *Biochemistry*. 46(16):4785-4792.

Brogden N. K. and Brogden K. A. (2011). Will new generations of modified antimicrobial peptides improve their potential as pharmaceuticals? *Int J Antimicrob Agents*. 38(3):217-225.

Diaz-Achirica P., Prieto S., Ubach J., Andreu D., Rial E. and Rivas L. (1994). Permeabilization of the mitochondrial inner membrane by short cecropin-A-melittin hybrid peptides. *Eur J Biochem*. 224(1):257-263.

Diaz-Achirica P., Ubach J., Guinea A., Andreu D. and Rivas L. (1998). The plasma membrane of Leishmania donovani promastigotes is the main target for CA(1-8)M(1-18), a synthetic cecropin A-melittin hybrid peptide. *Biochem J*. 330 (Pt 1):453-460.

Fernandez-Reyes M., Diaz D., de la Torre B. G., Cabrales-Rico A., Valles-Miret M., Jimenez-Barbero J., Andreu D. and Rivas L. (2010). Lysine N(epsilon)-trimethylation, a tool for improving the selectivity of antimicrobial peptides. *J Med Chem*. 53(15):5587-5596.

Ferre R., Melo M. N., Correia A. D., Feliu L., Bardaji E., Planas M. and Castanho M. (2009). Synergistic effects of the membrane actions of cecropin-melittin antimicrobial hybrid peptide BP100. *Biophys J*. 96(5):1815-1827.

Fischbach M. A. and Walsh C. T. (2009). Antibiotics for emerging pathogens. *Science*. 325(5944):1089-1093.

Haney E. F. and Hancock R. E. (2013). Peptide design for antimicrobial and immunomodulatory applications. *Biopolymers*. 100(6):572-583.

Huang T. C., Toraya H., Blanton T. N. and Wu Y. (1993). X-ray powder diffraction analysis of silver behenate, a possible low-angle diffraction standard. *J Appl Cryst*. 26(2):180-184.

Juvvadi P., Vunnam S., Merrifield E. L., Boman H. G. and Merrifield R. B. (1996). Hydrophobic effects on antibacterial and channel-forming properties of cecropin A-melittin hybrids. *J Pept Sci*. 2(4):223-232.

Keller S., Vargas C., Zhao H., Piszczek G., Brautigam C. A. and Schuck P. (2012). High-precision isothermal titration calorimetry with automated peak-shape analysis. *Anal Chem*. 84(11):5066-5073.

Koltover I., Salditt T., Rädler J. O. and Safinya C. R. (1998). An Inverted Hexagonal Phase of Cationic Liposome-DNA Complexes Related to DNA Release and Delivery. *Science*. 281(5373):78-81.

Ladokhin A. S., Selsted M. E. and White S. H. (1997). Sizing membrane pores in lipid vesicles by leakage of co-encapsulated markers: pore formation by melittin. *Biophys J*. 72(4):1762-1766.

Ladokhin A. S. and White S. H. (1999). Folding of amphipathic alpha-helices on membranes: energetics of helix formation by melittin. *J Mol Biol*. 285(4):1363-1369.

Ladokhin A. S. and White S. H. (2001). 'Detergent-like' permeabilization of anionic lipid vesicles by melittin. *Biochim Biophys Acta*. 1514(2):253-260.

Leal C., Bouxsein N. F., Ewert K. K. and Safinya C. R. (2010). Highly efficient gene silencing activity of siRNA embedded in a nanostructured gyroid cubic lipid matrix. *J Am Chem Soc*. 132(47):16841-16847.

Mansour S. C., Pena O. M. and Hancock R. E. (2014). Host defense peptides: front-line immunomodulators. *Trends Immunol*. 35(9):443-450.

McClare C. W. (1971). An accurate and convenient organic phosphorus assay. *Anal Biochem*. 39(2):527-530.

Melo M. N., Ferre R., Feliu L., Bardaji E., Planas M. and Castanho M. A. (2011). Prediction of antibacterial activity from physicochemical properties of antimicrobial peptides. *PLoS One*. 6(12):e28549.

Milani A., Benedusi M., Aquila M. and Rispoli G. (2009). Pore forming properties of cecropin-melittin hybrid peptide in a natural membrane. *Molecules*. 14(12):5179-5188.

Nguyen L. T., Haney E. F. and Vogel H. J. (2011). The expanding scope of antimicrobial peptide structures and their modes of action. *Trends Biotechnol*. 29(9):464-472.

Pistolesi S., Pogni R. and Feix J. B. (2007). Membrane insertion and bilayer perturbation by antimicrobial peptide CM15. *Biophys J*. 93(5):1651-1660.

Pozo Navas B., Lohner K., Deutsch G., Sevcsik E., Riske K. A., Dimova R., Garidel P. and Pabst G. (2005). Composition dependence of vesicle morphology and mixing properties in a bacterial model membrane system. *Biochim Biophys Acta*. 1716(1):40-48.

Rädler J. O., Koltover I., Salditt T. and Safinya C. R. (1997). Structure of DNA-Cationic Liposome Complexes: DNA Intercalation in Multilamellar Membranes in Distinct Interhelical Packing Regimes. *Science*. 275(5301):810-814.

Roveri N., Bigi A., Castellani P. P., Foresti E., Marchini M. and Strocchi R. (1980). [Study of rat tail tendon by x-ray diffraction and freeze-etching technics]. *Boll Soc Ital Biol Sper*. 56(9):953-959.

Sato H. and Feix J. B. (2006). Osmoprotection of bacterial cells from toxicity caused by antimicrobial hybrid peptide CM15. *Biochemistry*. 45(33):9997-10007.

Scheidt H. A., Klingler J., Huster D. and Keller S. (2015). Structural Thermodynamics of myr-Src(2-19) Binding to Phospholipid Membranes. *Biophys J*. 109(3):586-594.

Schwieger C. and Blume A. (2007). Interaction of poly(L-lysines) with negatively charged membranes: an FT-IR and DSC study. *Eur Biophys J*. 36(4-5):437-450.

Seelig J. (2004). Thermodynamics of lipid-peptide interactions. *Biochim Biophys Acta*. 1666(1-2):40-50.

Teixeira V., Feio M. J. and Bastos M. (2012). Role of lipids in the interaction of antimicrobial peptides with membranes. *Prog Lipid Res*. 51(2):149-177.

Teixeira V., Feio M. J., Rivas L., De la Torre B. G., Andreu D., Coutinho A. and Bastos M. (2010). Influence of Lysine Nε-Trimethylation and Lipid Composition on the Membrane Activity of the Cecropin A-Melittin Hybrid Peptide CA(1−7)M(2−9). *J Phys Chem B*. 114(49):16198-16208.

Vargas C., Klingler J. and Keller S. (2013). Membrane partitioning and translocation studied by isothermal titration calorimetry. *Methods Mol Biol*. 1033:253-271.

Wade D., Boman A., Wahlin B., Drain C. M., Andreu D., Boman H. G. and Merrifield R. B. (1990). All-D amino acid-containing channel-forming antibiotic peptides. *Proc Natl Acad Sci U S A*. 87(12):4761-4765.

Yeung A., Gellatly S. and Hancock R. (2011). Multifunctional cationic host defence peptides and their clinical applications. *Cell Mol Life Sci*. 68(13):2161-2176.

CHAPTER 6. Structural diversity and mode of action on lipid membranes of three lactoferrin candidacidal peptides

Biochimica et Biophysica Acta 1828 (2013) 1329–1339

Contents lists available at SciVerse ScienceDirect

Biochimica et Biophysica Acta

journal homepage: www.elsevier.com/locate/bbamem

Structural diversity and mode of action on lipid membranes of three lactoferrin candidacidal peptides

Tânia Silva [a,b,c], Regina Adão [a], Kamran Nazmi [d], Jan G.M. Bolscher [d], Sérgio S. Funari [e], Daniela Uhríková [f], Margarida Bastos [a,*]

[a] Centro de Investigação em Química CIQ(UP), Department of Chemistry & Biochemistry, Faculty of Sciences, University of Porto, Portugal
[b] IBMC — Instituto de Biologia Molecular e Celular, Universidade do Porto, Portugal
[c] ICBAS — Instituto de Ciências Biomédicas Abel Salazar, Universidade do Porto, Portugal
[d] Academic Centre Dentistry Amsterdam (ACTA), Department of Oral Biochemistry, University of Amsterdam and VU University Amsterdam, Amsterdam, The Netherlands
[e] HASYLAB, DESY, Hamburg, Germany
[f] Faculty of Pharmacy, Comenius University, Bratislava, Slovak Republic

ARTICLE INFO

Article history:
Received 9 October 2012
Received in revised form 25 January 2013
Accepted 28 January 2013
Available online 4 February 2013

Keywords:
Antimicrobial peptides
Lactoferrin peptides
DSC
CD
SAXD

ABSTRACT

The structure and membrane interactions of three antimicrobial peptides from the lactoferrin family were investigated through different techniques. Circular dichroism shows that the peptides adopt a secondary structure in the presence of DMPC/DMPG, and DSC reveals that they all interact with these membranes, albeit differently, whereas only LFchimera has an effect in pure zwitterionic membranes of DMPC. DSC further shows that membrane action is weakest for LFcin17-30, increases for LFampin265-284 and is largest for LFchimera. These differences are clearly reflected in a different structure upon interaction, as revealed by SAX. This technique shows that LFcin17-30 only induces membrane segregation (two lamellar phases are apparent upon cooling from fluid phase), whereas LFampin265-284 induces micellization of the membrane with structure compatible to a micellar cubic phase of space group Pm3n, and LFchimera leads to membrane destruction through the formation of two cubic phases, Pn3m and Im3m. These structural results show a remarkable parallel with the ones obtained previously by freeze fracture microscopy of the effect of these peptides against *Candida albicans*.

1. Introduction

We continue to face a reemergence of infectious diseases, mainly due to the increasing resistance of the pathogens to current therapies and the lack of new and more effective antimicrobial drugs. One potential and interesting alternative to conventional antibiotics is the use of antimicrobial peptides (AMPs). Natural AMPs are present in almost all living organisms as a primary defense mechanism against invading pathogens, with remarkably different structures and bioactivity profiles [1].

AMPs are considered membrane-active agents leading to cell death by acting on the phospholipid membrane [2]. Within this broad umbrella, it is recognized today that they do not act through a universal mechanism. Different mechanisms have been proposed, consistent with experimental results, providing possible ways for the peptides to disrupt the membrane, leading to cell death. All rely on the same main factor for initial action — adsorption of AMPs onto the membrane due to electrostatic interactions between the cationic peptides and the headgroups of anionic phospholipids. Thereafter, accumulation and positional change eventually lead to the formation of pores, membrane permeabilization or membrane micellization [1,3–7]. In some cases internal targets have also been described [5,8–11].

Independently of the details of the mechanism of action the interaction must be as selective as possible regarding the distinction between mammalian cells (higher eukaryotes) and pathogen cells, such as bacteria (prokaryotic cells) or lower eukaryotes as fungi and protozoan. Cytoplasmic membranes of mammalian cells expose predominantly zwitterionic phosphatidylcholine (PC) and sphingomyelin to the extracellular side [1]. On the other hand, cytoplasmic bacterial membranes are mainly composed of zwitterionic phosphatidylethanolamine (PE) and negatively charged phosphatidylglycerol (PG) conferring an overall

Abbreviations: AMPs, antimicrobial peptides; CD, circular dichroism; DMPC, dimyristoylphosphatidylcholine; DMPG, dimyristoylphosphatidylglycerol; DSC, differential scanning calorimetry; IMPs, intra-membranous particles; LC_{50}, lethal concentration that causes 50% of cell death; LFampin265-284, lactoferrampin 265–284; LFchimera, LFcin17-30-K-LFampin265-284; LFcin17-30, lactoferricin 17–30; LUVs, large unilamellar vesicles; MLVs, multilamellar vesicles; P:L, peptide-to-lipid molar ratio; PC, phosphatidylcholine; PE, phosphatidylethanolamine; PG, phosphatidylglycerol; SAXD, small angle X-ray diffraction; WAXD, wide angle X-ray diffraction

* Corresponding author at: Centro Investigação em Química CIQ(UP), Department of Chemistry and Biochemistry, Faculty of Sciences, University of Porto, Rua do Campo Alegre, 4169-007 Porto, Portugal. Tel.: +351 220402511; fax: +351 220402659.
E-mail address: mbastos@fc.up.pt (M. Bastos).

0005-2736/$ – see front matter © 2013 Elsevier B.V. All rights reserved.
http://dx.doi.org/10.1016/j.bbamem.2013.01.022

negative charge to the membrane [1,12]. Lower eukaryotes, such as fungi and protozoa also have PC, but they have higher amounts of exposed anionic phospholipids, like phosphatidylserine, than mammalian cells [1,13,14]. Indeed it is this differential composition that justifies the unifying electrostatic character of the initial interaction, as well as the ability of the AMPs to act preferentially against pathogens.

Biophysical studies can provide important information on the details of AMPs interaction with the membranes and thus help to unravel their mechanism of action, by providing insight into the effects of the peptides on the membrane structure and information on peptide location. Different techniques have been employed, such as calorimetry, spectroscopy, X-ray diffraction and others [3,12,15–28].

X-ray diffraction studies can give quantitative information on the effects of AMPs on membrane structure, namely if they are capable of altering the phospholipid structure and organization, as well as phase behavior. This information thus allows correlation of these possible changes in lipid polymorphism with models for the mechanism of action of AMPs [12,22,23,28]. Growing evidence shows that lipid cubic phases are ubiquitous in the biological world as they have been detected in the plasma membrane of archaebacteria, as well as in the endoplasmic reticulum and mitochondria of mammalian cells. These phases are also involved in biological processes such as membrane fusion, fat digestion and in the reorganization of cell membrane composition [1,29–32]. In the AMP research area, some reports started to appear in the literature indicating the ability of AMPs to induce cubic phases. So far most studies have revealed the existence of bicontinuous (single or double) cubic phases [12,19,24–28,33–35] and a recent one reported a micellar cubic phase [36].

Previously, Bolscher et al. [37,38] have obtained freeze-fracture results on the action of peptides of the lactoferrin family against *Candida albicans*, showing that the peptides have a quite different effect on the membrane of this pathogen. In the present work we studied the action of these peptides on model membranes of DMPC/DMPG (3:1), considered to be a good model system for *C. albicans*, by a variety of biophysical techniques. We found that lactoferricin 17–30 (LFcin17-30) induces phase segregation and is the peptide with lowest membrane activity, lactoferrampin 265–284 (LFampin265-284) induces a micellar cubic phase (Pm3n) [36], which to the best of our knowledge is the first experimental evidence of such phase in the context of antimicrobial peptide/membrane interaction. Finally LFchimera, a hybrid peptide between the first two [16], induces two cubic phases of Pn3m and Im3m symmetry. These results parallel their effect on *C. albicans* as derived from freeze-fracture electron microscopy, indicating a remarkable agreement between simple model systems and living organisms.

2. Materials and methods

2.1. Peptide synthesis, purification and characterization

LFcin17-30, LFampin265-284 and LFchimera were synthesized by solid phase peptide synthesis using Fmoc-protected amino acids (Orpegen Pharma GmbH, Heidelberg, Germany) in a Syro II synthesizer (Biotage, Uppsala Sweden) as described previously [16]. The chimerical peptide comprises a single C-terminal amidated lysine substituted at the α- and ε-amino groups with the two peptides via the C-terminal site and leaving two N-termini as free ends. Peptides were purified to a purity of at least 95% by semipreparative RP-HPLC (Jasco Corporation Tokyo, Japan) on a Vydac C18-column (218MS510; Vydac, Hesperia, CA, USA) and the authenticity of the peptides was confirmed by MALDI-TOF mass spectrometry on a Microflex LRF mass spectrometer equipped with an additional gridless reflectron (Bruker Daltonik, Bremen, Germany) as described previously [39]. In Table 1 we provide basic information of the peptides, together with their LC_{50} and their ultrastructural effects against *C. albicans*, as obtained previously by Bolscher et al. [37,38].

2.2. Preparation of liposomes

1,2-dimyristoyl-*sn*-glycero-3-phosphocholine (DMPC) was dissolved in chloroform, and its mixture with 1,2-dimyristoyl-*sn*-glycero-3-[phospho-*rac*-(1-glycerol)] (DMPG) at a molar ratio of 3:1 was dissolved in chloroform/methanol (3:1 (v/v)). Both lipids were from Avanti Polar Lipids, Alabama, USA. A film was prepared thereafter in round bottom flasks by drying the sample under a stream of nitrogen, and was kept under vacuum for 3 h to remove all traces of organic solvents. After drying, the lipid film was first warmed for 30 min at *ca.* 10 °C above the temperature of the gel-to-liquid crystalline phase transition (T_m) in a thermostated water bath, and afterwards hydrated with buffer, either HEPES (10 mM HEPES, 100 mM NaCl, pH 7.4) or PBS (9.3 mM, 154 mM NaCl, pH 7.2), kept at the same temperature. The multilamellar vesicles (MLVs) were obtained by alternating gentle vortex with short periods in the thermostated water bath at ~35 °C. After this the MLVs were frozen in liquid nitrogen and thawed in a water bath at 35 °C, and this process was repeated 5 times.

Large unilamellar vesicles (LUVs) were obtained from the MLVs by extrusion in a 10 ml stainless steel extruder (Lipex Biomembranes, Vancouver, BC, Canada), inserted in a thermostated cell with a re-circulating water bath, at 35 °C. The samples were passed several times through polycarbonate filters (Nucleopore, Pleasanton, CA, USA) of decreasing pore size (600, 200 and 100 nm; 5, 5 and 10 times, respectively), under inert (N_2) atmosphere.

Size distribution of extruded vesicles was determined by *qels* analysis (Malvern Zeta Sizer 5000, Malvern Instruments, Malvern, Worcestershire,UK) using a helium-neon laser (633 nm) as a source of incident light, and operating at a scattering angle of 90° and at 37 °C. Mean particle size was thus determined as being of 106 ± 4 nm (average and standard deviation of 6 independent measurements). The phospholipid concentration was determined by the phosphomolibdate method [40].

2.3. Differential scanning calorimetry

Differential scanning calorimetry (DSC) was performed in a Micro-DSCIII microcalorimeter (SETARAM, Caluire, France) essentially as described previously [41]. In brief, samples were run against HEPES buffer in the reference cell, and blank experiments with HEPES buffer in both cells were also performed for subsequent blank correction. The solution or suspension volume used in each cell was of around 0.8 ml, and the masses of solution in sample and reference cells were subsequently matched by weighing ±0.00005 g. Two successive heating and cooling scans were performed for each sample, the heating scan at a scanning rate of 0.5 °C/min and the cooling scan at 3 °C/min, over the temperature range of 10–35 °C. The results provided here always refer to the second heating scan, as we have observed that small differences can exist between first and second scans, but not thereafter. The sample mixtures were prepared immediately before the DSC run, by adding the desired amount of peptide (LFcin17-30, LFampin265–284 or LFchimera) stock solution (in HEPES buffer) to the LUVs suspension of DMPC or DMPC/DMPG (3:1). Samples with peptide-to-lipid molar ratios (P:L) from 1:197 to 1:29 were used. All procedures regarding sample preparation and handling (lag time at low temperature, time between mixtures, and start of the experiment) were kept constant in all experiments, to ensure that all samples had the same thermal history. The instrument was electrically calibrated for temperature and the scan rate with the SETARAM Calibration Unit. The Micro-DSCIII software was used for blank subtraction (run with buffer solution on both cells (sample and reference)). T_m and the $\Delta_{trans}H$ were calculated by integration of the heat capacity versus temperature curve (*Cp* versus Temperature). A linear baseline was used to calculate the integral areas under the curves [41].

Table 1
Properties of synthetic lactoferrin peptides.

Peptide	LFcin17-30	LFampin265-284	LFchimera[a]
Sequence	FKCRRWQWRMKKLG	DLIWKLLSKAQEKFGKNKSR	FKCRRWQWRMKKLG–K DLIWKLLSKAQEKFGKNKSR
Charge[b]	+6	+4	+12
Freeze fracture microscopy[c]	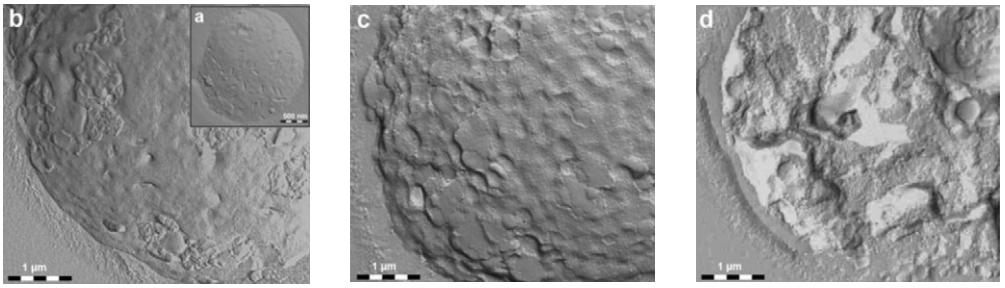		
LC_{50}[d]	1.5	1.2	0.5

[a] The carboxyl group of the linking lysine (C-terminal) is in carboxamide form.
[b] Calculated overall charge at pH = 7.0.
[c] From previously published results [37,38]. Insert (a) is the control. The scale is embedded in each figure.
[d] From previously published results [37,38]; LC_{50} is the peptide lethal concentration that causes 50% of *C. albicans* death determined in a 5 mM NaCl containing phosphate buffer.

2.4. Circular dichroism

Circular dichroism (CD) experiments were carried out in a Jasco 720 spectropolarimeter (Japan Spectroscopy Co., Tokyo) equipped with a rectangular cell, path length of 1 mm. Scans were performed between 175 and 250 nm, bandwidth 1.0 nm, and resolution of 100 mdeg. The measurements were performed in 2 mM HEPES, 100 mM NaCl, pH 7.4. Spectra of pure liposome preparations were performed in the same solvent media at the concentrations used in liposome/peptide mixture. These were used as blank experiments to be subtracted from the liposome/peptide spectra. The peptide concentration in buffer was 36 μM. Liposome concentrations were: 6 mM for DMPC and 3 mM for DMPC/DMPG (3:1), in both cases with a P:L ratio of 1:167. The peptide solution and liposome suspension were mixed just prior to each measurement and incubated at 35 °C for 30 min and measurements were performed thereafter at the same temperature. Each spectrum was the average of nine accumulations. After blank correction, the observed ellipticity was converted to a mean residue molar ellipticity (θ) ($deg \cdot cm^2 \cdot dmol^{-1}$), based on the total amount of peptide in the mixture.

2.5. X-ray diffraction studies

Peptide solution in the same buffer used for preparing the liposomes was added to the liposome suspension at different P:L molar ratios, and the mixtures were incubated for 30 min at 35 °C. The samples were then centrifuged at 13 000 rpm in a microcentrifuge at least for 15 min, and transferred thereafter into glass capillaries (Spezialglas Markröhrchen 1.5 mm capillaries, Glass Technik & Konstruktion — Müller & Müller OHG, Germany). In the transfer care was taken to always have a significant amount of supernatant in the capillaries, to guarantee that all samples were studied at high water contents. The capillaries were sealed by flame, and stored at 4 °C, at least 3 days before use.

Small angle X-ray diffraction (SAXD) and wide angle X-ray diffraction (WAXD) experiments were performed at the synchrotron soft condensed matter beamline A2 in HASYLAB at Deutsches Elektronen Synchrotron (DESY), Hamburg, Germany, using a monochromatic radiation of λ = 0.15 nm wavelength. Diffractograms were taken at selected temperatures, where the sample was equilibrated for 5 min before exposure to radiation, or by performing up and down temperature scans at a scan rate 1 °C/min, where diffractograms were recorded for 10 s every minute. The heating and cooling of the sample were regulated by a thermocouple connected to the temperature controller JUMO IMAGO 500 (JUMO GmbH & Co. KG, Fulda, Germany). The evacuated double-focusing camera was equipped with a linear position sensitive detector for WAXD and a 2D MarCCD detector or a linear position sensitive detector for SAXD. The raw data were normalized against the incident beam intensity. The SAXD patterns were calibrated using Ag behenate [42] or rat tail collagen [43] and the WAXD patterns by tripalmitin or polyethylene terephthalate [44,45]. Each diffraction peak was fitted by Lorentzians above a linear background by use of the Peakfit or Origin software programs, in order to derive the lattice parameters. For cubic phases, the lattice parameter was determined as the slope of the dependence of $s(Å^{-1})$ vs. $\sqrt{(h^2+k^2+l^2)}$, passing through the origin (0,0), where h, k, l are Miller indices. The uncertainty assigned to the lattice parameters is half of the interval of maximum width that can be obtained through calculation of minimum and maximum values for lattice parameters from the slope above together with its statistical standard error, as obtained from the regression. For lamellar phases, the obtained uncertainty never exceeds ±0.1 Å, and thus from hereafter we will not quote the uncertainty for the lattice parameter in lamellar phases. The reported uncertainties for cubic phase lattice parameters are calculated as above and presented together with the lattice parameter value throughout the text.

3. Results

3.1. Differential scanning calorimetry

DSC experiments show the influence of both lipid charge and peptide-to-lipid molar ratio (P:L) on the thermotropic behavior of the peptide/lipid systems. The endotherms obtained for each peptide, LFcin17-30, LFampin265-284 and LFchimera, with the model membranes of DMPC and DMPC/DMPG (3:1), are shown in Figs. 1 and 2, respectively.

The thermodynamic description is based on the parameters characterizing the gel-to-liquid crystalline phase transition of the liposomes, namely transition temperature (T_m) and the corresponding enthalpy change (ΔH). By comparing the calorimetric profiles obtained for the pure liposomes and the liposome/peptide mixtures at the various P:L ratios allow us to derive the influence of the peptides on this thermotropic transition. The obtained thermodynamic parameters are listed in Tables 2 and 3, where values for the pure lipid systems are also shown. In order to overcome the slight differences that may occur for different lipid samples, measurements of the same peptide/lipid system were always performed with liposome suspension from the same preparation batch.

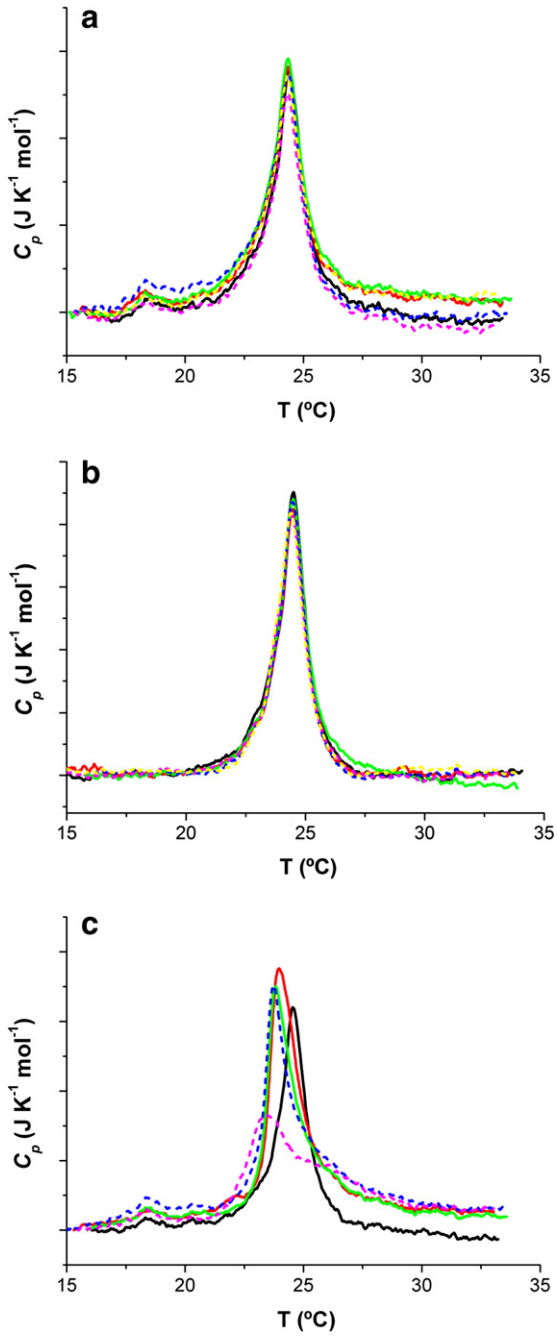

Fig. 1. DSC curves for DMPC and DMPC/peptide mixtures of varying composition. The lipid concentration was 3.0 ± 0.3 mM in all experiments. (a) LFcin17-30; (b) LFampin265-284 and (c) LFchimera. Pure lipid (solid black); P:L = 1:196 (solid gray); P:L = 1:129 (solid light gray); P:L = 1:96 (dash black); P:L = 1:46 (dash gray); P:L = 1:29 (dash light gray). Maximal P:L molar ratio used was 1:46 for LFchimera.

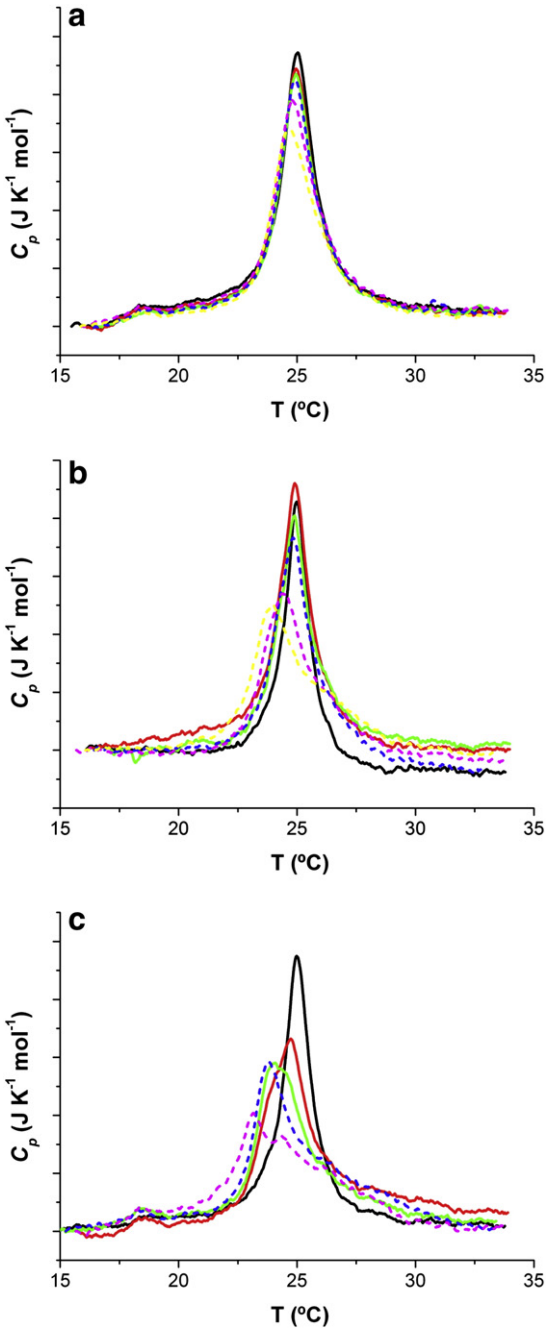

Fig. 2. DSC curves for DMPC/DMPG (3:1) and DMPC/DMPG (3:1)/peptide mixtures of varying composition. The lipid concentration was 3.0 ± 0.3 mM in all experiments. (a) LFcin17-30; (b) LFampin265-284 and (c) LFchimera. Pure lipid (solid black); P:L = 1:196 (solid gray); P:L = 1:129 (solid light gray); P:L = 1:96 (dash black); P:L = 1:46 (dash gray); P:L = 1:29 (dash light gray). Maximal P:L molar ratio used was 1:46 for LFchimera.

The phase transition observed for LUVs of pure DMPC is characterized by a temperature of 24.5 °C and an enthalpy change that varies between 19 and 27 kJ·mol^{-1} (Table 2) for different sample preparations. The ΔH_{trans} value observed for the sample used together with LFchimera is significantly higher than the other two (stated uncertainty between samples ± 3 kJ·mol^{-1}), but the same sample was used for all mixtures with this peptide, and the results are consistent within sample. The observed thermodynamic parameters are in very good agreement with literature values [41,46,47]. The calorimetric profile for the pure lipid system is a symmetric and cooperative peak. As regarding the peptide/lipid mixtures, we can see that LFcin17-30 and LFampin265-284 do not alter the gel-to-liquid crystalline transition, as the curves are superimposable for all tested P:L ratios and the parameters T_m and ΔH_{trans} are the same, within the stated uncertainty (Fig. 1a and b, and Table 2). As for LFchimera, it is clear that this peptide interacts with the zwitterionic lipid system for all P:L ratios, and as a result we observe a progressive decrease of T_m as the peptide content in the mixture increases, reflecting a better interaction with the liquid crystalline phase, and the appearance of a shoulder at the high temperature side for the highest P:L ratios (Fig. 1c and Table 2), which is indicative of domain segregation in the membrane [41]. The ΔH_{trans} values decrease with increasing peptide content, indicating a progressive

Table 2
Thermodynamic parameters T_m and ΔH_{trans} for the gel to liquid crystalline phase transition of DMPC liposomes for different P:L ratios.

	T_m[a] (°C)			ΔH_{trans}[b] (kJ mol^{-1})		
(P:L)	LFcin17-30	LFampin265-284	LFchimera	LFcin17-30	LFampin265-284	LFchimera[c]
0	24.4	24.5	24.4	22	19	27
1:196	24.4	24.5	23.7	21	21	26
1:129	24.4	24.5	23.6	22	21	23
1:96	24.4	24.5	23.5	20	19	23
1:46	24.3	24.5	23.3	20	18	23
1:29	24.3	24.4	–	21	18	–

[a] T_m estimated uncertainty is ±0.1 °C (same liposomes preparation, used for the full P:L series) and ±0.3 °C (within samples).
[b] ΔH_{trans} estimated uncertainty is ±0.5 kJ mol^{-1} (same liposomes preparation, used for the full P:L series) and ±3 kJ mol^{-1} (within samples).
[c] The value for pure lipid is significantly higher than for the other peptides, but is consistent within the same preparation (series) for this peptide.

destabilization of the membrane organization, and thus probably a deeper insertion of the peptide in the hydrocarbon moiety.

As regarding the mixed system DMPC/DMPG (3:1), we can see that an interaction exists for the three peptides, with strength that increases in the order LFcin17-30, LFampin265-284 and LFchimera (Fig. 2). This is reflected in a very small change in the thermodynamic parameters for LFcin17-30 that is higher for LFampin265–284, and much more significant for LFchimera. In all cases we observe a decrease in T_m and ΔH_{trans} (Table 3). For LFcin17-30, although the decrease in both parameters is within the quoted uncertainty, the observed trend is clearly downwards (Fig. 2a). For LFampin265-284 the differences are already outside the error limits at the highest P:L ratios, and overall the trend in both parameters is towards lower values. It should be stressed that for this peptide a significant change in shape occurs already at P:L ratio 1:46, as a very distorted curve with significantly higher width is observed, showing a large reduction in the cooperativity of the transition. This indicates the onset of a significant structural change in the membrane at higher P:L ratios (Fig. 2b).

For LFchimera the decrease in both parameters is significant for all P:L ratios, and although overall the shape of the calorimetric profile is somewhat similar to the one observed for DMPC, it is clear that the effect is much stronger (Fig. 2c). Again we see a trend for T_m and ΔH_{trans} to decrease as peptide content in the mixtures increases. This is reasonable, as on one hand the system is still predominantly zwitterionic (DMPC is 75% of the lipid content of the membrane), and on the other the electrostatic favorable contribution in the case of the partially negatively charged system DMPC/DMPG (3:1) is expected to increase the interaction, as seen in the results. Further, the profile is significantly different from the ones observed for the constituent peptides. We observed the same differential pattern in DSC studies of the three peptides with DMPG liposomes, where LFchimera had a completely disruptive behavior already at low P:L ratios, at odds with the other two peptides, that only presented a significant interaction as the P:L ratio increases [16]. This was also seen by Haney et al. in a DSC study with DPPG liposomes [18]. Again these results are in line with the effect that these peptides show on *C. albicans*, as it will be discussed further.

Finally in order to try to shed some light in the observed lipid/peptide cubic organization for the mixture DMPC/DMPG (3:1) and LFampin265-284 at high peptide contents [36] we did perform some further DSC experiments at higher P:L ratios for this system, and the obtained results can be seen in Fig. 3. A clear peak splitting is observed, as anticipated in the highest ratio of previous collection of results. Overall the transitions occur between 20 and 30 °C, and when we did the deconvolution of the overall DSC curves, two peaks were obtained, one at lower and the other at higher temperature as compared to the pure lipid mixture. At 1:12 the first transition is about one degree higher than the ones observed for 1:8 and 1:3, whereas the higher temperature transition occurs at about the same temperature (within estimated uncertainty) irrespective of P:L ratio.

3.2. Circular dichroism

The secondary structures of LFcin17-30, LFampin265-284 and LFchimera were examined by CD in HEPES buffer and in the presence of the liposome systems. CD spectra of the peptides at a concentration of 36 μM in the aqueous buffer (2 mM HEPES, 100 mM NaCl, pH = 7.4) are shown in Fig. 4, together with the CD spectra obtained in the presence of DMPC and DMPC/DMPG (3:1) liposomes. Measurements at different peptide concentrations in aqueous buffer showed that the peptide structures are not significantly affected by peptide concentration within the concentration range of 15 to 50 μM (results not shown). Therefore, only one concentration is plotted for each peptide in buffer. As for peptide/liposome mixtures, we have tested several combinations, and observed that all provide the same secondary structure information. Therefore, we only plot the ones that provided the best quality spectra.

All peptides show a predominantly random coil structure in buffer. In the presence of DMPC the structure remains practically the same for LFampin265-284, whereas LFcin17-30 changes slightly the minima to higher wavelengths and more negative ellipticity values between 210 and 230 nm, indicating a more significant contribution of β-structure to the overall CD signal (Fig. 4a and b). In the case of LFchimera, we have a mixture of structures, where the minimum around 200 nm moves to about 217 nm, characteristic of the presence

Table 3
Thermodynamic parameters T_m and ΔH_{trans} for the gel to liquid crystalline phase transition of DMPC/DMPG (3:1) liposomes for different P:L ratios.

	T_m[a] (°C)			ΔH_{trans}[b] (kJ mol^{-1})		
(P:L)	LFcin17-30	LFampin265-284	LFchimera	LFcin17-30	LFampin265-284	LFchimera
0	25.0	25.0	24.8	23	21	26
1:196	25.0	24.9	24.7	22	21	26
1:129	25.0	24.9	24.5	22	19	24
1:96	25.0	24.8	23.7	22	19	21
1:46	24.8	24.4	23.2	22	20	20
1:29	24.6	23.9	–	21	18	–

[a] T_m estimated uncertainty is ±0.1 °C (same liposomes preparation, used for the full P:L series) and ±0.3 °C (within samples).
[b] ΔH_{trans} estimated uncertainty is ±0.5 kJ mol^{-1} (same liposomes preparation, used for the full P:L series) and ±3 kJ mol^{-1} (within samples).

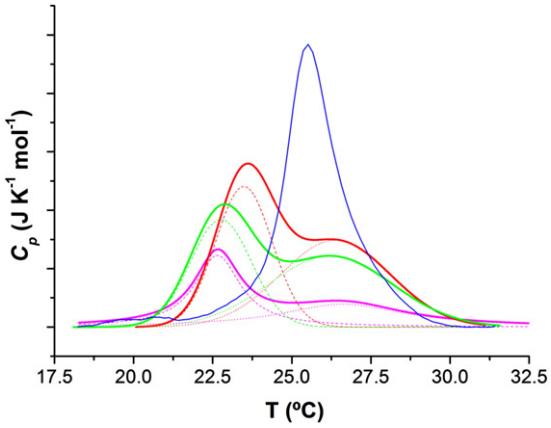

Fig. 3. DSC curves for DMPC/DMPG (3:1) and DMPC/DMPG (3:1)/LFampin 265–284 mixtures at high P:L ratios. The lipid concentration was 6.0 ± 0.3 mM in all experiments. Pure lipid (solid black); P:L = 1:12 (heavy solid black); P:L = 1:8 (heavy solid gray); P:L = 1:3 (heavy solid light gray). The dashed (low temperature peak) and dotted (high temperature peak) lines represent the deconvoluted curves for each P:L ratio.

of β-structure (Fig. 4c). This could indicate that although LFcin17-30 and LFampin265-284 alone do hardly interact with DMPC liposomes, as revealed from DSC and CD, when bound together in LFchimera they contribute to the mixture of structures observed by CD for this peptide's interaction with zwitterionic lipids.

In the presence of DMPC/DMPG (3:1), both LFampin265-284 and LFchimera show the predominance of α-helix structure, with well-defined minima around 208 and 222 nm (Fig. 4b and c). Nevertheless the α-helix structure is better defined in the case of LFampin265-284. Finally LFcin17-30 shows CD spectra in this lipid mixture that clearly reflects a mixture of α-helix and β-structure (Fig. 4a). We should stress that in a previous paper we showed that this peptide presents the structure of a β-turn in the presence of purely negatively charged membranes of DMPG [16], and it is thus reasonable that this structure already appears in the DMPC/DMPG (3:1) lipid mixture, although to a smaller extent.

Overall, it is clear that the structure of the peptides changes in the presence of membranes, and that the structure adopted depends on the peptide and the lipid mixture.

3.3. X-ray diffraction

Curiously, SAXD experiments revealed that each of the three studied peptides induces different structural changes in DMPC/DMPG (3:1) membrane. The structural changes are temperature dependent, and we present typical diffraction patterns at selected temperatures with the aim to shed more light into the mechanism of peptide–membrane interaction.

The SAXD and WAXD results obtained for LFcin17-30 and DMPC/DMPG (3:1) at selected temperatures, for a P:L ratio 1:8 (mol/mol) can be found in Fig. 5. Despite the high peptide to lipid molar ratio in the sample, SAXD did not indicate the occurrence of membrane disruption. As described in the Materials and methods section, prior to interaction with the peptide the DMPC/DMPG (3:1) mixture forms a dispersion of unilamellar (or oligolamellar) vesicles. Such dispersion does not have a long range order and SAX diffraction shows a broad peak with intensity at the level of background (not shown). In the gel phase, the phospholipid acyl chains are fully extended, packed hexagonally and oriented more or less perpendicularly to the surface of the bilayer, a structural feature documented by a peak in WAX diffraction. For our pure DMPC/DMPG (3:1) mixture the temperature of gel to liquid crystalline phase transition was found to be $T_m = 25$ °C by our DSC experiments (Table 3). The diffractogram obtained for the mixture LFcin17-30 and DMPC/DMPG (3:1) taken at 10 °C

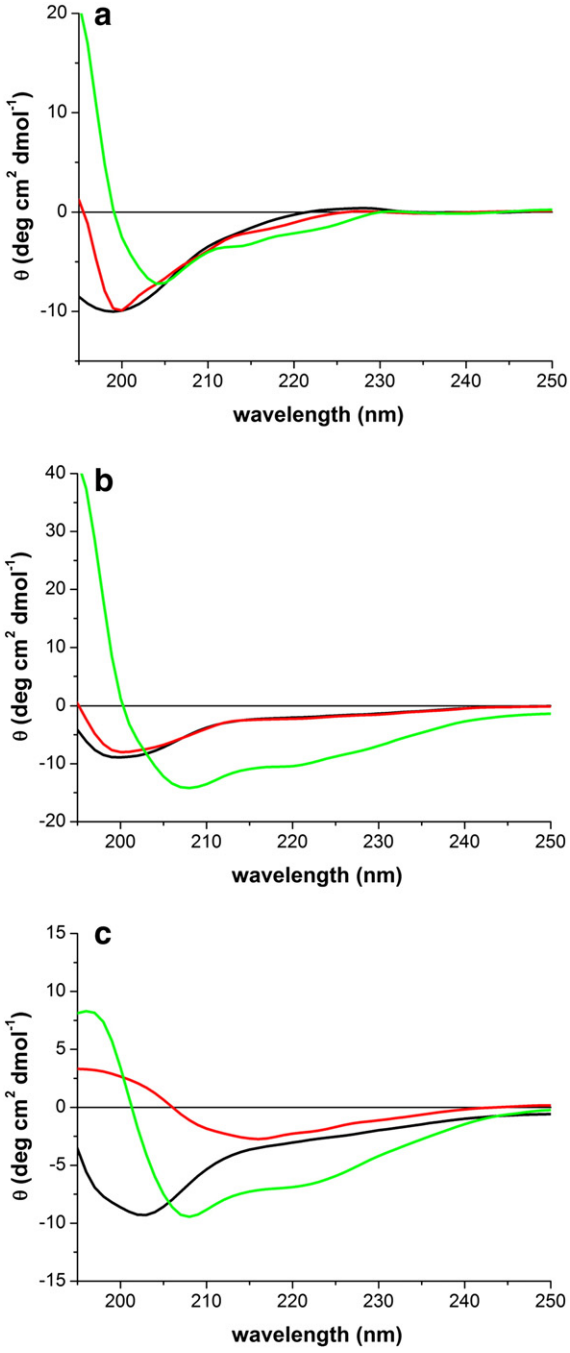

Fig. 4. CD spectra of (a) LFcin17-30, (b) LFampin265-284 and (c) LFchimera at 35 °C in: buffer (peptide concentration 36 μM) (solid black); DMPC 6 mM (dash gray); and DMPC/DMPG (3:1) 3 mM (dotted light gray). P:L ratio in peptide/LUV mixtures was 1:167.

corresponds well with the description above and shows no evidence of interaction of the AMP with the DMPC/DMPG (3:1) membrane. However, heating the system above the phase transition temperature of the mixture, we observe a lamellar phase with a repeat distance d slightly decreasing with increasing temperature — $d = 61.7$ and 58.5 Å at 35 and 50 °C, respectively. The WAXD pattern, on the other hand, exhibits wide diffuse scattering in the range ~0.18–0.35 Å^{-1}, characteristic for phospholipid liquid-like carbon chains (Fig. 5). This indicates that the peptide has a better interaction with the membrane in liquid crystalline resulting in structural changes due to charge screening of both DMPC/DMPG membrane and LFcin17-30. Cooling down the mixture, we identified two distinct

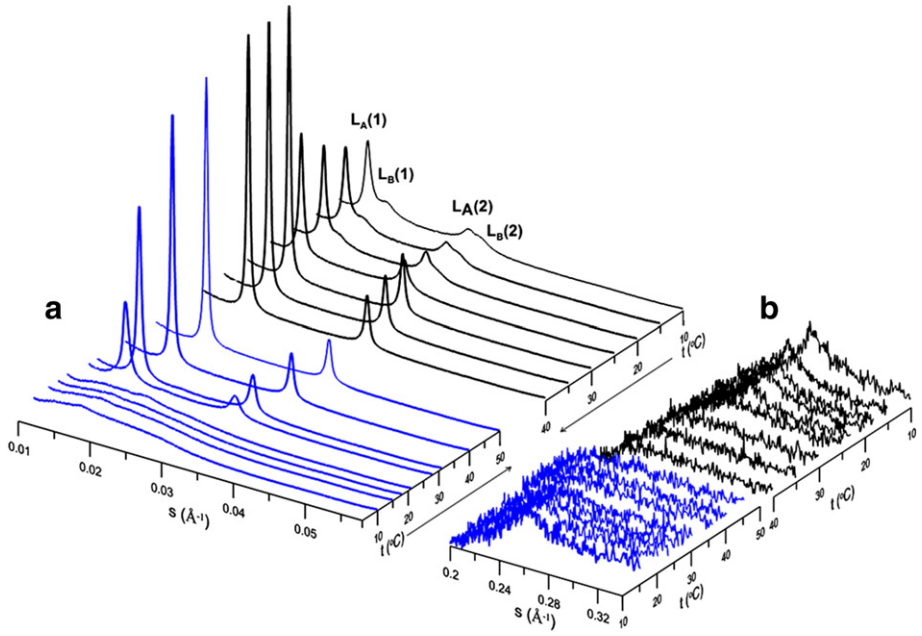

Fig. 5. SAXD (a) and WAXD (b) patterns for a peptide/lipid mixture of LFcin17-30 and DMPC/DMPG (3:1) for P:L = 1:8 (mol/mol), at selected temperatures. The lipid concentration was 12 mM.

lamellar phases (L_A and L_B) at temperatures below T_m (Fig. 5), with repeat distances $d_A = 70.9$ Å and $d_B = 65.7$ Å at 10 °C, an indication that the cooling process leads to a non-homogeneous distribution of the components in the system.

The other two peptides of the lactoferrin family show a more disruptive behavior against the DMPC/DPMG (3:1) membrane. Our previously published X-ray diffraction study on the system with LFampin265-284 and DMPC/DMPG (3:1) revealed the membrane disintegration through a micellar cubic phase of space group Pm3n [36]. By performing SAXD measurements at increasing temperatures we observed that the cubic phase Pm3n occurs in a temperature range where the pure DMPC/DMPG (3:1) mixture was still in the gel state. Fig. 6 shows SAX diffractograms of mixtures of LFampin265-284 with DMPC/DMPG (3:1) at two P:L molar ratios (1:8 and 1:5) and selected temperatures. At both P:L ratios and ~20 °C we observe a cubic

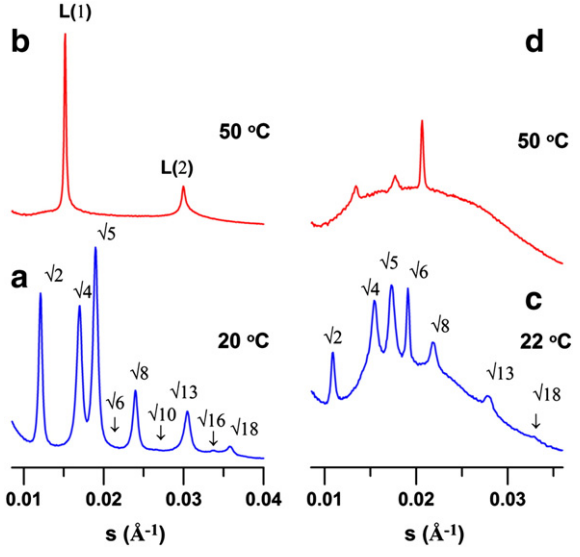

Fig. 6. SAX diffractograms for mixtures of LFampin265-284 with DMPC/DMPG (3:1) at different temperatures and P:L molar ratios: (a) and (b): P:L = 1:8; (c) and (d): P:L = 1:5. Intensities are plotted in logarithmic scale.

phase of Pm3n space group (Fig. 6a, c). The lattice parameters depend on P:L ratio, as the value obtained for a P:L ratio 1:5 was $a = 129.0 \pm 0.1$ Å, whereas for 1:8 we obtained $a = 119.4 \pm 0.1$ Å, determined as described in the Materials and methods section. The unit cell dimension of Pm3n cubic phase was also found to be dependent on temperature, with the cell dimension slightly decreasing as the temperature increased. The Pm3n phase is usually observed at high water content and is supposed to consist of discrete micelles of amphiphiles arranged on a cubic lattice and separated by a continuous film of water.

The phase transition accompanying the disappearance of the cubic phase involves massive structural changes in the mixture, which in SAX is reflected in a broad, not well resolved peak [36]. At higher temperatures, we detected a lamellar L_α phase. The onset of the L_α phase was found to depend on P:L molar ratio — for P:L = 1:8 it was observed at ~29 °C, whereas for P:L = 1:5 the L_α phase was not detected until ~60 °C. Bellow this temperature, diffractograms show 2–3 peaks above a broad background as (Fig. 6), probably due to scattering on partly ordered intermediated structures in the process of cubic phase disappearance.

LFchimera was identified as the peptide with much stronger disruptive effect on the model membrane, as revealed by the DSC results (Section 3.1, Fig. 2c and Table 3).

We examined its effect on the DMPC/DMPG (3:1) membrane at several P:L molar ratios. At low molar ratio (P:L = 1:38) the peptide does not disrupt the membrane, but in the temperature range of 15–40 °C we observe a lamellar phase with periodicities 64.2 and 56.3 Å at 20 and 40 °C, respectively (not shown). This shows that although the peptide initially interacts with unilamellar or oligolamellar vesicles at low P:L ratio it has the ability to build a multilamellar structure. At the same temperatures, we found $d_{DMPC} = 66.5$ and 62.0 Å, where d_{DMPC} is the repeat distance of DMPC bilayer stacking. The observed lower spacing (~6 Å) at 40 °C indicates that either the peptide mediates a closer approach between two opposite charged bilayers due to membrane/AMP charge compensation or the thickness of the membrane itself is reduced after AMP intercalation. As we increase P:L ratio, SAX diffractograms already detected changes in the lamellar organization, but at temperatures below T_m and for P:L = 1:30 we only observe a not well resolved phase of higher symmetry (not shown), that becomes better defined

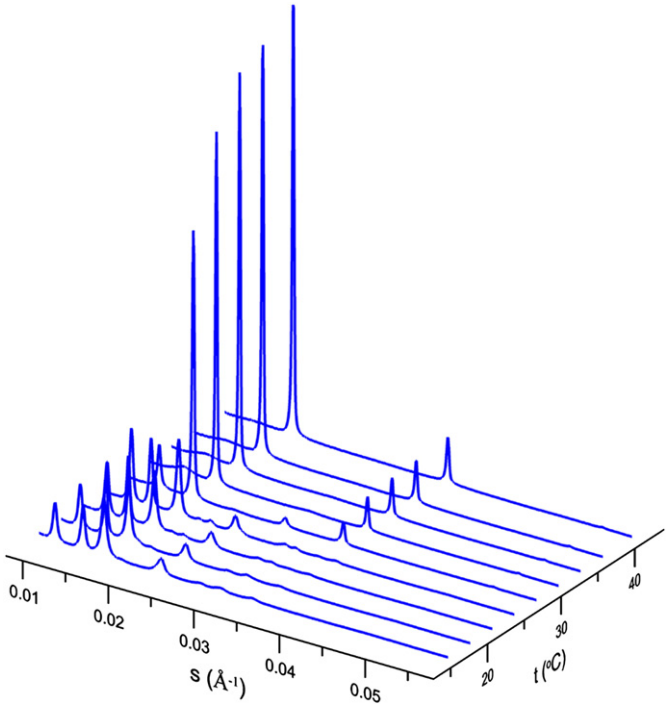

Fig 7. SAX diffractograms of a heating scan between 15 and 40 °C for LFchimera and DMPC/DMPG (3:1) at a P:L ratio 1:21.

on cooling. This parallels our previous findings (see above) of a better compatibility with the fluid phase, as expected. Increasing the LFchimera content to molar ratio P:L = 1:21, the membrane was disrupted and SAXD clearly confirmed the presence of non-lamellar phase(s) (Figs. 7 and 8). In Fig. 7 we show diffractograms of a heating scan between 15 and 40 °C for this peptide with DMPC/DMPG (3:1) at this later P:L ratio, where the peaks corresponding to a phase or phases of higher symmetry are clearly seen.

Two representative diffractograms at 24 and 30 °C with respective peak assignment are presented in Fig. 8. At low temperature, the deconvolution of the diffraction pattern revealed the coexistence of

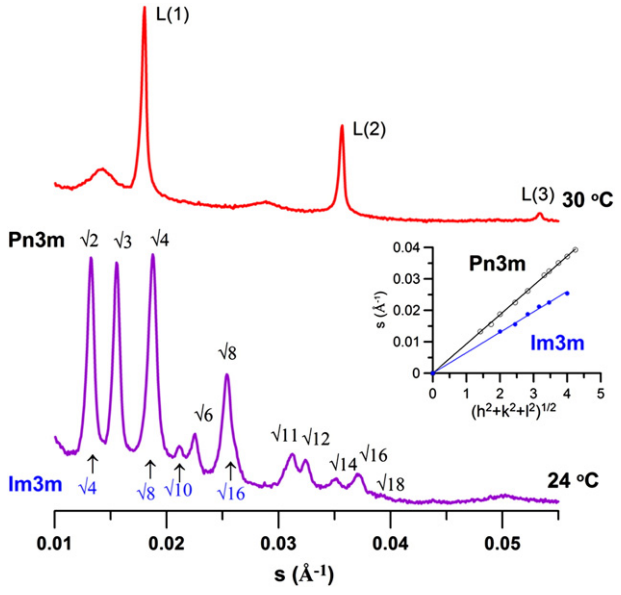

Fig. 8. SAXD patterns for a peptide/lipid mixture of LFchimera and DMPC/DMPG (3:1) for P:L = 1:21 (mol/mol), at selected temperatures, 30 and 24 °C. Insert: a plot of s ($Å^{-1}$) vs. $\sqrt{(h^2+k^2+l^2)}$ for all observed reflections at 24 °C.

two cubic phases with reflections compatible with Pn3m and Im3m space groups. The lattice parameters $a_{Pn3m} = 107.9 \pm 0.3$ Å and $a_{Im3m} = 155.6 \pm 0.9$ Å at 24 °C were determined as described in the Material and methods section, with $R^2 = 0.9999$ and 0.9997, respectively. The ratio of the unit cell parameters for the two cubic phases is $a_{Im3m}/a_{Pn3m} \sim 1.4$. On increasing temperature above ~25 °C both cubic phases vanish and we observe two diffuse peaks with intensities decreasing with temperature, and finally merging in the background (Figs. 7 and 8). Concurrently a lamellar phase is detected, with periodicity $d \sim 56.5–54.9$ Å in the range of 27–40 °C, thus decreasing as the temperature increases.

4. Discussion

The determination of the structure of AMPs upon interaction with membranes, together with the characterization of the changes observed in the membrane structure as a result of this interaction, can help to unravel the antimicrobial peptide's mechanism of action. In the present study we address these two aspects through DSC, CD and SAXD studies on model membranes, and compare them with previous results of their effects on *C. albicans* (Table 1) [37,38]. The structural characterization derived from SAXD using model membranes and from freeze-fracture with *C. albicans* allows a comparison of results derived from two widely different approaches, namely with model and pathogen membranes.

The designed lactoferrin chimera and its constituent peptides presented high candidacidal activity, as can be seen by the low values of LC_{50} previously obtained [37,38] and provided in Table 1. Freeze-fracture electron microscopy of the yeast showed that the peptides induce different levels of membrane damage [37,38]. All peptides clearly affected the membrane morphology of *C. albicans*, albeit differently (Table 1). LFcin17-30 had the weakest effect on the membrane, altering significantly the distribution of the intra-membranous particles (IMP) as compared to control, into IMP-free and IMP-dense areas, suggesting possible IMP aggregation and/or lipid segregation (Table 1, b). LFampin265–284 had a much stronger effect, indicating substantial weakening of the cytoplasmic membrane, as evidenced by the appearance of disruptions into vesicle-like structures (Table 1, c). Finally LFchimera severely destroyed the membrane (Table 1, d).

Our DSC results showed that LFcin17-30 and LFampin265-284 do not interact with the model membranes formed from zwitterionic DMPC, whereas LFchimera does. Measurements performed with DPPC liposomes and LFampin265-284 [48] as well as with similar peptides, LFcin17-41 [49], LFcin17-31 [21] and LFampin268-284 [17] also show that the thermotropic profile of the liposomes is not affected by the presence of the peptides, up to a P:L ratio of 1:10. All these results indicate that LFcin and LFampin peptides do not significantly alter the structural organization of bilayers of zwitterionic lipids. It is interesting to note that LFchimera is the result of a special link between LFcin17-30 and LFampin265-284 through an additional lysine [16], and it shows significant interaction with DMPC liposomes, at odds with the constituent peptides. This synergism has been observed for this peptide [16,18,37,50,51], and probably reflects its very high charge (+12), that along with its amphipatic structure leads to the partition to zwitterionic membranes. In line with the critical importance of charge in AMP/membrane interaction, a strong correlation was recently found between the net positive charge of peptides and their capacity to induce anionic lipid clustering, which was found to be independent of their secondary structure [52]. Overall, the obtained results of the interaction of these peptides with zwitterionic membranes are in agreement with the non-hemolytic behavior of LFcin17-30 and LFampin265-284, and the mild hemolytic character of LFchimera [51,53,54].

All three peptides change their secondary structure upon interaction with the membranes, as long as the membrane has significant negative charge (25% in our case), as shown by the CD results. Only in the case of

LFchimera an altered secondary structure in the presence of pure DMPC membranes is observed, in line with the DSC results. Again this effect might follow from a high charge and amphipaticity, with a mixture of secondary structures that would maximize the electrostatic and hydrophobic interactions.

In the present work we observed the predominance of α-helix structure upon interaction with DMPC/DMPG membranes for LFampin265-284 and LFchimera. The presence of significant amounts of α-helix was also found for LFampin268-284 [17] and LFampin265-284 [18,48] in the presence of SDS micelles. Strøm et al. [55] have studied LFcin17-31, and they obtained a percentage of helicity of only 4% for this peptide in contact with SDS, indicating that in the presence of purely negative micelles this peptide does hardly adopts a helical structure. Haney et al. [18] have studied these three peptides, LFcin17-30, LFampin265-284 and LFchimera by a variety of techniques, but their CD results are also obtained in the presence of SDS micelles. Again, they found that for LFcin17-30 the intensity of the negative peaks characteristic of α-helix structure is fairly weak, whereas for LFampin265-284 and LFchimera strong negative minima are present. These results are in line with the ones reported here for DMPC/DMPG (3:1) liposomes, as well as with our previous results in the presence of DMPG [16].

The biological importance of cubic phases was addressed in the seminal work of Luzatti and collaborators [32]. In recent years, Lohner et al. addressed this issue by X-ray scattering in the context of AMPs [12], and the presence of cubic phases upon AMP interaction is now documented both with simple model membranes [19,36,56] as well as with lipid extracts from pathogenic agents [26,27]. Further, their importance has been stressed in recent reviews [1,23,28]. The induction of cubic phases by AMPs, mostly by lowering the lamellar to non-lamellar phase boundary of lipid membranes, could indicate that the peptides act by promoting an extensive bilayer curvature, leading eventually to either the formation of pores, mainly of the toroidal type [28] or even to membrane disruption (micellization). The formation of non-lamellar phases could also alter lipid domains in the cellular membrane that are important for many biological processes such endocytosis, or even the activity of membrane proteins that most of the time depend on these domains, culminating into impairment of the membrane function [33,34]. Most reported work so far points to the induction of cubic phases, mostly of Pn3m and Im3m symmetry, as we have found for LFchimera. In the present report it was very interesting to find that three peptides from the same family, lactoferrin, have quite different effects on membranes of the same composition. LFcin17-30 only induces segregation of the lipid moiety, and leads to the formation of two lamellar phases in the gel phase, on cooling, with repeat distances $d_A = 70.9$ Å and $d_B = 65.7$ Å at 10 °C. At this temperature, neutral DMPC itself forms a gel lamellar phase with the repeat distance of ~60.1 Å. This value is comparable with the periodicity of L_B phase $d_B = 65.7$ Å indicating thus the domain with less AMP. Lowering the temperature beyond T_m may affect differently the mobility of individual membrane's components, which together with the tendency for effective charge compensation results in a segregation of the membrane components. For systems polyelectrolyte–cationic membrane it was suggested that the presence of negatively charged DNA between bilayers can induce a partial lateral segregation of cationic surfactants to minimize the electrostatic energy of the whole system, i.e., lateral "demixing" in the plane of the bilayer can occur [57]. It has been proven experimentally that the polyelectrolyte-bound population is enriched with oppositely charged lipid, while the polyelectrolyte-free lipid population is correspondingly depleted [58,59]. These observations correlate very well with the membrane lipid segregation observed by freeze-fracture, and consequent protein reorganization.

LFcin17-30 was found to be the peptide among the three studied here with lowest membrane activity against *C. albicans*. It is indeed remarkable that our SAX results indicate that for LFcin17-30, only a segregation effect on the lipid mixture takes place, as revealed by the appearance of two lamellar phases upon cooling, and the peptide does not induce a cubic phase. This peptide's mild effect on the membrane also agrees with previous reports of internal targets for LFcin peptides [8–11], as well as with the slower kinetics observed against *Leishmania* [50]. All these results lead us to propose that peptides that only induce a mild membrane effect, like LFcin17-30, as observed by SAXD (segregation) are likely to have internal targets as part of their mode of action, as long as they are known to be active.

LFampin265-284 induces a micellar cubic phase of Pm3n type on the model membranes of DMPC/DMPG, compatible with a detergent-like action that would cause plasma membrane solubilization [36]. The DSC results obtained for DMPC/DMPG (3:1) and LFampin265-284 at high peptide contents (Fig. 3) allowed us to shed some light in the observed lipid/peptide cubic organization for the mixture. Overall we can see that a transition is still observed by DSC in a temperature range where we already observe the presence of a cubic phase by SAX. As it is known that the transition to cubic phase is a low energy one, thus not easily detectable by DSC [60], the peaks observed must be related to a transition between gel and liquid crystalline phases. This transition is compatible with the peak we observe in WAX at 20 °C (not shown) indicative of the presence of gel phase. Further, it can account for what we previously hypothesized [36], i.e., that not all lipids are involved in the cubic phase and that the volume fraction of non-lamellar phase depends on temperature and P:L ratio. Thus the results from both methods taken together show that the cubic phase must coexist with a lamellar phase, whose presence is reflected in SAX diffractograms in the high background observed for both 1:5 and 1:8 P:L mixtures. Further, by DSC we see that above 30 °C the mixture is completely in liquid crystalline state, which is compatible with the observed peaks of an organized lamellar phase whose onset we see by SAX at 29 °C [36] for the 1:8 mixture. For the mixture with high peptide content (1:5) the lamellar phase only appears at high temperature, probably because the volume fraction involved in the cubic phase is higher at this peptide content.

As mentioned before in the results' section, two peaks are clearly seen in DSC, thus the mixture is not homogeneous. The first appears at a temperature lower than T_m of the pure lipid mixture, leading to the onset of gel to liquid crystalline transition at ~22.6 °C. This decreased stability should facilitate the transition to a cubic arrangement, and in fact we could see by SAXD that for the mixture 1:8 the onset of cubic phase appearance could be observed already at ~22 °C. The DSC tracing also shows a very broad transition (between ~20 and 32 °C), in a temperature range that coincides with the presence of cubic phase. Thus from ~20 °C there is a fraction of the peptide/lipid membrane that starts to have a transition to liquid crystalline state and subsequently can undergo a transition to cubic phase in this temperature range, whereas the remaining fraction is still in the gel phase until ~26 °C. This last fraction shows a very broad, non-cooperative transition that could be responsible for the observed high background in the diffractograms in this temperature range. At temperatures above the disappearance of the cubic phase a massive system reorganization takes place, as pointed out before [36]. The observation of L_α at high temperatures can seem surprising, as micellar phase Pm3n is commonly known to change either to a micellar solution or to a hexagonal phase. It must be stressed that we do not suggest that the origin of the L_α phase at high temperature is a transition from the cubic Pm3n phase. As the temperature is raised, the cubic phase vanishes and a redistribution of charged AMP induces massive structural changes. Further, as we suggested earlier [36] and our DSC results here confirm, part of the lipid mixture is not involved in the cubic phase. We found a repeat distance $d = 65.9$ Å of L_α phase at 50 °C (P:L = 1:8), and DMPC multilamellar vesicles show at this temperature a repeat distance of 60.7 Å. The higher spacing observed as compared to pure DMPC can be accounted for either to the presence of the peptide between the lipid bilayers or as due to a residual charge imbalance in the system.

It is worth noting that the micellization that we could retrieve by SAXD, aside from being the first reported micellar cubic phase in the context of antimicrobial/peptide membrane interactions, is a result that parallels the findings by freeze-fracture for LFampin265-284 when in contact with *C. albicans*, showing again a remarkable agreement between the results with model and actual pathogens' membranes.

SAXD results for LFchimera show the presence of cubic phase, and for the P:L ratio 1:21 the coexistence of two cubic phases (Pn3m and Im3m) was clearly resolved. The ratio obtained of the unit cell parameters for the two cubic phases was a_{Im3m}/a_{Pn3m} ~1.4, showing a significant deviation from the ideal Bonnet relation 1.28, for coexisting cubic phases related to the minimal surfaces for a system in thermodynamic equilibrium [61,62]. For AMPs/model membranes, epitaxial relationships between coexisting cubic phases and hexagonal or lamellar phases were reported previously [19,23,26,27,63]. The transitions from liquid crystalline lamellar to cubic phase as well as within different cubic phases occur in a narrow range, and coexistence of phases has been reported, as well as hysteresis. Therefore the system might not have been able to reach thermodynamic equilibrium, and that could justify the deviation of the ratio of lattice parameters from the ideal Bonnet relation. Further, the Bonnet transformation is derived from a mathematical treatment of coexisting infinite minimal surfaces (IMS), and relates the primitive and diamond (and gyroid) surfaces via intermediate self-interacting minimal surfaces, and real systems can deviate from this theoretical prediction, either because they do not conform to it or because the system is not at equilibrium [63]. As the temperature increases above the range of cubic phase stability the lipid network is disrupted. Some released lipid/AMP fragments can initially keep some symmetry in their organization, which in SAXD is observed as two diffuse peaks. With heating, their volume fraction in the sample decreases as documented by the observed decrease in the intensity of the diffuse peaks, while simultaneously we observe the increase in the intensity of peaks related to a lamellar phase. The released lipid or lipid/AMP fragments are reorganized into the lamellar phase to decrease the free energy of the whole system. The retrieved periodicity of the lamellar phase (d~54.9 Å at 40 °C) is smaller than for DMPC membrane at the same temperature (d_{DMPC}~62.0 Å), and closer to the periodicity (d~56.3 Å at 40 °C) derived from our system at low P:L molar ratio where DMPC/DMPG membrane was not disrupted (P:L = 1:38). At molar ratio P:L = 1:30 SAXD detected the membrane disruption by LFchimera (see Results section). Thus our experiments indicate the value ~1:34(±4) as a critical for the DMPC/DMPG (3:1) membrane disruption by LFchimera.

Finally we would like to point out that the formation of two cubic phases, of symmetry Pn3m and Im3m, would lead to total membrane disruption, in a way that parallels what was observed by freeze-fracture. It should be noted that Bolscher et al. [37] refer the presence of some vesicular structures as observed in freeze-fracture experiments also in the case of LFchimera, together with a massive membrane disruption. This peptide is very complex, both due to its extremely high positive charge as well as to its unusual link of constituent peptides through a lysine side chain. In our SAXD experiments with the simple model system of DMPC/DMPG (3:1) we could only assign the presence of two cubic phases, Pn3m and Im3m. Nevertheless, the possibility of other structures to be formed upon interaction with the more complex membrane of *C. albicans* cannot be discarded.

Thus, overall we could find a remarkable match between the effect of these peptides on *C. albicans* membrane as observed by freeze-fracture and the structural features they revealed in a simple model membrane system particularly suited to mimic *C. albicans* (known to have a significant PC content). This has several important consequences: i) it indicates that structural studies involving simple model membranes can provide very important information as regarding different modes of action of AMPs; and ii) the conclusions that can be drawn are indeed much more sound when accompanied by measurements involving real pathogens.

Disclosure statement

The authors declare that they have no conflict of interest.

Acknowledgements

This research received funding from the EC's 7th Framework Program (FP7/2007-2013) under grant agreement no. 226716 (HASYLAB project II-20090024 EC), and financial support from FCT/CIQ(UP) to MB and TS, MŠ SR grant VEGA 1/1224/12 to DU, SK-PT-0015-10 to DU, MB and TS, a PhD grant (SFRH/BD/77564/2011) to TS, and a grant from the University of Amsterdam for research into the focal point Oral Infections and Inflammation to JGMB and KN.

References

[1] V. Teixeira, M.J. Feio, M. Bastos, Role of lipids in the interaction of antimicrobial peptides with membranes, Prog. Lipid Res. 51 (2012) 149–177.
[2] M.A.R.B. Castanho, Membrane-active peptides: methods and results on structure and function, IUL Biotechnology Series, vol. 9, International University Line, La Jolla, CA, USA, 2010, p. 692.
[3] Y. Shai, A. Makovitzky, D. Avrahami, Host defense peptides and lipopeptides: modes of action and potential candidates for the treatment of bacterial and fungal infections, Curr. Protein Pept. Sci. 7 (2006) 479–486.
[4] L.T. Nguyen, E.F. Haney, H.J. Vogel, The expanding scope of antimicrobial peptide structures and their modes of action, Trends Biotechnol. 29 (2011) 464–472.
[5] K.A. Brogden, Antimicrobial peptides: pore formers or metabolic inhibitors in bacteria? Nat. Rev. Microbiol. 3 (2005) 238–250.
[6] H.W. Huang, Action of antimicrobial peptides: two-state model, Biochemistry 39 (2000) 8347–8352.
[7] L. Yang, T.A. Harroun, T.M. Weiss, L. Ding, H.W. Huang, Barrel-stave model or toroidal model? A case study of melittin pores, Biophys. J. 81 (2001) 1475–1485.
[8] H.H. Haukland, H. Ulvatne, K. Sandvik, L.H. Vorland, The antimicrobial peptides lactoferricin B and magainin 2 cross over the bacterial cytoplasmic membrane and reside in the cytoplasm, FEBS Lett. 508 (2001) 389–393.
[9] H. Ulvatne, O. Samuelsen, H.H. Haukland, M. Kramer, L.H. Vorland, Lactoferricin B inhibits bacterial macromolecular synthesis in *Escherichia coli* and *Bacillus subtilis*, FEMS Microbiol. Lett. 237 (2004) 377–384.
[10] J.S. Mader, A. Richardson, J. Salsman, D. Top, R. de Antueno, R. Duncan, D.W. Hoskin, Bovine lactoferricin causes apoptosis in Jurkat T-leukemia cells by sequential permeabilization of the cell membrane and targeting of mitochondria, Exp. Cell Res. 313 (2007) 2634–2650.
[11] J.L. Gifford, H.N. Hunter, H.J. Vogel, Lactoferricin: a lactoferrin-derived peptide with antimicrobial, antiviral, antitumor and immunological properties, Cell. Mol. Life Sci. 62 (2005) 2588–2598.
[12] K. Lohner, E.J. Prenner, Differential scanning calorimetry and X-ray diffraction studies of the specificity of the interaction of antimicrobial peptides with membrane-mimetic systems, Biochim. Biophys. Acta 1462 (1999) 141–156.
[13] M.K. Wassef, T.B. Fioretti, D.M. Dwyer, Lipid analyses of isolated surface membranes of *Leishmania donovani* promastigotes, Lipids 20 (1985) 108–115.
[14] A. Singh, T. Prasad, K. Kapoor, A. Mandal, M. Roth, R. Welti, R. Prasad, Phospholipidome of *Candida*: each species of *Candida* has distinctive phospholipid molecular species, OMICS 14 (2010) 665–677.
[15] V.V. Andrushchenko, H.J. Vogel, E.J. Prenner, Interactions of tryptophan-rich cathelicidin antimicrobial peptides with model membranes studied by differential scanning calorimetry, Biochim. Biophys. Acta 1768 (2007) 2447–2458.
[16] J.G. Bolscher, R. Adão, K. Nazmi, P.A. van den Keybus, W. van 't Hof, A.V. Nieuw Amerongen, M. Bastos, E.C. Veerman, Bactericidal activity of LFchimera is stronger and less sensitive to ionic strength than its constituent lactoferricin and lactoferrampin peptides, Biochimie 91 (2009) 123–132.
[17] E.F. Haney, F. Lau, H.J. Vogel, Solution structures and model membrane interactions of lactoferrampin, an antimicrobial peptide derived from bovine lactoferrin, Biochim. Biophys. Acta 1768 (2007) 2355–2364.
[18] E.F. Haney, K. Nazmi, J.G. Bolscher, H.J. Vogel, Structural and biophysical characterization of an antimicrobial peptide chimera comprised of lactoferricin and lactoferrampin, Biochim. Biophys. Acta 1818 (2012) 762–775.
[19] A. Hickel, S. Danner-Pongratz, H. Amenitsch, G. Degovics, M. Rappolt, K. Lohner, G. Pabst, Influence of antimicrobial peptides on the formation of nonlamellar lipid mesophases, Biochim. Biophys. Acta 1778 (2008) 2325–2333.
[20] H.W. Huang, Molecular mechanism of antimicrobial peptides: the origin of cooperativity, Biochim. Biophys. Acta 1758 (2006) 1292–1302.
[21] W. Jing, J.S. Svendsen, H.J. Vogel, Comparison of NMR structures and model-membrane interactions of 15-residue antimicrobial peptides derived from bovine lactoferricin, Biochem. Cell Biol. 84 (2006) 312–326.
[22] C.-C. Lee, Y. Sun, S. Qian, Huey W. Huang, Transmembrane pores formed by human antimicrobial peptide LL-37, Biophys. J. 100 (2011) 1688–1696.

[23] G. Pabst, D. Zweytick, R. Prassl, K. Lohner, Use of X-ray scattering to aid the design and delivery of membrane-active drugs, Eur. Biophys. J. (2012) 1–15.
[24] E.J. Prenner, R.N. Lewis, R.N. McElhaney, The interaction of the antimicrobial peptide gramicidin S with lipid bilayer model and biological membranes, Biochim. Biophys. Acta 1462 (1999) 201–221.
[25] E.J. Prenner, R.N. Lewis, K.C. Neuman, S.M. Gruner, L.H. Kondejewski, R.S. Hodges, R.N. McElhaney, Nonlamellar phases induced by the interaction of gramicidin S with lipid bilayers. A possible relationship to membrane-disrupting activity, Biochemistry 36 (1997) 7906–7916.
[26] E. Staudegger, E.J. Prenner, M. Kriechbaum, G. Degovics, R.N. Lewis, R.N. McElhaney, K. Lohner, X-ray studies on the interaction of the antimicrobial peptide gramicidin S with microbial lipid extracts: evidence for cubic phase formation, Biochim. Biophys. Acta 1468 (2000) 213–230.
[27] D. Zweytick, S. Tumer, S.E. Blondelle, K. Lohner, Membrane curvature stress and antibacterial activity of lactoferricin derivatives, Biochem. Biophys. Res. Commun. 369 (2008) 395–400.
[28] E.F. Haney, S. Nathoo, H.J. Vogel, E.J. Prenner, Induction of non-lamellar lipid phases by antimicrobial peptides: a potential link to mode of action, Chem. Phys. Lipids 163 (2010) 82–93.
[29] J. Erbes, C. Czeslik, W. Hahn, R. Winter, M. Rappolt, G. Rapp, On the existence of bicontinuous cubic phases in dioleoylphosphatidylethanolamine, Ber. Bunsenges. Phys. Chem. 98 (1994) 1287–1293.
[30] G. Tresset, The multiple faces of self-assembled lipidic systems, PMC Biophys. 2 (2009) 3.
[31] Z.A. Almsherqi, T. Landh, S.D. Kohlwein, Y. Deng, Chapter 6: cubic membranes the missing dimension of cell membrane organization, Int. Rev. Cell Mol. Biol. 274 (2009) 275–342.
[32] V. Luzzati, Biological significance of lipid polymorphism: the cubic phases, Curr. Opin. Struct. Biol. 7 (1997) 661–668.
[33] K. Lohner, New strategies for novel antibiotics: peptides targeting bacterial cell membranes, Gen. Physiol. Biophys. 28 (2009) 105–116.
[34] K. Lohner, S.E. Blondelle, Molecular mechanisms of membrane perturbation by antimicrobial peptides and the use of biophysical studies in the design of novel peptide antibiotics, Comb. Chem. High Throughput Screen. 8 (2005) 241–256.
[35] S.L. Keller, S.M. Gruner, K. Gawrisch, Small concentrations of alamethicin induce a cubic phase in bulk phosphatidylethanolamine mixtures, Biochim. Biophys. Acta 1278 (1996) 241–246.
[36] M. Bastos, T. Silva, V. Teixeira, K. Nazmi, J.G.M. Bolscher, S.S. Funari, D. Uhríková, Lactoferrin-derived antimicrobial peptide induces a micellar cubic phase in a model membrane system, Biophys. J. 101 (2011) L20–L22.
[37] J. Bolscher, K. Nazmi, J. van Marle, W. van 't Hof, E. Veerman, Chimerization of lactoferricin and lactoferrampin peptides strongly potentiates the killing activity against *Candida albicans*, Biochem. Cell Biol. 90 (2012) 378–388.
[38] M.I. van der Kraan, J. van Marle, K. Nazmi, J. Groenink, W. van 't Hof, E.C. Veerman, J.G. Bolscher, A.V. Nieuw Amerongen, Ultrastructural effects of antimicrobial peptides from bovine lactoferrin on the membranes of *Candida albicans* and *Escherichia coli*, Peptides 26 (2005) 1537–1542.
[39] J.G. Bolscher, M.J. Oudhoff, K. Nazmi, J.M. Antos, C.P. Guimaraes, E. Spooner, E.F. Haney, J.J. Garcia Vallejo, H.J. Vogel, W. van't Hof, H.L. Ploegh, E.C. Veerman, Sortase A as a tool for high-yield histatin cyclization, FASEB J. 25 (2011) 2650–2658.
[40] C.W.F. McClare, An accurate and convenient organic phosphorous assay, Anal. Biochem. 39 (1971) 527–530.
[41] F. Abrunhosa, S. Faria, P. Gomes, I. Tomaz, J.C. Pessoa, D. Andreu, M. Bastos, Interaction and lipid-induced conformation of two cecropin–melittin hybrid peptides depend on peptide and membrane composition, J. Phys. Chem. B 109 (2005) 17311–17319.
[42] T.C. Huang, H. Toraya, T.N. Blanton, Y. Wu, X-ray powder diffraction analysis of silver behenate, a possible low-angle diffraction standard, J. Appl. Crystallogr. 26 (1993) 180–184.
[43] N. Roveri, A. Bigi, P.P. Castellani, E. Foresti, M. Marchini, R. Strocchi, Study of rat tail tendon by X-ray diffraction and freeze-etching technics, Boll. Soc. Ital. Biol. Sper. 56 (1980) 953–959.
[44] D. Chapman, The polymorphism of glycerides, Chem. Rev. 62 (1962) 433–456.
[45] M. Kellens, W. Meeussen, H. Reynaers, Crystallization and phase transition studies of tripalmitin, Chem. Phys. Lipids 55 (1990) 163–178.
[46] LIPIDAT, http://www.lipidat.tcd.ie/, (Last access on October 2012).
[47] R.A. Parente, B.R. Lentz, Phase behavior of large unilamellar vesicles composed of synthetic phospholipids, Biochemistry 11 (1984) 2353–2362.
[48] E.F. Haney, K. Nazmi, J.G. Bolscher, H.J. Vogel, Influence of specific amino acid side-chains on the antimicrobial activity and structure of bovine lactoferrampin, Biochem. Cell Biol. 90 (2012) 362–377.
[49] H.J. Vogel, D.J. Schibli, W. Jing, E.M. Lohmeier-Vogel, R.F. Epand, R.M. Epand, Towards a structure-function analysis of bovine lactoferricin and related tryptophan- and arginine-containing peptides, Biochem. Cell Biol. 80 (2002) 49–63.
[50] T. Silva, M.A. Abengozar, M. Fernandez-Reyes, D. Andreu, K. Nazmi, J.G. Bolscher, M. Bastos, L. Rivas, Enhanced leishmanicidal activity of cryptopeptide chimeras from the active N1 domain of bovine lactoferrin, Amino Acids 43 (2012) 2265–2277.
[51] N. Leon-Sicairos, A. Canizalez-Roman, M. de la Garza, M. Reyes-Lopez, J. Zazueta-Beltran, K. Nazmi, B. Gomez-Gil, J.G. Bolscher, Bactericidal effect of lactoferrin and lactoferrin chimera against halophilic Vibrio parahaemolyticus, Biochimie 91 (2009) 133–140.
[52] P. Wadhwani, R.F. Epand, N. Heidenreich, J. Burck, A.S. Ulrich, R.M. Epand, Membrane-active peptides and the clustering of anionic lipids, Biophys. J. 103 (2012) 265–274.
[53] M.I. van der Kraan, J. Groenink, K. Nazmi, E.C. Veerman, J.G. Bolscher, A.V. Nieuw Amerongen, Lactoferrampin: a novel antimicrobial peptide in the N1-domain of bovine lactoferrin, Peptides 25 (2004) 177–183.
[54] M.I. van der Kraan, K. Nazmi, A. Teeken, J. Groenink, W. van 't Hof, E.C. Veerman, J.G. Bolscher, A.V. Nieuw Amerongen, Lactoferrampin, an antimicrobial peptide of bovine lactoferrin, exerts its candidacidal activity by a cluster of positively charged residues at the C-terminus in combination with a helix-facilitating N-terminal part, Biol. Chem. 386 (2005) 137–142.
[55] M.D. Strom, O. Rekdal, W. Stensen, J.S. Svendsen, Increased antibacterial activity of 15-residue murine lactoferricin derivatives, J. Pept. Res. 57 (2001) 127–139.
[56] K. Lohner, F. Prossnigg, Biological activity and structural aspects of PGLa interaction with membrane mimetic systems, Biochim. Biophys. Acta 1788 (2009) 1656–1666.
[57] R. Bruinsma, J. Mashl, Long-range electrostatic interaction in DNA–cationic lipid complexes, Europhys. Lett. 41 (1998) 165–170.
[58] P. Mitrakos, P.M. MacDonald, DNA induced lateral segregation of cationic amphiphiles in lipid bilayer membranes as detected via 2H NMR, Biochemistry 35 (1996) 16714–16722.
[59] D. Uhrikova, M. Hanulova, S.S. Funari, R.S. Khusainova, F. Sersen, P. Balgavy, The structure of DNA-DOPC aggregates formed in presence of calcium and magnesium ions: a small-angle synchrotron X-ray diffraction study, Biochim. Biophys. Acta 1713 (2005) 15–28.
[60] R.N. Lewis, D.A. Mannock, R.N. McElhaney, Differential scanning calorimetry in the study of lipid phase transitions in model and biological membranes: practical considerations, Methods Mol. Biol. 400 (2007) 171–195.
[61] G. Lindblom, L. Rilfors, Cubic phases and isotropic structures formed by membrane lipids — possible biological relevance, Biochim. Biophys. Acta 988 (1989) 221–256.
[62] C. Oguey, J.-F. Sadoc, Crystallographic aspects of the Bonnet transformation for periodic minimal surfaces (and crystals of films), J. Phys. I France 3 (1993) 839–854.
[63] M. Hanulová, Interaction of antimicrobial peptides with lipid membranes, Departments Physik der Universität Hamburg, vol. PhD, Hamburg, Hamburg, 2008.

Biochimica et Biophysica Acta 1828 (2013) 2796

Contents lists available at ScienceDirect

Biochimica et Biophysica Acta

journal homepage: www.elsevier.com/locate/bbamem

Corrigendum

Corrigendum to "Structural diversity and mode of action on lipid membranes of three lactoferrin candidacidal peptides" [Biochim. Biophys. Acta 1828 (2013) 1329–1339]

Tânia Silva[a,b,c], Regina Adão[a], Kamran Nazmi[d], Jan G.M. Bolscher[d], Sérgio S. Funari[e], Daniela Uhríková[f], Margarida Bastos[a,*]

[a] Centro de Investigação em Química CIQ(UP), Department of Chemistry & Biochemistry, Faculty of Sciences, University of Porto, Portugal
[b] IBMC — Instituto de Biologia Molecular e Celular, Universidade do Porto, Portugal
[c] ICBAS — Instituto de Ciências Biomédicas Abel Salazar, Universidade do Porto, Portugal
[d] Academic Centre Dentistry Amsterdam (ACTA), Department of Oral Biochemistry, University of Amsterdam and VU University Amsterdam, Amsterdam, The Netherlands
[e] HASYLAB, DESY, Hamburg, Germany
[f] Faculty of Pharmacy, Comenius University, Bratislava, Slovak Republic

There were errors in the figure legends for Figures 1, 2, 3, 4, and 5. The correct legends appear below.

Fig. 1. DSC curves for DMPC and DMPC/peptide mixtures of varying composition. The lipid concentration was 3.0 ± 0.3 mM in all experiments. (a) LFcin17–30; (b) LFampin265–284; (c) LFchimera. Pure lipid (solid black); P:L = 1:196 (solid red); P:L = 1:129 (solid green); P:L = 1:96 (dash blue); P:L = 1:46 (dash pink); P:L = 1:29 (dash yellow). Maximal P:L molar ratio used was 1:46 for LFchimera.

Fig. 2. DSC curves for DMPC/DMPG (3:1) and DMPC/DMPG (3:1)/peptide mixtures of varying composition. The lipid concentration was 3.0 ± 0.3 mM in all experiments. (a) LFcin17–30; (b) LFampin265–284; (c) LFchimera. Pure lipid (solid black); P:L = 1:196 (solid red); P:L = 1:129 (solid green); P:L = 1:96 (dash blue); P:L = 1:46 (dash pink); P:L = 1:29 (dash yellow). Maximal P:L molar ratio used was 1:46 for LFchimera.

Fig. 3. DSC curves for DMPC/DMPG (3:1) and DMPC/DMPG (3:1)/LFampin 265–284 mixtures at high P:L ratios. The lipid concentration was 6.0 ± 0.3 mM in all experiments. Pure lipid (solid blue); P:L = 1:12 (solid red); P:L = 1:8 (solid green); P:L = 1:3 (solid magenta). The dashed (low temperature peak) and dotted (high temperature peak) lines represent the deconvoluted curves for each P:L ratio.

Fig. 4. CD spectra of (a) LFcin17–30, (b) LFampin265–284 and (c) LFchimera at 35 °C in: buffer (peptide concentration 36 μM) (black); DMPC 6 mM (red); and DMPC/DMPG (3:1) 3 mM (green). P:L ratio in peptide/LUV mixtures was 1:167.

Fig. 5. SAXD (a) and WAXD (b) patterns for a peptide/lipid mixture of LFcin17–30 and DMPC/DMPG (3:1) for P:L = 1:8 (mol/mol), at selected temperatures. In blue the diffractograms from the heating, and in black from the cooling scans. The lipid concentration was 12 mM.

DOI of original article: http://dx.doi.org/10.1016/j.bbamem.2013.01.022.
* Corresponding author at: Centro Investigação em Química CIQ(UP), Department of Chemistry and Biochemistry, Faculty of Sciences, University of Porto, Rua do Campo Alegre, 4169-007 Porto, Portugal. Tel.: +351 220402511; fax: +351 220402659.
E-mail address: mbastos@fc.up.pt (M. Bastos).

0005-2736/$ – see front matter
http://dx.doi.org/10.1016/j.bbamem.2013.03.018

CHAPTER 7. Killing of *Mycobacterium avium* by lactoferricin peptides: improved activity of arginine- and D-amino acids-containing molecules

AAC
Journals.ASM.org

Killing of *Mycobacterium avium* by Lactoferricin Peptides: Improved Activity of Arginine- and D-Amino-Acid-Containing Molecules

Tânia Silva,[a,b,c] Bárbara Magalhães,[a] Sílvia Maia,[b] Paula Gomes,[b] Kamran Nazmi,[d] Jan G. M. Bolscher,[d] Pedro N. Rodrigues,[a,c] Margarida Bastos,[b] Maria Salomé Gomes[a,c]

IBMC (Instituto de Biologia Molecular e Celular), Universidade do Porto, Porto, Portugal[a]; CIQ(UP), Centro de Investigação em Química, Departamento de Química e Bioquímica, Faculdade de Ciências, Universidade do Porto, Porto, Portugal[b]; ICBAS (Instituto de Ciências Biomédicas Abel Salazar), Universidade do Porto, Porto, Portugal[c]; Department of Oral Biochemistry, Academic Center for Dentistry Amsterdam (ACTA), University of Amsterdam and VU University Amsterdam, Amsterdam, The Netherlands[d]

Mycobacterium avium **causes respiratory disease in susceptible individuals, as well as disseminated infections in immunocompromised hosts, being an important cause of morbidity and mortality among these populations. Current therapies consist of a combination of antibiotics taken for at least 6 months, with no more than 60% overall clinical success. Furthermore, mycobacterial antibiotic resistance is increasing worldwide, urging the need to develop novel classes of antimicrobial drugs. One potential and interesting alternative strategy is the use of antimicrobial peptides (AMP). These are present in almost all living organisms as part of their immune system, acting as a first barrier against invading pathogens. In this context, we investigated the effect of several lactoferrin-derived AMP against *M. avium*. Short peptide sequences from both human and bovine lactoferricins, namely, hLFcin1-11 and LFcin17-30, as well as variants obtained by specific amino acid substitutions, were evaluated. All tested peptides significantly inhibited the axenic growth of *M. avium*, the bovine peptides being more active than the human. Arginine residues were found to be crucial for the display of antimycobacterial activity, whereas the all-D-amino-acid analogue of the bovine sequence displayed the highest mycobactericidal activity. These findings reveal the promising potential of lactoferricins against mycobacteria, thus opening the way for further research on their development and use as a new weapon against mycobacterial infections.**

The genus *Mycobacterium* includes several species capable of causing disease in humans and other animals. *Mycobacterium tuberculosis* is one of the most deadly human pathogens, killing 1 million to 2 million people every year (1), while *Mycobacterium avium* and *Mycobacterium intracellulare* are frequent opportunistic pathogens of immunosuppressed individuals and people with chronic respiratory distress (2, 3). Equipped with a complex lipid-rich cell envelope and adapted to proliferate inside the host's macrophages, mycobacteria tend to cause persistent infections, which are difficult to cure, requiring long treatment regimens that rely on the combination of several drugs. The increasing emergence of drug-resistant strains of mycobacteria makes the treatment of these diseases even more challenging (1).

The vast array of antimicrobial peptides (AMP) produced by virtually all living organisms as natural barriers against infection is a new and promising source of potential antimicrobial weapons. Although they have little sequence homology, the vast majority of AMP contain a high proportion of hydrophobic and cationic amino acids, and when in contact with bacterial membranes, they adopt amphipathic structures (4). The fact that AMP are active against a wide variety of microorganisms, combined with the observation that both the L and D enantiomers are active, supports the notion that the target of these peptides is a general structure conserved across different bacterial species, such as the cytoplasmic membrane (5, 6). Thus, it is thought that electrostatic attraction is responsible for the initial approach between the cationic peptide and the negatively charged phospholipids usually present at the pathogen's surface (4). Downstream events that lead to bacterial killing are not yet fully understood (4, 6). Acting in such a fundamental and conserved biological target as the bacterial membrane, AMP are believed to be less prone to the development of secondary microbial resistance than other types of antibiotics (4, 7). Therefore, a deeper understanding of the mechanisms of action of AMP, along with the establishment of structure-activity relationships, is an essential step toward the identification and development of more active molecules with improved therapeutic characteristics and possibly higher specificity toward pathogens of interest.

Lactoferricins are naturally occurring peptides, formed by the cleavage of the highly cationic N1 terminal domain of the iron-binding protein lactoferrin. Bovine lactoferricin is composed by 25 amino acids, corresponding to residues 17 to 41 in the native protein (5, 8), and has broad-spectrum antimicrobial activity (5, 9–15). A shorter version of bovine lactoferricin containing amino acids 17 to 30 (LFcin17-30) was found to have even higher antimicrobial activity (16). A human peptide with the first 11 amino acids from human lactoferrin (hLFcin1-11) was also demonstrated to be active against a great variety of bacteria, including antibiotic-resistant strains, and fungi, especially *Candida albicans* (17–21), and was already used in different preclinical and clinical trials, where its overall safety was proved (20, 22).

In the present work, we investigated the activity against *M. avium* of hLFcin1-11 and LFcin17-30, as well as peptides obtained

Received 19 December 2013 **Returned for modification** 22 March 2014
Accepted 3 April 2014
Published ahead of print 7 April 2014
Address correspondence to Maria Salomé Gomes, sgomes@ibmc.up.pt.

doi:10.1128/AAC.02728-13

TABLE 1 Antimicrobial activities of lactoferricin peptides against *Mycobacterium avium*

Peptide	Amino acid sequence	Mol wt[a]	Charge[b]	Activity (μM) (mean ± SD) against *M. avium* strain[c]					
				2447 SmT		2-151 SmT		2-151 SmD	
				IC_{50}	IC_{90}	IC_{50}	IC_{90}	IC_{50}	IC_{90}
hLFcin1-11	G**RRRR**SVQWCA	1,374	+5	15.8 ± 4.5	34.6 ± 22.4	11.0 ± 4.1	65.8 ± 19.3	15.2 ± 2.9	37.9 ± 15.9
hLFcin1-11 all K	G**KKKK**SVQWCA	1,262	+5	39.1 ± 6.9[d]					
LFcin17-30	F**KCRR**WQW**R**M**KK**LG	1,923	+6	14.2 ± 1.5	18.9 ± 4.0	8.0 ± 1.5	22.8 ± 9.1	12.4 ± 0.3	21.5 ± 4.0
D-LFcin17-30	F**KCRR**WQW**R**M**KK**LG	1,923	+6	10.7 ± 0.9[e]	14.4 ± 1.9				
LFcin17-30 all K	F**KCKK**WQW**K**M**KK**LG	1,839	+6	18.0 ± 2.1[e,f,g]	34.4 ± 8.2[e,f]				
LFcin17-30 all R	F**RCRR**WQW**R**M**RR**LG	2,007	+6	10.8 ± 1.6[e]	19.3 ± 4.8				

[a] Molecular weight.
[b] Calculated overall charge at pH 7.0.
[c] Each value represents the average for at least three independent experiments, with the corresponding SD indicated. IC_{50} is the peptide concentration that inhibits 50% of mycobacterial viability at 7 days of incubation. IC_{90} is the peptide concentration that inhibits 90% of mycobacterial viability at 7 days of incubation.
[d] $P < 0.0001$ (compared to results for the parental peptide, hLFcin1-11).
[e] $P < 0.05$ (compared to results for the parental peptide, LFcin17-30).
[f] $P < 0.05$ (compared to results for LFcin17-30 all R, by cross-comparison within the bovine peptides).
[g] $P < 0.0001$ (compared to results for hLFcin1-11 all K, by cross-comparison within all peptides).

from these by specific amino acid substitutions, to test the importance of various factors on the potency of AMP against that pathogen.

MATERIALS AND METHODS

Peptides. Human lactoferricins (hLFcin1-11 and hLFcin1-11 all K) (Table 1) were prepared as C-terminal amides by standard Fmoc/^{t}Bu [1-(9*H*-fluoren-9-yl)-methoxycarbonyl)/*tert*-butyl chemistry] solid-phase peptide synthesis on a Liberty1 microwave (MW) peptide synthesizer (CEM Corporation, Mathews, NC, USA) (23). Briefly, Fmoc-Rink-amide resin (NovaBiochem, Switzerland) was preswelled for 15 min in *N*,*N*-dimethylformamide (DMF) (VWR International, Portugal) and then transferred into the MW reaction vessel. The initial Fmoc deprotection step was carried out using 20% piperidine in DMF containing 0.1 M 1-hydroxybenzotriazole (HOBt) (Sigma-Aldrich, Germany) in two MW irradiation pulses: 30 s at 24 W plus 3 min at 28 W, with the temperature in both cases being no higher than 75°C. The Fmoc-protected C-terminal amino acid (Bachem, Switzerland) was then coupled to the resin, using 5 molar equivalents (eq) of the Fmoc-protected amino acid in DMF (0.2 M), 5 eq of 0.5 M *N*,*N*,*N*′,*N*′-tetramethyl-*O*-(1*H*-benzotriazol-1-yl)uronium hexafluorophosphate/HOBt in DMF, and 10 eq of 2 M *N*-ethyl-*N*,*N*-diisopropylamine (DIPEA) (Sigma-Aldrich, Germany) in *N*-methylpyrrolidone (NMP) (VWR International, Portugal); the coupling step was carried out for 5 min at 35-W MW irradiation, with a maximum temperature reaching 75°C. The remaining amino acids were sequentially coupled in the C → N direction by means of similar deprotection and coupling cycles, except for incorporation of the following: (i) Fmoc-Arg(Pbf)-OH, whose coupling was done in two steps, 25 min with no MW irradiation (room temperature), followed by 5 min of coupling at 25 W, and (ii) Fmoc-Cys(Trt)-OH and Fmoc-Trp(Boc)-OH, both also coupled in two steps, first 2 min of coupling without MW irradiation (room temperature) and then 4 min of coupling at 25 W, with the maximum temperature reaching 50°C. Following completion of sequence assembly, the peptides were released from the resin with the concomitant removal of side chain protecting groups, by a 3-h acidolysis at room temperature using a trifluoroacetic acid (TFA) (VWR International, Portugal)-based cocktail containing triisopropylsilane (TIS) (Sigma-Aldrich, Germany) and water as scavengers (TFA-TIS-H_2O, 95:2.5:2.5 [vol/vol/vol]). Crude products were purified by reverse-phase (RP) liquid chromatography on a Vydac C_{18} column (238TPB1520; Vydac, Hesperia, CA, USA) to a purity of at least 95%, as confirmed by high-performance liquid chromatography (HPLC) analysis on a Hitachi-Merck LaChrom Elite system equipped with a quaternary pump, a thermostated (Peltier effect)-automated sampler, and a diode-array detector (DAD). Pure peptides were quantified by UV absorption spectroscopy (Helios Gama, Spectronic Unicam), and their molecular weights were confirmed to be as expected by electrospray ionization/ion trap mass spectroscopy (ESI/IT MS) (LCQ-DecaXP LC-MS system; ThermoFinnigan).

Bovine lactoferricins (LFcin17-30, D-LFcin17-30, LFcin17-30 all R, and LFcin17-30 all K) (Table 1) were synthesized by solid-phase peptide synthesis using Fmoc-protected amino acids (Orpegen Pharma GmbH, Heidelberg, Germany) in a Syro II synthesizer (Biotage, Uppsala, Sweden) as described previously (24). Peptides were purified to a purity of at least 95% by semipreparative RP-HPLC (Jasco Corporation Tokyo, Japan) on a Vydac C_{18} column (218MS510; Vydac, Hesperia, CA, USA), and the authenticity of the peptides was confirmed by matrix-assisted laser desorption ionization–time of flight (MALDI-TOF) mass spectrometry on a Microflex LRF mass spectrometer equipped with an additional gridless reflectron (Bruker Daltonik, Bremen, Germany) as described previously (25).

All purified peptides were freeze-dried, after which peptide stock solutions were prepared in phosphate-buffered saline (PBS) (pH = 7.4) and stored at −20°C until use.

Bacteria. The strains of *Mycobacterium avium* used in this study were clinical isolates. Strain 2447 smooth transparent variant (SmT) was provided by F. Portaels (Institute of Tropical Medicine, Antwerp, Belgium); strains 2-151, either SmT or SmD (smooth-domed), was provided by J. Belisle (Colorado State University, Fort Collins, CO, USA).

Mycobacteria were grown to mid-log phase in Middlebrook 7H9 medium (Difco, Sparks, MD) containing 0.05% of Tween 80 (Sigma, St. Louis, MO) and 10% of ADC supplement (albumin-dextrose-catalase) at 37°C. Bacteria were harvested by centrifugation, washed twice with saline containing 0.05% Tween 80, resuspended in the same solution, and briefly sonicated in order to disrupt bacterial clumps. The suspension was stored in aliquots at −80°C until use. Just before use, an aliquot was quickly thawed and diluted to the appropriate concentration.

Effect of antimicrobial peptides on the viability of *M. avium* in axenic cultures. *M. avium* was grown in Middlebrook 7H9 medium to exponential phase (bacterial growth was monitored by measuring the optical density at 600 nm). Bacteria were seeded at 10^6 CFU per well into 96-well flat bottom plates and incubated with the peptides in a final volume of 200 μl. Each condition was tested in triplicate. The plates were incubated at 37°C in a humid atmosphere. After 1, 2, 4, or 7 days of incubation, bacterial viability was measured by a CFU assay. A bacterial suspension from each well was serially diluted in water containing 0.05% Tween 80. The dilutions were plated in Middlebrook 7H10 agar medium (Difco, Sparks, MD) and supplemented with OADC (oleic acid-albumin-dextrose-catalase), and the colonies were counted after 7 days at 37°C. The

difference, in terms of $\log_{10}$ CFU/ml, between the first and the last days of incubation was designated "log increase."

IC_{50} and IC_{90} (peptide concentration that inhibits 50% or 90% of mycobacterial growth after 7 days of incubation) values were obtained by fitting CFU data through a four-parameter dose-response sigmoidal curve using the GraphPad Prism software program (GraphPad Software Inc., La Jolla, CA). The reported final values correspond to the average of at least three independent experiments, with the corresponding standard deviation (SD) indicated.

Statistical analysis was performed with GraphPad Prism software using one-way analysis of variance (ANOVA) with adjustment for multiple comparisons in two ways: (i) comparing each value to a control (the corresponding parental peptide) and (ii) performing cross-comparisons among all peptides (within each family). The statistical significance, adjusted *P* value, and confidence intervals were obtained through the Bonferroni method for a chosen 95% significance.

SEM. *M. avium* 2447 SmT was grown in Middlebrook 7H9 medium to exponential phase. Approximately 10^6 CFU of bacteria were incubated with the peptides (25 μM) for 2 days at 37°C. After incubation, cytospin centrifugation (1,000 rpm, 2 min) (Cytospin 4; Thermo Scientific) was used to concentrate the bacteria in glass coverslips previously coated with APES (3-aminopropyltriethoxysilane) to promote bacterial adherence. Bacteria were fixed with 2.5% glutaraldehyde solution in 0.1 M sodium cacodylate buffer (supplemented with 5 mM $MgCl_2$ and 5 mM $CaCl_2$; pH = 7.2) for 2 h, followed by postfixation with 1% osmium tetroxide (OsO_4) in 0.1 M sodium cacodylate buffer (1 h). Bacteria were then dehydrated by successive incubations with increasing concentrations of ethanol (10 to 100%), dried in a critical point dryer (CPD7501; Polaron), and sputter coated with a gold/palladium thin film (50 s with a 15-mA current) using SPI Module sputter coater equipment. The scanning electron microscopy (SEM) exam was performed using a high-resolution (Schottky) environmental scanning electron microscope with X-ray microanalysis and electron backscattered diffraction analysis: Quanta 400 FEG ESEM/EDAX Genesis X4M.

TEM. A suspension of *M. avium* 2447 SmT in exponential growth phase was incubated with the peptides (25 μM) for 2 days at 37°C. Bacteria were fixed with a 4% formaldehyde and 1.25% glutaraldehyde solution in 0.1 M sodium cacodylate buffer (supplemented with 5 mM $MgCl_2$ and 5 mM $CaCl_2$; pH = 7.2) overnight at 4°C (first 3 h at room temperature), followed by postfixation with 1% osmium tetroxide (OsO_4) in 0.1 M sodium cacodylate buffer (1 h) and 1% uranyl acetate in water (30 min), gradually dehydrated in ethanol (25 to 100%), included with propylene oxide, and embedded in Epon resin (26, 27). Ultrathin sections were stained with lead citrate and uranyl citrate for 15 min each, and the samples were observed and photographed in a Jeol JEM-1400 transmission electron microscope (TEM).

RESULTS

Antimycobacterial activity of lactoferricin peptides. Human and bovine lactoferricin peptides (hLFcin1-11 and LFcin17-30) were evaluated for their antimicrobial activities against three different strains of *M. avium* (2-151 SmT, 2447 SmT, and 2-151 SmD) (28). Both peptides were active against the three strains in axenic cultures, with an IC_{50} of ≤15 μM (Table 1). The bovine peptide tended to be more active than the human one, exhibiting lower IC_{90} values for all *M. avium* strains. The activities of each peptide were similar between the *M. avium* strains (Table 1).

Arginine residues were reported to be critical for the antimicrobial activity of lactoferricins (5, 8, 29). hLFcin1-11 has four arginine residues, and LFcin17-30 has three (Table 1). In order to investigate whether these residues were important for the display of antimycobacterial activity, we synthesized and tested lactoferricin analogues in which arginine residues were replaced by lysine (all-K variants). Lysine was chosen because it has the same charge as arginine, and hence any differences in activity would not be attributable to the alteration of overall positive charge. Since bovine LFcin17-30 has three lysine residues, we also tested a variant of this peptide in which all lysines were replaced by arginines (all-R variant).

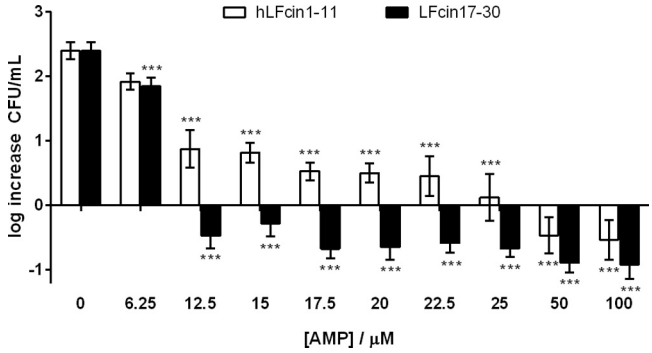

FIG 1 Direct effect of human and bovine lactoferricin on *M. avium* viability at 7 days of incubation. *M. avium* 2447 SmT was incubated with hLFcin1-11 or LFcin17-30 at 0, 6.25, 12.5, 15, 17.5, 20, 22.5, 25, 50, and 100 μM concentrations. *M. avium* viability was determined by measuring CFU after 7 days of incubation. Statistical analysis was performed using one-way ANOVA (Bonferroni test): ***, $P < 0.001$. The results of one experiment out of three are shown.

When tested against *M. avium* 2447 SmT in axenic culture, the all-K variants of each peptide were significantly less active than the corresponding original peptide (Table 1) ($P < 0.0001$ for IC_{50} for human peptides; $P = 0.0329$ for IC_{50} and $P = 0.0074$ for IC_{90} for bovine peptides). Conversely, the all-R variant of LFcin17-30 was slightly more active than the original peptide (Table 1) (for IC_{50}, $P = 0.0377$). Of note, even in the all-K variants, the bovine peptide exhibited a stronger antimicrobial activity than the human peptide ($P < 0.0001$) (Table 1).

Given that one of the limitations of therapeutic applications of peptides is their sensitivity to proteolysis, we thought it would be interesting to know whether replacement of all native amino acids in LFcin17-30 by their D enantiomers (less prone to degradation) would preserve the peptide's activity against *M. avium*. Remarkably, the all-D LFcin17-30 sequence (D-LFcin17-30) was found to be significantly more active than the corresponding native peptide (Table 1) (for IC_{50}, $P = 0.0455$).

We observed in all cases an abrupt decrease in mycobacterial viability at peptide concentrations around 12.5 μM, which translated into very close values for IC_{50} and IC_{90} (Table 1). This suggested that a critical concentration threshold may exist for the peptides to exert their activity. To test this hypothesis, we assessed the effect of the human and bovine parental peptides, hLFcin1-11 and LFcin17-30, on *M. avium* 2447 SmT using narrower concentration intervals in the 12.5 to 25 μM range. As shown in Fig. 1, this experiment confirmed the existence of a threshold concentration and further showed that the dose-effect correlation is different for the two peptides. For hLFcin1-11, there is a gradual decrease in the viability of *M. avium* as the peptide concentration increases, whereas for LFcin17-30, there is a critical inhibitory concentration above which the increase in the peptide concentration has no further effect on mycobacterial viability.

To assess in detail the time dependence of the action of lactoferricin peptides against *M. avium* 2447 SmT, the antimicrobial activity was determined by CFU at the end of 1, 2, and 4 days of

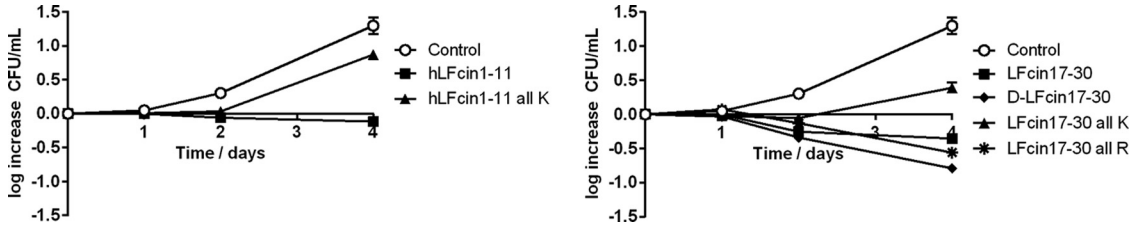

FIG 2 Direct effect of lactoferricins on *M. avium* viability at 1, 2, and 4 days of incubation. *M. avium* 2447 SmT was incubated with hLFcin1-11, hLFcin1-11 all K, LFcin17-30, D-LFcin17-30, LFcin17-30 all K, or LFcin17-30 all R at 0 and 12.5 μM. *M. avium* viability was determined by measuring CFU after 1, 2, and 4 days of incubation. The results of one experiment out of three are shown.

incubation. No significant effects were seen up to 1 day. All peptides showed significant inhibitory activity after 2 days of incubation at 12.5 μM (Fig. 2) and 25 μM (not shown). For the most active peptides (hLFcin1-11, LFcin17-30, D-LFcin17-30, and LFcin17-30 all R), mycobacterial death was observed at 4 days (Fig. 2).

Similar to what was observed at 7 days of incubation, at shorter times the bovine peptides tended to be more active than the human ones, and the peptides with arginines (human or bovine) were more active than those with lysines.

Surface and ultrastructural alterations in *M. avium* induced by lactoferricins. To gain a better understanding of the mechanisms of antimicrobial action of lactoferricin peptides against *M. avium*, we performed scanning electron microscopy (SEM) and transmission electron microscopy (TEM) to identify surface and ultrastructural alterations in the bacteria upon peptide treatment. After 2 days of incubation with lactoferricins at 25 μM, SEM analysis of *M. avium* 2447 SmT revealed overall shape deformations (Fig. 3, left panel, arrow), increased roughness of the bacterial surface, and the accumulation of biological material outside the cells (Fig. 3, left panel, arrowhead), this last suggesting leakage of intracellular content. Ultrastructural alterations were also seen using TEM, namely, condensation of cytoplasmic dense material, such as proteins (Fig. 3, right panel, empty arrow), once again with the suggestion of leakage of intracellular material, indicated by accumulation of material extracellularly (Fig. 3; right panel, arrowhead), as well as translucent cytoplasm and a high number of "ghost" cells (Fig. 3, right panel, asterisk). In agreement with the previous results for activity, the bovine peptides induced more severe structural alterations in the bacteria than the human ones, especially D-LFcin17-30 and LFcin17-30 all R (Fig. 3).

DISCUSSION

Considering the potential of AMP as new alternative therapies to fight infectious diseases and the urgent need to develop more efficient therapies for infections caused by mycobacteria, we tested several lactoferricin peptides against *Mycobacterium avium*. Aside from the antimicrobial activity, toxicity is a fundamental parameter in possible future use. hLFcin1-11 has already been used in different preclinical and clinical trials, where its overall safety was proved (20, 22), and LFcin17-30 has been shown to be nontoxic for erythrocytes and rat hepatocytes up to a 50 μM concentration (30). In the present work, we found that both the human and bovine lactoferricins (hLFcin1-11 and LFcin17-30, respectively) were active against *M. avium* strains of different virulences, the bovine peptide being more active than the human one.

AMP vary widely in many aspects, such as length, sequence, structure, and source, but they share important common traits, such as a positive charge, presumed to be fundamental for interaction with the negatively charged surface of pathogen cells (4, 6), and amphipathicity, which enables better interaction with the hydrophobic part of the microbial membrane, leading to its disruption (31, 32). Arginine residues were previously suggested to be important for the antimicrobial activity of lactoferricins (5, 8, 29) and also to potentiate the internalization of peptides (33–35). Therefore, we studied lactoferricin variants with arginines replaced by lysines and vice versa. As shown in Table 1 and Fig. 2, all peptides, human and bovine, with all arginines replaced by lysines were less active against *M. avium*, whereas when lysines were replaced by arginines, the peptides were more active. This shows that arginine residues are crucial for the antimicrobial activity of these peptides against *M. avium*. The contribution of arginine for activity is probably not charge related, since it bears the same charge as lysine (+1). The higher activities of peptides with arginine residues could be the result of the presence of the bulky guanidinium group on the side chain, enabling a better interaction with the membranes, since multiple hydrogen bonds can in this case be formed with the lipid headgroups around, whereas lysines can interact with only one (5, 8, 33, 35, 36). Arginine can also establish stronger cation-π interactions, which occur mainly between aromatic residues (e.g., tryptophan) and residues with positively charged side chains (e.g., arginines and lysines), that could allow the peptides to penetrate deeper into the membrane (8, 33, 35, 36). Moreover, arginines can form hydrogen bonds while establishing cation-π interactions, with tryptophan, for instance, whereas lysines cannot (8, 33, 35, 36). All these factors combined may have contributed to a more efficient activity against mycobacteria (5, 8, 29, 33, 36).

Due to the large diversity of AMP and of their properties, there is most probably no universal mechanism for their action. In this work, we have contributed to the elucidation of the mechanism of action of lactoferricins against *M. avium*. Our observation that the D enantiomer of LFcin17-30 is more active than the L form suggests that antimycobacterial activity is not dependent on chiral centers, such as specific protein receptors, which is in agreement with previous observations made for lactoferricin and other AMP, such as magainin, cecropin, melittin, and protegrin, against other pathogens (5, 6, 37–39). One of the major drawbacks of the use of AMP in the clinic is their susceptibility to proteases and other plasma components, resulting in low metabolic stability and bioavailability (40). One way to overcome this problem is to use D peptides, which are more resistant to protease activity (32, 41). This seems to be the case for LFcin17-30, which exhibited a higher activity against *M. avium* with all D-amino acids, indicating that

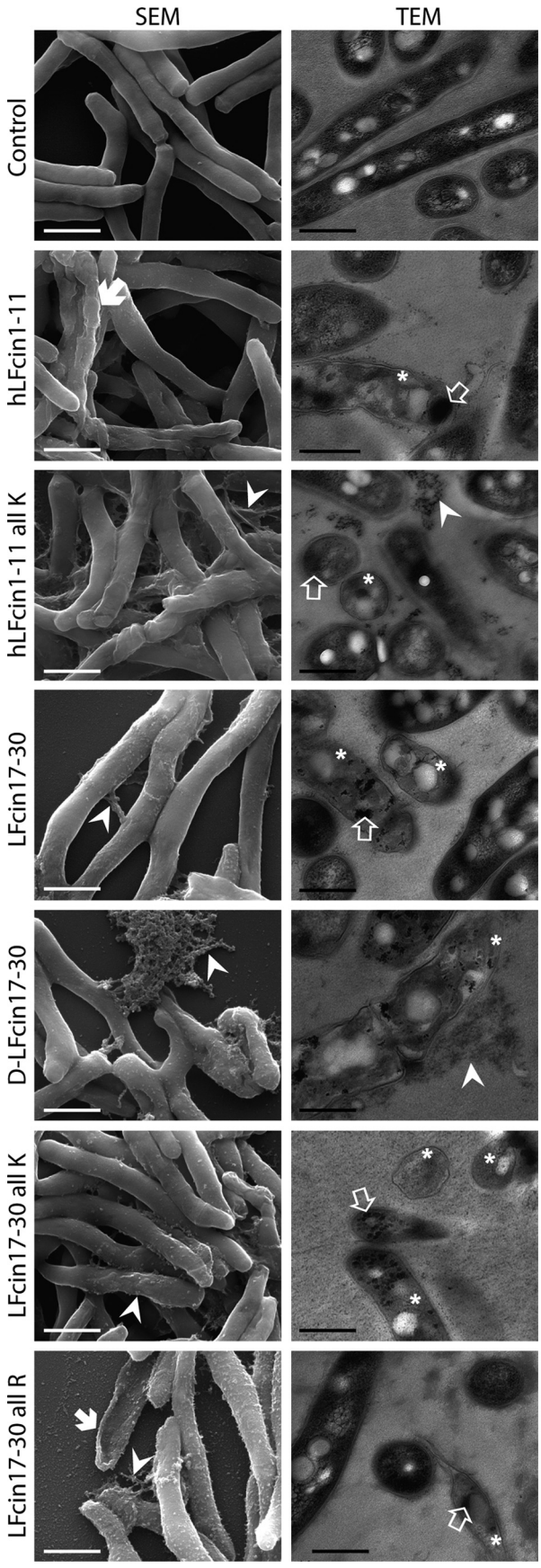

this can be used advantageously in comparison to the L enantiomer.

The concentration-effect curves obtained for the antimicrobial activities of lactoferricins did not show a gradual decrease. Around 12.5 μM, there was a sharp drop in mycobacterial viability, more pronounced in the case of the bovine peptide, reflected in very close values for IC_{50} and IC_{90}. This observation is in line with some models of AMP activity that predict the existence of a threshold concentration for their antimicrobial activity (4).

M. avium is a slow-growing mycobacterium, and thus we used 7 days of culture to determine lactoferricin activity. However, previous reports showed that LFcin17-30 is able to exert antimicrobial activity against other pathogens in about 1 h (24, 42–44). In order to evaluate the kinetics of the activity of lactoferricins against *M. avium*, we performed several assays with shorter culture times. We did not observe any significant decrease in the number of viable mycobacterial cells in less than 2 days of incubation, with peptide concentrations up to 25 μM (data not shown). This "delay" in activity against *M. avium* compared to that against other pathogens can be explained by the particular characteristics of the mycobacterial cell wall, as well as an intrinsic low rate of proliferation. *Mycobacterium* species are characterized by a complex hydrophobic envelope of extremely low fluidity and high impermeability, which contributes to the capacity of the pathogen to survive inside the host and resist chemotherapy (45, 46). Furthermore, the possibility of an internal target for the action of these peptides against *M. avium* cannot be discarded. In fact, there are numerous evidences in the literature pointing to the probable existence of an internal target for lactoferricins (5, 47–49).

Finally, electron microscopy studies showed that all lactoferricin peptides tested induced significant changes both in the surface and in the ultrastructural organization of the mycobacterial cells. In agreement with the bacterial viability assays, D-LFcin17-30 and the all-R variant showed the most drastic effects on the mycobacterial morphostructure. However, these studies did not allow us to obtain definitive information on what is the target (or targets) of the peptides. The observed accumulation of biological material outside the cells, seen by both SEM and TEM, and the presence of translucent cytoplasm and a high number of "ghost" cells (TEM) indicate leakage and are compatible with cell membrane permeabilization. Clearer evidences that the peptides act by permeabilization, such as the appearance of vesicular budding and disappearance of the cell wall or membrane, were not observed. A mechanism of action that includes crossing over the bacterial surface and acting on internal targets has been proposed for bovine lactoferricins. The higher activity of lactoferricins containing arginines also supports this hypothesis, since this amino acid is often correlated with peptides that exert their activity on internal targets (33–35), as opposed to lysines, which are usually described as cru-

FIG 3 Surface and ultrastructural alterations in *M. avium* induced by lactoferricins at 2 days of incubation. *M. avium* 2447 SmT was incubated with hLFcin1-11, hLFcin1-11 all K, LFcin17-30, D-LFcin17-30, LFcin17-30 all K, or LFcin17-30 all R at 25 μM for 2 days. Cells were observed and photographed in a scanning electron microscope (left panels) and in a transmission electron microscope (right panels). Representative pictures are shown. Bar = 1 μm (left panels) or 0.5 μm (right panels). Symbols: arrow, shape deformations; arrowhead, increased roughness and accumulation of intracellular material outside; empty arrow, condensation of cytoplasmic material; asterisk, translucent cytoplasm and ghost cells.

cial for membrane-lytic activities. In recent studies, we have shown that LFcin17-30 has a mild effect on model membranes, acting by lipid segregation instead of leading to full membrane disruption, as observed for other membrane-active peptides (50). Further, Haukland et al. (47) showed that lactoferricin is found in the cytoplasm of *Staphylococcus aureus* and *Escherichia coli*, and Ulvatne et al. (49) showed that it inhibits the macromolecular synthesis (DNA, RNA, and protein synthesis) of *E. coli* and *Bacillus subtilis*. The alterations seen suggest that the mechanism of action of the studied lactoferricins against mycobacteria is not confined to the cell wall or membrane but probably also includes action on internal targets, leading to impairment of several intracellular processes, such as DNA replication, DNA, RNA, and protein synthesis, protein folding, etc., which eventually culminates in cell death.

In summary, key molecular features of lactoferricin-based peptides for the display of antimycobacterial activity were identified, contributing to the understanding of their mechanism of action against mycobacteria. Hence, this work demonstrates that lactoferricin-related AMP are promising molecules for development of clinically useful weapons to treat infections caused by mycobacteria.

ACKNOWLEDGMENTS

This research received support from FCT (Fundação para a Ciência e Tecnologia), Lisbon, Portugal, and European Social Fund through projects Pest-C/QUI/UI0081/2011 and PEst-C/QUI/UI0081/2013, awarded to CIQ(UP); "NORTE-07-0124-FEDER-000002-Host-Pathogen Interactions," cofunded by Programa Operacional Regional do Norte (ON.2, O Novo Norte), under the Quadro de Referência Estratégico Nacional (QREN), awarded to IBMC; and POFC, COMPETE program FCOMP-01-0124-FEDER-009400 and project PTDC/CTM/101484/2008, awarded to CIQUP. T.S. receives Ph.D. grant SFRH/BD/77564/2011 from FCT. This work also benefited from a grant from the University of Amsterdam for research into the focal point of oral infections and inflammation to J.G.M.B. and K.N.

We thank Instituto Nacional de Engenharia Biomédica (INEB), Porto, Portugal, for giving access to the critical point dryer essential for SEM experiments, Rui Fernandes from the Histology and Electron Microscopy Service of Instituto de Biologia Molecular e Celular (IBMC), Porto, Portugal, for technical assistance with transmission electron microscopy, and Daniela Silva from Centro de Materiais da Universidade do Porto (CEMUP), Porto, Portugal, for technical assistance with scanning electron microscopy.

REFERENCES

1. **Villemagne B, Crauste C, Flipo M, Baulard AR, Deprez B, Willand N.** 2012. Tuberculosis: The drug development pipeline at a glance. Eur. J. Med. Chem. **51:**1–16. http://dx.doi.org/10.1016/j.ejmech.2012.02.033.
2. **Cook JL.** 2010. Nontuberculous mycobacteria: opportunistic environmental pathogens for predisposed hosts. Br. Med. Bull. **96:**45–59. http://dx.doi.org/10.1093/bmb/ldq035.
3. **Karakousis PC, Moore RD, Chaisson RE.** 2004. *Mycobacterium avium* complex in patients with HIV infection in the era of highly active antiretroviral therapy. Lancet Infect. Dis. **4:**557–565. http://dx.doi.org/10.1016/S1473-3099(04)01130-2.
4. **Teixeira V, Feio MJ, Bastos M.** 2012. Role of lipids in the interaction of antimicrobial peptides with membranes. Prog. Lipid Res. **51:**149–177. http://dx.doi.org/10.1016/j.plipres.2011.12.005.
5. **Gifford JL, Hunter HN, Vogel HJ.** 2005. Lactoferricin: a lactoferrin-derived peptide with antimicrobial, antiviral, antitumor and immunological properties. Cell. Mol. Life Sci. **62:**2588–2598. http://dx.doi.org/10.1007/s00018-005-5373-z.
6. **Lohner K, Blondelle SE.** 2005. Molecular mechanisms of membrane perturbation by antimicrobial peptides and the use of biophysical studies in the design of novel peptide antibiotics. Comb. Chem. High Throughput Screen. **8:**241–256. http://dx.doi.org/10.2174/1386207053764576.
7. **Nguyen LT, Haney EF, Vogel HJ.** 2011. The expanding scope of antimicrobial peptide structures and their modes of action. Trends Biotechnol. **29:**464–472. http://dx.doi.org/10.1016/j.tibtech.2011.05.001.
8. **Chan DI, Prenner EJ, Vogel HJ.** 2006. Tryptophan- and arginine-rich antimicrobial peptides: structures and mechanisms of action. Biochim. Biophys. Acta **1758:**1184–1202. http://dx.doi.org/10.1016/j.bbamem.2006.04.006.
9. **Bellamy W, Wakabayashi H, Takase M, Kawase K, Shimamura S, Tomita M.** 1993. Killing of Candida albicans by lactoferricin B, a potent antimicrobial peptide derived from the N-terminal region of bovine lactoferrin. Med. Microbiol. Immunol. **182:**97–105.
10. **Leon-Sicairos N, Reyes-Lopez M, Ordaz-Pichardo C, de la Garza M.** 2006. Microbicidal action of lactoferrin and lactoferricin and their synergistic effect with metronidazole in Entamoeba histolytica. Biochem. Cell Biol. **84:**327–336. http://dx.doi.org/10.1139/o06-060.
11. **Omata Y, Satake M, Maeda R, Saito A, Shimazaki K, Yamauchi K, Uzuka Y, Tanabe S, Sarashina T, Mikami T.** 2001. Reduction of the infectivity of Toxoplasma gondii and Eimeria stiedai sporozoites by treatment with bovine lactoferricin. J. Vet. Med. Sci. **63:**187–190. http://dx.doi.org/10.1292/jvms.63.187.
12. **Turchany JM, Aley SB, Gillin FD.** 1995. Giardicidal activity of lactoferrin and N-terminal peptides. Infect. Immun. **63:**4550–4552.
13. **Jenssen H, Hancock RE.** 2009. Antimicrobial properties of lactoferrin. Biochimie **91:**19–29. http://dx.doi.org/10.1016/j.biochi.2008.05.015.
14. **Oo TZ, Cole N, Garthwaite L, Willcox MD, Zhu H.** 2010. Evaluation of synergistic activity of bovine lactoferricin with antibiotics in corneal infection. J. Antimicrob. Chemother. **65:**1243–1251. http://dx.doi.org/10.1093/jac/dkq106.
15. **Sanchez-Gomez S, Japelj B, Jerala R, Moriyon I, Fernandez Alonso M, Leiva J, Blondelle SE, Andra J, Brandenburg K, Lohner K, Martinez de Tejada G.** 2011. Structural features governing the activity of lactoferricin-derived peptides that act in synergy with antibiotics against Pseudomonas aeruginosa in vitro and in vivo. Antimicrob. Agents Chemother. **55:**218–228. http://dx.doi.org/10.1128/AAC.00904-10.
16. **Groenink J, Walgreen-Weterings E, van 't Hof W, Veerman ECI, Nieuw Amerongen AV.** 1999. Cationic amphipathic peptides, derived from bovine and human lactoferrins, with antimicrobial activity against oral pathogens. FEMS Microbiol. Lett. **179:**217–222. http://dx.doi.org/10.1111/j.1574-6968.1999.tb08730.x.
17. **Wiesner J, Vilcinskas A.** 2010. Antimicrobial peptides: the ancient arm of the human immune system. Virulence **1:**440–464. http://dx.doi.org/10.4161/viru.1.5.12983.
18. **Dijkshoorn L, Brouwer CP, Bogaards SJ, Nemec A, van den Broek PJ, Nibbering PH.** 2004. The synthetic N-terminal peptide of human lactoferrin, hLF(1-11), is highly effective against experimental infection caused by multidrug-resistant Acinetobacter baumannii. Antimicrob. Agents Chemother. **48:**4919–4921. http://dx.doi.org/10.1128/AAC.48.12.4919-4921.2004.
19. **Lupetti A, Paulusma-Annema A, Welling MM, Dogterom-Ballering H, Brouwer CP, Senesi S, Van Dissel JT, Nibbering PH.** 2003. Synergistic activity of the N-terminal peptide of human lactoferrin and fluconazole against Candida species. Antimicrob. Agents Chemother. **47:**262–267. http://dx.doi.org/10.1128/AAC.47.1.262-267.2003.
20. **Brouwer CP, Rahman M, Welling MM.** 2011. Discovery and development of a synthetic peptide derived from lactoferrin for clinical use. Peptides **32:**1953–1963. http://dx.doi.org/10.1016/j.peptides.2011.07.017.
21. **Brouwer CP, Welling MM.** 2008. Various routes of administration of (99m)Tc-labeled synthetic lactoferrin antimicrobial peptide hLF 1-11 enables monitoring and effective killing of multidrug-resistant Staphylococcus aureus infections in mice. Peptides **29:**1109–1117. http://dx.doi.org/10.1016/j.peptides.2008.03.003.
22. **Velden WJ, van Iersel TM, Blijlevens NM, Donnelly JP.** 2009. Safety and tolerability of the antimicrobial peptide human lactoferrin 1-11 (hLF1-11). BMC Med. **7:**44. http://dx.doi.org/10.1186/1741-7015-7-44.
23. **Brandt M, Gammeltoft S, Jensen K.** 2006. Microwave heating for solid-phase peptide synthesis: general evaluation and application to 15-mer phosphopeptides. Int. J. Peptide Res. Ther. **12:**349–357. http://dx.doi.org/10.1007/s10989-006-9038-z.
24. **Bolscher JG, Adão R, Nazmi K, van den Keybus PA, van 't Hof W, Nieuw Amerongen AV, Bastos M, Veerman EC.** 2009. Bactericidal activity of LFchimera is stronger and less sensitive to ionic strength than its

constituent lactoferricin and lactoferrampin peptides. Biochimie **91:**123–132. http://dx.doi.org/10.1016/j.biochi.2008.05.019.
25. **Bolscher JG, Oudhoff MJ, Nazmi K, Antos JM, Guimaraes CP, Spooner E, Haney EF, Vallejo JJ, Vogel HJ, van't Hof W, Ploegh HL, Veerman EC.** 2011. Sortase A as a tool for high-yield histatin cyclization. FASEB J. **25:**2650–2658. http://dx.doi.org/10.1096/fj.11-182212.
26. **Silva MT, Macedo PM.** 1983. The interpretation of the ultrastructure of mycobacterial cells in transmission electron microscopy of ultrathin sections. Int. J. Lepr. Other Mycobact. Dis. **51:**225–234.
27. **Silva MT, Macedo PM.** 1984. Ultrastructural characterization of normal and damaged membranes of Mycobacterium leprae and of cultivable mycobacteria. J. Gen. Microbiol. **130:**369–380.
28. **Gomes MS, Florido M, Cordeiro JV, Teixeira CM, Takeuchi O, Akira S, Appelberg R.** 2004. Limited role of the Toll-like receptor-2 in resistance to Mycobacterium avium. Immunology **111:**179–185. http://dx.doi.org/10.1111/j.0019-2805.2003.01807.x.
29. **Kang JH, Lee MK, Kim KL, Hahm KS.** 1996. Structure-biological activity relationships of 11-residue highly basic peptide segment of bovine lactoferrin. Int. J. Pept. Protein Res. **48:**357–363.
30. **van der Kraan MI, Nazmi K, Teeken A, Groenink J, van 't Hof W, Veerman EC, Bolscher JG, Nieuw Amerongen AV.** 2005. Lactoferrampin, an antimicrobial peptide of bovine lactoferrin, exerts its candidacidal activity by a cluster of positively charged residues at the C-terminus in combination with a helix-facilitating N-terminal part. Biol. Chem. **386:**137–142. http://dx.doi.org/10.1515/BC.2005.017.
31. **Shai Y, Makovitzky A, Avrahami D.** 2006. Host defense peptides and lipopeptides: modes of action and potential candidates for the treatment of bacterial and fungal infections. Curr. Protein Pept. Sci. **7:**479–486. http://dx.doi.org/10.2174/138920306779025620.
32. **Hancock RE, Sahl HG.** 2006. Antimicrobial and host-defense peptides as new anti-infective therapeutic strategies. Nat. Biotechnol. **24:**1551–1557. http://dx.doi.org/10.1038/nbt1267.
33. **Hansen M, Kilk K, Langel U.** 2008. Predicting cell-penetrating peptides. Adv. Drug Deliv. Rev. **60:**572–579. http://dx.doi.org/10.1016/j.addr.2007.09.003.
34. **Mitchell DJ, Kim DT, Steinman L, Fathman CG, Rothbard JB.** 2000. Polyarginine enters cells more efficiently than other polycationic homopolymers. J. Pept. Res. **56:**318–325. http://dx.doi.org/10.1034/j.1399-3011.2000.00723.x.
35. **Rothbard JB, Jessop TC, Lewis RS, Murray BA, Wender PA.** 2004. Role of membrane potential and hydrogen bonding in the mechanism of translocation of guanidinium-rich peptides into cells. J. Am. Chem. Soc. **126:**9506–9507. http://dx.doi.org/10.1021/ja0482536.
36. **Torcato IM, Huang YH, Franquelim HG, Gaspar D, Craik DJ, Castanho MA, Troeira Henriques S.** 2012. Design and characterization of novel antimicrobial peptides, R-BP100 and RW-BP100, with activity against Gram-negative and Gram-positive bacteria. Biochim. Biophys. Acta **1828:**944–955. http://dx.doi.org/10.1016/j.bbamem.2012.12.002.
37. **Merrifield EL, Mitchell SA, Ubach J, Boman HG, Andreu D, Merrifield RB.** 1995. D-Enantiomers of 15-residue cecropin A-melittin hybrids. Int. J. Pept. Protein Res. **46:**214–220.
38. **Wade D, Boman A, Wahlin B, Drain CM, Andreu D, Boman HG, Merrifield RB.** 1990. All-D amino acid-containing channel-forming antibiotic peptides. Proc. Natl. Acad. Sci. U. S. A. **87:**4761–4765. http://dx.doi.org/10.1073/pnas.87.12.4761.
39. **Wakabayashi H, Matsumoto H, Hashimoto K, Teraguchi S, Takase M, Hayasawa H.** 1999. N-Acylated and D enantiomer derivatives of a nonamer core peptide of lactoferricin B showing improved antimicrobial activity. Antimicrob. Agents Chemother. **43:**1267–1269.
40. **Rotem S, Mor A.** 2009. Antimicrobial peptide mimics for improved therapeutic properties. Biochim. Biophys. Acta **1788:**1582–1592. http://dx.doi.org/10.1016/j.bbamem.2008.10.020.
41. **Haug BE, Strom MB, Svendsen MJSM.** 2007. The medicinal chemistry of short lactoferricin-based antibacterial peptides. Curr. Med. Chem. **14:**1–18. http://dx.doi.org/10.2174/092986707779313435.
42. **Flores-Villasenor H, Canizalez-Roman A, Reyes-Lopez M, Nazmi K, de la Garza M, Zazueta-Beltran J, Leon-Sicairos N, Bolscher JG.** 2010. Bactericidal effect of bovine lactoferrin, LFcin, LFampin and LFchimera on antibiotic-resistant Staphylococcus aureus and Escherichia coli. Biometals **23:**569–578. http://dx.doi.org/10.1007/s10534-010-9306-4.
43. **Lopez-Soto F, Leon-Sicairos N, Nazmi K, Bolscher JG, de la Garza M.** 2010. Microbicidal effect of the lactoferrin peptides lactoferricin17-30, lactoferrampin265-284, and lactoferrin chimera on the parasite Entamoeba histolytica. Biometals **23:**563–568. http://dx.doi.org/10.1007/s10534-010-9295-3.
44. **Silva T, Abengozar MA, Fernandez-Reyes M, Andreu D, Nazmi K, Bolscher JG, Bastos M, Rivas L.** 2012. Enhanced leishmanicidal activity of cryptopeptide chimeras from the active N1 domain of bovine lactoferrin. Amino Acids **43:**2265–2277. http://dx.doi.org/10.1007/s00726-012-1304-0.
45. **Abdallah AM, Gey van Pittius NC, Champion PA, Cox J, Luirink J, Vandenbroucke-Grauls CM, Appelmelk BJ, Bitter W.** 2007. Type VII secretion—mycobacteria show the way. Nat. Rev. Microbiol. **5:**883–891. http://dx.doi.org/10.1038/nrmicro1773.
46. **Nigou J, Gilleron M, Puzo G.** 2003. Lipoarabinomannans: from structure to biosynthesis. Biochimie **85:**153–166. http://dx.doi.org/10.1016/S0300-9084(03)00048-8.
47. **Haukland HH, Ulvatne H, Sandvik K, Vorland LH.** 2001. The antimicrobial peptides lactoferricin B and magainin 2 cross over the bacterial cytoplasmic membrane and reside in the cytoplasm. FEBS Lett. **508:**389–393. http://dx.doi.org/10.1016/S0014-5793(01)03100-3.
48. **Liu Y, Han F, Xie Y, Wang Y.** 2011. Comparative antimicrobial activity and mechanism of action of bovine lactoferricin-derived synthetic peptides. Biometals **24:**1069–1078. http://dx.doi.org/10.1007/s10534-011-9465-y.
49. **Ulvatne H, Samuelsen O, Haukland HH, Kramer M, Vorland LH.** 2004. Lactoferricin B inhibits bacterial macromolecular synthesis in Escherichia coli and Bacillus subtilis. FEMS Microbiol. Lett. **237:**377–384. http://dx.doi.org/10.1111/j.1574-6968.2004.tb09720.x.
50. **Silva T, Adao R, Nazmi K, Bolscher JG, Funari SS, Uhrikova D, Bastos M.** 2013. Structural diversity and mode of action on lipid membranes of three lactoferrin candidacidal peptides. Biochim. Biophys. Acta **1828:**1329–1339. http://dx.doi.org/10.1016/j.bbamem.2013.01.022.

CHAPTER 8. Lactoferricin peptides increase macrophage's capacity to kill *Mycobacterium avium*

Lactoferricin peptides increase macrophage's capacity to kill *Mycobacterium avium*

Tânia Silva [a,b,c,d], Kamran Nazmi [e], Nuno Vale [f], Tânia Moniz [f], Ana Carolina Moreira [a,b], Maria Rangel [g], Jan G. M. Bolscher [e], Paula Gomes [f], Pedro N. Rodrigues [a,b,d], Margarida Bastos [c], Maria Salomé Gomes [a,b,d,#]

[a] Instituto de Investigação e Inovação em Saúde, Universidade do Porto, Porto, Portugal;

[b] IBMC – Instituto de Biologia Molecular e Celular, Universidade do Porto, Porto, Portugal;

[c] CIQ-UP – Centro de Investigação em Química, Departamento de Química e Bioquímica, Faculdade de Ciências, Universidade do Porto, 4169-007 Porto, Portugal;

[d] ICBAS – Instituto de Ciências Biomédicas Abel Salazar, Universidade do Porto, Porto, Portugal;

[e] Department of Oral Biochemistry, Academic Center for Dentistry Amsterdam (ACTA), University of Amsterdam and VU University Amsterdam, Amsterdam, The Netherlands;

[f] UCIBIO/REQUIMTE, Departamento de Química e Bioquímica, Faculdade de Ciências, Universidade do Porto, 4169-007 Porto, Portugal;

[g] UCIBIO/REQUIMTE, Instituto de Ciências Biomédicas de Abel Salazar, Universidade do Porto, 4050-313 Porto, Portugal.

Address correspondence to Maria Salomé Gomes, sgomes@ibmc.up.pt.

Abstract

The incidence of infections caused by nontuberculous mycobacteria (NTM) is increasing worldwide. Within this group, bacteria from the *Mycobacterium avium* complex (MAC) are the main cause of disease, especially disseminated disease in immunocompromised hosts (*e.g.* HIV-infected patients). Treatment of NTM is currently long, toxic, costly and usually extrapolated from the tuberculosis experience. Moreover, antibiotic resistance development is increasing, pressing the need for new antimicrobial alternatives. Antimicrobial peptides (AMP) are ubiquitous in nature and are active components of the host antimicrobial defence mechanisms.

We have previously reported that a shorter version of bovine lactoferricin along with variants obtained by specific amino acid substitutions were active against *Mycobacterium avium* growing in broth culture. In the present work, those same peptides were tested against *M. avium* growing inside its host cells, macrophages. We found that only the D enantiomer of lactoferricin was active alone against mycobacteria, but all peptides were active when combined with the conventional antibiotic ethambutol. We then sought to understand the mechanisms behind mycobacterial death. For that, the distribution and sub-cellular localization of lactoferricins inside *M. avium*-infected macrophages were evaluated, as well as the peptides ability to modulate the macrophage's antimicrobial mechanisms. We found that lactoferricins do not localize to *M. avium*-harbouring phagosomes and while they significantly induce the production of IL-6 and TNF by infected macrophages, this production does not explain the AMP anti-mycobacterial action.

Further studies are needed to clarify lactoferricin's mode of action.

Introduction

Nontuberculous mycobacteria (NTM) include more than 150 species and are important causes of morbidity and mortality. NTM are ubiquitous in the environment, being present in soil and water. The incidence of NTM infections, predominantly caused by species of the *Mycobacterium avium* complex (MAC), is increasing worldwide, surpassing in some regions the number of infections caused by *Mycobacterium tuberculosis* (Cassidy *et al.* 2009, Brode *et al.* 2014). Disseminated infections by NTM occur mainly in patients with a compromised immune system, such as HIV-infected patients, patients with cancer, organ or stem cell transplants, among others. Pulmonary disease can also occur, most frequently affecting patients with underlying lung disease such as chronic obstructive pulmonary disease or older women and also appearing as nosocomial infections after surgery (revised in (Weiss and Glassroth 2012, Orme and Ordway 2014, Henkle and Winthrop 2015)). Mycobacteria are equipped with a unique and complex highly impermeable cell wall, and as facultative intracellular pathogens are able to proliferate inside host cells, such as macrophages, resisting chemotherapy and causing persistent infections that are difficult to eradicate (Flannagan *et al.* 2009, Guenin-Mace *et al.* 2009). Treatment regimens are based on a combination of several drugs taken from months to years, and in general have limited efficacies (Brown-Elliott *et al.* 2012, Philley and Griffith 2015). Furthermore, mycobacterial antibiotic resistance is increasing worldwide, urging the need to develop novel classes of antimicrobial drugs (Falzon *et al.* 2015).

Antimicrobial peptides (AMP) are a large number of antimicrobial molecules widespread in nature as part of the host defence mechanisms, constituting potential new antimicrobial therapies (Yeung *et al.* 2011). Although their mode of action is still under debate, they are thought to act in a multiple hit strategy, which probably contributes to their high efficacy and large spectrum of activity. AMP can act directly on the pathogens, either by disrupting the membrane due to pore formation and/or micellization, or by acting on internal targets (Nguyen *et al.* 2011). They can also act by immunomodulation, being involved in several processes such as, modulation of pro- and anti-inflammatory responses, chemoattraction, cellular differentiation, angiogenesis and wound healing, enhanced bacterial clearance, autophagy and apoptosis, among others (Mansour *et al.* 2014). The nature of the peptide's target, the cytoplasmic membrane, a conserved and essential structure across different species, together with the fact that both L and D enantiomers are active (indicating a non-receptor mediated activity) (Haug *et al.* 2007), suggest that these compounds are less prone to the development of microbial resistance than conventional antibiotics.

Lactoferricin peptide is obtained by pepsin digestion of the highly cationic N1 terminal domain of the iron-binding protein lactoferrin (Bellamy *et al.* 1992b, Kuwata *et al.* 1998). The bovine lactoferricin is constituted by 25 amino acids (17 to 41 in the native protein) (Bellamy *et al.* 1992a), and has broad-spectrum of activity (reviewed in (Gifford *et al.* 2005)). A shorter version, with amino acids 17 to 30 (LFcin17-30), was found to be even more active (Groenink *et al.* 1999). In the previous chapter we have shown that arginine residues are crucial for the antimicrobial activity of LFcin17-30 against *M. avium* growing in broth culture, and that the D enantiomer (D-LFcin17-30) was even more active than the L form (chapter 7). In the present work, LFcin17-30 and its variants were tested against *M. avium* growing inside mouse macrophages, alone or in combination with the conventional antibiotic ethambutol, and found that the D-LFcin17-30 was the most active peptide. We further tried to establish the mechanism by which this peptide exerts its activity against intracellular *M. avium*.

Material and Methods

Peptides

Bovine lactoferricins (LFcin17-30, D-LFcin17-30, LFcin17-30 all K and LFcin17-30 all R) (Table 1) were synthesized by solid phase peptide synthesis using 9-fluorenyl-methoxycarbonyl (Fmoc) chemistry with a Syro II synthesizer (Biotage, Uppsala, Sweden) as described previously (Bolscher *et al.* 2011). Peptide synthesis grade solvents were obtained from Actu-All Chemicals (Oss, The Netherlands), the preloaded NovaSyn TGA resins from Novabiochem (Merck Schuchardt, Hohenbrunn, Germany) and the N-α-Fmoc-amino acids from Orpegen Pharma (Heidelberg, Germany) and Iris Biotech (Marktredwitz, Germany). LFcin17-30 and D-LFcin17-30, were labelled in synthesis with 5(6)-carboxytetramethylrhodamine (TAMRA; Novabiochem) by coupling TAMRA to the ε-aminogroup of a C-terminally additional lysine residue using Fmoc-Lys(ivDde)-OH, resulting in a labelling stoichiometry of 1:1, without any free TAMRA remaining. Briefly, the peptide was synthesized as described above on Fmoc-Lys(ivDde)-OH coupled to NovaSyn TGR resin (Novabiochem) with the N-terminal amino acid protected by N-α-t.-Boc. Subsequently, the ivDde-protecting group at the C-terminal Lys was released by hydrazinolysis (2% hydrazine hydrate in 1-methyl-2-pyrrolidone, NMP) followed by overnight incubation with 1.5 eq. TAMRA in (NMP) containing 1.5 eq. 1-hydroxybenzotriazole (HObt), 1.7 eq. 2-1[H-benzotriazole-1-yl]-1,1,3,3-tetramethylaminium tatrafluoroborate (TBTU) and 70 µL N,N-diisopropylethylamine (DIPEA) in a final volume of 2ml. Next, the peptide containing resin was washed twice with NMP and twice with 20% piperidine, followed by three times washing with consecutively NMP, isopropyl alcohol (IPA) and dichloromethane (DCM). Subsequently, the peptide was detached from the resin and deprotected as described previously (Bolscher *et al.* 2011).

Peptides were purified to a purity of at least 95% by semipreparative RP-HPLC (Jasco Corporation Tokyo, Japan) on a Vydac C18-column (218MS510; Vydac, Hesperia, CA, USA) and the authenticity of the peptides was confirmed by MALDI-TOF mass spectrometry on a Microflex LRF mass spectrometer equipped with an additional gridless reflectron (Bruker Daltonik, Bremen, Germany) as described previously (Bolscher *et al.* 2011).

All purified peptides were freeze-dried. Peptide stock solutions were prepared in Phosphate Buffered Saline (PBS, pH = 7.4), with 10 % DMSO in the case of the labelled peptides, and stored at -20 °C until use.

Bacteria

In this work two strains of *Mycobacterium avium* were used: i) *M. avium* strain 2447 smooth transparent variant (SmT), originally isolated by Dr. F. Portaels (Institute of Tropical Medicine, Antwerp, Belgium) from an AIDS patient, and ii) *M. avium* 104:pMV306 (*hsp*60/*gfp*) expressing green fluorescent protein (*M. avium*-GFP) (Parker and Bermudez 1997) for confocal microscopy experiments.

Mycobacteria were grown to mid-log phase in Middlebrook 7H9 medium (Difco, Sparks, MD) containing 0.05% of Tween 80 (Sigma, St. Louis, MO) and 10% of albumin-dextrose-catalase supplement (ADC) at 37 °C. Bacteria were harvested by centrifugation, washed twice with saline containing 0.05% Tween 80, re-suspended in the same solution and briefly sonicated in order to disrupt bacterial clumps. The suspension was stored in aliquots at -80 °C until use. Just before macrophage infection, an aliquot was quickly thawed and diluted to the appropriate concentration.

Bone Marrow derived Macrophages (BMM)

Macrophages were derived from the bone marrow of male BALB/c, C57BL/6 and C57BL/6.TNF-alpha deficient mice (*Tnf*$^{-/-}$) bred at the IBMC animal facility. TNF-alpha deficient breeder mice were originally purchased from B&K Universal (East Yorkshire, United Kingdom).

Each femur and tibia was flushed with Hank's Balanced Salt Solution (HBSS, Gibco, Paisley, U.K.). The resulting cell suspension was centrifuged and re-suspended in Dulbecco's Modified Eagle's Medium (DMEM, Gibco, Paisley, U.K.) supplemented with 10 mM glutamine, 10 mM HEPES, 1 mM sodium pyruvate, 10% Fetal Bovine Serum (FBS, Gibco, USA) and 10% of L929 cell conditioned medium (LCCM) as a source of Macrophage Colony Stimulating Factor (M-CSF). Cells were cultured overnight at 37 °C in a 7% CO_2 atmosphere to remove fibroblasts. Non-adherent cells were collected with cold HBSS medium, washed and seeded at the concentration of $4x10^5$ cells/mL and incubated at 37 °C in a 7% CO_2 atmosphere. Four days after seeding, 10% of LCCM was added to the culture medium and on the 7th day, the medium was renewed. Cells were used at day 10 of culture, when fully differentiated into macrophages.

Macrophage infection and quantification of bacterial growth

BMM were cultured in 24-wells culture plates. At day 10 of culture, 10^6 Colony Forming Units (CFU) of *M. avium* 2447 SmT in DMEM were added to each well and cells were

incubated for 4 h at 37 °C in a 7% CO_2 atmosphere. After incubation, cells were washed several times with warm HBSS to remove non-internalized bacteria, and re-incubated with new medium, DMEM with 10% FBS and 10% LCCM, with or without 40 µM of peptide, alone or in combination with the antibiotic ethambutol (7.2 µM of ethambutol dihydrochloride, Sigma, St. Louis, MO, USA). Each condition was tested in triplicates.

After 5 days in culture, the intracellular growth of *M. avium* 2447 SmT was evaluated by colony forming units (CFU). Macrophages were lysed, using 0.1% saponin. The bacterial suspensions were serially diluted in water containing 0.05% Tween 80 and plated in Middlebrook 7H10 agar medium (Difco, Sparks, MD) supplemented with oleic acid-albumin-dextrose-catalase (OADC). The number of colonies was counted after 7 days at 37 °C. The results were expressed as percentage of growth of mycobacteria in each well relative to the growth of mycobacteria in the non-treated infected wells (control), in each experiment. The reported final values correspond to the average of at least three independent experiments with the corresponding standard deviation. Statistics were performed with GraphPad Prism 6 (GraphPad Software, Inc., La Jolla, CA, USA) using two-way ANOVA with Sidak's multiple comparisons test.

Measurement of macrophage viability

Viability of BALB/c BMM cultured in 96-wells culture plates, was determined by resazurin reduction. After 24 h of infection and peptide treatment (see above), supernatant was removed and cells were incubated with new medium (DMEM/ 10% FBS/ 10% LCCM) containing 125 µM resazurin (Sigma, St. Louis, MO, USA), for 24 h at 37 °C in a 7% CO_2 atmosphere. The fluorescence of resorufin, resulting from the conversion from resazurin by viable cells, was measured at λ_{ex} = 560 nm and λ_{em} = 590 nm. The results are expressed as the percentage of viable cells relative to the corresponding non-peptide-treated infected cells.

Confocal Microscopy

BALB/c BMM were cultured in µ-Slide 8 well plates (ibidi GmbH, Germany). At the 10th day of culture, macrophages were infected, as described above, with either GFP-expressing *M. avium* or *M. avium* 2447 SmT. After infection, LFcin17-30-TAMRA or D-LFcin17-30-TAMRA were added (10 µM, final concentration) to the cell culture medium. Simultaneously, ethambutol (7.2 µM, final concentration), was added to some infected wells with GFP-expressing *M. avium*. Fluorescein-conjugated dextran (10,000 MW) (22.5

μM, final concentration) (Molecular Probes, Invitrogen) or MitoTracker® Green FM (200 nM, final concentration) (Molecular Probes, Invitrogen), were added to *M. avium* 2447 SmT-infected macrophages for endosomal or mitochondrial labelling, respectively. Fluorescein-conjugated dextran was added along with the peptides, immediately after infection and incubated for 2 h, whereas MitoTracker® Green FM was incubated for 30 min prior visualization.

Macrophages were observed and photographed live, using a Laser Scanning Confocal Microscope Leica TCS SP5II (Laser Microsystems, Germany) with the 63x oil objective. Immediately before visualization, cells were washed with cold PBS and kept in RPMI medium without phenol red (Life Technologies, Paisley, U.K.).

Cytokine production

Cytokine production was evaluated in the supernatant of macrophage cultures, 24 h after infection and peptide treatment. The levels of six different cytokines (IL-12p70, TNF-alpha, INF-γ, CCL2, IL-10 and IL-6) were determined using the BD™ Cytometric Bead Array (CBA) Mouse Inflammation Kit (BD Biosciences, San Jose, CA, USA) following the manufacturer's instructions. Briefly, standards and samples were incubated for 2 h, with a mixture of capture beads for each cytokine, and with a mixture of phycoerythrin (PE)-conjugated antibodies as detection reagent. Afterwards, the wells were washed, the supernatant discarded, and the beads were re-suspended with Wash buffer. The standards and samples were then acquired in a BD FACSCanto™ II cytometer (BD, Biosciences, San Jose, CA, USA), and the results analysed using the FCAP Array™ software (BD, Biosciences, San Jose, CA, USA). The results represent the average of three independent experiments, and are presented as the fold increase relative to the uninfected control in each experiment. Statistical analysis was performed with GraphPad Prism 6 (GraphPad Software, Inc., La Jolla, CA, USA) using one-way ANOVA with Tukey's multiple comparisons test.

HPLC

Peptides (LFcin17-30 and D-LFcin17-30) were incubated with DMEM, supplemented as stated above, at 37 °C for 4 days. At the end of 0, 0.5, 2, 4, 8, 24, 48, 72 and 96 h an aliquot was taken from each mixture and analysed through high performance liquid chromatography (HPLC). The HPLC (Hitachi Elite Autosampler L-2200, Pump L-2130, Diode Array Detector L-2455 and Column OvenL-2300) was performed with a C18

reverse phase column with 150 mm (Merck). Each analysis, with an injection volume of 40 µL, was done in 30 min with 0-100% of acetonitrile (with H_2O+0.05% TFA as solvent A) at a flow rate of 1 mL/min and the detection was at 220 nm.

The chromatograms were analysed with EZChrom Elite™ software and the peaks integrated in order to extract the area. The results were then presented as the percentage of the remaining peptide in relation to the amount of peptide present in time zero.

Results

1- Lactoferricin peptides are not toxic to primary mouse macrophages up to 40 µM.

In the previous chapter (chapter 7) we showed that bovine lactoferricin, LFcin17-30, its variants with all arginines substituted by lysines and *vice-versa* (LFcin17-30 all K and LFcin17-30 all R, respectively), and the variant with all amino acids in the D-form (D-LFcin17-30), killed *M. avium* in axenic cultures. In this chapter, we decided to investigate whether those peptides were able to kill mycobacteria when they are growing inside macrophages, their natural host cell. Before testing the peptides for their antimicrobial activity, we evaluated their potential toxicity towards bone marrow derived macrophages (BMM). In figure 1, we show that the peptides did not exert a significant toxic effect on macrophages up to 80 µM with the exceptions of the D-form (D-LFcin17-30) and the variant with all arginines (LFcin17-30 all R), which had a significant toxic effect at 80 but not at 40 µM.

2- Lactoferricin peptides inhibit *M. avium* growth inside macrophages and synergize with ethambutol

Given that the peptides were not toxic to macrophages up to 40 µM, we next evaluated their effect on *M. avium* growing inside these cells. Since one of the possible applications of AMP is the co-administration with conventional antibiotics, we included ethambutol in this assay. Ethambutol is known to have a low effect on mycobacteria growing inside macrophages (Deshpande *et al.* 2010), making it a good model to assess the possible synergistic effect of AMP.

Bone marrow derived macrophages were obtained from BALB/c mice and infected with *M. avium* 2447 SmT and the non-internalized bacteria were washed-out. The different peptides were added at 40 µM, and ethambutol was added at 7.2 µM. After 5 days in culture, the number of intracellular bacteria per culture well was quantified in a CFU assay. The results obtained are shown in figure 2.

Among the peptides tested, only D-LFcin17-30 significantly inhibited the intramacrophagic growth of *M. avium* (52% reduction, $P<0.0001$). The other peptides and ethambutol alone did not caused inhibition of *M. avium* growth. Interestingly, when given to the macrophages in combination with ethambutol, all peptides had a significant inhibitory effect. Even in combination with ethambutol, D-LFcin17-30 was still the most active peptide (73% reduction in *M. avium* growth relative to the control; $P<0.0001$).

Since D-LFcin17-30 was the only peptide with significant antimycobacterial activity inside macrophages, we decided to proceed with this peptide together with its L-form, LFcin17-30, to investigate their mechanisms of antibacterial activity inside macrophages.

3- D-LFcin17-30 is more resistant to degradation by medium components than LFcin17-30.

In order to understand the reason why D-LFcin17-30 had a stronger effect on the intramacrophagic growth of *M. avium* than LFcin17-30, and considering that peptide degradation is one of the factors that can impact on efficacy, we evaluated the kinetics of degradation of both peptides in the presence of the cell culture medium used in the infection assays. As expected, the peptide composed of amino acids in the D-form was significantly more resistant to degradation, persisting in the medium at a higher concentration up to 96 h of incubation, with no more than 30% of degradation, whereas 50% of degradation happens for the L-form of the peptide, before 24 h of incubation, being completely degraded after 96 h (figure 3).

4- Lactoferricins do not co-localize with *M. avium* inside macrophages.

In order to understand possible mechanisms by which lactoferricins inhibited the intramacrophagic growth of *M. avium,* we started by characterizing the intracellular distribution of the peptides inside *M. avium*-infected macrophages. For that, we used peptides labelled with TAMRA (a rhodamine derivative) on the C-terminal together with a strain of *M. avium* expressing GFP; and fluorescein-labelled markers of endosomes and of mitochondria. Representative images of the assays with LFcin17-30 are shown in figure 4 and those with D-LFcin17-30 are shown in figure 5.

The two peptides exhibited a similar distribution inside macrophages and neither LFcin17-30 nor D-LFcin17-30 co-localized with *M. avium*. Figures 4A and 5A depict representative pictures of BALB/c BMM 2 hours after infection with *M. avium*-GFP and lactoferricin treatment. The exclusion of the peptides from mycobacteria-containing vesicles was not altered by the treatment with ethambutol (figures 4B and 5B), by the incubation time (20 min up to 24 h) (data not shown), or the time of peptide addition, either immediately after infection (figures 4 and 5) or 4 to 5 days after infection (data not shown).

Since the intracellular distribution of both peptides had a vesicular appearance, we studied their co-localization with the endocytic pathway. For that, *M. avium*-infected macrophages were co-incubated with peptides and dextran for 2 h, and we found that

both peptides extensively co-localized with endosomes and lysosomes (figures 4C and 5C), suggesting they are internalized by this pathway. Importantly, neither LFcin17-30 nor D-LFcin17-30 significantly localized with mitochondria, which indicates that they do not exert a toxic effect in this organelle (figures 4D and 5D).

5- Lactoferricins increase macrophage production of pro-inflammatory cytokines

Since lactoferricins decreased *M. avium* viability inside macrophages without a direct interaction with the bacteria (figures 4 and 5), we asked whether they had a modulatory effect on macrophage function.

For that, we used macrophage supernatants to measure the levels of several cytokines 24 hours after infection with *M. avium* and treatment with the peptides. In figure 6, we can see that the treatment with lactoferricins significantly increased the production of TNF-alpha and IL-6 by BMM infected with *M. avium*, with no significant differences between the two peptides. IL-10, CCL2, IL-12p40 and IFN-gamma were not significantly induced either by *M. avium* infection or by peptide treatments (data not shown).

6- The antimicrobial effects of lactoferricins inside macrophages are NOT dependent on the production of TNF-alpha and/or IL-6 by macrophages.

Since both peptides increased the production of TNF-alpha by *M. avium* infected macrophages and macrophage activation by TNF-alpha can lead to intracellular killing of mycobacteria (Appelberg and Orme 1993, Appelberg *et al.* 1994), we asked whether this cytokine was necessary for the antibacterial effect of the peptides. We took BMM from *Tnf*$^{-/-}$ mice and from congenic C57BL/6 wild-type mice, infected them with *M. avium* 2447 SmT, treated with LFcin17-30 or D-LFcin17-30 and measured *M. avium* growth after 5 days. Our results, presented in figure 7, showed that, similarly to what was observed before in BALB/c macrophages (figure 2), only D-LFcin17-30 significantly inhibited the growth of *M. avium* inside its host cell (figure 7). More interestingly, the effect of D-LFcin17-30 on *M. avium* intracellular growth was similar on C57BL/6 or *Tnf*$^{-/-}$ BMM, leading us to conclude that TNF-alpha is not necessary for the antibacterial effect of this peptide. By measuring cytokine levels in macrophage supernatants, as described above, we confirmed that *Tnf*$^{-/-}$ BMM were not producing TNF-alpha and also found that these macrophages did not have a significant production of IL-6, showing that the effect of the peptide is also IL-6-independent (data not shown).

Discussion

In this chapter we show that the D enantiomer of lactoferricin strongly inhibits *M. avium* growth inside infected-macrophages, and lactoferricin variants cooperate with the antibiotic ethambutol to inhibit intracellular *M. avium* growth. Although the exact mechanism of action was not elucidated, we gathered evidences indicating that the peptides act by increasing antimicrobial effects of the macrophage.

Following the work on the direct antimicrobial activity of a set of lactoferricin peptides against *Mycobacterium avium* (chapter 7), we proceed to test those peptides on *M. avium*-infected macrophages. Although LFcin17-30, its variants with arginines substituted by lysines and *vice-versa* (LFcin17-30 all K and LFcin17-30 all R), and the D enantiomer (D-LFcin17-30) were all active against *M. avium* in axenic cultures, only D-LFcin17-30 induced a significant decrease in the mycobacterial growth inside macrophages.

The combination of antimicrobial peptides with conventional antibiotics is of great potential interest as it could reduce the dosages of each compound, diminish the probability of resistance, and also reduce the treatment time. The advantageous combination of ethambutol and iron chelators in the control of *M. avium* growth inside macrophages has recently been reported (Moniz *et al.* 2015). Ethambutol acts by impairing the biosynthesis of the cell wall, increasing cell permeability and potentiating the action of other drugs (Hoffner *et al.* 1990, Rastogi *et al.* 1990, Brown-Elliott *et al.* 2012). In the clinic, ethambutol is used in combination with other antimycobacterial drugs not only as a strategy to prevent the appearance of resistant strains, but also due to its high toxicity when given alone in high doses (Brown-Elliott *et al.* 2012, Egelund *et al.* 2015). In the present work, the administration of ethambutol with lactoferricins resulted in a significant inhibition of *M. avium* growth. This improvement in the antimycobacterial activity of both compounds is probably related with increased cell permeability induced by either ethambutol or by the peptides, allowing for the compounds to enter the cell more easily, potentiating their activity. However, D-LFcin17-30 was still the most active peptide even when combined with ethambutol, which in this case did not bring a significant improvement to the peptide's effect. For this reason, we proceed to investigate the mechanism by which the D enantiomer of LFcin17-30 exerts its antimycobacterial activity.

Due to their peptidic nature, AMP are highly susceptible to proteases and other plasma components. This feature is one of the obstacles to AMP application in the clinic, as it results in low stability and bioavailability, limiting AMP application to topical agents (Seo *et al.* 2012). One strategy employed to overcome this problem is the use of non-natural D enantiomers of amino acids, since in principle, they are more resistant to proteolytic

activity (Deslouches *et al.* 2013). In the case of the peptides studied in this work, D-LFcin17-30 was capable of resisting degradation, persisting in cell culture medium at a higher concentration over time than LFcin17-30, a probably crucial factor for the higher antimycobacterial activity. Wakabayashi *et al.* in 1999 reported a similar effect for a D enantiomer of a lactoferricin derivative (LFcin20-29) (Wakabayashi *et al.* 1999). The fact that the D enantiomer is more active than the L one, also reveals that the observed antimicrobial effect is probably not related to chiral receptors, since they would not recognized D-amino acids. As reported in the previous chapter, these peptides exhibit a direct inhibitory effect against *M. avium* in broth culture (chapter 7), being able to interact directly with the mycobacteria. Thus, we hypothesized that the inhibition of the mycobacterial growth could be the result of a direct effect on the mycobacteria, such as a disruption of the cell membrane, or the activity on an intracellular target in *M. avium*. In order to clarify this aspect, the distribution and sub-cellular localization inside *M. avium* infected macrophages of LFcin17-30 and D-LFcin17-30 was assessed. Contrarily to what was expected, our localization studies showed that none of the peptides co-localized with *M. avium* when growing inside macrophages. This result was not altered by the presence of ethambutol, the incubation time or the time-point of peptide addition after infection. These peptides seem to follow an endocytic pathway, co-localizing with fluorescein-conjugated dextran, never reaching the mycobacteria-harbouring phagosomes. Thus, we sought other possible effects of D-LFcin17-30 on the *M. avium*-infected macrophages that could be leading to a better clearance of the mycobacteria.

The administration of LFcin17-30 and D-LFcin17-30 was accompanied by an increase in the levels of TNF-alpha and IL-6 produced by *M. avium*-infected macrophages. TNF-alpha is involved in macrophage activation, being able to induce intracellular killing of mycobacteria (Bermudez and Young 1988, Appelberg and Orme 1993, Appelberg *et al.* 1994). Also, TNF-deficient mice infected with *M. avium* do not resist the infection (Florido and Appelberg 2007). IL-6 is a cytokine involved in the modulation of inflammation and the acute phase response. It is also able to induce the development of IL-17-producing T cells that are involved in the host response to mycobacterial infections (Torrado and Cooper 2010). Although both peptides increased the levels of TNF-alpha and IL-6, these are not essential for the antimicrobial effect of D-LFcin17-30, since their absence did not interfere with the peptide's effect. We did not find evidences supporting a role of nitrites in the antimicrobial effect of D-LFcin17-30 (data not shown). Furthermore, several works reported that oxygen and nitrogen reactive species are not required for the antimycobacterial mechanisms of *M. avium*-infected macrophages (Gomes *et al.* 1999, Gomes and Appelberg 2002).

Lactoferricin has been reported to have multiple roles on the host immune response. Besides its direct antimicrobial activity towards several pathogens, lactoferricin can selectively kill cancer cells (Yoo *et al.* 1997, Mader *et al.* 2005, Furlong *et al.* 2006, Mader *et al.* 2007, Furlong *et al.* 2010, Pan *et al.* 2013) and can inhibit septic shock by binding to endotoxins (Yamauchi *et al.* 1993). Recently, it was described that apoptosis and autophagy are involved in lactoferricin-induced death of cancer cells (Pan *et al.* 2013).

Autophagy is a host cell effector mechanism used as a quality control for the removal of protein aggregates and damaged organelles. Under stress conditions (*e.g.* infection), the cell can activate autophagy for survival (Deretic and Levine 2009, Mansilla Pareja and Colombo 2013). In the case of mycobacterial infections, vitamin D3 induces not only the production of antimicrobial peptides such as cathelicidin, but also induces autophagy, both playing a role in the control of the pathogen growth within the macrophage (Gutierrez *et al.* 2004, Yuk *et al.* 2009, Selvaraj *et al.* 2015). Therefore one of the mechanism by which D-LFcin17-30 inhibits the growth of *M. avium* inside macrophages could be the induction of autophagy, which will be investigated in future studies.

M. avium, similarly to other pathogenic mycobacteria, is capable of living and proliferating inside macrophages by inhibiting the formation of a phagolysosome, which would constitute a harsh environment for the bacteria growth (Appelberg 2006b). One possible way to interfere with the pathogen growth would be to interfere with this process, favouring the maturation of the compartment where the mycobacteria are living and thus restricting the access to nutrients or exposing the mycobacteria to toxic compounds (Appelberg 2006a, Appelberg 2006b, Gomes *et al.* 2008). In future experiments, we will investigate whether D-LFcin17-30 acts through this pathway.

In summary, in this work we showed that a D enantiomer of lactoferricin is active against *M. avium* growing inside mouse macrophages, by a mechanism that is independent of direct contact with the bacteria. The exact mechanism behind the peptide's activity is still not clear, but is probably related with modulation of the macrophage's capacity to kill *M. avium*.

Acknowledgments

This research received support from Fundação para a Ciência e Tecnologia (FCT), Lisbon, Portugal, and European Social Fund through project PEst-C/QUI/UI0081/2013 awarded to CIQ-UP; “NORTE-07-0124-FEDER-000002-Host-Pathogen Interactions” of the Programa Operacional Regional do Norte (ON.2 - O Novo Norte), under the Quadro de Referência Estratégico Nacional (QREN) and funded by Fundo Europeu de Desenvolvimento Regional (Feder) was awarded to IBMC. TS receives a PhD grant SFRH/BD/77564/2011 from FCT.

NV and PG thank FCT and FEDER for funding through UID/MULTI/04378/2013 and co-financed by ON.2 in the framework of project NORTE-07-0162-FEDER-000111. NV thanks also FCT for funding project grant IF/00092/2014.

This work also benefited from a grant from the University of Amsterdam for research into the focal point Oral Infections and Inflammation, attributed to JGMB and KN.

The authors would like to thank Paula Sampaio from Advanced Light Microscopy Unit of Instituto de Biologia Molecular e Celular (IBMC) da Universidade do Porto, Porto, Portugal, for technical assistance on fluorescence confocal microscopy; João Relvas and Renato Socodato from the Glial Cell Biology group of Instituto de Biologia Molecular e Celular (IBMC) da Universidade do Porto, Porto, Portugal, for kindly providing the C57BL/6 TNF-deficient mice.

Tables

Table 1 – Properties of synthetic lactoferrin peptides.

Peptide	**Amino Acid sequence**	**MW**	**Charge** [a]
LFcin17-30	F**K**C**RR**WQW**R**M**KK**LG	1923	+6
D-LFcin17-30	F**K**C**RR**WQW**R**M**KK**LG	1923	+6
LFcin17-30 all K	F**K**C**KK**WQW**K**M**KK**LG	1839	+6
LFcin17-30 all R	F**R**C**RR**WQW**R**M**RR**LG	2007	+6

[a] Calculated overall charge at pH= 7.0

Figures

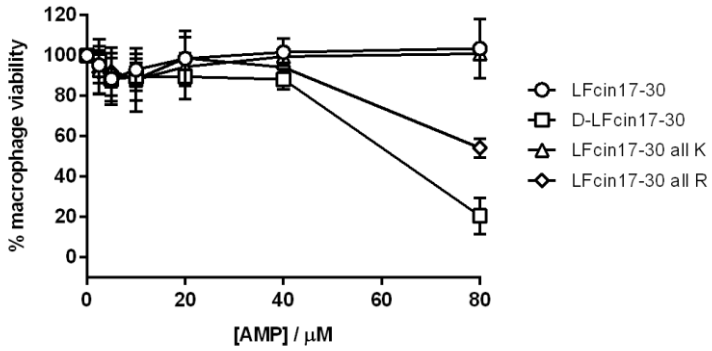

Figure 1 – Effect of lactoferricin peptides on macrophage viability. BALB/c mouse BMM were infected with *M. avium* 2447 SmT and incubated with LFcin17-30 (circles), D-LFcin17-30 (squares), LFcin17-30 all K (triangles) and LFcin17-30 all R (diamonds), for 24 h. At the end of this period, 10% resazurin 125 μM was added and 24 h later fluorescence was measured at 560/590 nm to evaluate cell viability. The graph shows the average ± standard deviation of two independent experiments, presented as the percentage of viable cells relative to the corresponding non-peptide-treated infected cells.

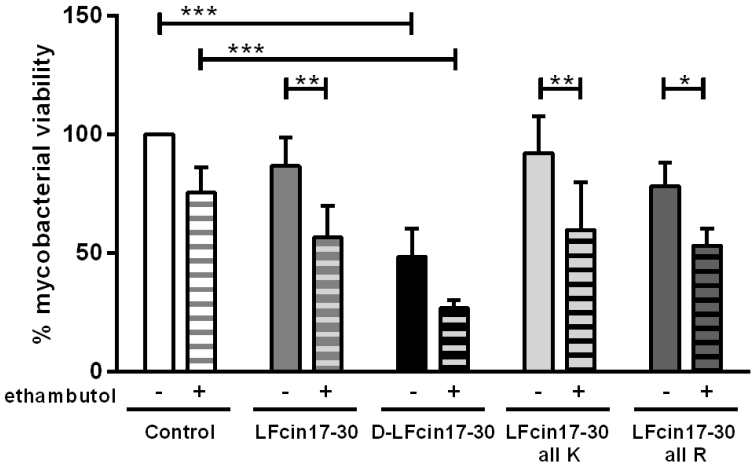

Figure 2 – Inhibition of the growth of *M. avium* inside BALB/c BMM by lactoferricin peptides alone or in combination with ethambutol. *M. avium* 2447 SmT growing inside BALB/c BMM were treated with 40 µM of LFcin17-30, D-LFcin17-30, LFcin17-30 all K or LFcin17-30 all R, alone (non-patterned bar) or in combination with 7.2 µM of ethambutol (patterned bar). After 5 days of incubation, bacteria were quantified by a CFU assay. The results represent the average + standard deviation of at least four independent experiments, and are expressed as the percentage of growth of mycobacteria in each well relative to the growth of mycobacteria in the non-treated infected wells (control), in each experiment. Statistics were performed using two-way ANOVA with Sidak's multiple comparisons test. * $P < 0.05$; ** $P < 0.01$; *** $P < 0.001$.

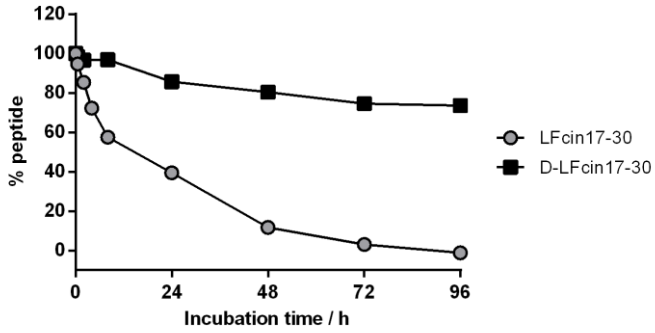

Figure 3 – Stability of lactoferricin peptides in culture medium. LFcin17-30 (grey circles) and D-LFcin17-30 (black squares), at 40 µM of final concentration, were incubated with DMEM/10%FBS/10% LCCM at 37 °C. After 0, 0.5, 2, 4, 8, 24, 48, 72 and 96 h of incubation an aliquot was taken and immediately analysed by RP-HPLC with a gradient from 100% solution A (0.05% TFA in water) to 100% solution B (acetonitrile). The results are presented as the percentage of the remaining peptide in relation to the amount of peptide present in time zero.

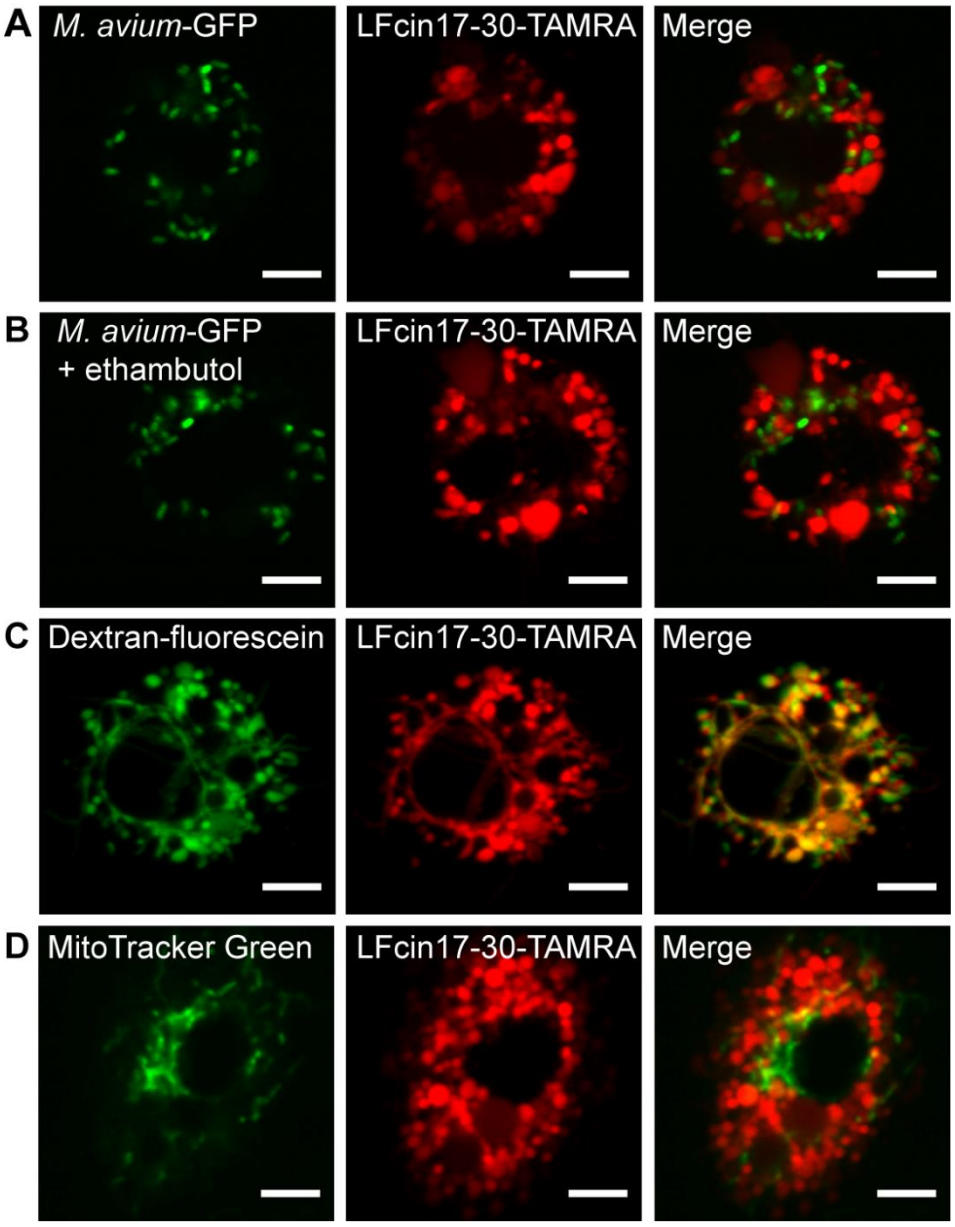

Figure 4 – Intracellular distribution and localization of LFcin17-30 in *M. avium* infected macrophages. Live cell imaging of BALB/c BMM infected with *M. avium*-GFP (A, B) or *M. avium* 2447 SmT (no fluorescent label, C, D) for 2 h, and treated with 10 µM LFcin17-30-TAMRA for 2 h. **A)** BMM infected with *M. avium* expressing GFP; **B)** BMM infected with *M. avium* expressing GFP and treated with 7.2 µM ethambutol for 2 h; **C)** BMM infected with *M. avium* 2447 SmT and incubated with 22.5 µM fluorescein-conjugated dextran for 2 h; **D)** BMM infected with *M. avium* 2447 SmT and incubated with 200 nM MitoTracker Green for 30 minutes. Macrophages were visualized and photographed in a Laser Scanning Confocal Microscope Leica TCS SP5II with 63x oil objective. One representative cell, of one representative experiment out of three, is shown for each condition. Bar scale: 5 µm.

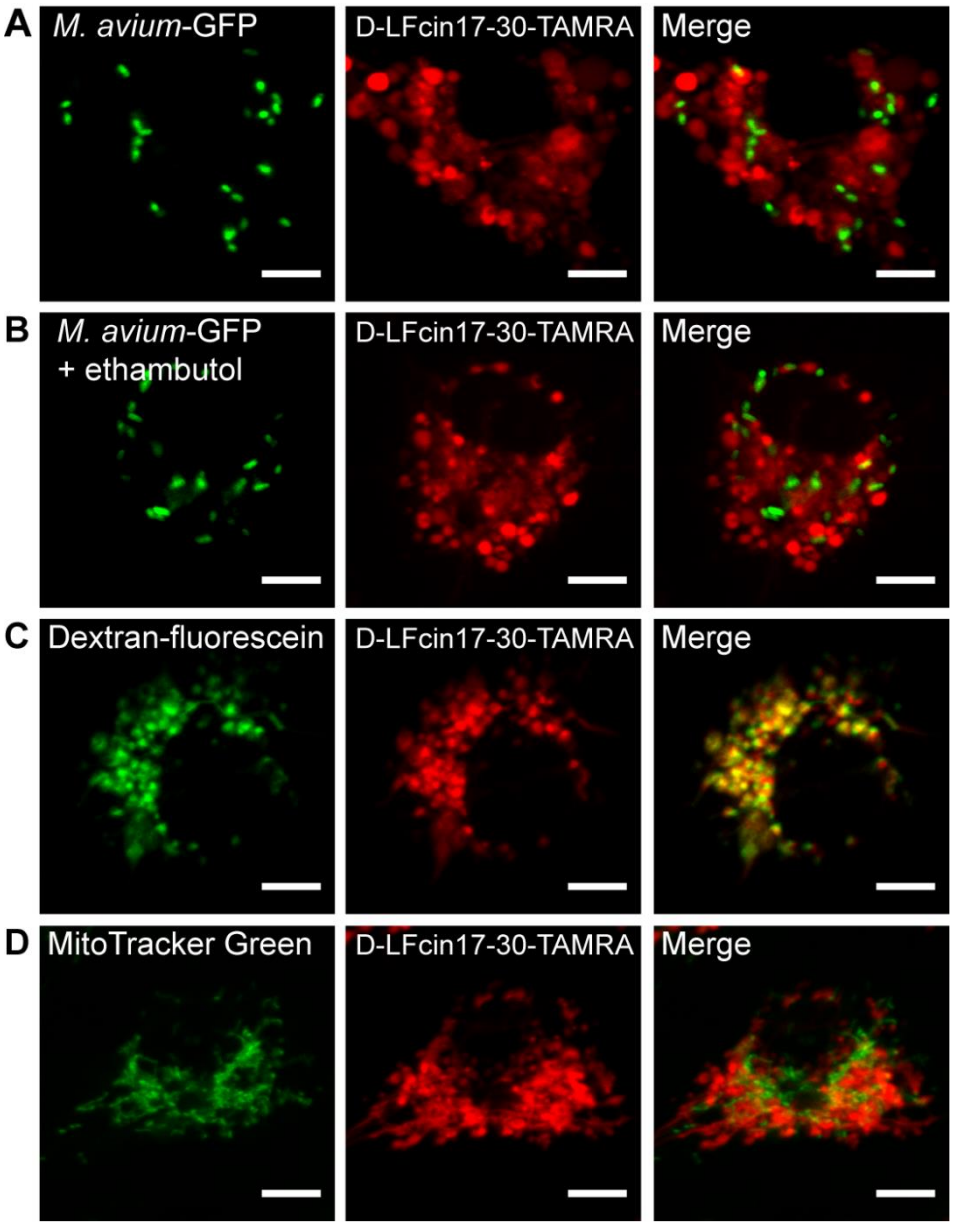

Figure 5 – Intracellular distribution and localization of D-LFcin17-30 in *M. avium* infected macrophages. Live cell imaging of BALB/c BMM infected with *M. avium*-GFP (A, B) or *M. avium* 2447 SmT (no fluorescent label, C, D) for 2 h, and treated with 10 µM D-LFcin17-30-TAMRA for 2 h. **A)** BMM infected with *M. avium* expressing GFP; **B)** BMM infected with *M. avium* expressing GFP and treated with 7.2 µM ethambutol for 2 h; **C)** BMM infected with *M. avium* 2447 SmT and incubated with 22.5 µM fluorescein-conjugated dextran for 2 h; **D)** BMM infected with *M. avium* 2447 SmT and incubated with 200 nM MitoTracker Green for 30 minutes. Macrophages were visualized and photographed in a Laser Scanning Confocal Microscope Leica TCS SP5II with 63x oil objective. One representative cell, of one representative experiment out of three, is shown for each condition. Bar scale: 5 µm.

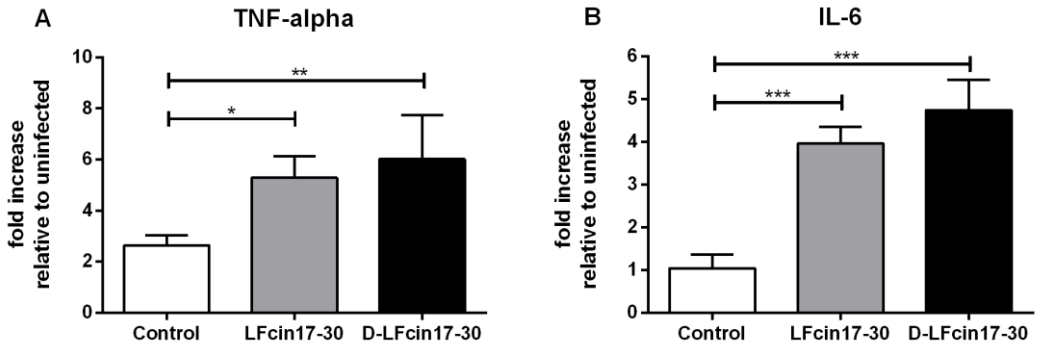

Figure 6 – Cytokine production by *M. avium* infected macrophages treated with lactoferricin peptides. 24 h after infection and treatment with LFcin17-30 (grey) or D-LFcin17-30 (black), the levels of TNF-alpha (A) and IL-6 (B) were determined in the supernatant of BALB/c BMM, using the BD™ Cytometric Bead Array (CBA) Mouse Inflammation Kit. The samples were acquired in a BD FACSCanto™ II cytometer, and analysed using the FCAP Array™ software. The graphs represent the average + standard deviation of three independent experiments, presented as the fold increase relative to uninfected control macrophages. Statistical analysis was performed using one-way ANOVA with Tukey's multiple comparisons test. * $P < 0.05$; ** $P < 0.01$; *** $P < 0.001$.

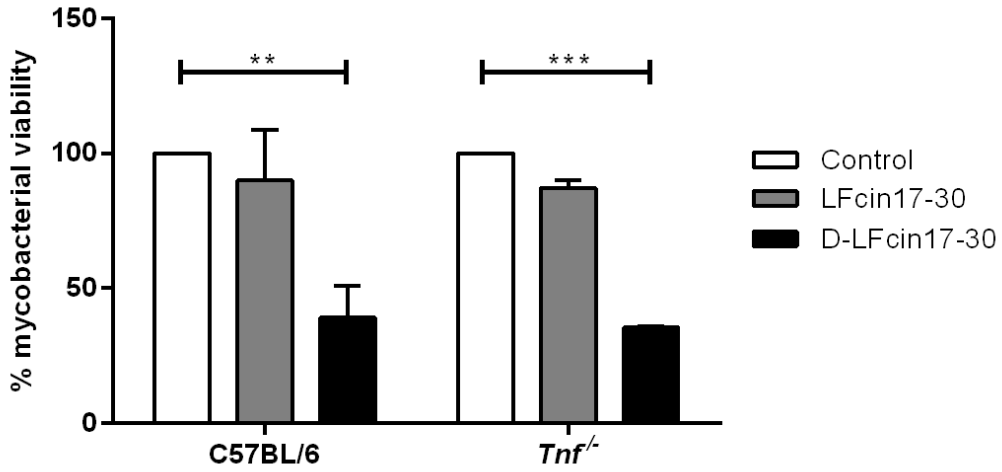

Figure 7 – Effect of lactoferricin peptides on C57BL/6 and *Tnf*$^{-/-}$ BMM infected with *M. avium*. *M. avium* 2447 SmT growing inside C57BL/6 and *Tnf*$^{-/-}$ BMM were treated with 40 µM of LFcin17-30 (grey) or D-LFcin17-30 (black). After 5 days of incubation, bacteria were quantified by a CFU assay. The graph represents the average of two independent experiments, expressed as the percentage of growth of mycobacteria in each well relative to the growth of mycobacteria in the non-treated infected wells (control), in each experiment. Statistics were performed using two-way ANOVA with Tukey's multiple comparisons test. ** $P < 0.01$; *** $P < 0.001$.

References

Appelberg R. (2006a). Macrophage nutriprive antimicrobial mechanisms. *J Leukoc Biol*. 79(6):1117-1128.

Appelberg R. (2006b). Pathogenesis of Mycobacterium avium infection: typical responses to an atypical mycobacterium? *Immunol Res*. 35(3):179-190.

Appelberg R., Castro A. G., Pedrosa J., Silva R. A., Orme I. M. and Minoprio P. (1994). Role of gamma interferon and tumor necrosis factor alpha during T-cell-independent and -dependent phases of Mycobacterium avium infection. *Infect Immun*. 62(9):3962-3971.

Appelberg R. and Orme I. M. (1993). Effector mechanisms involved in cytokine-mediated bacteriostasis of Mycobacterium avium infections in murine macrophages. *Immunology*. 80(3):352-359.

Bellamy W., Takase M., Wakabayashi H., Kawase K. and Tomita M. (1992a). Antibacterial spectrum of lactoferricin B, a potent bactericidal peptide derived from the N-terminal region of bovine lactoferrin. *J Appl Bacteriol*. 73(6):472-479.

Bellamy W., Takase M., Yamauchi K., Wakabayashi H., Kawase K. and Tomita M. (1992b). Identification of the bactericidal domain of lactoferrin. *Biochim Biophys Acta*. 1121(1-2):130-136.

Bermudez L. E. and Young L. S. (1988). Tumor necrosis factor, alone or in combination with IL-2, but not IFN-gamma, is associated with macrophage killing of Mycobacterium avium complex. *J Immunol*. 140(9):3006-3013.

Bolscher J. G., Oudhoff M. J., Nazmi K., Antos J. M., Guimaraes C. P., Spooner E., Haney E. F., Vallejo J. J., Vogel H. J., van't Hof W., Ploegh H. L. and Veerman E. C. (2011). Sortase A as a tool for high-yield histatin cyclization. *FASEB J*. 25(8):2650-2658.

Brode S. K., Daley C. L. and Marras T. K. (2014). The epidemiologic relationship between tuberculosis and non-tuberculous mycobacterial disease: a systematic review. *Int J Tuberc Lung Dis*. 18(11):1370-1377.

Brown-Elliott B. A., Nash K. A. and Wallace R. J., Jr. (2012). Antimicrobial susceptibility testing, drug resistance mechanisms, and therapy of infections with nontuberculous mycobacteria. *Clin Microbiol Rev*. 25(3):545-582.

Cassidy P. M., Hedberg K., Saulson A., McNelly E. and Winthrop K. L. (2009). Nontuberculous mycobacterial disease prevalence and risk factors: a changing epidemiology. *Clin Infect Dis*. 49(12):e124-129.

Deretic V. and Levine B. (2009). Autophagy, immunity, and microbial adaptations. *Cell Host Microbe*. 5(6):527-549.

Deshpande D., Srivastava S., Meek C., Leff R. and Gumbo T. (2010). Ethambutol optimal clinical dose and susceptibility breakpoint identification by use of a novel pharmacokinetic-pharmacodynamic model of disseminated intracellular Mycobacterium avium. *Antimicrob Agents Chemother*. 54(5):1728-1733.

Deslouches B., Steckbeck J. D., Craigo J. K., Doi Y., Mietzner T. A. and Montelaro R. C. (2013). Rational design of engineered cationic antimicrobial peptides consisting exclusively of arginine and tryptophan, and their activity against multidrug-resistant pathogens. *Antimicrob Agents Chemother*. 57(6):2511-2521.

Egelund E. F., Fennelly K. P. and Peloquin C. A. (2015). Medications and monitoring in nontuberculous mycobacteria infections. *Clin Chest Med*. 36(1):55-66.

Falzon D., Mirzayev F., Wares F., Baena I. G., Zignol M., Linh N., Weyer K., Jaramillo E., Floyd K. and Raviglione M. (2015). Multidrug-resistant tuberculosis around the world: what progress has been made? *Eur Respir J*. 45(1):150-160.

Flannagan R. S., Cosio G. and Grinstein S. (2009). Antimicrobial mechanisms of phagocytes and bacterial evasion strategies. *Nat Rev Microbiol*. 7(5):355-366.

Florido M. and Appelberg R. (2007). Characterization of the deregulated immune activation occurring at late stages of mycobacterial infection in TNF-deficient mice. *J Immunol*. 179(11):7702-7708.

Furlong S. J., Mader J. S. and Hoskin D. W. (2006). Lactoferricin-induced apoptosis in estrogen-nonresponsive MDA-MB-435 breast cancer cells is enhanced by C6 ceramide or tamoxifen. *Oncol Rep*. 15(5):1385-1390.

Furlong S. J., Mader J. S. and Hoskin D. W. (2010). Bovine lactoferricin induces caspase-independent apoptosis in human B-lymphoma cells and extends the survival of immune-deficient mice bearing B-lymphoma xenografts. *Exp Mol Pathol*. 88(3):371-375.

Gifford J. L., Hunter H. N. and Vogel H. J. (2005). Lactoferricin: a lactoferrin-derived peptide with antimicrobial, antiviral, antitumor and immunological properties. *Cell Mol Life Sci*. 62(22):2588-2598.

Gomes M. S. and Appelberg R. (2002). NRAMP1- or cytokine-induced bacteriostasis of Mycobacterium avium by mouse macrophages is independent of the respiratory burst. *Microbiology*. 148(10):3155-3160.

Gomes M. S., Flórido M., Pais T. F. and Appelberg R. (1999). Improved Clearance of Mycobacterium avium Upon Disruption of the Inducible Nitric Oxide Synthase Gene. *J Immunol*. 162(11):6734-6739.

Gomes M. S., Sousa Fernandes S., Cordeiro J. V., Silva Gomes S., Vieira A. and Appelberg R. (2008). Engagement of Toll-like receptor 2 in mouse macrophages infected with Mycobacterium avium induces non-oxidative and TNF-independent anti-mycobacterial activity. *Eur J Immunol*. 38(8):2180-2189.

Groenink J., Walgreen-Weterings E., van 't Hof W., Veerman E. C. I. and Nieuw Amerongen A. V. (1999). Cationic amphipathic peptides, derived from bovine and human lactoferrins, with antimicrobial activity against oral pathogens. *FEMS Microbiol Lett*. 179(2):217-222.

Guenin-Mace L., Simeone R. and Demangel C. (2009). Lipids of pathogenic Mycobacteria: contributions to virulence and host immune suppression. *Transbound Emerg Dis*. 56(6-7):255-268.

Gutierrez M. G., Master S. S., Singh S. B., Taylor G. A., Colombo M. I. and Deretic V. (2004). Autophagy is a defense mechanism inhibiting BCG and Mycobacterium tuberculosis survival in infected macrophages. *Cell*. 119(6):753-766.

Haug B. E., Strom M. B. and M. Svendsen J. S. M. (2007). The Medicinal Chemistry of Short Lactoferricin-Based Antibacterial Peptides. *Current Medicinal Chemistry*. 14(1):1-18.

Henkle E. and Winthrop K. L. (2015). Nontuberculous mycobacteria infections in immunosuppressed hosts. *Clin Chest Med*. 36(1):91-99.

Hoffner S. E., Svenson S. B. and Beezer A. E. (1990). Microcalorimetric studies of the initial interaction between antimycobacterial drugs and Mycobacterium avium. *J Antimicrob Chemother*. 25(3):353-359.

Kuwata H., Yip T. T., Tomita M. and Hutchens T. W. (1998). Direct evidence of the generation in human stomach of an antimicrobial peptide domain (lactoferricin) from ingested lactoferrin. *Biochim Biophys Acta*. 1429(1):129-141.

Mader J. S., Richardson A., Salsman J., Top D., de Antueno R., Duncan R. and Hoskin D. W. (2007). Bovine lactoferricin causes apoptosis in Jurkat T-leukemia cells by sequential permeabilization of the cell membrane and targeting of mitochondria. *Exp Cell Res*. 313(12):2634-2650.

Mader J. S., Salsman J., Conrad D. M. and Hoskin D. W. (2005). Bovine lactoferricin selectively induces apoptosis in human leukemia and carcinoma cell lines. *Mol Cancer Ther*. 4(4):612-624.

Mansilla Pareja M. E. and Colombo M. I. (2013). Autophagic clearance of bacterial pathogens: molecular recognition of intracellular microorganisms. *Frontiers in Cellular and Infection Microbiology*. 3:54.

Mansour S. C., Pena O. M. and Hancock R. E. (2014). Host defense peptides: front-line immunomodulators. *Trends Immunol*. 35(9):443-450.

Moniz T., Silva D., Silva T., Gomes M. S. and Rangel M. (2015). Antimycobacterial activity of rhodamine 3,4-HPO iron chelators against Mycobacterium avium: analysis of the contribution of functional groups and of chelator's combination with ethambutol. *Med Chem Commun*. 6(12):2194-2203.

Nguyen L. T., Haney E. F. and Vogel H. J. (2011). The expanding scope of antimicrobial peptide structures and their modes of action. *Trends Biotechnol*. 29(9):464-472.

Orme I. M. and Ordway D. J. (2014). Host response to nontuberculous mycobacterial infections of current clinical importance. *Infect Immun*. 82(9):3516-3522.

Pan W. R., Chen P. W., Chen Y. L., Hsu H. C., Lin C. C. and Chen W. J. (2013). Bovine lactoferricin B induces apoptosis of human gastric cancer cell line AGS by inhibition of autophagy at a late stage. *J Dairy Sci*. 96(12):7511-7520.

Parker A. E. and Bermudez L. E. (1997). Expression of the green fluorescent protein (GFP) in mycobacterium avium as a tool to study the interaction between Mycobacteria and host cells. *Microb Pathog*. 22(4):193-198.

Philley J. V. and Griffith D. E. (2015). Treatment of slowly growing mycobacteria. *Clin Chest Med*. 36(1):79-90.

Rastogi N., Goh K. S. and David H. L. (1990). Enhancement of drug susceptibility of Mycobacterium avium by inhibitors of cell envelope synthesis. *Antimicrob Agents Chemother*. 34(5):759-764.

Selvaraj P., Harishankar M. and Afsal K. (2015). Vitamin D: Immuno-modulation and tuberculosis treatment. *Can J Physiol Pharmacol*. 93(5):377-384.

Seo M. D., Won H. S., Kim J. H., Mishig-Ochir T. and Lee B. J. (2012). Antimicrobial peptides for therapeutic applications: a review. *Molecules*. 17(10):12276-12286.

Torrado E. and Cooper A. M. (2010). IL-17 and Th17 cells in tuberculosis. *Cytokine Growth Factor Rev*. 21(6):455-462.

Wakabayashi H., Matsumoto H., Hashimoto K., Teraguchi S., Takase M. and Hayasawa H. (1999). N-Acylated and D enantiomer derivatives of a nonamer core peptide of lactoferricin B showing improved antimicrobial activity. *Antimicrob Agents Chemother*. 43(5):1267-1269.

Weiss C. H. and Glassroth J. (2012). Pulmonary disease caused by nontuberculous mycobacteria. *Expert Rev Respir Med*. 6(6):597-612; quiz 613.

Yamauchi K., Tomita M., Giehl T. J. and Ellison Iii R. T. (1993). Antibacterial activity of lactoferrin and a pepsin-derived lactoferrin peptide fragment. *Infect Immun*. 61(2):719-728.

Yeung A. T., Gellatly S. L. and Hancock R. E. (2011). Multifunctional cationic host defence peptides and their clinical applications. *Cell Mol Life Sci*. 68(13):2161-2176.

Yoo Y. C., Watanabe R., Koike Y., Mitobe M., Shimazaki K., Watanabe S. and Azuma I. (1997). Apoptosis in human leukemic cells induced by lactoferricin, a bovine milk protein-derived peptide: involvement of reactive oxygen species. *Biochem Biophys Res Commun*. 237(3):624-628.

Yuk J. M., Shin D. M., Lee H. M., Yang C. S., Jin H. S., Kim K. K., Lee Z. W., Lee S. H., Kim J. M. and Jo E. K. (2009). Vitamin D3 induces autophagy in human monocytes/macrophages via cathelicidin. *Cell Host Microbe*. 6(3):231-243.

PART III. FINAL REMARKS AND FUTURE PERSPECTIVES

CHAPTER 9. Final Remarks and Future Perspectives

Taking into account the potential advantageous use of antimicrobial peptides as new therapeutic alternatives, the purpose of this work was to enlighten the mechanisms of action by which two families of AMP exert their activity, as well as to assess their potential as antimycobacterial therapeutics. As discussed throughout this thesis, AMP are characterized by the possibility of acting on multiple fronts by a variety of mechanisms, being sometimes called “dirty-drugs”. The importance of antimicrobial peptides as potential alternatives to conventional antibiotics relies on the fact that these AMP represent a new antimicrobial paradigm. The antibiotics currently used in the clinic have a single defined target, most often a protein, which is common to all compounds within the same family. Thus, it is relatively easy for bacteria to develop resistance to the antibiotics by making a simple change in this target. At odds, the advantage of AMP relies on factors such as:

i) it would require an overall organization of the entire membrane for bacteria to modify the peptide’s target – the cytoplasmic membrane. This would affect all its constituents such as proteins, receptors, transport systems, among others, which is difficult to achieve without a significant loss of fitness;

ii) even if this was possible, as has already been reported for some peptides and pathogens (Maria-Neto *et al.* 2015), AMP have the possibility of acting on other targets such as proteins, nucleic acids and intracellular membranes and processes, not to mention their role in the immune system and in the modulation of host defence mechanisms;

iii) finally, AMP have evolved in almost all living organisms for many thousands of years. The fact that they keep their activity may indicate the low probability of resistance development by pathogens.

Despite these arguments, resistance development still raises many questions and concerns. What will happen if we increase the exposure of bacteria and other pathogens, to AMP; will they develop resistance then? What are the implications for our health, if resistance to our own immune system develops? And even if resistance would not be a problem, what are the risks of increasing the amounts of these immune system compounds in our bodies?

The results presented in this thesis reflect the heterogeneity of AMP pathways, as we report different mechanisms of action not only between peptides of two distinct families, but even for peptides within the same family. This clearly indicates that the way AMP acts

depends significantly on the peptide nature but also on the lipid composition of the target membrane.

Cecropin A-melittin hybrid ((CA(1-7)M(2-9) or CAM) was an extremely interesting peptide, due to its high capacity to interact with lipid membranes, in an interaction that can be observed by the naked eye, as they induce extensive precipitation and condensation of the membranes. Based on the results reported here (chapter 5), we propose that the peptide acts through the carpet model, leading eventually to membrane disruption and consequent cell death.

For most natural peptides, several problems are faced when their application in clinic is attempted. A large number of peptides exhibit cytotoxicity against eukaryotic membranes, and/or are highly degradable within our digestive system. Another very important issue is the high costs associated with peptide synthesis that has precluded extensive use of peptide of proven antimicrobial action. Thus, rational design is a strategy that must be used for peptide's improvement. The cecropin A-melittin hybrids are one of the first examples of rational design in the AMP field resorting to sequence hybridization (Boman *et al.* 1989). With this synthesis approach one can combine and optimize the individual characteristics of different peptides into one molecule, which was the case of cecropin A-melittin hybrid peptides that have higher antimicrobial activity than cecropin A alone, with reduced haemolytic activity as compared to melittin (Boman *et al.* 1989, Andreu *et al.* 1992). These were very promising agents that were extensively studied by us and many others (Andreu *et al.* 1992, Piers and Hancock 1994, Merrifield *et al.* 1995, Mancheño *et al.* 1996, Giacometti *et al.* 2004, Abrunhosa *et al.* 2005, Sato and Feix 2006, Saugar *et al.* 2006, Pistolesi *et al.* 2007, Bastos *et al.* 2008, Ferre *et al.* 2009, Milani *et al.* 2009, Teixeira *et al.* 2010, Salomone *et al.* 2012, Schlamadinger *et al.* 2012). Nevertheless, it has been reported that the peptide can have significant cytotoxicity (Fernandez-Reyes *et al.* 2010). Accordingly, biophysical studies revealed that CAM is capable of strongly interact with zwitterionic PC membranes, used to mimic the eukaryotic membranes (Abrunhosa *et al.* 2005, Bastos *et al.* 2008). Moreover, we have previously tested this peptide against *M. avium*, and although it was effective against the mycobacteria growing in broth culture, it exerted a significant toxic effect against macrophages (unpublished data). Nevertheless, other *in vivo* studies show that CAM is effective against the tested infection without significant toxicity (Alberola *et al.* 2004). Several strategies have been employed to try to overcome this problem, for instance by acylation of the N-terminal with fatty acids (Chicharro *et al.* 2001) or by lysine N-trimethylation (Fernandez-Reyes *et al.* 2010, Teixeira *et al.* 2010, Diaz *et al.* 2011). Overall no high improvement over the parental peptide was obtained. Another strategy could be the targeted delivery of the

peptide to the local of infection by encapsulating it into liposomes or other stable and non-toxic vehicles (Urban *et al.* 2012). It is therefore worthwhile to study this peptide and its variants with model membranes, to contribute to a deeper understanding of its mechanism of action. We would finally stress that as CAM is highly active against several pathogens, it will be of great interest to introduce it into the clinic, probably as a topical agent, or for localized infections. In order to achieve that goal, research must proceed to understand the action of this peptide and therefore, optimize this molecule and its characteristics.

In the case of lactoferrin peptides, we studied the mechanism of action of LFcin17-30 and LFampin265-284 (Groenink *et al.* 1999, van der Kraan *et al.* 2005a, van der Kraan *et al.* 2006), and also a hybrid peptide obtained from their connection through a lysine linker (LFchimera) (Bolscher *et al.* 2009a, Bolscher *et al.* 2012). These three peptides were previously tested against *M. avium*, but only LFcin17-30 showed promising activity (unpublished data). Therefore that was the peptide chosen to proceed the studies of this thesis to further investigate its antimycobacterial potential.

As regarding the interaction of these peptides with model membranes, we found that the three peptides act by three different mechanisms, in remarkable agreement with the results obtained on its action on *C. albicans* (chapter 6).

LFchimera, a hybrid peptide between LFcin17-30 and LFampin265-284, was the most potent peptide both against *C. albicans* and model membranes (chapter 6). Contrarily to CA(1-7)M(2-9), LFchimera is not a linear peptide constructed via a simple peptide bond. LFcin17-30 and LFampin265-284 are spatially close in the native protein lactoferrin, and are located in the N-terminal domain, which is thought to be one of the reasons responsible for many of the beneficial properties of LF. Thus, LFchimera was constructed in order to mimic the spatial topology of its constituent peptides in LF, coupling the C-terminals of LFcin17-30 and LFampin265-284 to an additional lysine, leaving the two N-terminals as free ends (Bolscher *et al.* 2009a, Bolscher *et al.* 2012, Haney *et al.* 2012b). In our studies with LFchimera, this peptide had the most disruptive behaviour destroying *C. albicans* membrane (Bolscher *et al.* 2012) probably through the formation of bicontinuous cubic phases (chapter 6). This strong activity of LFchimera has been reported against several different pathogens, being more active than its counterparts LFcin17-30 and LFampin265-284, even when these two were added simultaneously (Bolscher *et al.* 2009b, Leon-Sicairos *et al.* 2009, Flores-Villasenor *et al.* 2010, Lopez-Soto *et al.* 2010, Bolscher *et al.* 2012, Flores-Villasenor *et al.* 2012a, Silva *et al.* 2012, Kanthawong *et al.* 2014, Leon-Sicairos *et al.* 2014). This peptide is capable of inducing not only membrane permeabilization but also severe damages in the surface of the pathogens, supporting a mechanism of action that involves membrane disruption (Leon-Sicairos *et al.* 2009,

Flores-Villasenor *et al.* 2010, Bolscher *et al.* 2012, Silva *et al.* 2012, Kanthawong *et al.* 2014, Leon-Sicairos *et al.* 2014). Studies based on structural features of LFchimera have shown that although LFcin17-30 and LFampin265-284 are coupled in a special way that could bring the two peptides to closer spatial proximity, they do not interact with each other in LFchimera (Haney *et al.* 2012b). This suggests that the enhanced antimicrobial features of LFchimera are not related to a combined structural component between LFcin17-30 and LFampin265-284. Further, the leishmanicidal activity of this peptide was not hampered when its constituent peptides were joined by a simple peptide bond, or even when formed by dimers of LFcin17-30 or LFampin265-284 (Silva *et al.* 2012). Even so, their coupling is relevant, as the simultaneous addition of LFcin17-30 and LFampin265-284 results in a lower antimicrobial activity than that shown by LFchimera, showing possibly a synergistic effect between the mechanisms of action of the two individual peptides. Finally, another reason behind LFchimera strong activity is most probably its high positive charge as compared to the other two peptides (+12 for LFchimera, +4 for LFampin265-284 and +6 for LFcin17-30), enhancing electrostatic interactions with the negative phospholipids at the membranes' surface. Overall it seems that LFchimera acts primarily by disrupting the pathogen's membrane, probably through the formation of cubic phases. Nevertheless, since an intracellular target has been suggested for LFcin17-30, we cannot discard this possibility also for LFchimera.

LFchimera has a high potential as new therapeutics against several infections. In fact, Flores-Villasenor *et al.* have recently found that LFchimera can protect mice against a lethal infection with enterohemorrhagic *E. coli* (Flores-Villasenor *et al.* 2012a, Flores-Villasenor *et al.* 2012b). Therefore, it is of high interest to continue to investigate the mechanism of action of LFchimera and the structural features that are required for its activity. For that, further studies could be performed with model membranes of different lipid compositions and also with LFchimera variants, in order to understand what are the structural characteristics responsible for the peptide's activity and how it can be improved in terms of activity: Further synthesis costs are also a major concern that could lead tentatively to related AMPs with shorter amino acid sequences. The final goal will always be to assess its antimicrobial properties in *in vivo* models of infection for future clinical development.

LFampin265-284, found in the N-terminal domain of lactoferrin (van der Kraan *et al.* 2004, van der Kraan *et al.* 2005a, van der Kraan *et al.* 2006), interacts with fungal model membranes inducing the formation of a micellar cubic phase (Pm3n) (chapter 6) (Bastos *et al.* 2011). This was not only the first report describing such phase in the context of antimicrobial peptides and membrane interaction, but it is also in agreement with the

results obtained on *C. albicans*, where weakening of the membrane was observed by the appearance of vesicular-like structures (van der Kraan *et al.* 2005b). The formation of a micellar cubic phase clearly indicates that the mechanism of action of LFampin265-284 relies on membrane disruption. This is supported by other reports where membrane permeabilization and significant damage of the cell surface induced by LFampin was observed (van der Kraan *et al.* 2005b, Flores-Villasenor *et al.* 2010, Silva *et al.* 2012, Leon-Sicairos *et al.* 2014). The interaction of this peptide with membranes is tightly connected with its unique structural characteristics (Haney *et al.* 2012a). LFampin265-284 contains a positive and flexible C-terminal region that is separated from the helical structured N-terminal region. When approaching a membrane, the C-terminal will establish electrostatic interactions with the head groups of the negatively charged phospholipids, inducing the folding of the N-terminal domain into a α-helix. The helix will then penetrate into the membrane leading to its disruption, probably as we did propose through the formation of a micellar cubic phase, culminating in cell death (Haney *et al.* 2007, Adao *et al.* 2011, Bastos *et al.* 2011, Haney *et al.* 2012a). We can then hypothesize that within LFchimera this part of the molecule can be the main responsible for the membrane perturbation effects. This peptide has not been extensively explored in terms of antimicrobial activity. However, there are evidence that this peptide does not exert toxicity towards eukaryotic cells (van der Kraan *et al.* 2005a, Haney *et al.* 2009, Adao *et al.* 2011, Haney *et al.* 2012a), and thus, it can possibly be used as antimicrobial if its activity is properly studied and its features improved.

LFcin17-30 had the lowest membrane effect among the three lactoferrin peptides tested. On *C. albicans* membrane, LFcin17-30 induced an alteration on the distribution of intra-membranous particles (van der Kraan *et al.* 2005b) consistent with lipid segregation as seen by SAXD on model membranes (chapter 6). These findings support previous reports indicating that despite having a clear inhibitory effect against several pathogens, this peptide has mild membranolytic activity. In fact, different lactoferricin derivatives were found incapable of inducing significant leakage from model membranes and their antimicrobial activities were shown not to correlate with the levels of membrane interaction (Ulvatne *et al.* 2001, Nguyen *et al.* 2005, Jing *et al.* 2006). Moreover, LFcin17-30 exhibited a slow kinetics of membrane permeabilization in *Leishmania* and *C. albicans*, and induced small structural damages on the pathogens surface, as compared to more membrane-active peptides such as LFchimera (Bolscher *et al.* 2012, Silva *et al.* 2012, Leon-Sicairos *et al.* 2014). LFcin has also been found to translocate into the cytoplasm of *Staphylococcus aureus* and *Escherichia coli* (Haukland *et al.* 2001), and to inhibit the macromolecular synthesis (DNA, RNA, and protein synthesis) of *E. coli* and *Bacillus*

subtilis (Ulvatne *et al.* 2004). Finally, LFcin led to apoptosis in cancer cell lines by attacking the mitochondrial membrane (Mader *et al.* 2007). These observations suggest that the mechanism of action of LFcin is not confined to the cell surface but most probably includes action on internal targets, leading to impairment of several intracellular processes, which eventually culminate in cell death. Independently of how LFcin17-30 acts, it still has to interact with the membrane, cross it and reach its final target(s). The observed lipid segregation can be the means that allows LFcin17-30 internalization. Our work with LFcin17-30 and *Mycobacterium avium* can further support this mechanism of membrane perturbation to allow peptide internalization, to act eventually on intracellular targets (chapter 7 and 8).

When we tested LFcin17-30 variants against *M. avium* growing in broth culture, the replacement of all arginines by lysines (LFcin17-30 all K) significantly decreased the antimycobacterial activity, especially when compared to the variant with all arginines (LFcin17-30 all R) (chapter 7). Arginine residues have been found to be important for the antimicrobial activity of several AMP, including lactoferricin (Kang *et al.* 1996, Gifford *et al.* 2005, Chan *et al.* 2006), and there are also evidences that this amino acid plays a role in AMP internalization and is important for intracellular mechanisms of action (Mitchell *et al.* 2000, Rothbard *et al.* 2004, Hansen *et al.* 2008). Although these peptides induce significant changes in the surface and morphology of the cell, no clear evidences of permeabilization were observed (chapter 7), suggesting the existence of an intracellular target. The D enantiomer of LFcin17-30 was more active than the L peptide, probably due to its ability to resist proteolytic degradation (chapter 7). This also suggests that the mechanism of action of LFcin17-30 does not require the interaction with chiral receptors, since they would not recognize non-natural D amino acids. All the information gathered supports also the idea of a mechanism of action that involves membrane interaction to gain access to the intracellular environment, where the peptide will exert its main activity.

Moving to a more complex *in vitro* system, we proceeded to test LFcin17-30 and its variants against *M. avium* growing inside macrophages (chapter 8). Surprisingly, only D-LFcin17-30 induced a significant inhibition of the mycobacterial growth inside macrophages, and the combination with a conventional antibiotic ethambutol, did not result in a significant improvement over D-LFcin17-30 activity (chapter 8). As speculated above, the enhanced activity of D-LFcin17-30 is probably related to the ability to resist degradation. In chapter 7, we have determined that all lactoferricin peptides exhibited a direct antimycobacterial activity, probably by acting on internal targets, so the question now was – how is D-LFcin17-30 killing *M. avium* inside macrophages? The distribution and sub-cellular localization of lactoferricins inside *M. avium*-infected macrophages

showed no differences between LFcin17-30 and D-LFcin17-30. Strikingly, we showed that they do not co-localize with *M. avium*, following instead an endocytic pathway, never reaching the *M. avium*-harbouring phagosomes (chapter 8). Therefore, the only possible conclusion is that D-LFcin17-30 is modulating the macrophage antimicrobial mechanisms in order to promote *M. avium* killing. In fact, TNF-alpha and IL-6 were significantly enhanced in the supernatant of *M. avium*-infected macrophages treated with either LFcin17-30 or D-LFcin17-30, but this revealed to be irrelevant for the peptide's activity (chapter 8). Therefore, at this point we still do not know the reason behind D-LFcin17-30 activity against *M. avium* growing inside macrophages. Given recent suggestions that lactoferricin may be involved in the induction of autophagy and apoptosis (Pan *et al.* 2013) and that autophagy and antimicrobial peptides can contribute to the control of mycobacterial infections (Gutierrez *et al.* 2004, Yuk *et al.* 2009, Selvaraj *et al.* 2015) we intend to investigate the hypothesis that D-LFcin17-30 is inhibiting the growth of *M. avium* inside infected macrophages by inducing autophagy. A possible related mechanism is the interference with the maturation of mycobacteria-harbouring phagosomes with consequent restriction of the access to nutrients and/or exposure of mycobacteria to toxic environments (Appelberg 2006a, Appelberg 2006b, Gomes *et al.* 2008). These two possible mechanisms will be evaluated in the future in order to achieve a better understanding of the peptide's mechanism of action.

The studies presented here involving lactoferricin, and especially D-LFcin17-30, have shown the high potential of these peptides in the fight against mycobacterial infections. The mechanism by which this peptide exert its activity is probably not tightly connected to a specific protein and/or receptor. More, we speculate, based on our results so far, that this mechanism must involve a modulation of the macrophage capacity to fight the infection. Thus, the development of resistance appears to be very difficult for this particular peptide, increasing the interest on its applicability against relevant infections such as those caused by mycobacteria. Once the mechanism of action on *M. avium*-infected macrophages will be enlightened the obvious road will be to proceed to *in vivo* studies for the control of disseminated *M. avium* infection. If the obtained results will be promising, the next step will be to assess the antimycobacterial potential of D-LFcin17-30 on more relevant pathogens such as *M. tuberculosis*, although the efficacy on one species does not guarantee an efficiency on other. Since D-LFcin17-30 is highly resistant to proteolytic activity without harbouring significant toxicity towards host cells, parental administration of this peptide should be possible. In view of the results of our work, we believe it could potentially be used in the treatment of disseminated mycobacterial infections, or even the pulmonary infections caused not only by *M. tuberculosis* but also

by *M. avium* and other mycobacteria. If it will be shown that D-LFcin17-30 cannot be administered in this way, and should follow the road of other peptide agents as topical drugs, it can still be applied to mycobacterial infections, for instance for the treatment of ulcers caused by *M. ulcerans*.

Although further studies are needed in order to evaluate the effects of these peptides *in vivo*, data obtained in this thesis present new views on mechanism of action of antimicrobial peptides, both on model membranes and with pathogenic agents, that can be essential for the development of a new antimicrobial peptide able to control mycobacterial infections.

References

Abrunhosa F., Faria S., Gomes P., Tomaz I., Pessoa J. C., Andreu D. and Bastos M. (2005). Interaction and Lipid-Induced Conformation of Two Cecropin−Melittin Hybrid Peptides Depend on Peptide and Membrane Composition. *J Phys Chem B*. 109(36):17311-17319.

Adao R., Nazmi K., Bolscher J. G. and Bastos M. (2011). C- and N-truncated antimicrobial peptides from LFampin 265 - 284: Biophysical versus microbiology results. *J Pharm Bioallied Sci*. 3(1):60-69.

Alberola J., Rodriguez A., Francino O., Roura X., Rivas L. and Andreu D. (2004). Safety and efficacy of antimicrobial peptides against naturally acquired leishmaniasis. *Antimicrob Agents Chemother*. 48(2):641-643.

Andreu D., Ubach J., Boman A., Wahlin B., Wade D., Merrifield R. B. and Boman H. G. (1992). Shortened cecropin A-melittin hybrids. Significant size reduction retains potent antibiotic activity. *FEBS Lett*. 296(2):190-194.

Appelberg R. (2006a). Macrophage nutriprive antimicrobial mechanisms. *J Leukoc Biol*. 79(6):1117-1128.

Appelberg R. (2006b). Pathogenesis of Mycobacterium avium infection: typical responses to an atypical mycobacterium? *Immunol Res*. 35(3):179-190.

Bastos M., Bai G., Gomes P., Andreu D., Goormaghtigh E. and Prieto M. (2008). Energetics and partition of two cecropin-melittin hybrid peptides to model membranes of different composition. *Biophys J*. 94(6):2128-2141.

Bastos M., Silva T., Teixeira V., Nazmi K., Bolscher J. G. M., Funari S. S. and Uhríková D. (2011). Lactoferrin-Derived Antimicrobial Peptide Induces a Micellar Cubic Phase in a Model Membrane System. *Biophys J*. 101(3):L20-L22.

Bolscher J., Nazmi K., van Marle J., van 't Hof W. and Veerman E. (2012). Chimerization of lactoferricin and lactoferrampin peptides strongly potentiates the killing activity against Candida albicans. *Biochem Cell Biol*. 90(3):378-388.

Bolscher J. G., Adao R., Nazmi K., van den Keybus P. A., van 't Hof W., Nieuw Amerongen A. V., Bastos M. and Veerman E. C. (2009a). Bactericidal activity of

LFchimera is stronger and less sensitive to ionic strength than its constituent lactoferricin and lactoferrampin peptides. *Biochimie*. 91(1):123-132.

Bolscher J. G. M., Adão R., Nazmi K., van den Keybus P. A. M., van 't Hof W., Nieuw Amerongen A. V., Bastos M. and Veerman E. C. I. (2009b). Bactericidal activity of LFchimera is stronger and less sensitive to ionic strength than its constituent lactoferricin and lactoferrampin peptides. *Biochimie*. 91(1):123-132.

Boman H. G., Wade D., Boman I. A., Wahlin B. and Merrifield R. B. (1989). Antibacterial and antimalarial properties of peptides that are cecropin-melittin hybrids. *FEBS Lett*. 259(1):103-106.

Chan D. I., Prenner E. J. and Vogel H. J. (2006). Tryptophan- and arginine-rich antimicrobial peptides: structures and mechanisms of action. *Biochim Biophys Acta*. 1758(9):1184-1202.

Chicharro C., Granata C., Lozano R., Andreu D. and Rivas L. (2001). N-terminal fatty acid substitution increases the leishmanicidal activity of CA(1-7)M(2-9), a cecropin-melittin hybrid peptide. *Antimicrob Agents Chemother*. 45(9):2441-2449.

Diaz M. D., de la Torre B. G., Fernandez-Reyes M., Rivas L., Andreu D. and Jimenez-Barbero J. (2011). Structural framework for the modulation of the activity of the hybrid antibiotic peptide cecropin A-melittin [CA(1-7)M(2-9)] by Nepsilon-lysine trimethylation. *Chembiochem*. 12(14):2177-2183.

Fernandez-Reyes M., Diaz D., de la Torre B. G., Cabrales-Rico A., Valles-Miret M., Jimenez-Barbero J., Andreu D. and Rivas L. (2010). Lysine N(epsilon)-trimethylation, a tool for improving the selectivity of antimicrobial peptides. *J Med Chem*. 53(15):5587-5596.

Ferre R., Melo M. N., Correia A. D., Feliu L., Bardaji E., Planas M. and Castanho M. (2009). Synergistic effects of the membrane actions of cecropin-melittin antimicrobial hybrid peptide BP100. *Biophys J*. 96(5):1815-1827.

Flores-Villasenor H., Canizalez-Roman A., de la Garza M., Nazmi K., Bolscher J. G. and Leon-Sicairos N. (2012a). Lactoferrin and lactoferrin chimera inhibit damage caused by enteropathogenic Escherichia coli in HEp-2 cells. *Biochimie*. 94(9):1935-1942.

Flores-Villasenor H., Canizalez-Roman A., Reyes-Lopez M., Nazmi K., de la Garza M., Zazueta-Beltran J., Leon-Sicairos N. and Bolscher J. G. (2010). Bactericidal effect of

bovine lactoferrin, LFcin, LFampin and LFchimera on antibiotic-resistant Staphylococcus aureus and Escherichia coli. *Biometals*. 23(3):569-578.

Flores-Villasenor H., Canizalez-Roman A., Velazquez-Roman J., Nazmi K., Bolscher J. G. and Leon-Sicairos N. (2012b). Protective effects of lactoferrin chimera and bovine lactoferrin in a mouse model of enterohaemorrhagic Escherichia coli O157:H7 infection. *Biochem Cell Biol*. 90(3):405-411.

Giacometti A., Cirioni O., Kamysz W., D'Amato G., Silvestri C., Simona Del Prete M., Lukasiak J. and Scalise G. (2004). In vitro activity and killing effect of the synthetic hybrid cecropin A-melittin peptide CA(1-7)M(2-9)NH(2) on methicillin-resistant nosocomial isolates of Staphylococcus aureus and interactions with clinically used antibiotics. *Diagn Microbiol Infect Dis*. 49(3):197-200.

Gifford J. L., Hunter H. N. and Vogel H. J. (2005). Lactoferricin: a lactoferrin-derived peptide with antimicrobial, antiviral, antitumor and immunological properties. *Cell Mol Life Sci*. 62(22):2588-2598.

Gomes M. S., Sousa Fernandes S., Cordeiro J. V., Silva Gomes S., Vieira A. and Appelberg R. (2008). Engagement of Toll-like receptor 2 in mouse macrophages infected with Mycobacterium avium induces non-oxidative and TNF-independent anti-mycobacterial activity. *Eur J Immunol*. 38(8):2180-2189.

Groenink J., Walgreen-Weterings E., van 't Hof W., Veerman E. C. I. and Nieuw Amerongen A. V. (1999). Cationic amphipathic peptides, derived from bovine and human lactoferrins, with antimicrobial activity against oral pathogens. *FEMS Microbiol Lett*. 179(2):217-222.

Gutierrez M. G., Master S. S., Singh S. B., Taylor G. A., Colombo M. I. and Deretic V. (2004). Autophagy is a defense mechanism inhibiting BCG and Mycobacterium tuberculosis survival in infected macrophages. *Cell*. 119(6):753-766.

Haney E. F., Lau F. and Vogel H. J. (2007). Solution structures and model membrane interactions of lactoferrampin, an antimicrobial peptide derived from bovine lactoferrin. *Biochim Biophys Acta*. 1768(10):2355-2364.

Haney E. F., Nazmi K., Bolscher J. G. and Vogel H. J. (2012a). Influence of specific amino acid side-chains on the antimicrobial activity and structure of bovine lactoferrampin. *Biochem Cell Biol*. 90(3):362-377.

Haney E. F., Nazmi K., Bolscher J. G. and Vogel H. J. (2012b). Structural and biophysical characterization of an antimicrobial peptide chimera comprised of lactoferricin and lactoferrampin. *Biochim Biophys Acta*. 1818(3):762-775.

Haney E. F., Nazmi K., Lau F., Bolscher J. G. and Vogel H. J. (2009). Novel lactoferrampin antimicrobial peptides derived from human lactoferrin. *Biochimie*. 91(1):141-154.

Hansen M., Kilk K. and Langel U. (2008). Predicting cell-penetrating peptides. *Adv Drug Deliv Rev*. 60(4-5):572-579.

Haukland H. H., Ulvatne H., Sandvik K. and Vorland L. H. (2001). The antimicrobial peptides lactoferricin B and magainin 2 cross over the bacterial cytoplasmic membrane and reside in the cytoplasm. *FEBS Lett*. 508(3):389-393.

Jing W., Svendsen J. S. and Vogel H. J. (2006). Comparison of NMR structures and model-membrane interactions of 15-residue antimicrobial peptides derived from bovine lactoferricin. *Biochem Cell Biol*. 84(3):312-326.

Kang J. H., Lee M. K., Kim K. L. and Hahm K. S. (1996). Structure-biological activity relationships of 11-residue highly basic peptide segment of bovine lactoferrin. *Int J Pept Protein Res*. 48(4):357-363.

Kanthawong S., Puknun A., Bolscher J. G., Nazmi K., van Marle J., de Soet J. J., Veerman E. C., Wongratanacheewin S. and Taweechaisupapong S. (2014). Membrane-active mechanism of LFchimera against Burkholderia pseudomallei and Burkholderia thailandensis. *Biometals*. 27(5):949-956.

Leon-Sicairos N., Angulo-Zamudio U. A., Vidal J. E., Lopez-Torres C. A., Bolscher J. G., Nazmi K., Reyes-Cortes R., Reyes-Lopez M., de la Garza M. and Canizalez-Roman A. (2014). Bactericidal effect of bovine lactoferrin and synthetic peptide lactoferrin chimera in Streptococcus pneumoniae and the decrease in luxS gene expression by lactoferrin. *Biometals*. 27(5):969-980.

Leon-Sicairos N., Canizalez-Roman A., de la Garza M., Reyes-Lopez M., Zazueta-Beltran J., Nazmi K., Gomez-Gil B. and Bolscher J. G. (2009). Bactericidal effect of lactoferrin and lactoferrin chimera against halophilic Vibrio parahaemolyticus. *Biochimie*. 91(1):133-140.

Lopez-Soto F., Leon-Sicairos N., Nazmi K., Bolscher J. G. and de la Garza M. (2010). Microbicidal effect of the lactoferrin peptides lactoferricin17-30, lactoferrampin265-284, and lactoferrin chimera on the parasite Entamoeba histolytica. *Biometals*. 23(3):563-568.

Mader J. S., Richardson A., Salsman J., Top D., de Antueno R., Duncan R. and Hoskin D. W. (2007). Bovine lactoferricin causes apoptosis in Jurkat T-leukemia cells by sequential permeabilization of the cell membrane and targeting of mitochondria. *Exp Cell Res*. 313(12):2634-2650.

Mancheño J. M., Oñaderra M., Martínez del Pozo A., Díaz-Achirica P., Andreu D., Rivas L. and Gavilanes J. G. (1996). Release of Lipid Vesicle Contents by an Antibacterial Cecropin A−Melittin Hybrid Peptide. *Biochemistry*. 35(30):9892-9899.

Maria-Neto S., de Almeida K. C., Macedo M. L. and Franco O. L. (2015). Understanding bacterial resistance to antimicrobial peptides: From the surface to deep inside. *Biochim Biophys Acta*. 1848(11 Pt B):3078-3088.

Merrifield E. L., Mitchell S. A., Ubach J., Boman H. G., Andreu D. and Merrifield R. B. (1995). D-enantiomers of 15-residue cecropin A-melittin hybrids. *Int J Pept Protein Res*. 46(3-4):214-220.

Milani A., Benedusi M., Aquila M. and Rispoli G. (2009). Pore forming properties of cecropin-melittin hybrid peptide in a natural membrane. *Molecules*. 14(12):5179-5188.

Mitchell D. J., Kim D. T., Steinman L., Fathman C. G. and Rothbard J. B. (2000). Polyarginine enters cells more efficiently than other polycationic homopolymers. *J Pept Res*. 56(5):318-325.

Nguyen L. T., Schibli D. J. and Vogel H. J. (2005). Structural studies and model membrane interactions of two peptides derived from bovine lactoferricin. *J Pept Sci*. 11(7):379-389.

Pan W. R., Chen P. W., Chen Y. L., Hsu H. C., Lin C. C. and Chen W. J. (2013). Bovine lactoferricin B induces apoptosis of human gastric cancer cell line AGS by inhibition of autophagy at a late stage. *J Dairy Sci*. 96(12):7511-7520.

Piers K. L. and Hancock R. E. (1994). The interaction of a recombinant cecropin/melittin hybrid peptide with the outer membrane of Pseudomonas aeruginosa. *Mol Microbiol*. 12(6):951-958.

Pistolesi S., Pogni R. and Feix J. B. (2007). Membrane insertion and bilayer perturbation by antimicrobial peptide CM15. *Biophys J*. 93(5):1651-1660.

Rothbard J. B., Jessop T. C., Lewis R. S., Murray B. A. and Wender P. A. (2004). Role of membrane potential and hydrogen bonding in the mechanism of translocation of guanidinium-rich peptides into cells. *J Am Chem Soc*. 126(31):9506-9507.

Salomone F., Cardarelli F., Di Luca M., Boccardi C., Nifosi R., Bardi G., Di Bari L., Serresi M. and Beltram F. (2012). A novel chimeric cell-penetrating peptide with membrane-disruptive properties for efficient endosomal escape. *J Control Release*. 163(3):293-303.

Sato H. and Feix J. B. (2006). Osmoprotection of bacterial cells from toxicity caused by antimicrobial hybrid peptide CM15. *Biochemistry*. 45(33):9997-10007.

Saugar J. M., Rodriguez-Hernandez M. J., de la Torre B. G., Pachon-Ibanez M. E., Fernandez-Reyes M., Andreu D., Pachon J. and Rivas L. (2006). Activity of cecropin A-melittin hybrid peptides against colistin-resistant clinical strains of Acinetobacter baumannii: molecular basis for the differential mechanisms of action. *Antimicrob Agents Chemother*. 50(4):1251-1256.

Schlamadinger D. E., Wang Y., McCammon J. A. and Kim J. E. (2012). Spectroscopic and computational study of melittin, cecropin A, and the hybrid peptide CM15. *J Phys Chem B*. 116(35):10600-10608.

Selvaraj P., Harishankar M. and Afsal K. (2015). Vitamin D: Immuno-modulation and tuberculosis treatment. *Can J Physiol Pharmacol*. 93(5):377-384.

Silva T., Abengozar M. A., Fernandez-Reyes M., Andreu D., Nazmi K., Bolscher J. G., Bastos M. and Rivas L. (2012). Enhanced leishmanicidal activity of cryptopeptide chimeras from the active N1 domain of bovine lactoferrin. *Amino Acids*. 43(6):2265-2277.

Teixeira V., Feio M. J., Rivas L., De la Torre B. G., Andreu D., Coutinho A. and Bastos M. (2010). Influence of Lysine Nε-Trimethylation and Lipid Composition on the Membrane Activity of the Cecropin A-Melittin Hybrid Peptide CA(1−7)M(2−9). *J Phys Chem B*. 114(49):16198-16208.

Ulvatne H., Haukland H. H., Olsvik O. and Vorland L. H. (2001). Lactoferricin B causes depolarization of the cytoplasmic membrane of Escherichia coli ATCC 25922 and fusion of negatively charged liposomes. *FEBS Lett*. 492(1-2):62-65.

Ulvatne H., Samuelsen O., Haukland H. H., Kramer M. and Vorland L. H. (2004). Lactoferricin B inhibits bacterial macromolecular synthesis in Escherichia coli and Bacillus subtilis. *FEMS Microbiol Lett*. 237(2):377-384.

Urban P., Valle-Delgado J. J., Moles E., Marques J., Diez C. and Fernandez-Busquets X. (2012). Nanotools for the delivery of antimicrobial peptides. *Curr Drug Targets*. 13(9):1158-1172.

van der Kraan M. I., Groenink J., Nazmi K., Veerman E. C., Bolscher J. G. and Nieuw Amerongen A. V. (2004). Lactoferrampin: a novel antimicrobial peptide in the N1-domain of bovine lactoferrin. *Peptides*. 25(2):177-183.

van der Kraan M. I., Nazmi K., Teeken A., Groenink J., van 't Hof W., Veerman E. C., Bolscher J. G. and Nieuw Amerongen A. V. (2005a). Lactoferrampin, an antimicrobial peptide of bovine lactoferrin, exerts its candidacidal activity by a cluster of positively charged residues at the C-terminus in combination with a helix-facilitating N-terminal part. *Biol Chem*. 386(2):137-142.

van der Kraan M. I., Nazmi K., van 't Hof W., Amerongen A. V., Veerman E. C. and Bolscher J. G. (2006). Distinct bactericidal activities of bovine lactoferrin peptides LFampin 268-284 and LFampin 265-284: Asp-Leu-Ile makes a difference. *Biochem Cell Biol*. 84(3):358-362.

van der Kraan M. I., van Marle J., Nazmi K., Groenink J., van 't Hof W., Veerman E. C., Bolscher J. G. and Nieuw Amerongen A. V. (2005b). Ultrastructural effects of antimicrobial peptides from bovine lactoferrin on the membranes of Candida albicans and Escherichia coli. *Peptides*. 26(9):1537-1542.

Yuk J. M., Shin D. M., Lee H. M., Yang C. S., Jin H. S., Kim K. K., Lee Z. W., Lee S. H., Kim J. M. and Jo E. K. (2009). Vitamin D3 induces autophagy in human monocytes/macrophages via cathelicidin. *Cell Host Microbe*. 6(3):231-243.